National Library
of Canada

Bibliothèque nationale
du Canada

Canadian Theses Service

Service des thèses canadiennes

Ottawa, Canada
K1A 0N4

NOTICE

The quality of this microform is heavily dependent upon the quality of the original thesis submitted for microfilming. Every effort has been made to ensure the highest quality of reproduction possible.

If pages are missing, contact the university which granted the degree.

Some pages may have indistinct print especially if the original pages were typed with a poor typewriter ribbon or if the university sent us an inferior photocopy.

Previously copyrighted materials (journal articles, published tests, etc.) are not filmed.

Reproduction in full or in part of this microform is governed by the Canadian Copyright Act, R.S.C. 1970, c. C-30.

AVIS

La qualité de cette microforme dépend grandement de la qualité de la thèse soumise au microfilmage. Nous avons tout fait pour assurer une qualité supérieure de reproduction.

S'il manque des pages, veuillez communiquer avec l'université qui a conféré le grade.

La qualité d'impression de certaines pages peut laisser à désirer, surtout si les pages originales ont été dactylographiées à l'aide d'un ruban usé ou si l'université nous a fait parvenir une photocopie de qualité inférieure.

Les documents qui font déjà l'objet d'un droit d'auteur (articles de revue, tests publiés, etc.) ne sont pas microfilmés.

La reproduction, même partielle, de cette microforme est soumise à la Loi canadienne sur le droit d'auteur, SRC 1970, c. C-30.

NL-339 (r. 88/04)

Canada

THE UNIVERSITY OF ALBERTA

GAS EVOLUTION IN ATHABASCA OIL SANDS

by

DAVID HERMAN LLOYD PEACOCK

A THESIS
SUBMITTED TO THE FACULTY OF GRADUATE STUDIES AND RESEARCH
IN PARTIAL FULFILMENT OF THE REQUIREMENTS FOR THE DEGREE
OF MASTER OF SCIENCE

DEPARTMENT OF CIVIL ENGINEERING

EDMONTON, ALBERTA
SPRING 1988

Permission has been granted to the National Library of Canada to microfilm this thesis and to lend or sell copies of the film.

The author (copyright owner) has reserved other publication rights, and neither the thesis nor extensive extracts from it may be printed or otherwise reproduced without his/her written permission.

L'autorisation a été accordée à la Bibliothèque nationale du Canada de microfilmer cette thèse et de prêter ou de vendre des exemplaires du film.

L'auteur (titulaire du droit d'auteur) se réserve les autres droits de publication; ni la thèse ni de longs extraits de celle-ci ne doivent être imprimés ou autrement reproduits sans son autorisation écrite.

ISBN 0-315-42911-9

THE UNIVERSITY OF ALBERTA

RELEASE FORM

NAME OF AUTHOR DAVID HERMAN LLOYD PEACOCK

TITLE OF THESIS GAS EVOLUTION IN ATHABASCA OIL SANDS

DEGREE FOR WHICH THESIS WAS PRESENTED MASTER OF SCIENCE

YEAR THIS DEGREE GRANTED SPRING 1988

Permission is hereby granted to THE UNIVERSITY OF ALBERTA LIBRARY to reproduce single copies of this thesis and to lend or sell such copies for private, scholarly or scientific research purposes only.

The author reserves other publication rights, and neither the thesis nor extensive extracts from it may be printed or otherwise reproduced without the author's written permission.

(SIGNED) Dave Peacock

PERMANENT ADDRESS:
2731 LIONEL CRESENT S.W.
CALGARY, ALBERTA, CANADA
T3E 6B1

DATED MARCH 26 1988

THE UNIVERSITY OF ALBERTA

FACULTY OF GRADUATE STUDIES AND RESEARCH

The undersigned certify that they have read, and recommend to the Faculty of Graduate Studies and Research, for acceptance, a thesis entitled Gas Evolution in Athabasca Oil Sand submitted by David H. L. Peacock in partial fulfilment of the requirements for the degree of Master of Science.

J. O. Scott
....
Supervisor

....

....

Date. December 21, 1987

ABSTRACT

Geotechnical engineering design and construction in oil sands are often significantly influenced by the gases present in the oil sands. The evolution of the solution gases caused by a reduction in the pore pressures or by an increase in the temperature produces large volume changes and reduces the in situ shear srength of the oil sands.

Solubility, gas saturation pressures and the composition of the in situ gases which cause this deformation were evaluated by testing Athabasca oil sand samples under various conditions. Testing was carried out under undrained and drained conditions with a sealed oedometer testing apparatus. The samples tested under undrained conditions were subjected to a series of unloading pressure increments and the sample response was monitered with time. The individual increments provided data on the transient behaviour of the dissolved gases and the equilibrium data points were used to determine some equilibrium properties of the gas in the oil sands.

The time dependent response of the samples was modelled with a curve fitting technique. The equilibrium properties examined included the gas saturation pressure and the combined solubility coefficient of the gases in the oil sand. The combined solubility coefficient was obtained from the actual volume of gas evolved over a range of pressure obtained from the unloading undrained tests. This was compared theoretically from the ratio of gases measured from

a gas chromatograph combined with solubility data of the gases in bitumen as found in the literature.

The gas saturation pressure for the oil sand samples correlated well with the premining pore pressures for both the shallow lean oil sand and the deep rich oil sand samples. The gas composition averaged approximately 75% methane, 20% carbon dioxide and 5% nitrogen. The solubility coefficients of these gases in bitumen at 24°C were 0.074 $(cm^3/cm^3)/101$ kPa for the lean oil sand and 0.19 to 0.22 $(cm^3/cm^3)/101$ kPa for the rich oil sand.

The gases vented from the lean oil sand when the pore liquid saturation reached 82% to 89% and the rich oil sand samples vented at pore liquid saturations of 40% to 65%.

ACKNOWLEDGMENTS

I wish to acknowledge the financial support that I have received from the Alberta Oil Sands Technology and Research Authority (AOSTRA). The AOSTRA scholarship was a major source of financial support during my period of research. Also, the testing could not have gone forward without the drilling and sampling provided to the University program by the Mining Engineering Department of Syncrude Canada Ltd.,

The guidance, direction, advise and encouragement from Dr. J.D. Scott throughout the course of my studies is greatly appreciated. The interest in the topic of gas evolution in oil sands was initiated and developed by him. I would like to thank Dr. L. Hepler for his assistance in providing understanding of gas properties and how they apply to the oil sands. Dr. K. McCurdy from the University of Lethbridge deserves special credit as it was he who encouraged me to take engineering and see it as an opportunity to challenge the unknown.

I would like to acknowledge the assistance that I received from Steve Gamble and Christine Hereygers who assisted me in setting up the testing equipment and making the apparatus workable. I also appreciate the assistance that I received from Marcel Huculak in collating some of the test data and running several tests.

My wife Becky deserves special acknowledgment as she encouraged and supported me through the research years. Without her support and help the challenge to complete this

thesis would have been much more difficult. Special thanks must go to my parents who have instilled in me the qualities that I needed to develop as a mature person mentally and spiritually. They taught me that my talents and abilities are gifts from God and that I am primarily responsible to Him for the effective and honorable use of these abilities.

List of Symbols

P = Absolute pressure (kPa)

u = Gage pressure (kPa)

n = Porosity

C = Dissolved gas concentration in pore liquid

K = Henry's coefficient

X = Liquid mole fraction

H = Solubility coefficient (cm^3/cm^3)/101 kPa

P_n = Partial pressure from dissolved gas n

V_L = Volume of liquid at N.T.P.

V_G = Volume of gas at N.T.P.

D = Coefficient of Diffusivity (cm^2/sec)

V_{fg} = Incremental volume of free gas evolved at time t

V_2 = Final incremental volume of evolved free gas

A = Curve fitting parameter

E = Curve fitting parameter

I_D = Index of disturbance

N.T.P. = Normal temperature and pressure (20°Cand 101.4 kPa)

t = time

N = Number of moles of fluid

Subscripts

L = Liquid

G = Gas

W = Water

O = Bitumen or oil

LT = Total liquid

GT = Total gas

Table of Contents

Chapter Page

1. INTRODUCTION 1

1.1 STATEMENT OF PROBLEM 1

1.2 OBJECTIVES OF THE RESEARCH 3

1.3 DEFINITIONS 4

1.4 SCOPE OF THESIS 5

2. REVIEW OF SOME GAS PROPERTIES IN OIL SANDS 6

2.1 GASES PRESENT IN OIL SANDS 6

2.2 SOLUBILITY OF GASES IN OIL SANDS 10

2.3 DIFFUSIVITY OF GASES IN OIL SANDS 18

2.4 TIME DEPENDENCY OF GAS EVOLUTION FROM OIL SANDS .23

3. LABORATORY APPARATUS AND PROCEDURES 29

3.1 TESTING APPARATUS 29

3.1.1 The Test Cell 29

3.1.2 The Pressurization System 30

3.1.3 Displacement Measurements 31

3.1.4 Temperature Measurement Apparatus 33

3.1.5 Data Acquisition 34

3.1.6 Insulation 34

3.2 TESTING PROGRAM FOR TAILINGS SAND SAMPLES 35

3.2.1 Purpose of Testing Tailings Sand Samples ..35

3.2.2 Preparation of Tailings Sand Samples 36

3.2.3 Testing of Tailings Sand 37

3.3 SAMPLING PROCEDURES FOR OBTAINING OIL SAND SAMPLES ...39

3.3.1 Previous Sampling Techniques 39

3.3.2 Sampling Program and Sample Storage 40

3.3.3 Preparation of Oil Sand Samples for Testing 43

3.3.4 Procedure for Obtaining Gas Samples 44

3.4 EVALUATION OF THE TESTING PROGRAM 45

3.4.1 Sampling Procedure 45

3.4.2 Sample Preparation and Testing Procedures .48

3.4.2.1 Sample Preparation 48

3.4.2.2 Test Procedures 50

3.4.2.3 Effect of Temperature 53

3.4.3 Unloading Undrained Tests on Oil Sand 54

3.4.4 Unloading Drained Tests on Oil Sands 54

3.4.5 Gas Saturation Curve 55

3.4.6 Measurement of Gases 56

4. EXPERIMENTAL RESULTS 62

4.1 TRANSIENT TEST RESULTS 62

4.1.1 Transient behaviour of Tailings Sand Samples 62

4.1.2 Transient Behaviour of Oil Sand Samples ...65

4.2 EQUILIBRIUM TEST RESULTS 67

4.2.1 Gas Saturation Pressure 67

4.2.2 Gas Types 68

5. EVALUATION OF DATA 115

5.1 TIME DEPENDENT BEHAVIOUR 115

5.1.1 Time Dependent Behavior of Tailing Sand Samples 115

5.1.2 Time Dependent Behavior of Lean Athabasca Oil Sand 118

5.1.3 Drainage Mechanism 121

5.2 EQUILIBRIUM BEHAVIOR 123

5.2.1 Solubility Coefficients 123

5.2.1.1 Solubility of Carbon Dioxide in Water 124

5.2.1.2 Combined Solubility Coefficents of Gases in Oil Sand 126

5.2.1.3 Combined Solubility Coefficients from Gas Samples 128

5.2.2 Gas Saturation Pressure 129

5.2.3 Gases Present in Oil Sand 139

6. CONCLUSIONS AND RECOMMENDATIONS 180

6.1 CONCLUSIONS 180

6.1.1 Sampling 180

6.1.2 Testing 181

6.1.3 Equilibrium Properties of Oil Sand 182

6.1.4 Time Dependent Behaviour 185

6.2 RECOMMENDATIONS 187

References 190

APPENDIX A - DESCRIPTION OF APPARATUS AND CALIBRATIONS ..193

APPENDIX B - TESTING ON TAILING SAND SAMPLE AT 50°C 199

APPENDIX C - TESTING ON LEAN OIL SAND AT 6°C AND 60°C ...210

APPENDIX D - TESTING ON RICH OIL SAND AT 24°C 229

APPENDIX E --DIFFUSION EMPIRICAL MODEL 242

List of Tables

Table Page

2.1 Solubility coefficients calculated from work done by Svrcek and Mehrotra, 1982 25

3.1 Summary of oil sand samples' densities, saturation and index of disturbance 58

4.1 List of testing done on tailing sand samples 70

4.2 List of testing done on lean oil sand samples 71

4.3 List of testing done on rich oil sand samples 72

4.4 Bitumen, water and sand content of oil sand samples 73

4.5 Percentages of gases found in oil sand samples 74

5.1 E values obtained by curve fitting oil sand samples 142

5.2 Combined solubility coefficients obtained from unloading undrained tests 143

5.3 Combined solubility coefficients calculated from gases obtained from the gas samples 144

E.1 Relationship between E parameter and Diffusion Coefficient 250

E.2 Relationship between bubble radius and E parameter 251

List of Figures

Figure Page

2.1 Solubility coefficients of carbon dioxide, nitrogen and methane in bitumen from Svercek and Mehrotra, 1982 26

2.2 Relationship between the diffusion coefficient and the viscosity of the solvent 27

2.3 Effect of temperature on the viscosity of bitumen below 20°C --Huculak, 1985 28

3.1 Schematic of test setup for testing tailing sand samples 59

3.2 Picture of expanded rich oil sand due to expanding gas at -25°C 60

3.3 Increment D from unloading undrained test on RB-5-12 at 6°C 61

4.1 Grain size curve for tailing sand samples 75

4.2 Increment B from unloading undrained test on tailing sand sample T-525 76

4.3 Increment C from unloading undrained test on tailing sand sample T-525 77

4.4 Increment D from unloading undrained test on tailing sand sample T-525 78

4.5 Increment E from unloading undrained test on tailing sand sample T-525 79

4.6 Increment F from unloading undrained test on tailing sand sample T-525 80

4.7 Increment G from unloading undrained test on tailing sand sample T-525 81

4.8 Increment H from unloading undrained test on tailing sand sample T-525 82

4.9 Undrained equilibrium curve for tailing sand sample T-525 83

4.10 Stress vs. strain cuve for tailing sand sample T-525 84

4.11 Increment H from unloading undrained test on tailing sand sample T-350 at 50°C 85

Figure Page

4.12 Grain size curve for samples from a lean oil sand sample and a rich oil sand sample 86

4.13 Increment D from unloading undrained test on lean oil sand sample B-224 at 24°C 87

4.14 Increment E from unloading undrained test on lean oil sand sample B-224 at 24°C 88

4.15 Increment F from unloading undrained test on lean oil sand sample B-224 at 24°C 89

4.16 Increment G from unloading undrained test on lean oil sand sample B-224 at 24°C 90

4.17 Increment H from unloading undrained test on lean oil sand sample B-224 at 24°C 91

4.18 Increment I from unloading undrained test on lean oil sand sample B-224 at 24°C 92

4.19 Increment J from unloading undrained test on lean oil sand sample B-224 at 24°C 93

4.20 Increment K from unloading undrained test on lean oil sand sample B-224 at 24°C 94

4.21 Undrained equilibrium curve for lean oil sand sample B-224 at 24°C 95

4.22 Stress vs. strain curve for lean oil sand sample B-224 at 24°C 96

4.23 Increment A from unloading undrained test on rich oil sand sample RB-5-5 at 24°C 97

4.24 Increment B from unloading undrained test on rich oil sand sample RB-5-5 at 24°C 98

4.25 Increment C from unloading undrained test on rich oil sand sample RB-5-5 at 24°C 99

4.26 Increment D from unloading undrained test on rich oil sand sample RB-5-5 at 24°C 100

4.27 Increment E from unloading undrained test on rich oil sand sample RB-5-5 at 24°C 101

4.28 Increment F from unloading undrained test on rich oil sand sample RB-5-5 at 24°C 102

Figure Page

4.29 Increment G from unloading undrained test on rich oil sand sample RB-5-5 at 24°C 103

4.30 Increment H from unloading undrained test on rich oil sand sample RB-5-5 at 24°C 104

4.31 Increment I from unloading undrained test on rich oil sand sample RB-5-5 at 24°C 105

4.32 Increment J from unloading undrained test on rich oil sand sample RB-5-5 at 24°C 106

4.33 Increment K from unloading undrained test on rich oil sand sample RB-5-5 at 24°C 107

4.34 Undrained equilibrium curve for rich oil sand sample RB-5-5 at 24°C 108

4.35 Stress vs.strain curve for rich oil sand sample RB-5-5 at 24°C 109

4.36 Unloading drained test on lean oil sand sample B-222 at 24°C with a vertical load of 8 kPa 110

4.37 Unloading drained test on lean oil sand sample B-223 at 24°C with a vertical load of 300 kPa 111

4.38 Unloading drained test on lean oil sand sample B-225A at 24°C with a vertical load of 120 kPa 112

4.39 Unloading drained test on rich oil sand sample RB-5-1 at 24°C with a vertical load of 8 kPa 113

4.40 Effect of temperature on the gas saturation pressure for lean oil sand samples and a rich oil sand sample 114

5.1 E values obtained by curve fitting data from T-525G 145

5.2 E values obtained by curve fitting data from T-525H 146

5.3 Combination of E values from Sobkowicz's data and from sample T-525 147

5.4 E values obtained by curve fitting data from T-350F 148

Figure Page

5.5 E values obtained by curve fitting data from T-350G 149

5.6 E values obtained by curve fitting data from T-350H 150

5.7 E values obtained by curve fitting data from B-223G 151

5.8 E values obtained by curve fitting data from B-223H 152

5.9 E values obtained by curve fitting data from B-224J 153

5.10 E values obtained by curve fitting data from B-224K 154

5.11 E values obtained by curve fitting data from B-225G 155

5.12 E values obtained by curve fitting data from the unloading drained test (B-222) 156

5.13 E values obtained by curve fitting data from the unloading drained test (B-225A) 157

5.14 E values obtained by curve fitting data from the unloading drained test (B-223) 158

5.15 Fracturing of lean oil sand sample observed after testing 159

5.16 Fracturing of rich oil sand sample observed after testing 160

5.17 E values obtained by curve fitting data from the unloading undrained test (B-5-5H) 161

5.18 E values obtained by curve fitting data from the unloading undrained test (B-5-5I) 162

5.19 E values obtained by curve fitting data from the unloading undrained test (B-5-5J) 163

5.20 E values obtained by curve fitting data from the unloading undrained test (B-5-5K) 164

Figure Page

5.21 E values obtained by curve fitting data from the unloading undrained test (RB-5-2L) 165

5.22 E values obtained by curve fitting data from the unloading undrained test (B-5-2M) 166

5.23 Solubility coefficient (H) for carbon dioxide in tailing sand sample at 24°C 167

5.24 Combined solubility coefficient for lean oil sand sample B-225 at 6°C 168

5.25 Combined solubility coefficient for lean oil sand sample B-224 at 24°C 169

5.26 Combined solubility coefficient for lean oil sand sample B-223 at 60°C 170

5.27 Combined solubility coefficient for rich oil sand sample RB-5-2 at 24°C 171

5.28 Combined solubility coefficient for rich oil sand sample RB-5-5 at 24°C 172

5.29 Combined solubility coefficient for rich oil sand sample RB-5-10 at 24°C 173

5.30 Combined solubility coefficient for rich oil sand sample RB-5-12 at 6°C 174

5.31 Combined solubility coefficient for rich oil sand sample RB-15-8 at 24°C 175

5.32 Sketch of the location from which the lean oil sand samples were taken 176

5.33 Sketch of the location from which the rich oil sand samples were taken 177

5.34 Theoretical combined solubility coefficients for oil sand samples at 24°C for a variety of bitumen/water ratios 178

5.35 Theoretical combined solubiliity coefficients for oil sand samples at 24°C for a variety of bitumen/water ratios 179

A.1 Calibration curve for the Celesco 2599 pore pressure transducer 195

Figure Page

A.2 Calibration curve for the Viatron 207 pore pressure transducer 196

A.3 Calibration curve for the Celesco 8414 pore pressure transducer 197

A.4 Calibration curve for the Hewlett Packard DCDT 100 LVDT 198

B.1 Increment A from the unloading undrained test at 50°C for T-350 200

B.2 Increment B from the unloading undrained test at 50°C for T-350 201

B.3 Increment C from the unloading undrained test at 50°C for T-350 202

B.4 Increment D from the unloading undrained test at 50°C for T-350 203

B.5 Increment E from the unloading undrained test at 50°C for T-350 204

B.6 Increment F from the unloading undrained test at 50°C for T-350 205

B.7 Increment G from the unloading undrained test at 50°C for T-350 206

B.8 Increment H from the unloading undrained test at 50°C for T-350 207

B.9 Stress strain curve for sample T-350 208

B.10 Unloading Undrained Equilibrium Curve obtained from T-350 209

C.1 Increment B from the unloading undrained test at 6°C for B-225 211

C.2 Increment C from the unloading undrained test at 6°C for B-225 212

C.3 Increment D from the unloading undrained test at 6°C for B-225 213

C.4 Increment E from the unloading undrained test at 6°C for B-225 214

C.5 Increment F from the unloading undrained test at 6°C for B-225 215

Figure Page

C.6 Increment G from the unloading undrained test at 6°C for B-225 216

C.7 Stress strain curve for sample B-225 217

C.8 Unloading Undrained Equilibrium Curve obtained from B-225 218

C.9 Increment A from the unloading undrained test at 60°C for B-223 219

C.10 Increment B from the unloading undrained test at 60°C for B-223 220

C.11 Increment C from the unloading undrained test at 60°C for B-223 221

C.12 Increment D from the unloading undrained test at 60°C for B-223 222

C.13 Increment E from the unloading undrained test at 60°C for B-223 223

C.14 Increment F from the unloading undrained test at 60°C for B-223 224

C.15 Increment G from the unloading undrained test at 60°C for B-223 225

C.16 Increment H from the unloading undrained test at 60°C for B-223 226

C.17 Stress strain curve for sample B-223 227

C.18 Unloading undrained Equilibrium Curve obtained from B-223 228

D.1 Increment D from the unloading undrained test at 24°C for RB-5-2 230

D.2 Increment E from the unloading undrained test at 24°C for RB-5-2 231

D.3 Increment F from the unloading undrained test at 24°C for RB-5-2 232

D.4 Increment G from the unloading undrained test at 24°C for RB-5-2 233

D.5 Increment H from the unloading undrained test at 24°C for RB-5-2 234

Figure Page

D.6 Increment I from the unloading undrained test at 24°C for RB-5-2 235

D.7 Increment J from the unloading undrained test at 24°C for RB-5-2 236

D.8 Increment K from the unloading undrained test at 24°C for RB-5-2 237

D.9 Increment L from the unloading undrained test at 24°C for RB-5-2 238

D.10 Increment M from the unloading undrained test at 24°C for RB-5-2 239

D.11 Stress strain curve for sample RB-5-2 240

D.12 Unloading Undrained Equilibrium Curve obtained from RB-5-2 241

E.1 Correlation between the diffusion empirical model and the E parameter 252

1. INTRODUCTION

1.1 STATEMENT OF PROBLEM

Some geotechnical problems in oil sands are the direct result of gases present in the oil sands. The evolution of the solution gases caused by a reduction in the pore pressures or by an increase in the temperature produces large volume changes and reduces the in situ shear strength of the oil sands.

The volume changes of the oil sands associated with gas evolution makes it difficult to collect quality geotechnical samples, predict and design foundations in oil sands and predict the behavior of tunnels and shafts in oil sands. The change in shear strength of the oil sands must also be considered in shaft and tunnel designs and also in slope stability design for mine pit slopes. Gas evolution is also of interest because it is a potential source of gas drive for in situ production of bitumen from oil sands.

Athabasca oil sands have a locked sand matrix that gives a high shear strength to the undisturbed sand which recompacted samples do not have (Dusseault and Morgenstern, 1979). The high strength due to the locked structure of the oil sands can be lost by disturbance of the sand matrix. Volume change due to the evolution of gases from the pore liquids is one mechanism which can cause the oil sands to become disturbed and break apart its locked structure.

The specific gas properties of the oil sands is an area which must be understood to determine the extent of the disturbance that gas evolution can have on the sand structure. This work is an undertaking to determine some gas properties of Athabasca oil sands and to make some quantitative statements which describe the extent of disturbance that can be expected in the oil sands due to gas evolution.

Gas exsolution has been defined by Sobkowicz (1982) for all gassy soils in general, including oil sands. Sobkowicz also developed an empirical model to analyze the transient behavior of gas evolution. However, no experimental data to use in his model was available to determine the time dependent behavior of gas evolution in oil sands. Also, the equilibrium behavior of the gases present within the oil sands has yet to be accurately assessed.

This research is an effort to determine some of the gas properties of Athabasca oil sands, the range of these properties, and how they affect the volume change characteristics of oil sands. The knowledge of these gas properties will provide information to design better sampling tools, to model in situ conditions and enable future research to more accurately determine the pressure required to saturate oil sand samples for testing purposes.

1.2 OBJECTIVES OF THE RESEARCH

To obtain the gas properties of oil sands the research was broken down into a series of five objectives.

1. Obtain field samples which had limited expansion during sampling and have therefore lost little or no gas.
2. Store the samples to prevent gas loss from the oil sand during storage.
3. Determine a preparation method of a sample for testing without losing gases from the oil sand during preparation.
4. Develop apparatus and test procedures which can measure the volume and rate of gas evolution from the oil sands during pore pressure reduction, confining stress release or a temperature increase.
5. Test a number of lean and rich bitumen oil sand specimens and analyze the results to isolate specific gas properties.

When all these objectives can be successfully attained and the individual gas properties of the oilsand determined, then the foundation is laid in understanding how gas evolution affects the geotechnical properties. This requires that both the equilibrium properties and the time dependent properties of gas evolution from the oil sand be quantified.

1.3 DEFINITIONS

Several terms must be defined to avoid confusion in the thesis.

a. Pressure.

Many gas properties are defined relative to the absolute pressure and not the gage pressure, however measurements such as pore pressure are always defined from gage pressure. To prevent confusion the gage pressure will be designated by "u" and and the absolute pressure by "P" as shown in equation 1.1.

$$P=u+P_{atm} \qquad 1.1$$

b. Gas Saturation Pressure.

The pressure of the gas inside the occluded bubble is higher than than the pressure of the surrounding liquid due to the interfacial tension caused by the skin of the bubble. The additional pressure caused by the interfacial tension can be significant if the bubble is small. Sobkowicz (1982) shows that bubbles larger than $3.5*10^{-6}$m in radius have a pressure increase due to interfacial tension which is insignificant. Most of the testing will involve bubbles with larger radii than this and as a result the pressure of the gas will be assumed to be equivalent to the pressure of the surrounding fluid.

c. Normal Temperature and Pressure (NTP).

When dealing with the volume of gas instead of the amount of gas, a consistent temperature and pressure is required to give uniformity to all data. Various definitions of NTP are available but the definition provided by the Compressed Gas Institute will be used where the normal pressure is 101.3 kPa and the normal temperature is 20°C.

1.4 SCOPE OF THESIS

The review in Chapter 2 discusses the data available from the literature on field observation of gas evolution from oil sands, gases that have been obtained from oil sand samples and the solubility and diffusivity of gases in bitumen.

The sampling and laboratory equipment required to obtain gas properties of oil sand are presented in Chapter 3. Also, the testing procedure developed for the experimental program is described in chapter 3.

Chapter 4 gives the experimental results from the testing program and these results are then analyzed in Chapter 5. In analyzing the test results the gas properties are broken down into the time dependent gas properties and the equilibrium gas properties of oil sands. These gas properties are analyzed over a range of bitumen contents of the oil sands and over a range of temperatures.

Finally, the test results are evaluated to determine the effect the gas evolution has on the volume change characteristics of the oil sand and the effectiveness of the sampling and testing procedures.

2. REVIEW OF SOME GAS PROPERTIES IN OIL SANDS

2.1 GASES PRESENT IN OIL SANDS

Gases are present in the bitumen and water within the oil sands. Geothermal heating has resulted in thermal degradation and maturing of the bitumen and, with time, has resulted in the production of various gases. In addition to the production of gases due to the thermal breakdown of bitumen, microbial degradation in the past assisted in the breakdown and is indicated by the presence of the gas neopentane (Jha, Montgomery and Strausz, 1977).

The presence of a gaseous phase within Athabasca oil sands has been known for many years. Hardy and Hemstock (1963) observed the effects of gas evolution in their testing procedures. However, no effort was made to determine the types of gases present or to quantify the effect of gas evolution on the test samples.

A major work in determining the gases found in Athabasca oil sand from the Syncrude and Suncor mine sites was from Strausz, Jha and Montgomery (1977), Jha, Montgomery and Strausz (1977) and Jha, Montgomery and Strausz (1979). They reported (in decreasing order of amounts) the presence of neopentane, methane, and acetaldehyde in Athabasca oil sand at 5°C. As the temperature was increased to 210°C a large quantity of carbon monoxide, sulpher dioxide and methane were measured. The gases collected at 5°C were considered to be the insitu constituent gases and any additional gases released at higher temperatures were the result of thermolysis. They did not take quantitative measurements of nitrogen, oxygen and carbon dioxide because of the problem of contamination from air.

When their sample of Athabasca oilsand was oxidized at 130°C, a large amount of carbon dioxide and carbon monoxide were released. Also larger amounts of most other gases previously observed were measured as well at this elevated temperature (Jha, Montgomery and Strausz, 1977). This oxidation rate slowed down as the temperature was lowered, but even with the temperature at 5°C the oxidation still occurred. This oxidation of the bitumen should quickly use up any in situ oxygen leaving the bitumen free of dissolved oxygen in situ.

The volume of gas obtained in testing was small and the authors considered the amounts of gases they obtained as a lower limit with many volatiles lost through storage and handling (Jha, Montgomery and Strausz, 1977).

Srajer and Barron (1978) tested the gases which evolved from the Athabasca oil sand during the construction of the Saline Creek tunnel. The volume of gases observed in the tunnel were very small and difficult to measure. Srajer (1977) also tested Saline Creek oil sand samples at 5°C and 25°C and the major gas constituents were carbon dioxide, carbon monoxide, neopentane, methane and acetaldehyde in decreasing order. Much more gas was obtained from these samples than the tunnel wall, but there was no correlation made with the insitu pore pressure. The total volume of gas collected increased 64% when the temperature was increased from 5°C to 25°C.

Gases were produced from the above Saline Creek oil sand samples in the laboratory by applying a vacuum to the sample and measuring the gases that come off the oil sand samples. This testing procedure was used by Jha, Montgomery and Strausz (1977) and by Srajer and Barron (1978) in obtaining their gas measurements. However, by placing the sample under a vacuum there should be little or no gas left in the sample even at 5°C. Any subsequent increase in temperature should not release any gas because very little should be left within the sample. However, by increasing the temperature there was not only an increase in the amount of gases produced but also as the temperature increased substantially new types of gases were released. The presence of different gases at higher temperatures indicates that the amount of gas within the oil sand is temperature dependent. The increased volumes of carbon dioxide, carbon monoxide and methane are due either to thermolysis or due to the gases being locked into the bitumen and only released at a higher temperature.

Srajer (1981) also tested gases coming from core samples taken at the Gulf Surmont lease. The gas desorption technique used in determining the amount of methane in coal was used to determine the gas quantities in the oil sand. A description of the gas desorption technique can be obtained from Kissel, McCulloch and Elder (1975) and Feng, Cheng and Augsten (1984). Four gas types were measured from these samples at 23°C including carbon dioxide, carbon monoxide, methane and ethane. The carbon monoxide and the ethane were consistently less than one percent of the total gas volume, the methane varied from 30-96% of the total volume and the carbon dioxide varied from 4-68% of the total gas volume. An effort was made to determine the amount of additional gas that would be obtained by heating the sample to 50°C but the results were not conclusive.

Robinson (1985) determined the types and amounts of gases that were released from Athabasca oil sand cores taken from the Syncrude mine site. He obtained gases in the ratio of 9% carbon dioxide, 37% methane, 37% nitrogen, and 17% oxygen. There was a lot of variability in his data and these proportions are only an average of some of the test results.

Martschuk, Chan and Slawinski (1985) obtained gas samples from the aquifer underlying the Athabasca oil sand at the Suncor mine site north of Fort McMurray. Their concern dealt primarily with lowering the pore pressure in the aquifer to prevent instability to the mine wall. The presence of gas became important not only from a safety perspective but also in determining the time required to lower the pore pressures as the presence of gas kept the pore pressures high and made pumping difficult. Several gas samples were taken which gave an average gas content of 61% methane, 30% nitrogen and 9% carbon dioxide.

In summary, efforts have been made by various people to obtain definitive gas compositions in Athabasca oil sands. Carbon dioxide, neopentane, carbon monoxide, methane and nitrogen were the most prominient gases found with smaller amounts of ethane present. The presence of oxygen was also noted in many samples but its quantity was not always reported. An increase in temperature increased the amounts and types of gases that were released by the oil sand.

2.2 SOLUBILITY OF GASES IN OIL SANDS

The volume of gas dissolved in the pore liquids at equilibrium will depend on the solubility of that individual gas within the pore liquids. At low pressures the volume of gas will obey Henry's Law (equation 2.1) which states that the weight fraction of gas dissolved in a liquid at equilibrium is proportional to the partial pressure of the gas (Hepler and Smith, 1975).

$$P_1 = K * X_1 \qquad 2.1$$

Often it is more convenient to measure the ratio of the volume of gas to the volume of pore liquid instead of the ratio of the masses. This can be done if the volume of the gas is measured at a constant temperature and pressure. Also, Henry's coefficient is not as familiar to geotechnical engineers as the solubility coefficient which is the inverse of Henry's coefficient. (This can be seen by observing that the solubility coeffiicient of air in water is approximately 0.02 (cm^3 of air/cm^3 of water)/atm and Henry's coeffiecient is approximately 50 atm/(cm^3 of air/cm^3 of water)). Rewriting equation 2.1 and using the solubility coefficient we get equation 2.2

$$X_1=\underline{H}*P_1 \qquad 2.2$$

To express the ratio of the volume of the dissolved gas to the volume of the liquid instead of the ratio of the mole fraction of the dissolved gas to the total liquid requires a relationship between the volume of the gas and liquid with their molecular value. If the amount of gas dissolved in the liquid is expressed as a gas from the ideal gas law then a solubility coefficient can be obtained in terms of the volume ratio rather than a mole ratio. By inserting this volume into equation 2.2 and defining H as the volumetric solubility coefficient it can be shown that

$$H = \underline{H}*V_L/((N_{TG} + N_{TL})) R*T \qquad 2.3$$

(Note that N is denoted as the number of moles instead of "n" as n is also used to define the porosity of the sample). This solubility coefficient can now be put into equation 2.2 and the mole fraction replaced with the volumetric fraction as shown in 2.2a.

$$Y_1=H*P_1 \tag{2.2a}$$

Although Henry's Law is technically a limit condition (it defines the slope of the curve as the pressure approaches zero) it is accurate enough at low concentrations of gas to be used to determine the amount of gas in solution at higher pressures. Work by Svrcek and Mehrotra (1982) show that gas saturation in bitumen is linear with gas pressure to at least 4 MPa for methane and carbon dioxide and to at least 2 MPa for nitrogen. Mehrotra and Svrcek (1982) also mixed these three gases in a ratio of 17% carbon dioxide, 1% methane and 82% nitrogen and the results provided a linear curve of solubility versus total gas pressure up to 2 MPa. Beyond these pressures the slope of the solubility curve deviates too much to be accurately measured by Henry's Law.

From the graphs given by Svrcek and Mehrotra (1982) values of the solubility coefficient can be obtained for each gas in bitumen. When the temperature of the bitumen increases, the amount of gas that can be dissolved in the bitumen is decreased and the solubility coefficient also decreases. Svrcek and Mehrotra (1982) also determined the solubility of gases in bitumen over a range of temperatures from 27°C to 100°C. The value of the solubility coefficients for nitrogen, methane and nitrogen over this temperature range is given in Table 2.1 and are shown in Figure 2.1.

It should be noted that the data from Svrcek and Mehrotra (1982) did have some scatter and variation and the curves drawn through those points did not always pass through the origin of their graphs. The values of the solubility coefficients are therefore not exact and should only be taken as a good first approximation. Lu et.al. (1986) have done additional work to correlate the solubility data and predict these solubilities theoretically but most of the data that was used was beyond the linear portion of the curve (where Henry's Law is not valid) and generally did not provide any improvement to the data already described.

In reality there is more than one gas present in the bitumen. For each of these gases there is an associated partial pressure required to keep the gas in solution. Dalton's Law (also known as the law of additive pressures) states that the total pressure of the mixture is equal to the sum of the partial pressures when the gases obey the ideal gas law. If there are several gases present and the ideal gas law and the ideal solution law applies, then the total pressure required to keep the gases in solution is the sum of the partial pressures of the gases as shown in equation 2.4.

$$P_T=P_1+P_2+\ldots \qquad 2.4$$

The ideal gas law applies for small concentrations of dissolved gases producing a pressure of not more than a few atmospheres. The law of ideal solutions was used as a first assumption to attempt to model the data from the test results and it will be shown in chapter 5 that the assumption produced results which were within the accuracy of the test data.

When the types of gases present are known and in what proportions they are present, the amount of dissolved gas in the oil sand can be determined from the solubility coefficients and the in situ pore pressure. To do this an expression must be derived from Henry's Law which will handle several gases in both water and bitumen. An expression is derived below which will handle several gases in one liquid and then combined with a second expression which puts the water and bitumen together and describes it as a single fluid.

With several gases dissolved at low concentrations in one fluid (assuming there is no interaction between the gases and the fluid), the total pressure required to maintain complete saturation is described by equation 2.4. If the ratio of the volume of gas (measured at atmospheric pressure) to the volume of the liquid is

$$V_{GT}/V_{LT}=V_{G1}/V_{LT}+V_{G2}/V_{LT}+\ldots=1.0 \qquad 2.5$$

then we can determine the total pressure required to maintain full saturation by rewriting equation 2.4 as shown in equation 2.6.

$$P_T=(V_{G1}/V_{LT})/H_1+(V_{G2}/V_{LT})/H_2+\ldots \qquad 2.6$$

Henry's law can now be rearranged to provide a combined solubility coefficient given the total gas volume, total liquid volume and total pressure as shown in equation 2.7.

$$H_C=(V_{GT}/V_{LT})/P_T \qquad 2.7$$

This combined solubility coefficient is valid only for several gases in one liquid. In oil sand there are two liquids (water and bitumen) and each gas will diffuse into both liquids. To determine the effect of both liquids the effect of one gas in water and bitumen is observed. The effect of one dissolved gas in two liquids will be calculated by combining the two liquids into one equivalent composite liquid which will hold as much dissolved gas as the combined water and bitumen.

When a gas is saturated in two immisible liquids the saturation pressure of the gas in both liquids is the same as show in equation 2.8.

$$P_1=(V_{GW}/V_W)/H_{GW}=(V_{GO}/V_O)/H_{GO} \qquad 2.8$$

For simplicity sake the volume of gas and liquids are set to unity as follows in equations 2.9 and 2.10 (the same volume units are assumed for both equations)

$$V_{GT}=V_{GW}+V_{GO}=1.0 \qquad 2.9$$

and

$$V_{LT}=V_W+V_O=1.0 \tag{2.10}$$

By combining equations 2.8 and 2.9 the volume of gas dissolved into water is obtained (equation 2.11).

$$V_{GW}=H_{GW}*V_W/ (H_{GO}*V_O+H_{GW}*V_W) \tag{2.11}$$

From this volume of gas dissolved in the water the saturation pressure required to keep one unit volume of gas saturated in the two liquids can be determined by combining equations 2.11 and 2.8.

$$P_1= 1/(H_{GO}*V_O+H_{GW}*V_W) \tag{2.12}$$

With this pressure and the total volume of gas and liquids described in equations 2.9 and 2.10, an average solubility coefficient can be obtained for the one gas in the composite liquid as shown in equation 2.13.

$$H_{AVE1}=(V_{GT}/V_{LT})/P_1 \tag{2.13}$$

In this manner the average solubility coefficient for each gas in water and bitumen can now be determined and the average solubility coefficients can be put into equation 2.6 and a combined solubility for several gases in bitumen and water can be obtained.

The combined solubility coefficients for various gases in bitumen can now be calculated from information obtained from the literature. Jha, Montgomery and Strausz (1977) measured the volume of gas in oil sand but the combined solubility coefficient could not be calculated because the volumes were very low and no pore pressure change was given with the results.

Srajer (1981) obtained volumes of gas from the testing done on the Gulf Surmont lease. The gas volumes that he obtained total 2.73 cm^3 of gas/kg of oilsand at 23°C. The samples were taken from a depth of 280-300 m below the ground surface and if the gas saturation pressure is assumed to equal the hydrostatic pressure and the insitu density is 2.1 g/cm^3, then the combined solubility coefficient is 0.0006(cm^3/cm^3)/101 kPa.

Robinson (1985) obtained gas volumes in his testing of oil sand core from Syncrude Canada and by analyzing his graphs a range of the combined solubility coefficient of 0.127-0.135 (cm^3/cm^3)/101 kPa is obtained.

Finally, Dusseault (1985) mentioned a test on Cold Lake oil sand core obtained with a pressurized core barrel which gave a combined solubility coefficient of 0.20 (cm^3/cm^3)/101 kPa.

Martschuk, Chan and Slawinski (1985) did their testing on the water in the aquifer underlying the oil sand. The combined solubility for their test data was calculated at between 0.064 (cm^3/cm^3)/101 kPa to 0.13 (cm^3/cm^3)/101 kPa.

This variation of the solubility coefficient and thus the volume of gas present within the oil sands is large and indicative of the problems associated with obtaining accurate gas measurements from oil sand bulk samples, cores, produced liquids or boreholes. None of the data obtained has given a consistent solubility coefficient as calculated by equation 2.6 and this is likely due to the loss of gas either in the sampling process, test preparation or testing of the sample.

2.3 DIFFUSIVITY OF GASES IN OIL SANDS

The diffusivity of gases was not specifically listed as an objective of this thesis in section 1.2 as it is not directly measured experimently nor is it directly used in analyzing any of the data. However, the diffusion coefficient is the gas property which directly affects the rate at which the gas will evolve from the pore liquids and any parameter which will affect the diffusion coefficient will alter the rate at which the gas will evolve. As a result, an understanding of the diffusion coefficient of gases is an important concept in the gas evolution process.

Work by others on the diffusivity of gases in oil and bitumen has been carried out to determine the amount of mass transfer that occurs due to diffusion and more recently with the rate of carbon dioxide diffusion into heavy oils and bitumen (dissolved carbon dioxide in bitumen reduces the viscosity and increases the mobility of the bitumen). The time required for this diffusion to occur is governed by Fick's second law (shown in Cartesian coordinates).

$$\partial C/\partial t=D*(\partial^2C/\partial x^2) \qquad 2.14$$

The actual diffusion process has been discussed by Verma (1977) and by Sobkowicz (1982) and will not be repeated here. However, information on the factors affecting the diffusion coefficient have been analyzed and will be reviewed here.

The work by McManamey and Woollen (1973) provided a relationship between the diffusion coefficient of carbon dioxide and the viscosity of the solvent (liquid). This range of viscosities is obtained from light liquids to medium oil with a viscosity of approximately 100 centipoise. The relationship is shown in Figure 2.2 and has been extrapolated to reach the viscosity of bitumen. The testing procedure measured the diffusion coefficient of carbon dioxide at atmospheric pressure.

Work by Schmidt, Leshchyshyn and Puttagunta (1982) on the diffusivity of carbon dioxide in Athabasca bitumen gives the only results in the literature on the diffusivity of gases in oil sands. Tests were carried out at 20°C and 200°C temperatures at a pressure of 4.8 MPa. There was some variability in the results but the two values given for the two temperatures are $0.286*10^{-5}$ cm^2/sec at 20°C and $3.46*10^{-5}$ cm^2/sec at 200°C. The viscosity of the Athabasca bitumen was not given with this data and to plot these points on Figure 2.2 the viscosity measurements used were obtained from Mehrotra and Svrcek (1982) (for the datum point measured at 20°C) and Robinson and Sim (1981) (for the datum point measured at 200°C) on carbon dioxide saturated Athabasca bitumen at 4.8 MPa.

It should be noted that the bitumen used by Schmidt was extracted from the oil sand, heated to 70°C to draw the bitumen into the sand sample and then left under a vacuum for one week to saturate the sample with bitumen and draw out all the air. With the bitumen subjected to a vacuum for one week the viscosity of the Athabasca bitumen may have been slightly altered by the loss of any volatiles.

Additional work by Schmidt has been reported by AOSTRA (1984) where the diffusion coefficient for carbon dioxide has been given for bitumen and water in a sand matrix. The diffusion coefficient obtained was $2.35 * 10^{-5}$ cm^2/sec but it was not plotted because the viscosity of the two phase liquid was not known.

Figure 2.3 (Huculak, 1985) shows viscosity testing on Athabasca bitumen from 20°C down to 6°C to determine the effect of temperature on bitumen viscosity when tested at atmospheric pressure. This figure confirms the conclusion that the bitumen viscosity rises dramatically as its temperature is lowered below 20°C. If the relationship shown in Figure 2.2 is accurate then the diffusion coefficient at 6°C should be lower and at -25°C (the temperature at which our samples were stored) should be almost negligible.

Denoyelle and Barden (1984) undertook to see how diffusivity was influenced by various pore media, pressure, and the presence of water with the oil. They reported that the inert porous media did not vary the diffusion coefficient over a range from no porous media to a fine sandstone. The effect of pressure was determined by collecting the available data on the diffusion coefficient of carbon dioxide in water over a range of pressures from atmospheric pressure to 10 MPa. Equation 2.15 was considered an acceptable fit to the data (the pressure is measured in atmospheres).

$$D=D_o * P \qquad 2.15$$

Denoyelle and Barden (1984) also determined the coefficient of diffusivity of carbon dioxide over a range of fluid viscosities at a pressure of 15 MPa. Their correlation is also plotted on Figure 2.2 along with the other data. Figure 2.2 shows that the diffusion coefficients for carbon dioxide in various fluids is fairly well understood. More work must be done to get specific values for bitumen to confirm the data given in this figure. The curves by McManamey and Woollen (1973) and Denoyelle and Barden (1984) provide the bounds for the diffusion coefficients of carbon dioxide in Athabasca bitumen at higher temperatures and lower viscosities. Specific tests on the diffusion coefficients of carbon dioxide in bitumen at higher viscosities are required to determine if the correlations can be extrapolated as shown in Figure 2.2.

Finally, Denoyelle and Barden checked the diffusion coefficient of carbon dioxide over a range of water and oil mixtures from pure water to pure oil for both light and heavy oil. The diffusion coefficient varied linearly (for both the light and heavy oil) between that of pure water and pure oil over the full range of water/oil mixtures.

Fu and Philips (1979) showed that the diffusivity of a gas within a fluid varied marginally with the shape and size of the gas molecule. The larger molecules and chain molecules tended to have a slightly larger diffusion coefficient than the smaller molecules.

In summary, the diffusion rate has been analyzed over a range of viscosities and a relationship between the viscosity and the diffusion coefficient is shown. This relationship shows that the diffusion coefficient is lowered as the viscosity of the solvent (liquid) increases. The presence of a varying sand matrix does not affect the diffusion coefficient,but the size and shape of the gas molecule does affect the diffusion coefficient.

The increase in viscosity of bitumen resulting from a drop in temperature to 6°C will decrease the diffusion coefficient and thus the rate at which the gas will evolve.

The use of lower temperatures is therefore an effective means to significantly slow the evolution of gas from the bitumen in oil sand masses or cores.

2.4 TIME DEPENDENCY OF GAS EVOLUTION FROM OIL SANDS

The work done by Sobkowicz (1982) dealt primarily with the time required for carbon dioxide to evolve from preformed samples with water as the pore fluid. In his testing the carbon dioxide saturated samples were monitored at very small time increments to determine the actual transient behaviour and then attempt to reproduce the data with a curve fitting equation.

Various types of curve fitting equations were tried and two equations were determined to most accurately reproduce the time dependent data from his results. Equation 2.16

$$\partial V_{fg}/\partial t=(V_2-V_{fg})/(t+A) \qquad 2.16$$

was the curve fitting equation which best fit his data. This equation has no theoretical basis and its value is only from its ability to model the data. Equation 2.17 was also used to fit a curve to the data.

$$\partial V_{fg}/\partial t=E*(V_2-V_{fg}) \qquad 2.17$$

However, this equation tended to overpredict the volume of gas evolved and predicted the rate of the gas evolution to be slightly faster than actually occurred. However, Sobkowicz felt that equation 2.17 more accurately represented the test data because the form of the equation is similar to the form of the actual diffusion equation it is modeling.

Also, as mentioned by Sobkowicz, the dissolved gas in the sample was able to diffuse through the membrane and this resulted in the measurment of lower gas volumes than actually existed for each of the test increments. It was felt that the loss of gas via diffusion through the membrane made equation 2.17 more accurate than equation 2.16 by increasing the volume of gas evolved as compared to the actual measured gas volumes.

This curve fitting equation (equation 2.17) was then incorporated into a general gas evolution equation which was able to give the transient pore pressure response which results from the gas evolution. This general model required information on the solubility data, compressibility of the sample, sample saturation and an E value from equation 2.17 to model the transient data that can be obtained at any pressure. The curve fitting equation will be used in Chapter 5 to analyze the data obtained from the tests done on tailing sand, lean oil sand and rich oil sand samples. The accuracy of equation 2.17 in modeling this data will also be reviewed in chapter 5.

Table 2.1 Solubility coefficients calculated from work done by Svrcek and Mehrotra, 1982

CARBON DIOXIDE		METHANE		NITROGEN	
Temperature (°C)	Solubility Coefficient of Carbon Dioxide in Bitumen (cm³/cm³)/ 101 kPa	Temperature (°C)	Solubility Coefficient of Methane in Bitumen (cm³/cm³)/ 101 kPa	Temperature (°C)	Solubility Coefficient of Nitrogen in Bitumen (cm³/cm³)/ 101 kPa
24	0.81	27.4	0.21	33.5	0.060
42	0.56	45	0.18	52.8	0.059
63	0.44	68	0.175	74.9	0.054
97	0.42	100	0.16	100.9	0.051 .

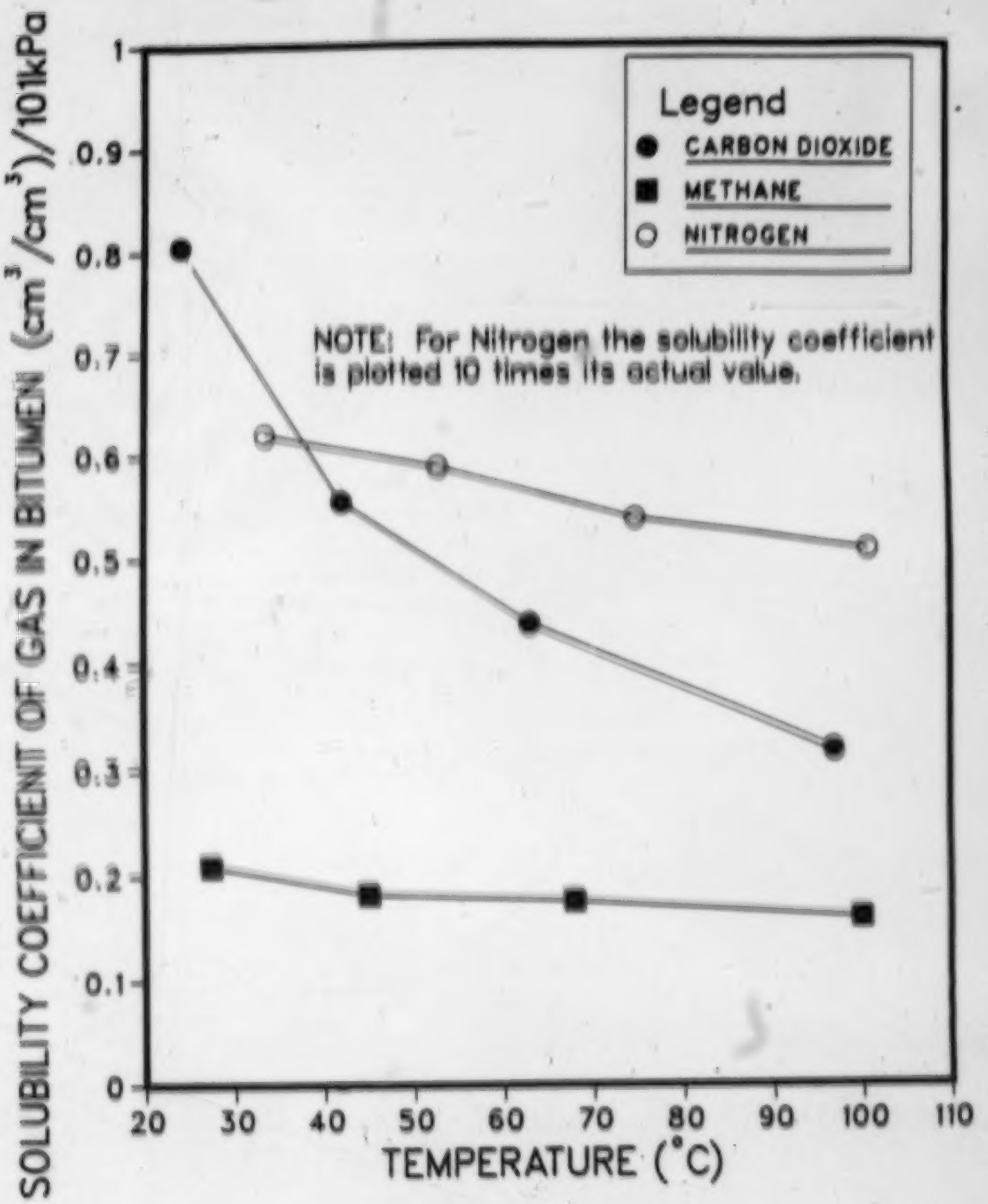

Figure 2.1 Solubility coefficients of carbon dioxide, nitrogen and methane in bitumen from Svercek and Mehrotra, 1982

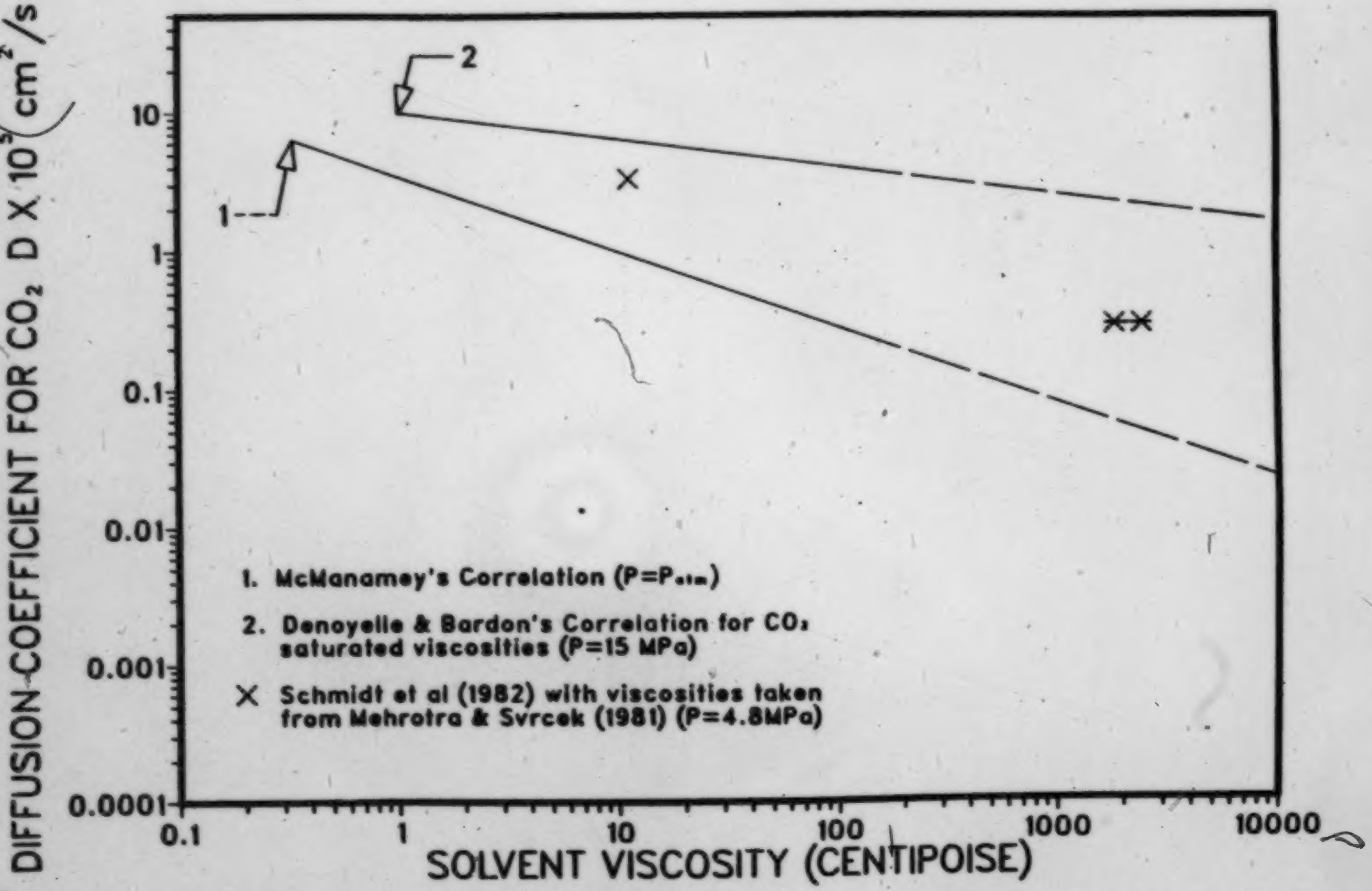

Figure 2.2 Relationship between the diffusion coefficient and the viscosity of the solvent

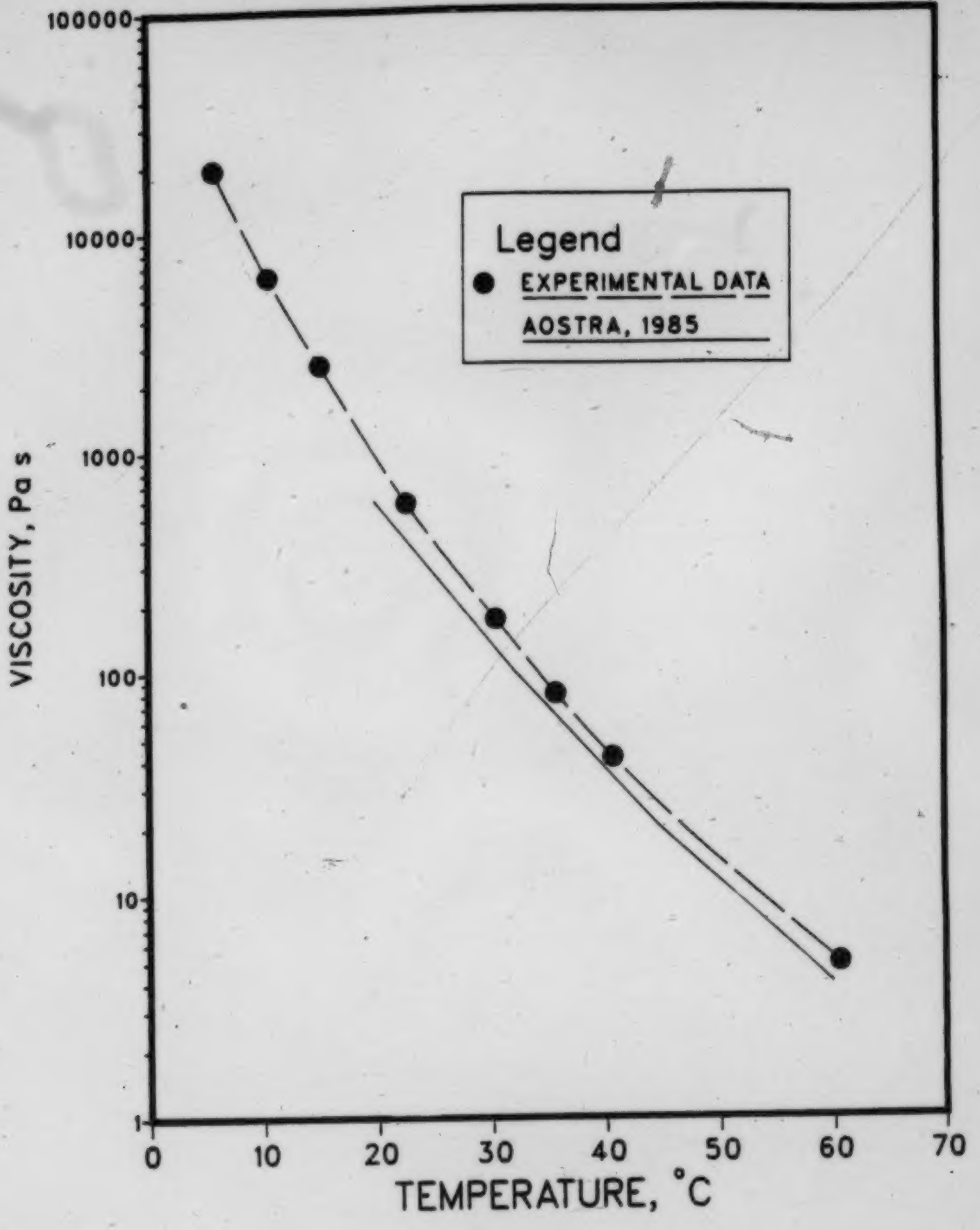

Figure 2.3 Effect of temperature on the viscosity of bitumen below 20°C --Huculak, 1985

3. LABORATORY APPARATUS AND PROCEDURES

3.1 TESTING APPARATUS

3.1.1 The Test Cell

The cell used in the experimental program is shown schematically in Figure 3.1. The oedometer is composed of a base, sample jacket, and piston. The sample jacket is held on the base by a top and bottom plate bolted together. The base of the oedometer has two ports for measuring pore pressure or to saturate the sample and an additional port to insert a thermocouple for measuring the temperature of the base of the sample. An O-ring is used as the seal between the base of the oedometer and the sample jacket.

The top plate rests on the sample jacket and is bolted down to the base plate. The pressure on the sample jacket compresses the O-ring in the oedometer base and this provides the sealed chamber for the sample.

The piston has two O-rings to reduce the friction along the sides of the sample and seal the chamber and an additional rider ring made from teflon to prevent the piston from jamming. There are three ports in the piston similar to the base with two drainage ports and one for a thermocouple.

A wire mesh (100 mesh grid) was installed at the top and bottom of the sample to prevent any air entry problems which might arise due to gas evolution.

3.1.2 The Pressurization System

An air pressure system was used to apply all loads and backpressure to the cell. The axial loading was performed through a diapham air cylinder to the piston of the oedometer. The air is forced into the cylinder against a diapham which in turn applies a force to the internal piston within the cylinder. This internal piston transfers the force to the oedometer piston either directly or through a concrete cylinder. The concrete cylinder was used whenever possible as it acts to reduce the loss of heat from the cell during the experiment.

The backpressure system was used for several different purposes and each of these will be discussed separately. When the oilsand was tested the backpressure system was required to saturate the oil sand sample in the oedometer at the onset of testing. In the tailing sand samples the water was first saturated with carbon dioxide in a bubble chamber. The chamber held over 2000 cm^3 of water and the gas pressure in maintained by a pressure relief valve at the top of the bubble chamber. The carbon dioxide gas from a pressurized bottle was bubbled into the bubble chamber from the bottom. This forced the carbon dioxide gas to bubble through all the water and fully saturate the water with gas at the pressure set by the pressure relief valve.

To force this fluid from the bubble chamber into the oedometer two independent pressure regulators and pressure transducers were required. One regulator forced the gas saturated water out of the bubble chamber into the oedometer against the backpressure of the second pressure regulator. The backpressure of the second regulator was kept higher than the saturation pressure to prevent premature gas evolution. The two pressure transducer procedure was used to moniter the pore pressure and prevent the pore pressures from falling below the gas saturation pressure. When the gas saturated water was in the oedometer the sample was saturated using one of the two pressure systems as the back pressure system. The equipment was originally designed by Sobkowicz (1982) and revised to meet any additional requirements for this work.

Due to the air pressure originating from the building's air compressor, there was some pressure flucuations which one regulator could not wholly remove. When two regulators were put in series, this problem was eliminated. The first regulator was set at the maximum required pressure and then the pressure was reduced to the desired value by the second regulator.

3.1.3 Displacement Measurements

The displacment measurements of the sample is one of the most important measurements of the test. Volumetric strains of 0.002%-0.004% were required to adequately observe the volume change of the sample during gas evolution. The difficulty in accurately measuring volumes this small was one reason the oedometer was selected as the test cell. With an oedometer the volume change of the sample is proportional to the change in vertical displacement of the piston. The use of a Linear Varying Displacement Transducer (LVDT) provided the required accuracy by measuring the vertical movement of the cell piston.

To obtain volumetric strains of 0.002%-0.004% there is a minimum volume of sample required to correspond to the minimum distance the LVDT will measure. With the LVDT used in the testing program (see Appendix A for details regarding the LVDT specifications) a minimum volume of 130 cm^3 was required. This translates into a height/diameter ratio of 0.37:1. This ratio will provide a sample which should not be dominated by frictional side effects. The oil sand samples were also wrapped with two to three layers of 0.025 cm thick teflon. The teflon reduced the the shear stresses between the sample and the cell wall and allowed the samples to freely expand vertically.

Initially the LVDT measured the relative displacment of the piston and the frame which held the cell apparatus. This proved inadequate because there is an asbestos plate between the cell and the frame which did not compress elastically. The asbestos was required to prevent the loss of heat through the base when higher or lower temperatures were used in the tests and as a result the apparatus was changed to have the LVDT measure the relative displacement between the piston and the cell. This reduced the measured equipment displacement values to negligible values as measured by testing an aluminium block over the range of loads used in the experimental program.

3.1.4 Temperature Measurement Apparatus

One of the objectives of this work was to observe the effect of varying temperatures on gas evolution. For temperatures below 24°C a constant temperature bath was used to lower the temperature of the sample. The glycol from the bath was circulated through a six millimeter copper tube which was wound around the sample jacket. The temperature of the bath could be kept constant down to -20°C which was well below the desired temperature of 4°C to 6°C.

To obtain accurate temperature measurement readings for the sample three type J thermocouples were used with one at the top and one at the bottom of the sample and the third in the sidewall of the oedometer jacket. These provided an accurate measurement of the temperature as described by Kosar(1983).

To measure temperatures higher than 24°C, a heater, a variable transformer and a digital temperature controller unit were used in conjunction with the thermocouples. The heater (described in Appendix A) surrounded the oedometer jacket and the oedometer base. This heated not only the sample but the piston above and the base below the sample to provide a uniform sample temperature.

The digital temperature controller unit regulated the heat provided to the sample through the heater. The interaction between the thermocouple in the sidewall of the oedometer jacket and the digital temperature controler unit were used to maintain a constant temperature to the sample.

The digital controler unit maintained the temperature of the sample within to 1-2°C. However this temperature variation produced a pore pressure change as high as 20-30 kPa in an undrained sample when subjected to a vertical effective stress. This change in pore pressure easily masked the pore pressure change due to gas evolution, and to reduce this effect a variable transformer was placed between the controller unit and the heater. The variable transformer could adjust the voltage going to the heater until the temperature of the sample (as measured by the thermocouples) remained at a constant value. This procedure provided accurate pore pressure measurements and a constant predetermined test temperatures within ± 0.1°C.

3.1.5 Data Acquisition

A Fluke Data Aquisition system was used to collect the data from the four pressure transducers, the three thermocouples and the LVDT. A description of the various measuring devices can be obtained from Appendix A.

3.1.6 Insulation

Two plates of asbestos were placed beneath the test cell to minimize the heat loss through the base. A shell of ceramic insulation was placed around the exterior and on the top of the test cell. The space between the oedometer and the shell was filled with loose ceramic insulation to minimize the heat loss through the sides and the top of the cell.

3.2 TESTING PROGRAM FOR TAILINGS SAND SAMPLES

3.2.1 Purpose of Testing Tailings Sand Samples

The previous testing done by Sobkowicz(1982) in determining the gas evolution process of carbon dioxide gas in water was done with Ottawa sand as the soil matrix and in a triaxial cell where all the stresses could be accurately controlled and measured. His testing showed that the process of gas evolution could be accurately monitored in a laboratory. Part of his work also indicated that problems with the membranes used to isolate the samples allowed the gas to evolve out of the sample chamber and into the surrounding water.

The oedometer was chosen for the test cell to eliminate the problem incurred with the membranes in the triaxial cell. The O-rings used to seal the oedometer chamber worked well in preventing the gas from diffusing out of the cell and enabled the testing to be carried on for days if necessary. An additional benefit of this particular oedometer was its ability to test samples at temperatures other than ambient temperatures. The oedometer could be heated up to 200°C and this provided an opportunity to determine the effect of temperature on the gas evolution process.

The tailing sand samples were tested in the oedometer to ensure that the results obtained by Sobkowicz from the triaxial cell could be effectively reproduced by the oedometer. The unloading undrained test devised by Sobkowicz (1982) was used in the oedometer and the transient volume and pore pressure results compared with those obtained from the triaxial tests. When the oedometer could successfully reproduce the results obtained from the triaxial test, then the results of testing oil sand samples with the oedometer could be considered accurate.

3.2.2 Preparation of Tailings Sand Samples

The quartz tailings sand was obtained from extraction tests done on Athabasca oil sand. The sand was sieved and all sand above the number 40 sieve and below the number 100 sieve was discarded. This was done to make the sand pack similar to the sand pack obtained from the Ottawa sand that was used by Sobkowicz (1982).

The tailings sand was placed into distilled water in the cell. The sand sample was vibrated under a 30 kPa load to increase the density of the sample. Distilled water was allowed to flow upward to flush out any remaining air trapped in the sample while the sample was being vibrated. After the water was allowed to flow upward through the sample for 10 minutes the piston was placed into the cell and the cell placing into the loading frame. The cell was then put under a backpressure to saturate the sample.

The gas saturated water was prepared in the bubble chamber as described in section 3.1.2. The gas saturated water was then flushed through the sample in three increments. About ten pore volumes were flushed through the sample with each increment with a two hour interval between each increment. This was done to allow the gas to diffuse to the connate water and provide a uniform concentration of solution gas throughout the pore liquid.

The differential pore pressure across the sample was small to maintain a slow fluid velocity and prevent bubble nucleation due to turbulence. Also, the gas saturated water was forced into the sample against a backpressure which was about 10 kPa higher than the gas saturation pressure. The pore pressure within the sample could not become lower than the gas saturation pressure and thus cause inadvertent gas evolution.

After the carbon dioxide was forced into the sample, the sample was left for several hours to allow the concentration of the solution gas to be evenly distributed throughout the whole sample before testing began.

3.2.3 Testing of Tailings Sand

In the testing that Sobkowicz (1982) performed on gas evolution in sand samples an unloading undrained test procedure was developed. The test involved reducing the total stress applied to the sample and measuring the volume change and pore pressure responses until undrained equilibrium was attained for the sample at that total stress increment (this procedure was called the unloading undrained equilibrium test by Sobkowicz).

A similar approach was used in these unloading undrained tests. The vertical load on the sample was unloaded incrementally under undrained conditions. For each unloading increment the pore pressure and the volume change of the sample was monitored with time until the pore pressure and the volume change approached equilibrium.

A total of eight unloading undrained tests were run on the tailing sand at this stage of the testing program. The first several tests were used to give an indication of the the effectiveness of the experimental procedure and to help in becoming familiar with the test equipment.

Three unloading undrained tests were carried out on these samples at 50°C to determine the effect of an elevated temperature on the rate of gas evolution. The samples were prepared in the same manner as the samples at room temperature and after the samples were saturated, the temperature of the sample and cell were increased to 50°C.

Finally one unloading undrained test was run at room temperature but special care was taken to ensure that the sample was run to equilibrium for each increment. The results from testing this sample were used to determine the solubility coefficient of the carbon dioxide saturated water.

3.3 SAMPLING PROCEDURES FOR OBTAINING OIL SAND SAMPLES

3.3.1 Previous Sampling Techniques

Most oil sands sampling has been done with a Christensen double tube core barrel with a PVC core liner. This sampler has provided samples which are long and generally quite continuous. This type of sampling produced valuable information of the geology of the site because it gave samples in long sections and the samples also gave accurate information of small stratigraphic changes in the oil sand.

During coring, the disturbance due to the cutting of the sample is small because the sample is cut smaller than the PVC core liner. The liner does not rotate and is smooth to provide a minimal amount of resistance to the sample as it enters the plastic tube. The sample is kept in the PVC liner by a core catcher as it is brought to the surface.

The extra space between the sample and the PVC liner creates a problem with this sampling technique. The gas evolution which occurs in a sample expands the sample radially to fill the space and this is enough disturbance to destroy the locked structure of the oil sand matrix. If the sample must come to the surface from quite a depth, the expansion is not only radial but also longitudinally along the plastic pipe. Logs from drillers will often show oil sands sample recovery ratios of over 100% indicating this longitudinal expansion.

Dusseault and Morgenstern (1977) attempted to prevent this expansion by circulating chilled diesel fuel in the borehole after the samples were cored but before the samples were brought to the surface. Upon arrival to the surface the samples were placed in dry ice and were kept frozen during storage and test sample preparation. The samples obtained in this manner were of much higher quality and some of the finer grained samples were of sufficient quality to test.

Dusseault and Scott(1985) describe the use of the Pitcher tube sampler in obtaining good quality samples of lean oilsand. The Pitcher tube sampler prevents the radial expansion that occurs with the triple tube samples and the mechanical restraint minimizes the longitudinal expansion until the sample can be frozen.

3.3.2 Sampling Program and Sample Storage

To obtain rich oil sand samples that have retained all of their solution gas the Pitcher tube sampler was chosen. There is too much gas lost by expansion from core taken with the triple tube sampler and it was hoped that the use of the Pitcher tube sampler would prevent this expansion and the associated gas loss.

The rich oil sand samples were obtained from Syncrude at the mine bench whose elevation was 291.5 m. At this location the original premining elevation was 17 m above the existing mining bench. The first 15 m below the bench consisted of lean oil sand and siltstones and below that level were two layers of rich oil sand separated by a layer of clay shale. The samples were obtained in the early spring when the temperature was around -20°C.

The depth below the mining bench chosen for sampling the rich oil sand was chosen from several criteria.

1. Previous sampling with the Pitcher Tube sampler in oil sand went to a depth of 14 m. The oil sand sampled at that time was lean, and quite dense and concerns still existed that the Pitcher Tube sampler could not obtain good quality samples at greater depths in richer oil sand where the pore pressures were higher.
2. There were two rich oil sand layers one at 15-29 m and the other at 34-42 m below the bench elevation of 291.5 m and below the original ground elevation of 308.5 m.
3. There were interbedded siltstone layers present in the rich oil sand and an attempt was made to avoid these because they tended to jam inside the tube and prevent the taking of quality samples.
4. The depths of sampling desired (over 35 m) was near the limit of previous sampling with the Pitcher Tube sampler at Syncrude in clay shale. This caused some concern as the oil sand of greatest interest was the lower layer of rich oil sand and the possibility of collecting a sample of any quality from this layer was unknown.

When the samples were brought to the surface the Shelby tubes were cut to the length of the oil sand sample, a metal plate was placed over the ends of the tube, the ends were capped and the tubes were placed in dry ice to quickly freeze the sample. The metal plate fitted flush over the ends of the tube to minimize the potential of contamination of the oil sand with the carbon dioxide from the sublimating dry ice.

Some expansion out the bottom of the tube was noted during sampling. When the samples were removed from the Shelby tubes and the densities determined, the majority of the expansion was due to movement near the end of the tube and only a small amount of the movement appears to have resulted from expansion of the overall sample within the tube.

The samples were frozen with dry ice on site and transported to the university packed in dry ice. The samples were then left in a freezer at the university at -25°C until they were to be tested. Throughout the storage time the samples were left in the capped tubes. A diagram of the borehole is shown in chapter 5 where the data from the testing program is discussed in conjuction with the location of the piezometers in the borehole and the pore pressures acting on the oil sand tested.

3.3.3 Preparation of Oil Sand Samples for Testing

To prepare the samples the first problem was in getting the samples out of the tube. Due to the cold temperatures the oil sand could not be pushed or extruded out of the tubes as the pressure required to force out the oil sand only buckled the tubes and heated the samples and causing them to expand. Various methods of cutting the metal tubes off the oil sand were tried with varying degrees of success. A bandsaw was used to cut the wall of the tube for the lean oil sand and worked with some success; any expansion due to the heating of the sample from cutting the sample was considered localized and acceptable. With the rich oil sand there were problems with too much expansion from this cutting method. Samples were then cut with a hacksaw and this proved to be much better as the samples could be kept cold and were never warmed up sufficiently to cause any volume change.

One tube was left uncapped after a sample was removed and after several hours the oil sand had pushed out the end of the tube. A picture of this tube can be seen in Figure 3.2. This expansion occurred at -25°C without a mechanical restraint on the end of the tube. The reason for this expansion will be discussed later but it was surprising considering the storage temperature.

The samples were 7.3 cm in diameter and the diameter of the testing chamber of the cell is 7.6 cm. To prevent the sample from being excessively disturbed in the test cell during loading by forcing the sample to expand to fit the diameter of the cell, teflon was put around the oil sand sample to increase its diameter. the thickness of the teflon was 0.025 cm and several wraps around the outside of the sample were required to increase the diameter of the sample to match that of the cell. The teflon also minimized frictional stresses developing between the wall of the cell and the sample as vertical volume change occurred due to gas evolution.

In setting up the cell for testing, the lines and the testing chamber were filled with distilled water. The frozen sample was placed into the water displacing some of the water within the cell and flushing air away from the sample. The piston was then put into the cell displacing the remaining excess water, the back pressure system was connected and the sample pressurized up to twice the anticipated gas saturation pressure.

3.3.4 Procedure for Obtaining Gas Samples

The oil sand samples used to obtain the gas samples were prepared in a different manner. The frozen oil sand sample was placed into the dry test chamber and the system alternately flushed with helium and placed under a vacuum. This was done for several minutes in an effort to remove as much of the air as possible from the cell and prevent any air contamination from influencing the results. The cell contents were placed under a vacuum one last time and the sample was allowed to thaw and the gases evolve. The sample was left for at several hours and then the gases were flushed with helium into an evacuated glass sampler. The gases from these oil sand samples were tested on a Hewlett Packard 5830A Gas Chromatograph to determine the types and percentages of gases present in the oil sand.

3.4 EVALUATION OF THE TESTING PROGRAM

3.4.1 Sampling Procedure

The purpose for using the pitcher tube sampler was described in section 3.3.2 with the main benefit being that the sample could be restrained in the horizontal direction and thus minimize the disturbance of the sand structure by the evolving gas. An indication of the amount of disturbance was defined by Dueassault and van Domselaar (1982) by using the disturbance index (equation 3.1).

$$I_D=(n_{sample}-n_{insitu})/n_{insitu} * 100 \qquad 5.1$$

The porosity of the samples tested and the material content are shown in Table 3.1. Also shown on this table is the disturbance index as described by Dusseault and van Domselaar (1982). According to them an undisturbed sample would have a disturbance index less than 10%, and as can be seen from Table 3.1, half of the samples tested were only slightly higher than this. Also, samples that were near the end of the Shelby tube tended to have a higher index of disturbance (samples RB-5-2 and RB-5-4) and this would be expected as there is insufficient frictional support to prevent the samples from expanding.

This disturbance of the samples is due to either:

1. The gas evolution within the sample after the sample is brought to the surface but before it was frozen.
2. The volume change from any existing gas in the sample as its pressure is reduced to atmospheric pressure when the sample is brought to the surface.

The oil sand samples were frozen in dry ice as soon they were brought to the surface. The exact time required to freeze the samples is not known, but most of the samples were placed in dry ice within 12 minutes from the time the sample was brought up to the surface. Under the assumption that the sample on dry ice is fully frozen within an hour the total amount of gas should be less than or equal to the amount of gas that evolved from a sample during the first hour of testing at in situ temperatures. Sample RB-5-12 (Figure 3.3) was tested at 6°C (in situ temperature) to determine the time rate of gas evolution at that temperature and the amount of gas that evolved in the first hour of this increment of the test was almost negligible. As a result the amount of gas evolving out of the sample as they were brought to the surface and frozen in dry ice is insignificant.

However, as previously noted, expansion of the samples occurred as they arrived at the surface and there are several possible explanations for this. If there is free gas present in the sample in situ, then the volume occupied by the gas will increase because the pressure is reduced on the sample as it is brought to the surface. When the oil sand samples were brought to the surface the samples could be seen "growing" out of the end of the Shelby tube. This expansion of the sample could be seen visually and only the quick capping and freezing of the samples prevented the sample from expanding more than they did.

Also, the presence of free gas in the samples is likely as the test samples all produced a gas saturation pressure greater than the measured pore pressures (this will be shown in the results in Chapter 5). The effect of the stripping of the overburden reduced the pore pressure and this effect could cause gas to evolve and be present in the oil sand in situ. The effect of the removal of overburden is discussed later in Chapter 5 where a correlation is made between the gas saturation pressure and the premining pore pressure.

Finally, Figure 3.2 shows an example of expansion which occurred in the cold room at -25°C when a Shelby tube was opened for several hours. This expansion indicates the gas bubbles were likely present and under considerable pressure. Despite the bitumen viscosity at -25°C the samples will expand if they are not mechanically restrained.

This expansion in the longitudinal direction appears to be limited to the ends of the tubes as the samples from the center of the tube had an acceptable density. Samples RB-5-1 and RB-5-2 were samples at the end of the Shelby tube and as the density was improving, all subsequent samples were taken from the middle of tubes RB-5 and RB-15.

In conclusion, the presence of gas in the samples is not due to the diffusion of solution gas into bubbles as the time required for the bubbles to form at the in situ temperature is greater than the time available. Instead, the free gas present in situ expanded due to a pressure change as the samples were brought to the surface. The gas bubbles in situ caused the core samples to expand longitudinally at the end of the tubes and the mechanical restraint prevented any lateral expansion. Frictional forces limited the longitudinal expansion to the end of the tubes and allowed very little expansion to occur in the middle of the Shelby tubes.

3.4.2 Sample Preparation and Testing Procedures

3.4.2.1 Sample Preparation

The purpose of the sample storage at -25°C as described in section 3.3.2. was to keep the gas dissolved in the bitumen and maintain the structural integrity of the sand. The cold temperature will decrease the diffusion rate of the gas in the bitumen and minimize the amount of gas diffusing from the sample. Any significant gas loss from this diffusion will be detected by variability in the test results over time. The results shown in Chapter 5 indicates that very little gas diffused out of the samples. The structural integrity of the sand structure will have to be tested in other work as there was insufficient time to determine this.

In preparing the samples the oil sand was kept at very cold temperatures (under dry ice) or expansion would occur and produce invalid results. Cooling the sample with dry ice produced a sample which was very rigid and did not allow the gas to evolve or the free gas to expand during the sample preparation phase. The only difficulty arose in maintaining the sample's low temperature as the sample was taken out of the Shelby tube and trimmed.

The use of a hacksaw to cut the Shelby tube and the sample kept the warming of the sample to a minimum. The sample could be cut very slowly and periodic breaks enabled the sample to be put back in dry ice where it could be recooled. Also, the sample could be prepared completely in the cold room at -25°C and this enabled the cutting to continue for a longer period of time than was possible outside the cold room. The use of this method to cut the samples produced a flat surface which required little or no milling of the sample for testing purposes.

3.4.2.2 Test Procedures

An important parameter in assuring the success of the testing program was the ability of the testing apparatus to keep all of the gas in the test chamber throughout the test. The undrained test on sample RB-5-12 was run at 6°C for over two months and as can be seen in Figure 3.3 the amount of gas present in the increment as measured by the volume change is quite constant by the end of the increment. There is some fluctuation in volume associated with the change in temperature of the sample and this masks any possible gas loss, but even with this variation it can be seen that there is little if any gas loss over the whole test period. The ability to test for such extended time periods permitted the testing of the oil sand at very low temperatures where the diffusion rate was very slow.

Volumetric changes due to thermal expansion was another problem that occurred in the testing the oil sand at temperatures other than room temperatures. In an undrained test the sample can experience volume changes due to thermal changes which can easily mask volume changes due to the pressure changes and gas evolution. Very accurate temperature measurements are required to prevent the thermal volume change and was best handled by a variable transformer. This procedure generated enough heat to match the heat loss of the system and minor fluctuations in temperature were easily handled.

The one drawback to this system was the necessity to manually adjust the variable transformer to adjust for minor temperature changes rather than electronically.

The effect of this volume change due to thermal changes is most dramatic at high effective stresses where small volume changes will dramatically change the vertical effective stress on the sample. This change in effective stress will be transferred to the pore pressure if there is a constant total stress. Without the variable transformer the fluctuations in temperature changed the volume of the sample enough that at high effective stresses the pore pressure would change 20-30 kPa. The use of a variable transformer and a constant temperature bath regulated the temperature of the sample to within ±0.1°C and the change in pore pressures to a similar magnitude.

At temperatures above room temperature the diffusion rate was rapid enough that the test could be finished in one day and careful monitoring of the thermcouples prevented temperature flucuations. At 6°C the diffusion rate was so slow that the test covered many days and the temperature in the laboratory would change several degrees throughout the course of the day. This temperature fluctuation produced pressure and volume changes in the sample as shown in Figure 3.3. The results can still be generally determined but the accuracy of the results is somewhat reduced.

The vertical pressure on the sample and the pore pressure were measured within ±0.5 kPa from the pressure transducers but the horizontal effective stress was an unknown quantity. The potential exists for arching to develop and the horizontal stresses to get locked in resulting in vertical stress/volume change curves which are inaccurate and difficult to reproduce. The presence of a potentially unsaturated sample makes the process even more difficult. The teflon tape wrapped in layers around the oilsand samples prevented the horizontal stresses from being locked into the cell and also allowed slippage in the vertical direction between the teflon layers during unloading. The teflon wrapped samples had pore pressure responses which were more consistent over a range of pressures while the sample was still saturated and under vertical effective stress (see Figure 4.26 and 4.35).

An important parameter associated with Sobkowicz's general gas exsolution model is the saturation of the sample. Small variations in the saturation of the sample (i.e. at the onset of nucleation) produced curve fitting problems of the actual transient pore pressure data. For the oedometer it is not possible to obtain the accuracy of the saturation level required to use this general model and this is due mainly to the inability of the oedometer to closely define the point of gas nucleation. In determining the E value from the general gas exsolution model a small variation in the amount of dissolved gas can cause significant fluctuations in the value and fit of the E parameter at low gas saturations. However, in determining the equilibrium gas properties this possibility of a small amount of undissolved gas is generally not significant.

3.4.2.3 Effect of Temperature

Various tailing sand and oil sand samples were tested at different temperatures to determine the effect of the temperature on the testing procedures. The tailing sand samples were tested at room temperature (24°C) and 50°C. The gas evolution at 50°C was so rapid that the sample reached equilibrium within a few minutes. This test at 50°C provided an effective test to obtain a procedure for testing at elevated temperatures. The use of a variable transformer to maintain a constant temperature was quite accurate and easily handled tests lasting one day.

The testing done on the lean oil sand and rich oil sand at temperatures of 6°C produced fluctuations in temperature and pressure. The equilibrium results are not affected by the fluctuating temperatures as the equilibrium data is taken when the temperature of the sample is at or near the initial temperature. The transient pore pressure data does vary (as shown by figure 3.3) and additional temperature monitoring equipment to obtain more accurate results. The oil sand samples were also tested at a range of temperatures up to 130°C to determine the gas saturation pressure. The saturation pressure at 130°C was 2700 kPa (see Figure 4.41) which is almost the limit for this test apparatus.

3.4.3 Unloading Undrained Tests on Oil Sand

These tests were performed similar to the unloading undrained tests done on the tailings sand samples. Each increment of the tests was run to equilibrium with the exception of the first few tests done on the lean oil sand. The time dependent behavior and the equilibrium conditions of the oil sand were determined from this set of unloading undrained tests.

The most critical measurements required from the unloading undrained test were the pore pressure measurement and the volumetric displacement measurement. The pressure transducers were accurate within ±0.5 kPa and problems with them were minor. The LVDT measured the vertical displacement (and thus the volumetric displacement) were accurate within 0.002% strain and few problems arose from this equipment.

3.4.4 Unloading Drained Tests on Oil Sands

In the unloading drained tests the pore pressure was reduced to atmospheric pressure for the saturated oil sand sample and the gas or liquid was allowed to drain out of the cell. The volume of gas or water was measured as they came out of the cell by displacing water in a plastic tube which lay horizontally at the same height as the cell. The displaced water was measured in a burette and the height of the water in the burette was kept at the same height as the top of the cell to prevent a pressure change. Mercury was placed into the horizontally laid plastic pipe to prevent the gases from dissolving into the water and giving erroneous volume readings.

The total volume due to gas evolution was the sum of the volume of gas and water measured by the burette and the volume change which occurred in the cell as measured by the LVDT.

3.4.5 Gas Saturation Curve

The gas saturation pressure for an oil sand sample at specific temperatures is an important equilibrium property to be determined. The temperature at which the sample is tested will affect the gas saturation pressure because the solubility of the gases in the pore liquids is temperature dependent.

To determine how much of an impact temperature has on the gas saturation pressure of the oil sand sample, an unloading undrained test was run on the sample until gas evolution started. The vertical load on the saturated oil sand sample was reduced incrementally and the pore pressure and volume change measurements were monitored. If unloading produced no gas evolution then the volume change was associated with a pore pressure drop. This volume change was the result of the compressibility change of the pore liquids and the sand matrix.

Unloading continued until the pore pressure was lowered just below the gas saturation pressure. The volume change continued but the pore pressure remained constant or slightly increased. After monitoring this for a few minutes the pore pressure was measured and considered to be the gas saturation pressure for that specific temperature.

The vertical load was reapplied to force the pore pressure up and resaturate the sample. The temperature was increased to the next temperature setting and the sample was allowed to come to thermal and volume change equilibrium. The sample was then incrementally unloaded to determine the gas saturation pressure at this temperature.

There was some concern that this test might produce a supersaturation of solution gas at the gas nucleation sites and that subsequent tests at different temperatures would give an inaccurate gas saturation pressure. To check for this the sample was initially tested twice at room temperature and once again at room temperature at the end of the test to make sure that the gas saturation pressure was consistent.

3.4.6 Measurement of Gases

The oedometer was not designed to accurately sample gases as the testing ports are small and the cell has many sharp corners. This arrangement makes it difficult to purge the cell of all the air as the air can get trapped in dead areas around the corners of the oedometer. Also, the small ports restrict the amount of helium that can be flushed through the testing chamber before the sample starts to thaw.

The procedure of alternating flushing with helium and placing the sample under a vacuum helped minimize the amount of air in the sample but it did not completely eliminate the problem.

Table 3.1 Summary of oil sand samples' densities, saturation and index of disturbance

Test No.	Initial Density gm/cm^3	Final Density gm/cm^3	Final Saturation %	Index of Disturbance %
B-222	2.11	1.93	73.7	8.8
B-223	2.08	*	*	10.1
B-224	2.08	1.97	82.3	13.3
B-225	2.10	2.04	89.2	10.3
B-226	2.07	1.98	86.9	11.7
RB-5-1	1.64	*	*	74.2
RB-5-2	1.73	*	*	55.3
RB-5-5	1.94	1.71	39.8	17.8
RB-5-6	1.81	*	*	39.8
RB-5-8	1.92	*	*	
RB-5-10	1.96	1.80	55.7	17.2
RB-5-12	1.96	1.85	64.6	17.0
RB-15-6	1.98	1.68	61.6	11.5
RB-15-8	1.95	1.82	62.9	14.4

* No final saturation
or density obtained

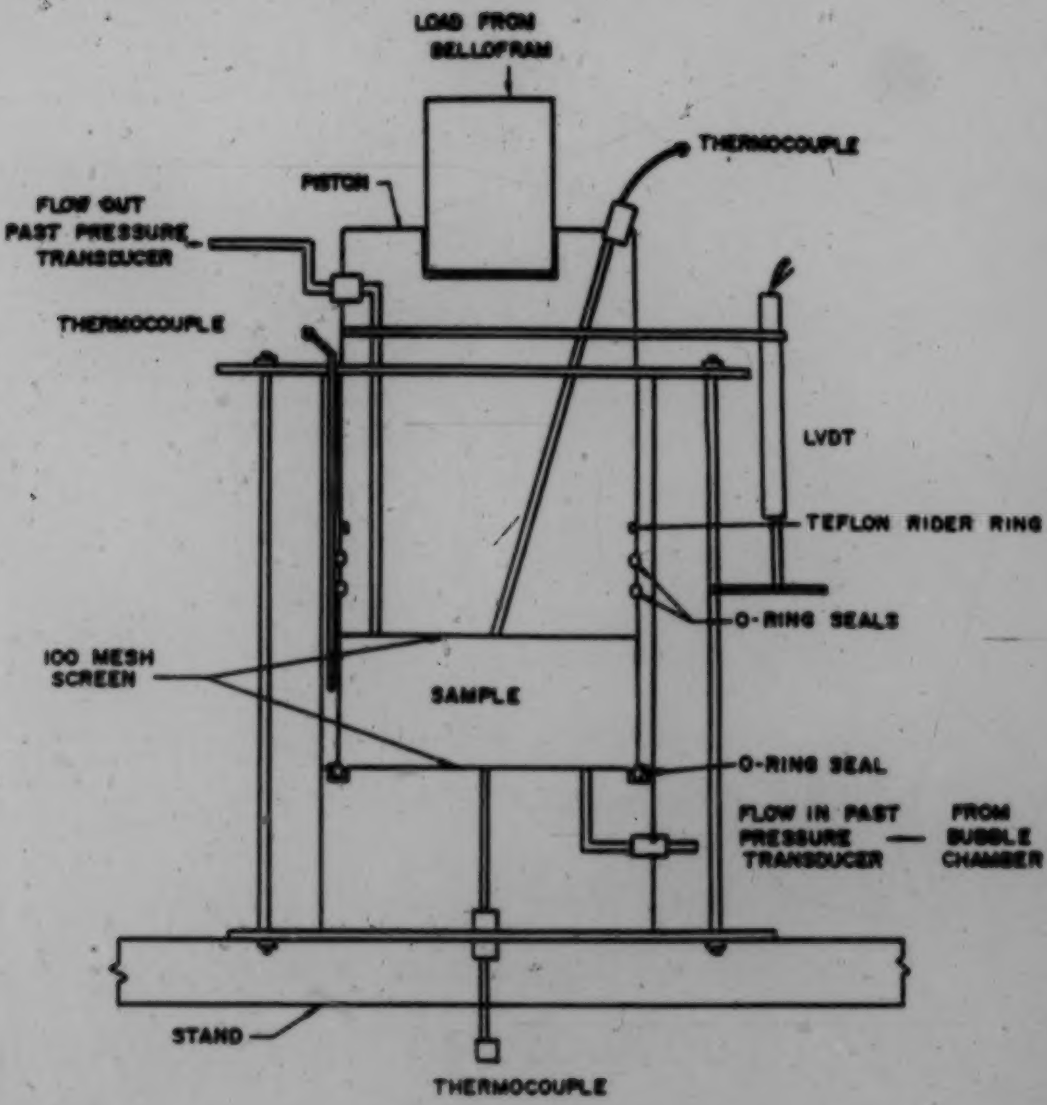
LOAD FROM BELLOFRAM
PISTON
THERMOCOUPLE
FLOW OUT PAST PRESSURE TRANSDUCER
THERMOCOUPLE
LVDT
TEFLON RIDER RING
O-RING SEALS
100 MESH SCREEN
SAMPLE
O-RING SEAL
FLOW IN PAST PRESSURE TRANSDUCER — FROM BUBBLE CHAMBER
STAND
THERMOCOUPLE

Figure 3.1 Schematic of test setup for testing tailing sand samples

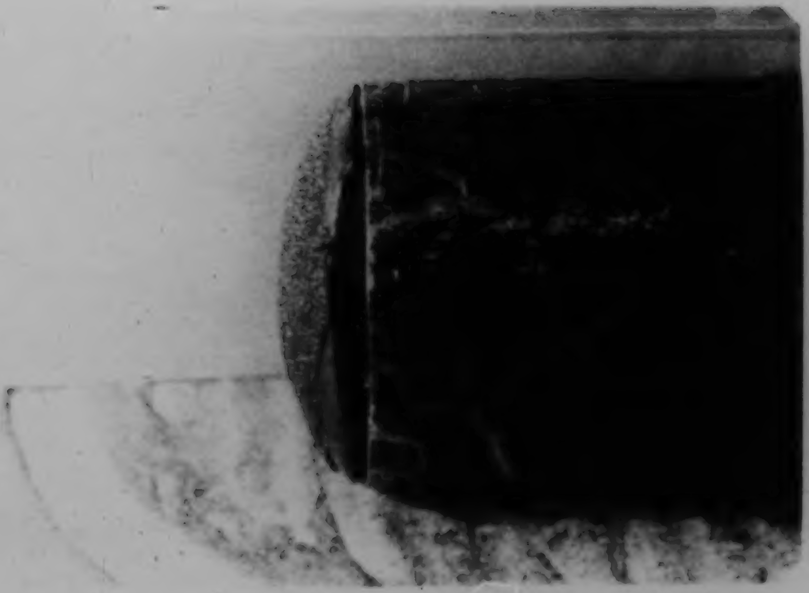

Figure 3.2 Picture of expanded rich oil sand due to expanding gas at -25°C

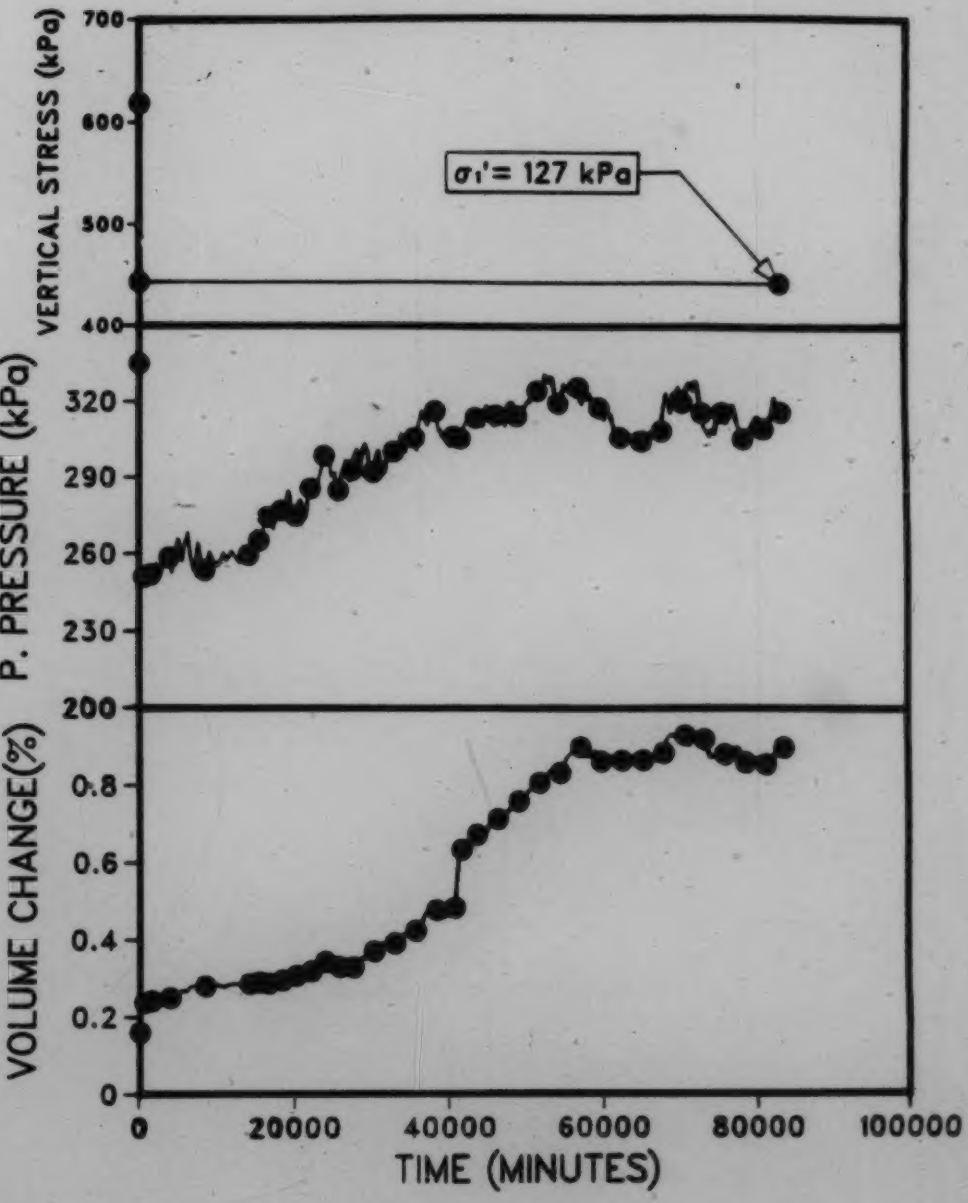

Figure 3.3 Increment D from unloading undrained test on RB-5-12 at 6°C

4. EXPERIMENTAL RESULTS

Chapter 4 will show the results of specific tests done on samples and representative figures from each test. This includes unloading undrained tests done on tailing sand samples, lean oil sand samples and rich oil sand samples. Other test results shown are from unloading drained tests from lean oil sand samples and rich oil sand samples, and gas samples from the lean and rich oil sand.

Several other unloading undrained tests were performed on tailing sand, lean oil sand and rich oil sand samples at a variety of temperatures. The test results will be mentioned, but the results will be shown in the appendices. Also, figures detailing the equilibrium properties will be shown and discussed in chapter 5.

4.1 TRANSIENT TEST RESULTS

4.1.1 Transient behaviour of Tailings Sand Samples

The testing program as described in section 3.2. resulted in a series of tests done on tailing sand samples, lean oil sand samples and rich oil sand samples. Table 4.1 lists the individual tests run on the tailing sand with with carbon dioxide saturated water as the pore liquid. Eight unloading undrained tests were carried out on tailing sand samples at 24°C to determine the rate of gas evolution, to verify the validity of the testing technique and to produce time dependent gas evolution results which could be compared with the results obtained by Sobkowicz (1982). Also, three unloading undrained tests were run at 50°C to determine the effect of elevated temperature on the rate at which the carbon dioxide evolved. One additional test (T-925) was run at 24°C to obtain the equilibrium volumes of evolved gas at various pressures to check our solubility coefficient.

The tailings sand used in these tests was sieved to provide a similar grain size distribution curve as was used by Sobkowicz (1982) in his testing program (Figure 4.1). The sand tended to be slightly finer than that of the sand used by Sobkowicz but the small variation should not have any significant effect on the diffusion rate of the carbon dioxide (Denoyelle and Bardon, 1984).

The purpose of testing the tailing sand samples was to show that the process of gas evolution could be measured accurately in an oedometer as well as in the triaxial cell as used by Sobkowicz (1982). A set of results from one test will be shown in this chapter as an example of the type of test results which were obtained at 24°C with the unloading undrained test on the tailing sand. An example of the test results at 50°C can be found in Appendix B. These two sets of data results are examples of the best results obtained in testing the tailing sand. The initial tests at both temperatures were used to monitor the effectiveness of the testing procedure and to make any minor changes where needed. The gas saturation pressure for the tailing sand samples at 24°C was set at 225 kPa. For sample T-525 the vertical stress at the beginning of the test was 525 kPa and the initial pore pressure was 240 kPa. Figures 4.2 to 4.8 show the the test data for each increment of unloading on sample T-525. Each figure contains the time dependent volume change and pore pressure change for an increment of the test. The stress strain curve for this sample and the undrained equilibrium curve are shown in Figures 4.9 and 4.10 respectively. The undrained equilibrium curve does not definitively show where the gas starts to evolve as it would do in the triaxial cell. This is due in part to the locking in of the horizontal stresses during the loading procedure and the poor pore pressure response that occurs in an oedometer from the total stress reduction.

The tailing sand was also tested at 50°C to determine the effect of temperature on gas evolution. The test procedure for these samples was the same as for the tailing sand samples at room temperature with care taken to ensure that the samples maintained a constant temperature of 50°C throughout the test. The amount of gas dissolved in the water was the same as for the tests at room temperature, but because the solubility of carbon dioxide in water decreases with temperature the saturation pressure is much higher at 770 kPa.

All data for each increment and the summary plots for test T-350 can be found in Appendix B. To show the rapidity at which the gas evolution occurred in the test at this temperature the test increment T-350H is shown in Figure

4.11. In this test the gas evolved so rapidly that the pressure and volume changes at the start of each increment were difficult to accurately read.

4.1.2 Transient Behaviour of Oil Sand Samples

The lean oil sand was much siltier than the sand used in the tailing sand samples; however the rich oil sand had a grain size which was quite similar to the tailing sand. The grain size analysis for both the lean oil sand and the rich oil sand is shown in Figure 4.12. A listing of the test program for the lean oil sand is shown in Table 4.2 and for the rich oil sand in Table 4.3. The majority of the testing dealt with the unloading undrained test procedure and the unloading drained test procedure which are described in section 3.3. The types of gases present in oil sand were obtained from the remainder of the test samples.

An unloading undrained test was performed on a lean oil sand sample to obtain the rate of gas evolution in lean oil sand. Figures 4.13 to 4.20 give the time dependent pore pressures and volume changes for each increment for this test on lean oil sand at 24°C. The stress strain curve and the unloading undrained equilibrium curve are also given in Figures 4.21 and 4.22. Increments 1 to 3 were not shown as the sample was above the saturation pressure and there was no time dependent behaviour exhibited.

In this test the sample was initially under a vertical stress of 480 kPa and the initial pore pressure was 195 kPa.

Similar tests were performed on lean oil sand at 6°C and 60°C and the data from these tests can be found in Appendix C.

An unloading undrained test was also done on rich oil sand at 24°C (sample RB-5-5). The test data for each unloading increment and the summary plots for sample RB-5-5 are shown in Figures 4.23 to 4.35. For this test the initial pore pressure was 650 kPa and the initial total vertical stress on the sample was 1370 kPa. Additional unloading undrained tests done on the rich oil sand can be found in Appendix D.

Unloading drained tests were also done on lean and rich oil sand samples. These tests were initially done to determine the effect of gas evolution under a constant vertical effective stress (equivilent to lowering the water table in the field and causing the gas to evolve) and to observe how gas evolution would occur. Also, it was hoped that the there would be an indication as to the time required for the gas to vent or drain from the sample and also the mode of drainage.

Three unloading drained tests were done on lean oil sand and one on a rich oil sand sample. The data obtained from the test on the lean oil sand are plotted in Figures 4.36 to 4.38 and tested under vertical loads of 8 kPa,120 kPa and 300 kPa. The data from the unloading undrained test on rich oil sand and a vertical load of 8 kPa is shown in Figure 4.39.

Table 4.4 lists the lean oil sand and rich oil sand samples and the weight percent of the bitumen, water and sand for each sample. This information will be used as the basis for determining the in-situ density of the samples and also for calculating the theoretical combined solubility coefficient from the gas samples.

4.2 EQUILIBRIUM TEST RESULTS

4.2.1 Gas Saturation Pressure

The presence of gases in the oil sand is described in section 3.4.6., but the amount of dissolved gas present is dependent upon the pore pressure which varies with depth. The gas saturation pressure (or the bubble point pressure) can be assumed to be equal to the in-situ pore pressure or it can be obtained experimentally by monitoring the volume change of the sample in an unloading undrained test. This correlation will be explored in chapter 5. The assumption that the gas saturation pressure is equal to the insitu pore pressure is a good approximation for oil sands but it can only be verified by the volume change measurements from the unloading undrained tests. The pore pressure in the lean oil sand was not measured with a piezometer but the level of the water table was measured in the borehole at 1.0 m below the surface. The lean oil sand samples tested were at a depth of 12.5 m and this would translate into a gas saturation pressure of 113 kPa. In the rich oil sand, there were two piezometers placed at the two levels of rich oil sand. The first piezometer was at a depth of 18.5 m below the bench level and the second was placed at a depth of 38.0 m below the bench. The first piezometer measured a pore pressure of 220 kPa and the second piezometer measured a pore pressure of 500 kPa.

These methods for determining the gas saturation pressure are obtained by analyzing the data obtained from various tests in various ways as shown in chapter 5. In addition, an unloading undrained test procedure described in section 3.4.5 was used to determine the gas saturation pressure for two lean oil sand samples and one rich oil sand sample over a range of temperatures. The data from these samples are combined in Figure 4.40 to give a saturation pressure versus temperature curve for the lean oil sand and the upper layer of the rich oil sand.

4.2.2 Gas Types

The gases obtained from the samples were measured on a gas chromatograph and the percentages of gases that were obtained from the various samples are shown in Table 4.5. Also listed on the table are the percentages of gases that exist when all the oxygen and some of the nitrogen in the ratio of the air is removed. The reason for the removal of the oxygen and the nitrogen from the sample will be discussed in section 5.3.2.3.

Most of the samples were tested at 24°C with the second lean oil sand sample being tested at 40°C. This second sample produced more methane than the samples tested at room temperature as shown in Table 4.5.

Table 4.1 List of testing done on tailing sand samples

Test No.	Description of Test Procedure
T-125--T-825 (8 tests)	Unloading Undrained test on Tailing Sand at 24°C. 6 samples were tested at 225 kPa and the remaining 2 tests at 550 kPa
T-925	Unloading Undrained test at 24°C with each increment measured on at equilibrium
T-150--T-350 (3 tests)	Unloading undrained tests on Tailing Sand at 50°C. The saturation pressure was 525 kPa

Table 4.2 List of testing done on lean oil sand samples

Test No.	Description of Test Procedure
B-222	Testing to determine the Gas Saturation Pressure at various Temperatures
B-223	Unloading Undrained test at 60°C, resaturated, and then an Unloading Drained test under a vertical load of 300 kPa at 24°C
B-224	Unloading Undrained test at 24°C
B-225	Unloading Undrained test at 6°C
B-225A	Unloading Drained test at 24°C under a vertical load of 120 kPa
B-226	Gas Saturation pressure determined at various temperatures and then an Unloading Drained test at 24°C
B-227	Gas sample taken
B-228	Gas sample taken

Table 4.3 List of testing done on rich oil sand samples

Test No.	Description of Test Procedure
RB-5-1	Gas Saturation pressure obtained at various temperatures and then an Unloading Drained test at 24°C and no vertical load
RB-5-2	Unloading undrained test on rich oil sand at 24°C
RB-5-5	Unloading undrained test on rich oil sand at 24°C
RB-5-10	Unloading undrained test on rich oil sand at 24°C
RB-5-12	Unloading undrained test on rich oil sand at 6°C
RB-15-8	Unloading undrained test on rich oil sand at 24°C
RB-5-4	Gas sample taken
RB-5-6	Gas sample taken
RB-5-7	Gas sample taken
RB-5-9	Gas sample taken
RB-15-1	Gas sample taken
RB-15-2	Gas sample taken

Table 4.4 Bitumen, water and sand content of oil sand samples

Sample No.	Bitumen Content wt.%	Water Content wt.%	Sand Content wt.%
B-221	4.4	9.0	86.6
B-224	2.1	11.9	86.0
B-226	2.6	10.4	87.0
RB-5-1	15.0	2.1	82.9
RB-5-5	17.6	5.1	77.4
RB-5-6	14.9	0.5	84.6
RB-5-8	15.2	1.4	83.4
RB-5-9	16.4	1.1	82.5
RB-51-1	14.9	1.6	83.5
RB-15-1	16.7	1.0	82.3
RB-15-2	17.0	1.4	81.6
RB-15-5	16.8	1.0	82.2

Table 4.5 Percentages of gases found in oil sand samples

Gas Sample No.	Sample Depth (m)	Gases Measured on Gas Chromatograph (%)				Gas Remaining with O_2 and some N_2 (%)			Temp °C
		O_2	N_2	CH_4	CO_2	N_2	CH_4	CO_2	
Air		21.3	78.7						24
B-227	12.8	12.6	47.2	30.7	9.1	1.6	75.9	22.5	24
B-228	12.8	7.1	28.4	60.4	9.2	1.6	92.1	6.30	40
RB-5-4	18.9	6.2	26.9	53.4	13.5	3.9	76.7	19.4	24
RB-5-7	18.9	13.0	54.5	28.4	4.0	16.6	73.1	10.3	30
RB-5-8	18.9	3.2	16.3	64.7	15.8	4.5	76.8	18.7	24
RB-15-1	39.6	3.7	16.0	66.5	13.8	2.2	81.4	16.4	24
RB-15-2	39.6	6.5	27.6	63.3	2.6	3.3	92.9	3.80	24

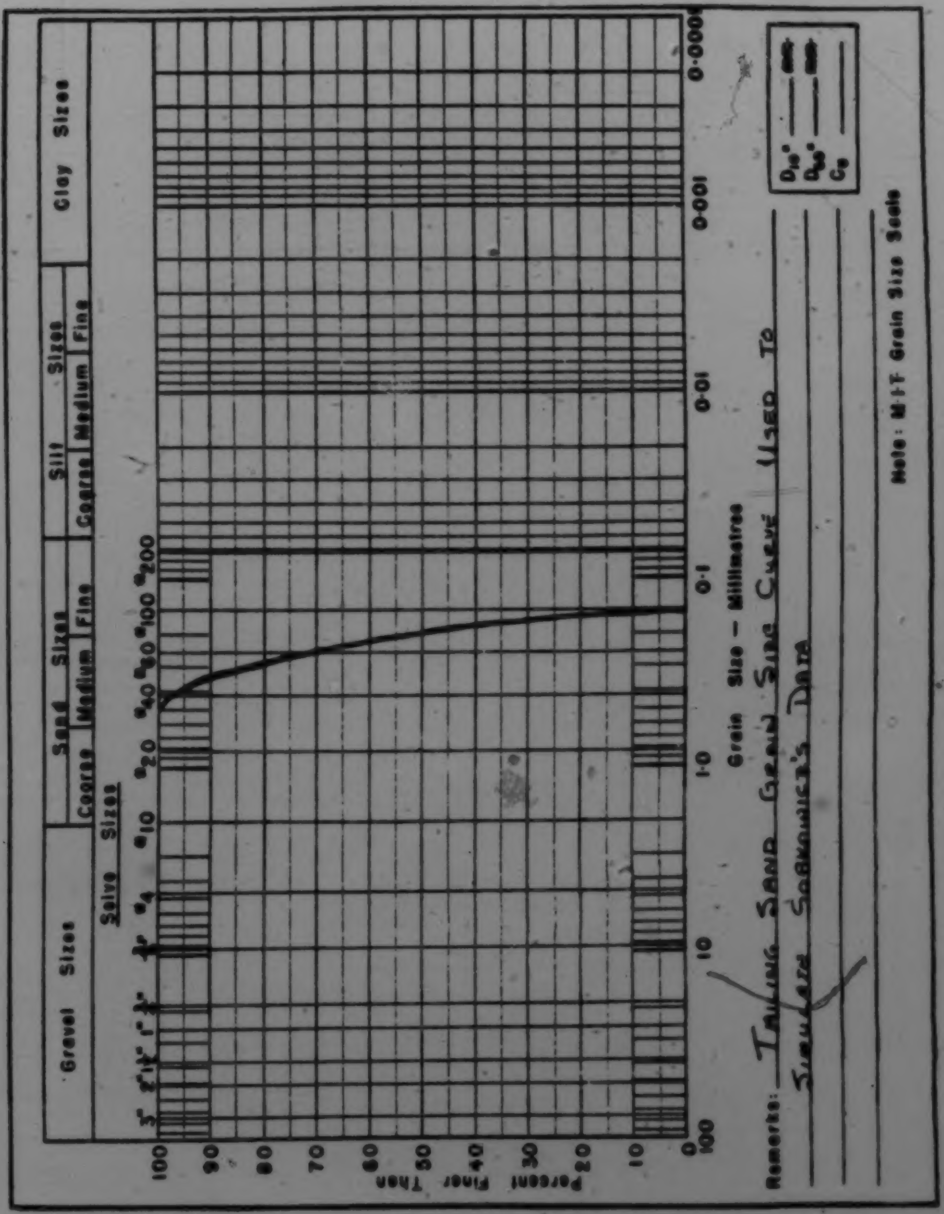

Figure 4.1 Grain size curve for tailing sand samples

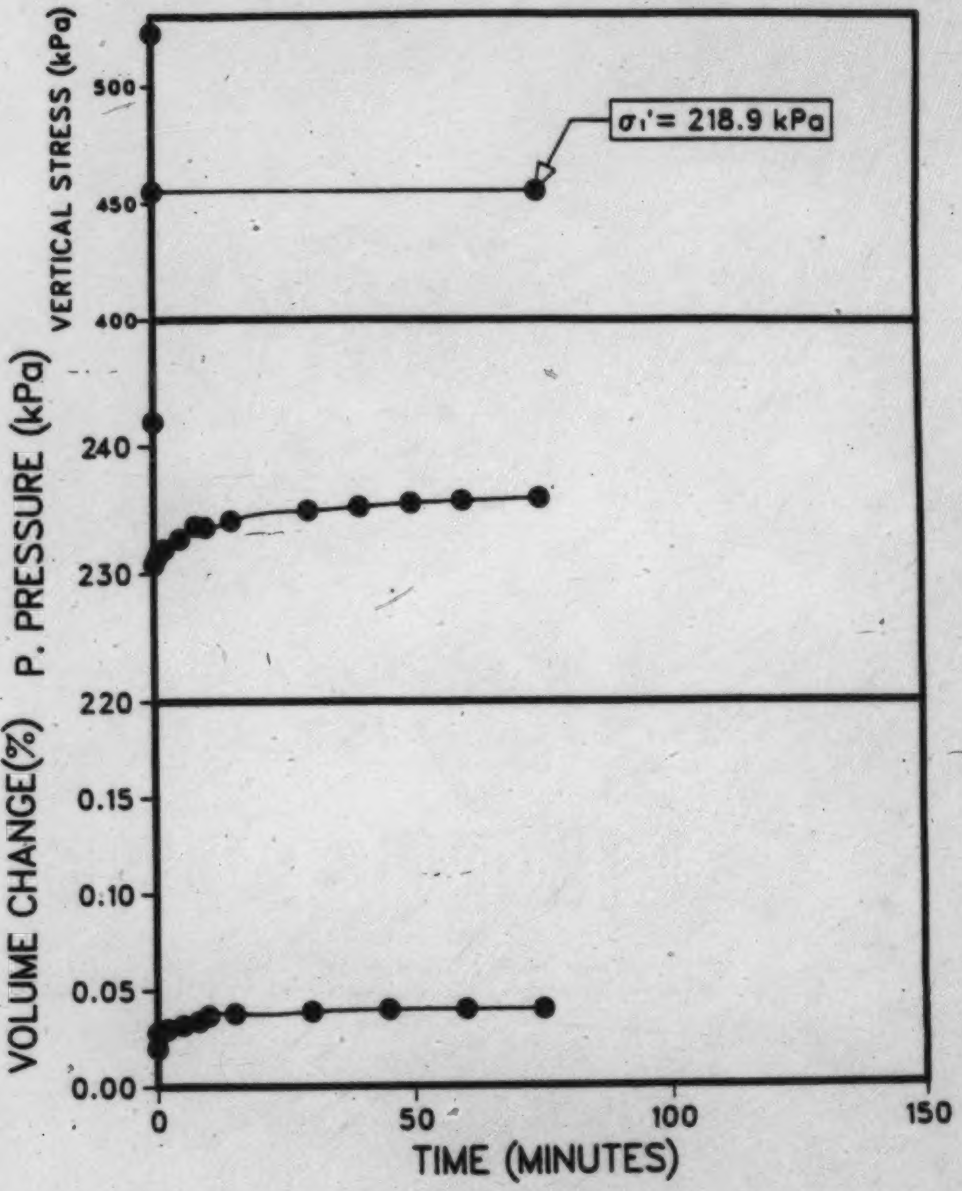

Figure 4.2 Increment B from unloading undrained test on tailing sand sample T-525

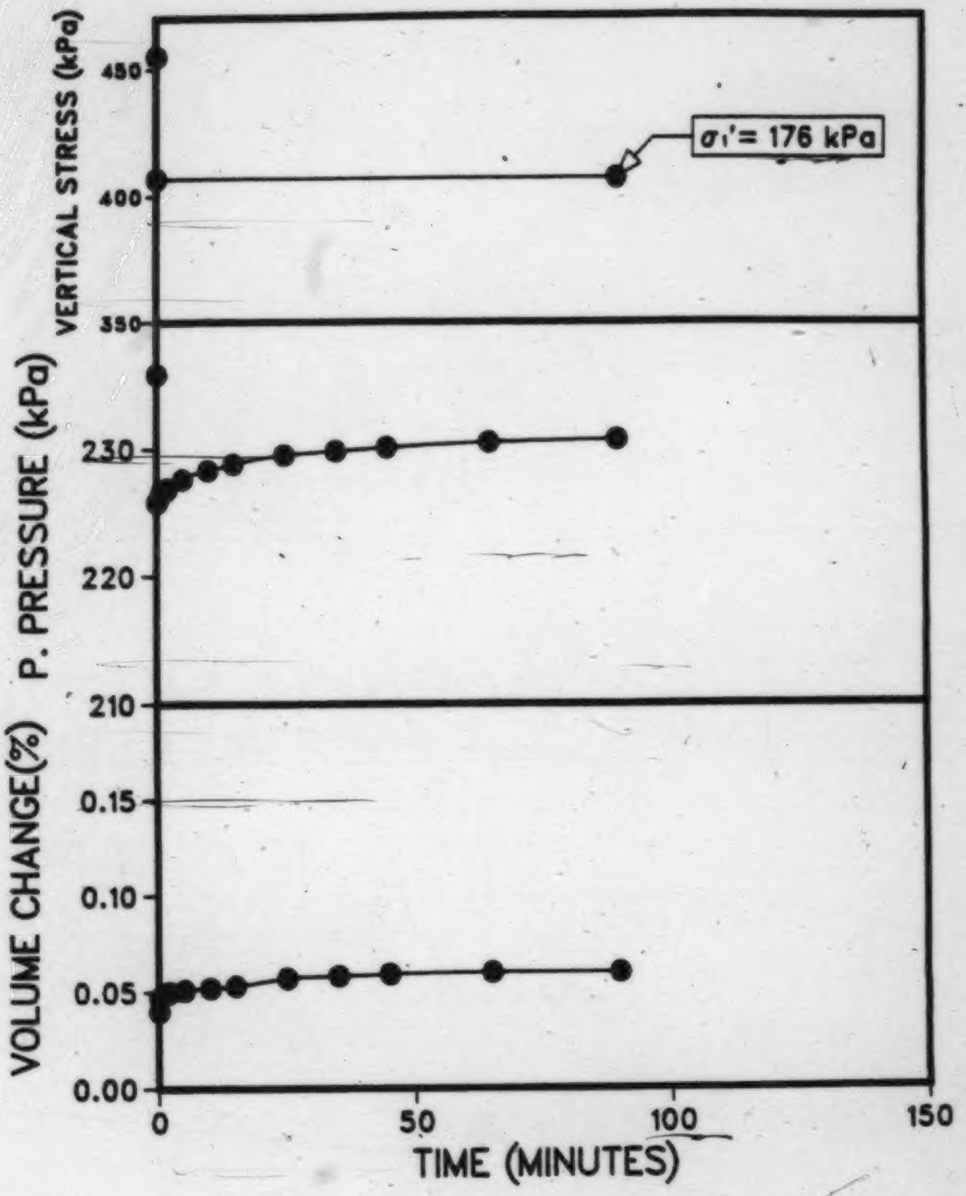

Figure 4.3 Increment C from unloading undrained test on tailing sand sample T-525

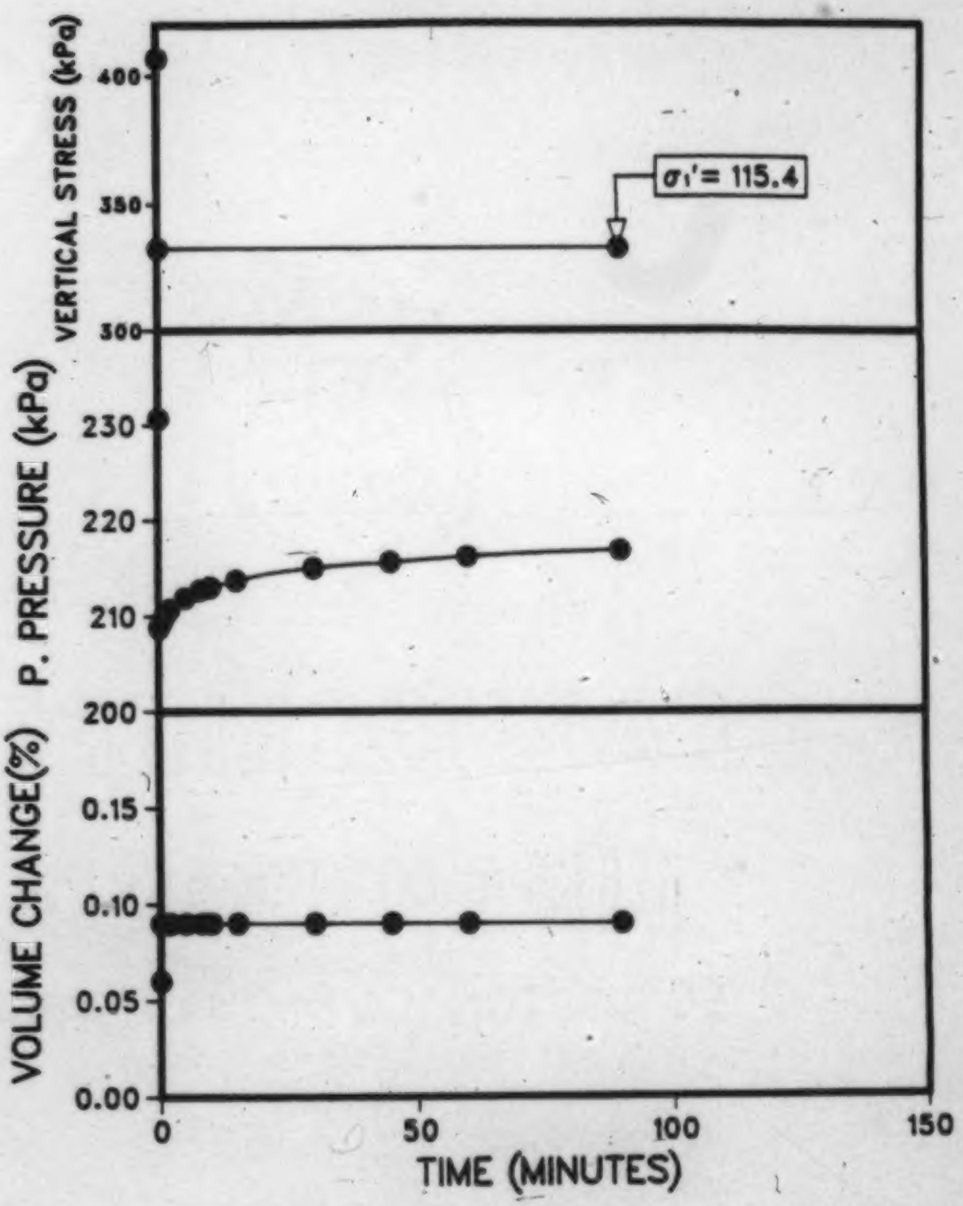

Figure 4.4 Increment D from unloading undrained test on tailing sand sample T-525

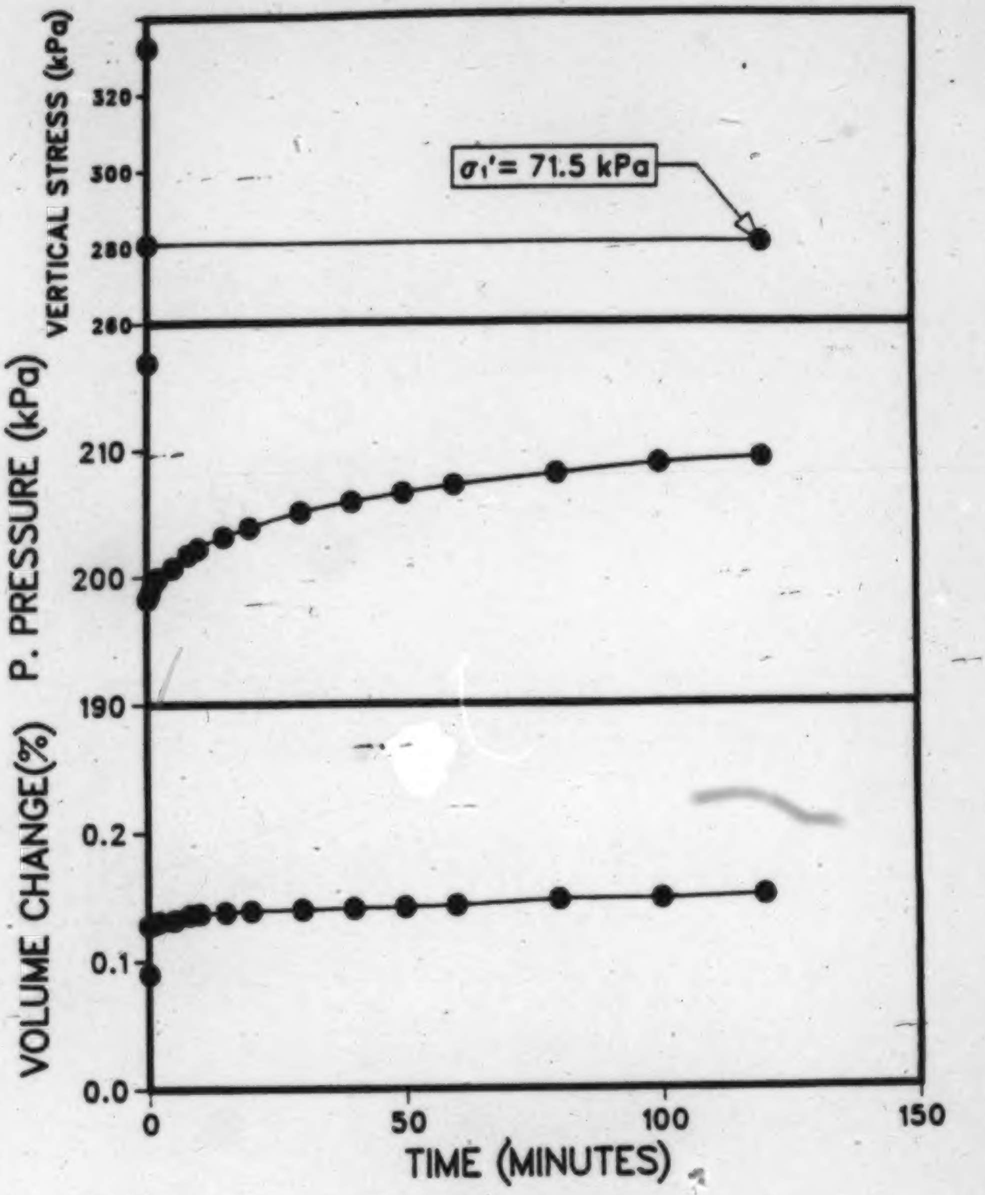

Figure 4.5 Increment E from unloading undrained test on tailing sand sample T-525

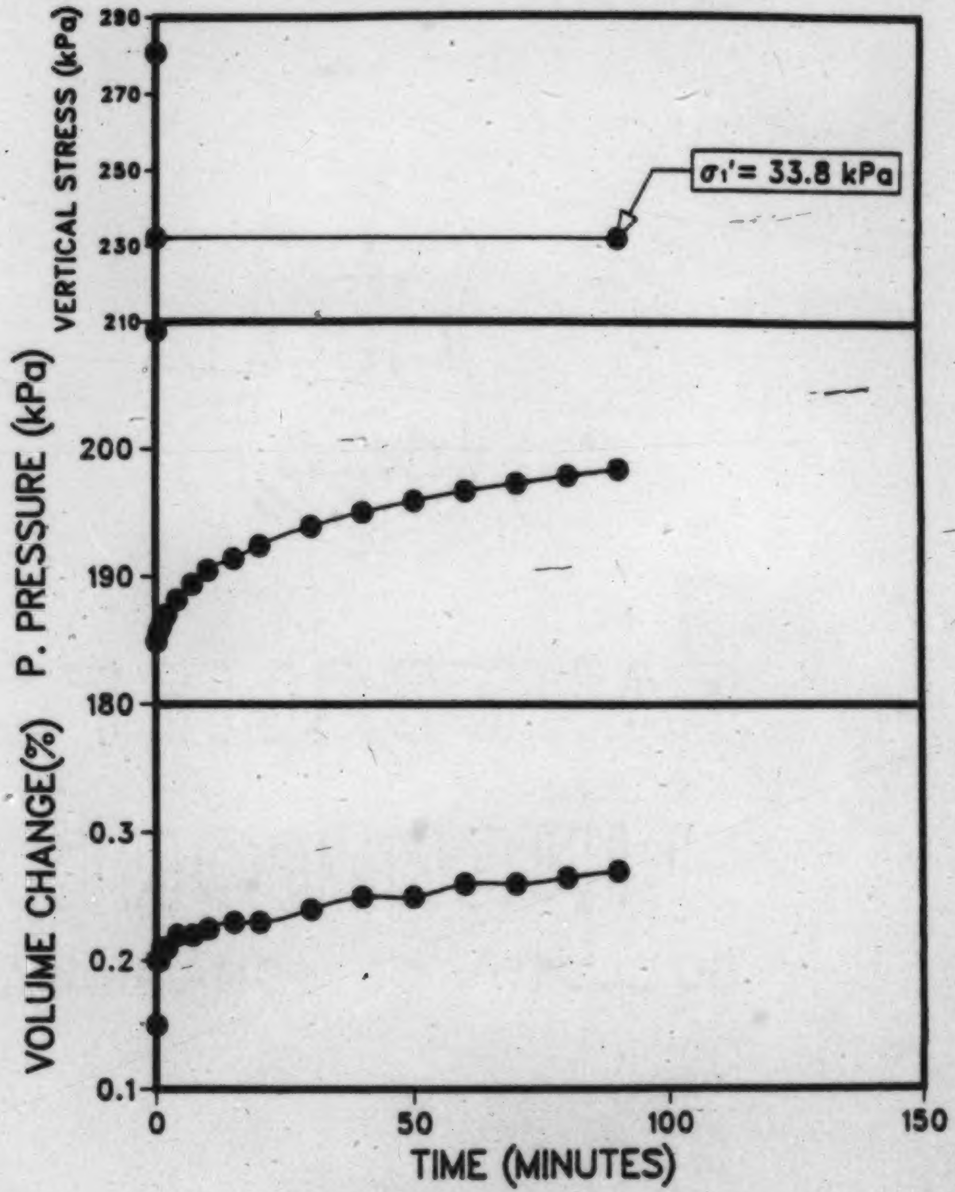

Figure 4.6 Increment F from unloading undrained test on tailing sand sample T-525

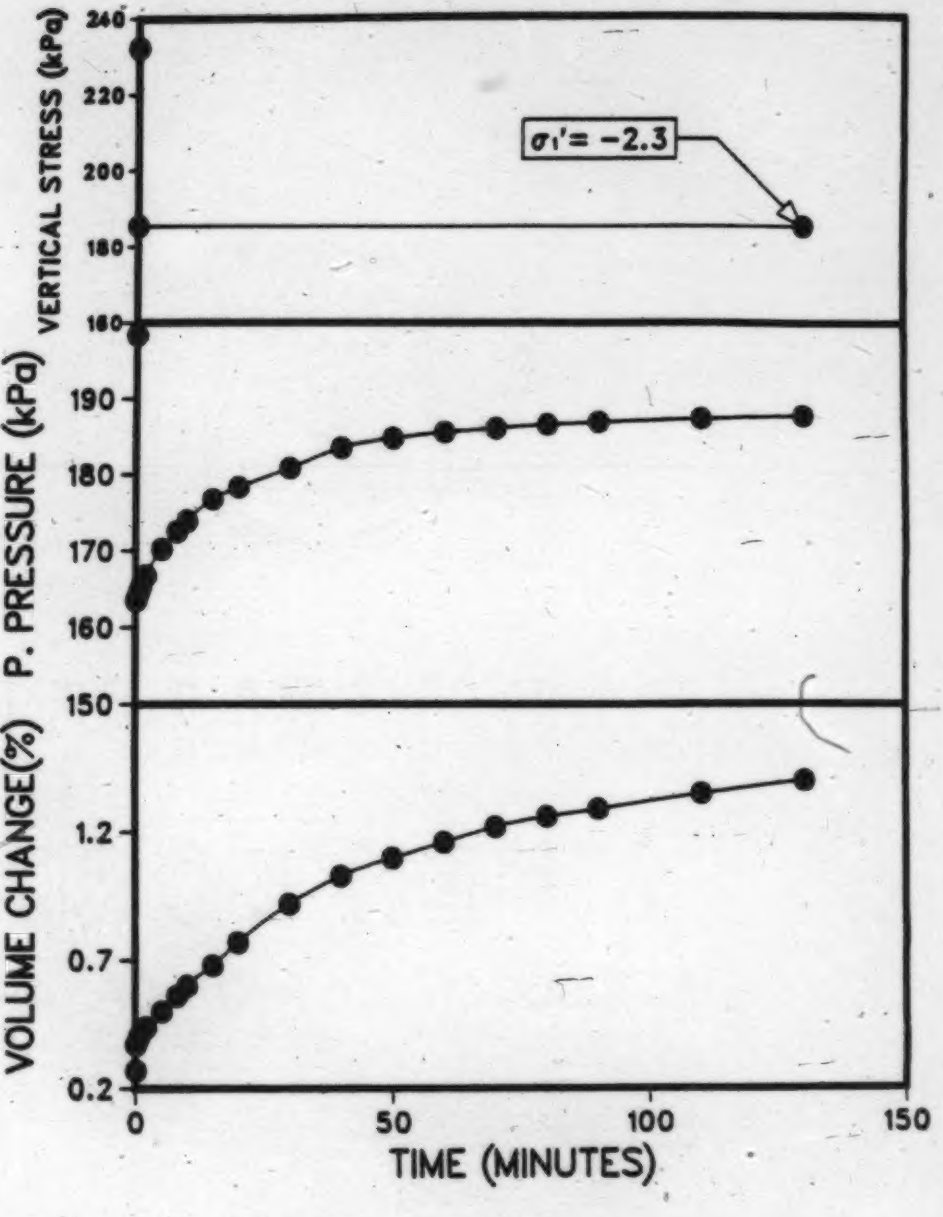

Figure 4.7 Increment G from unloading undrained test on tailing sand sample T-525

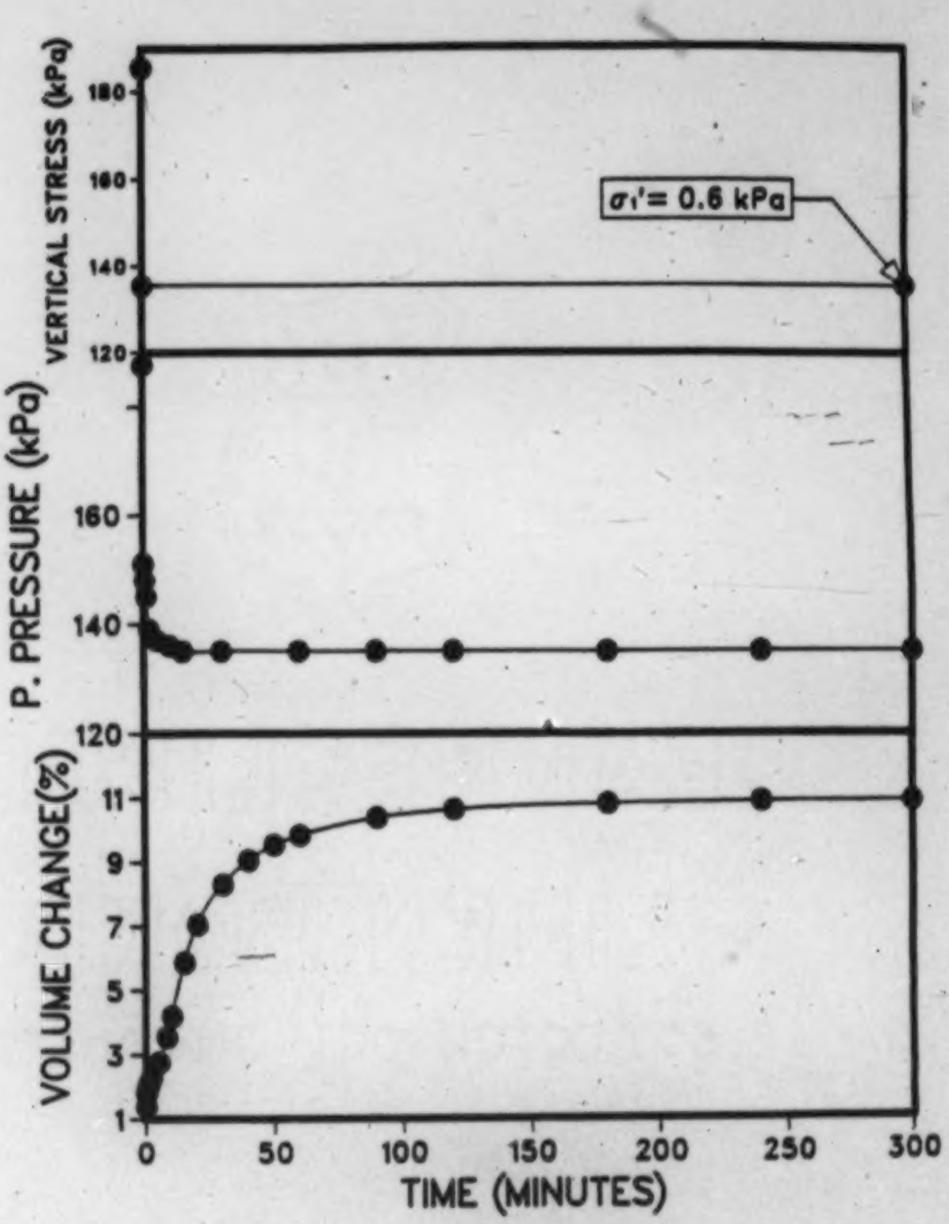

Figure 4.8 Increment H from unloading undrained test on tailing sand sample T-525

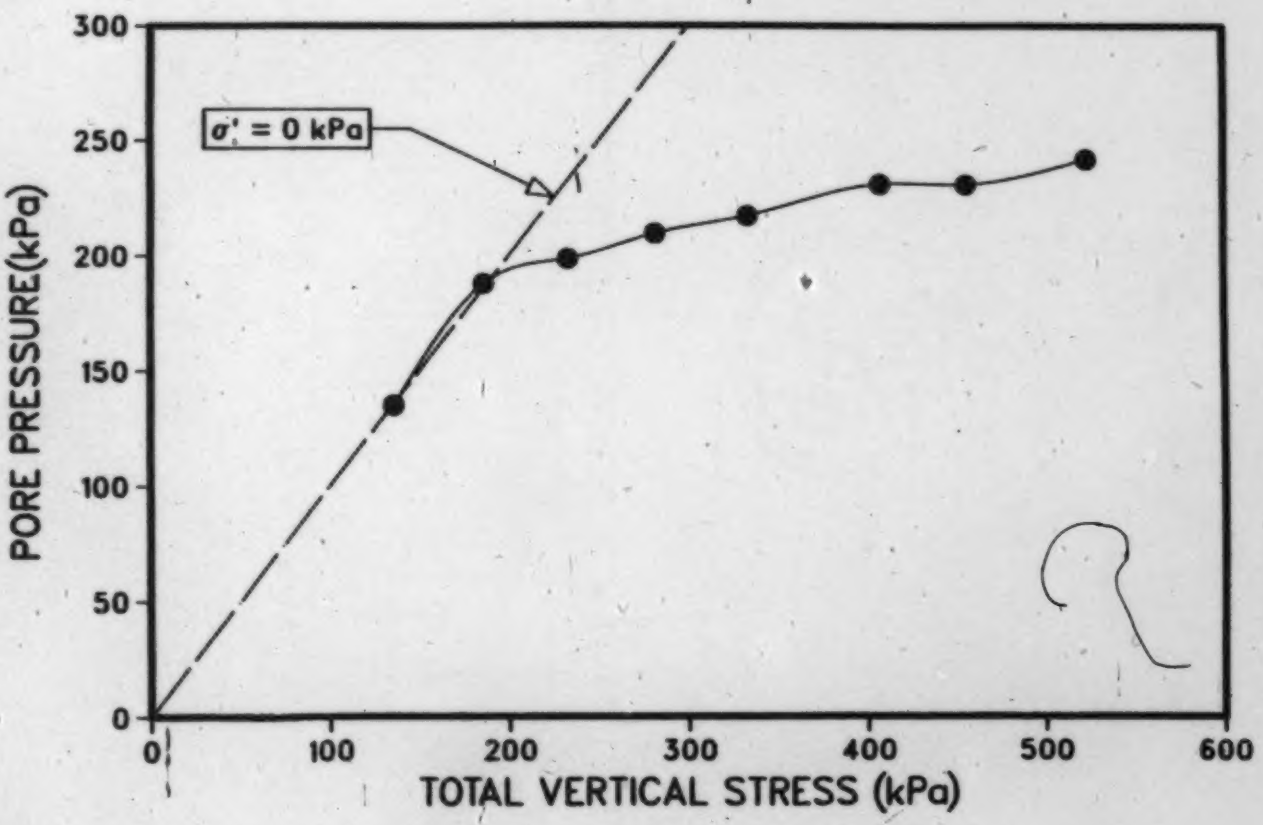

Figure 4.9 Undrained equilibrium curve for tailing sand sample T-525

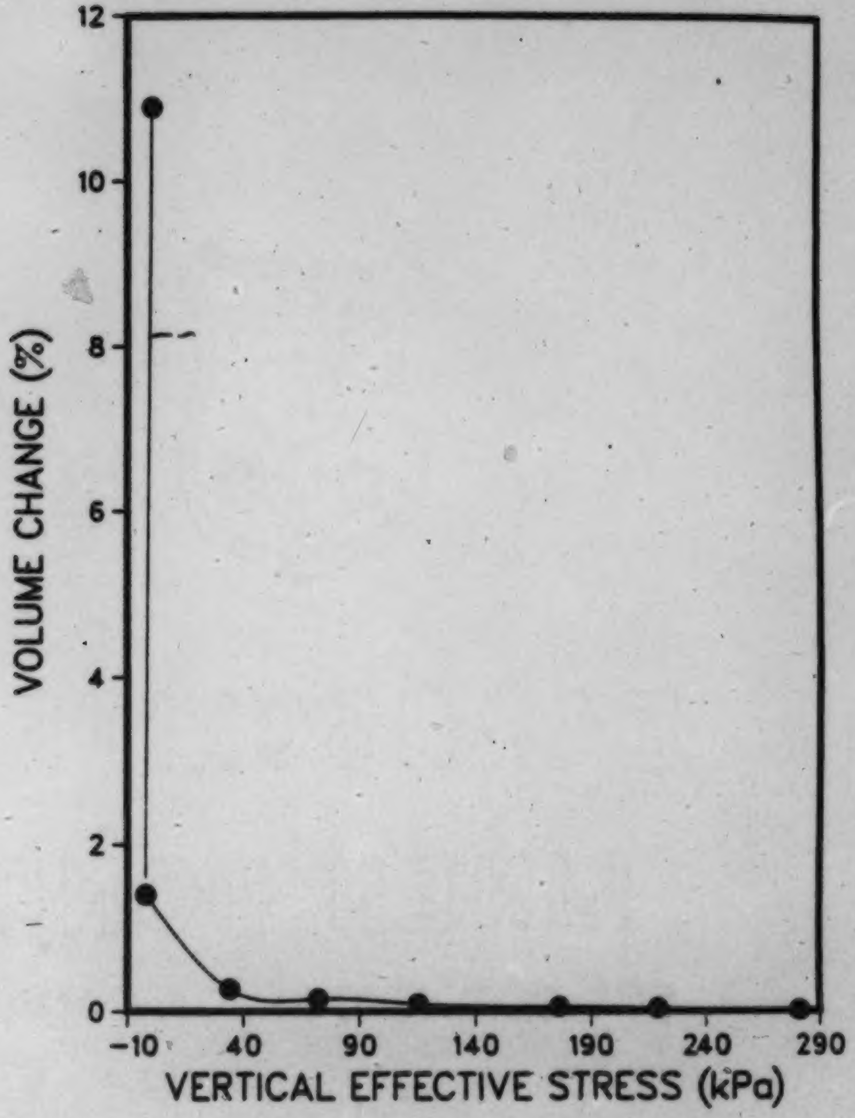

Figure 4.10 Stress vs. strain cuve for tailing sand sample T-525

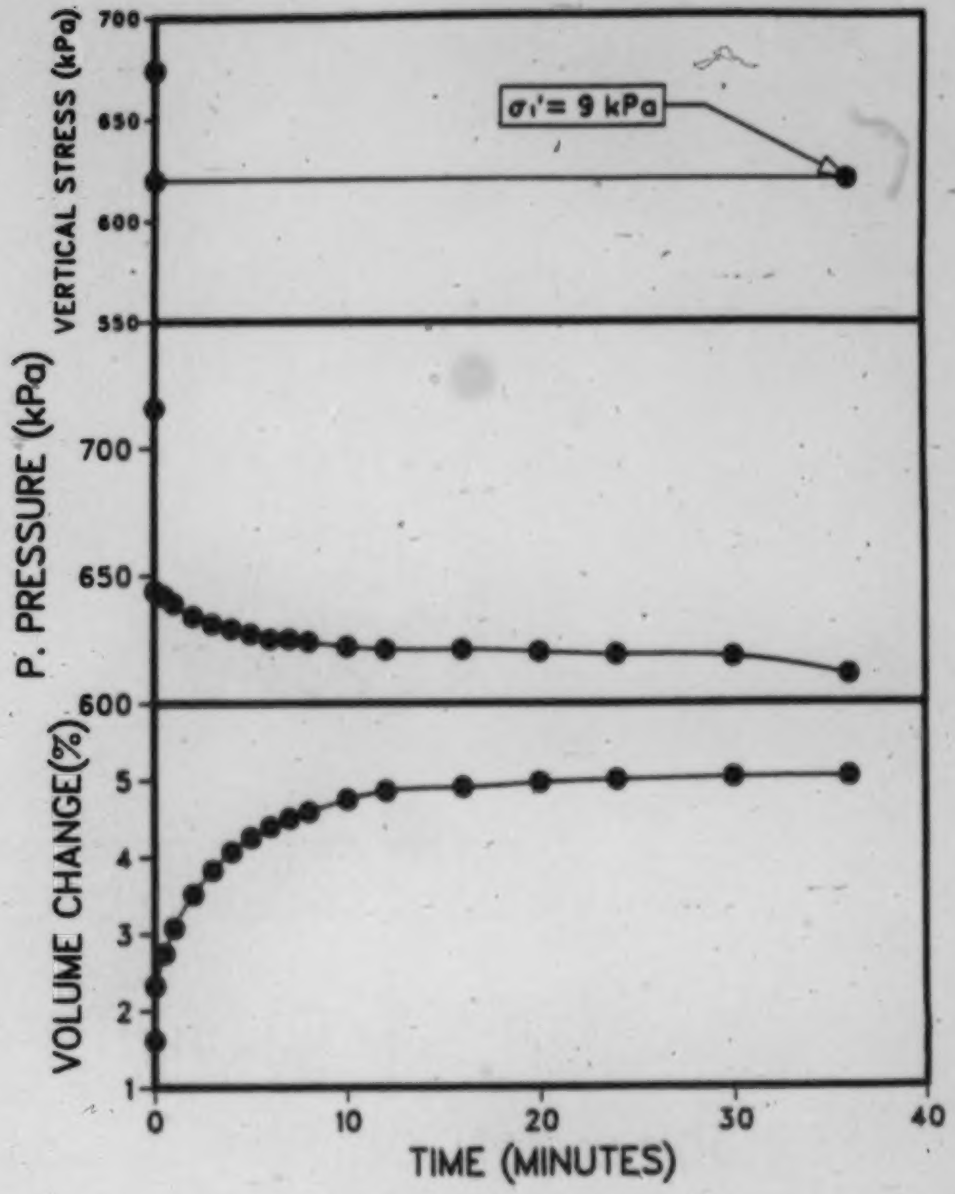

Figure 4.11 Increment H from unloading undrained test on tailing sand sample T-350 at 50°C

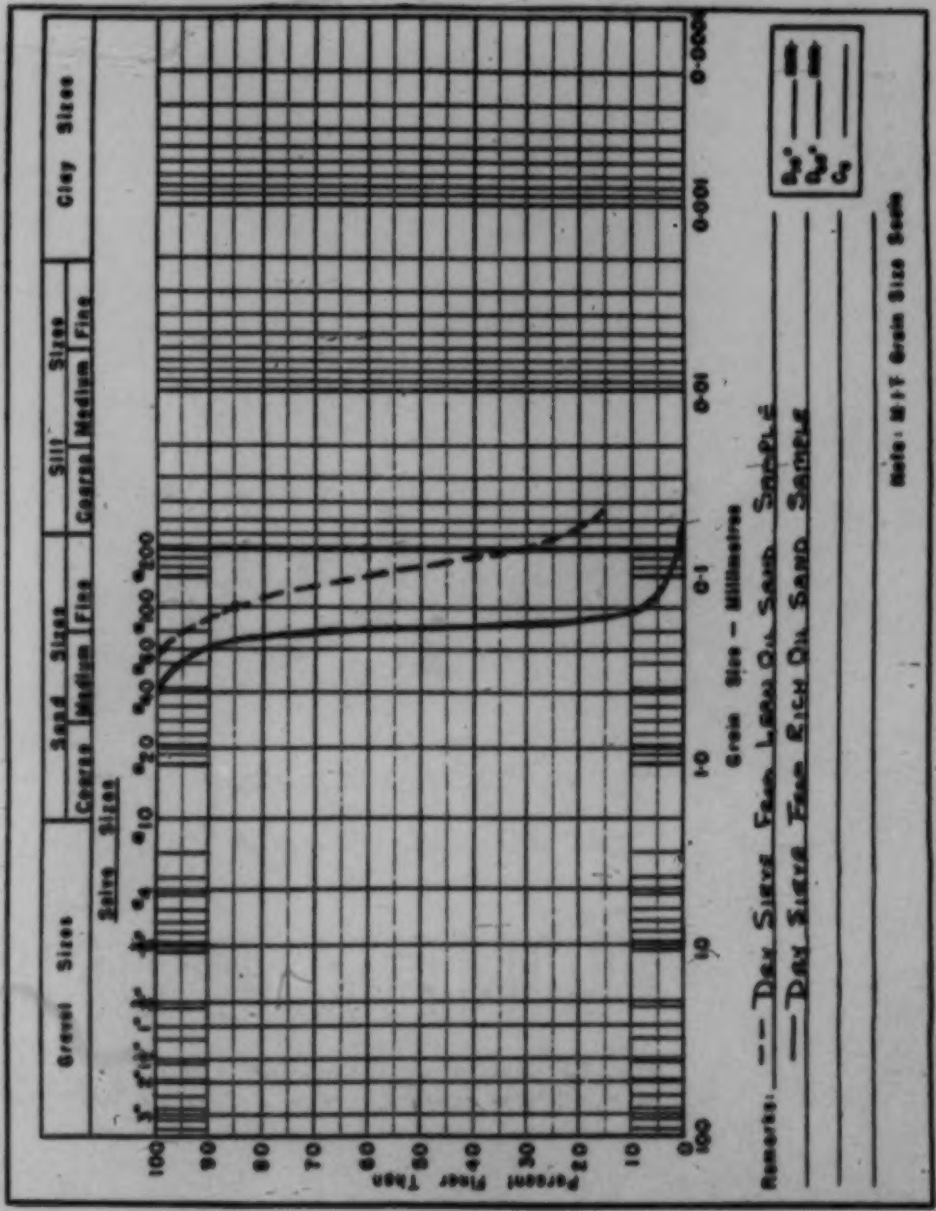

Figure 4.12 Grain size curve for samples from a lean oil sand sample and a rich oil sand sample

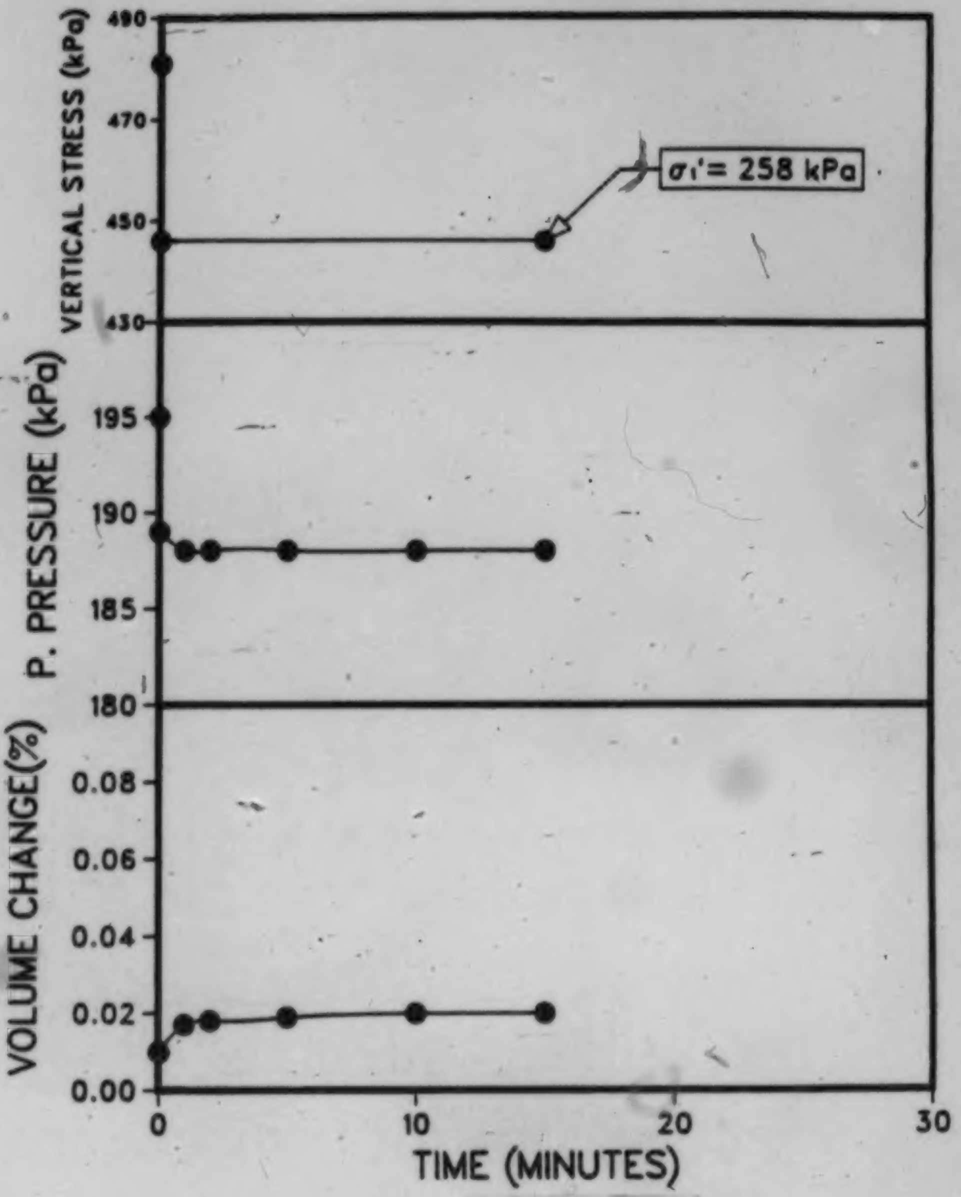

Figure 4.13 Increment D from unloading undrained test on lean oil sand sample B-224 at 24°C

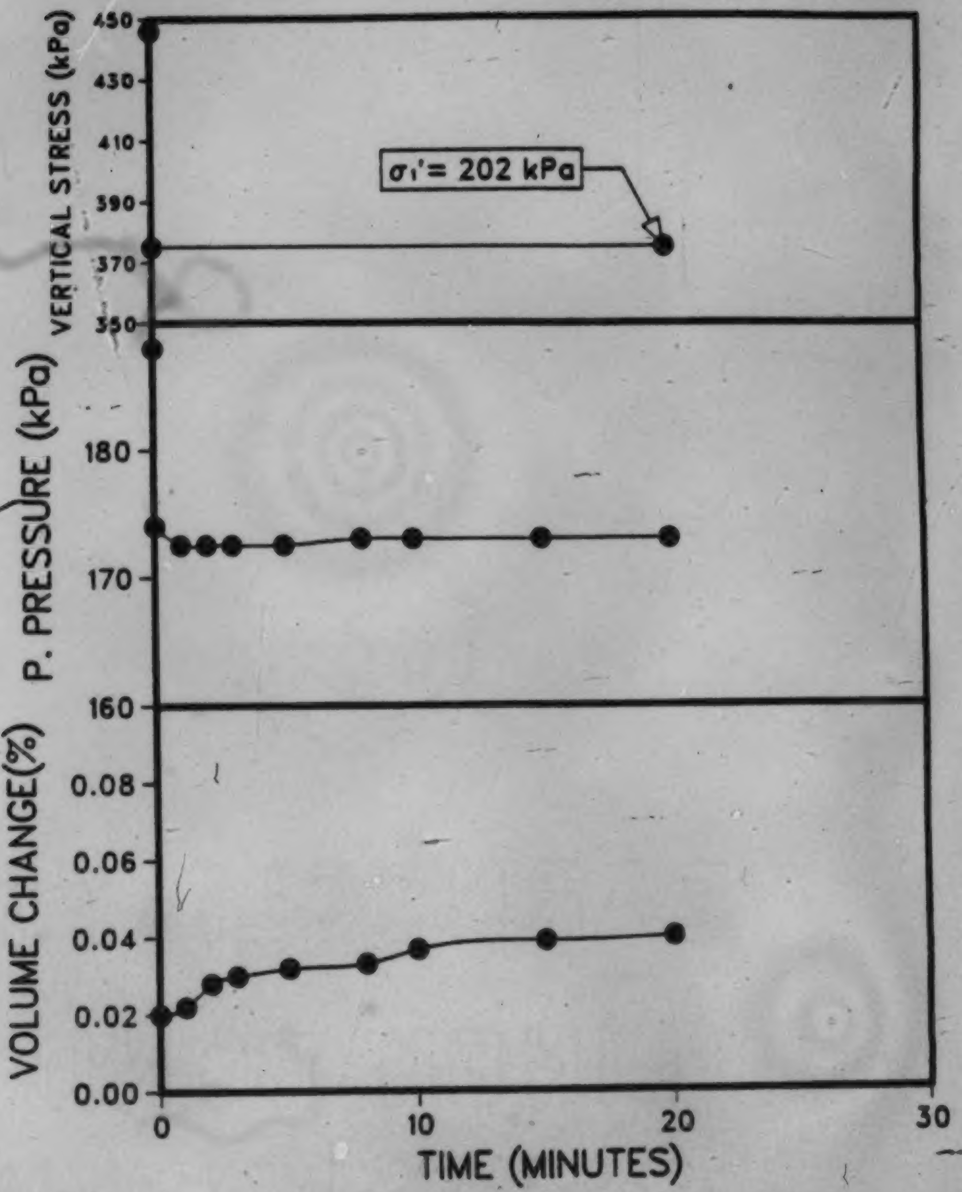

Figure 4.14 Increment E from unloading undrained test on lean oil sand sample B-224 at 24°C

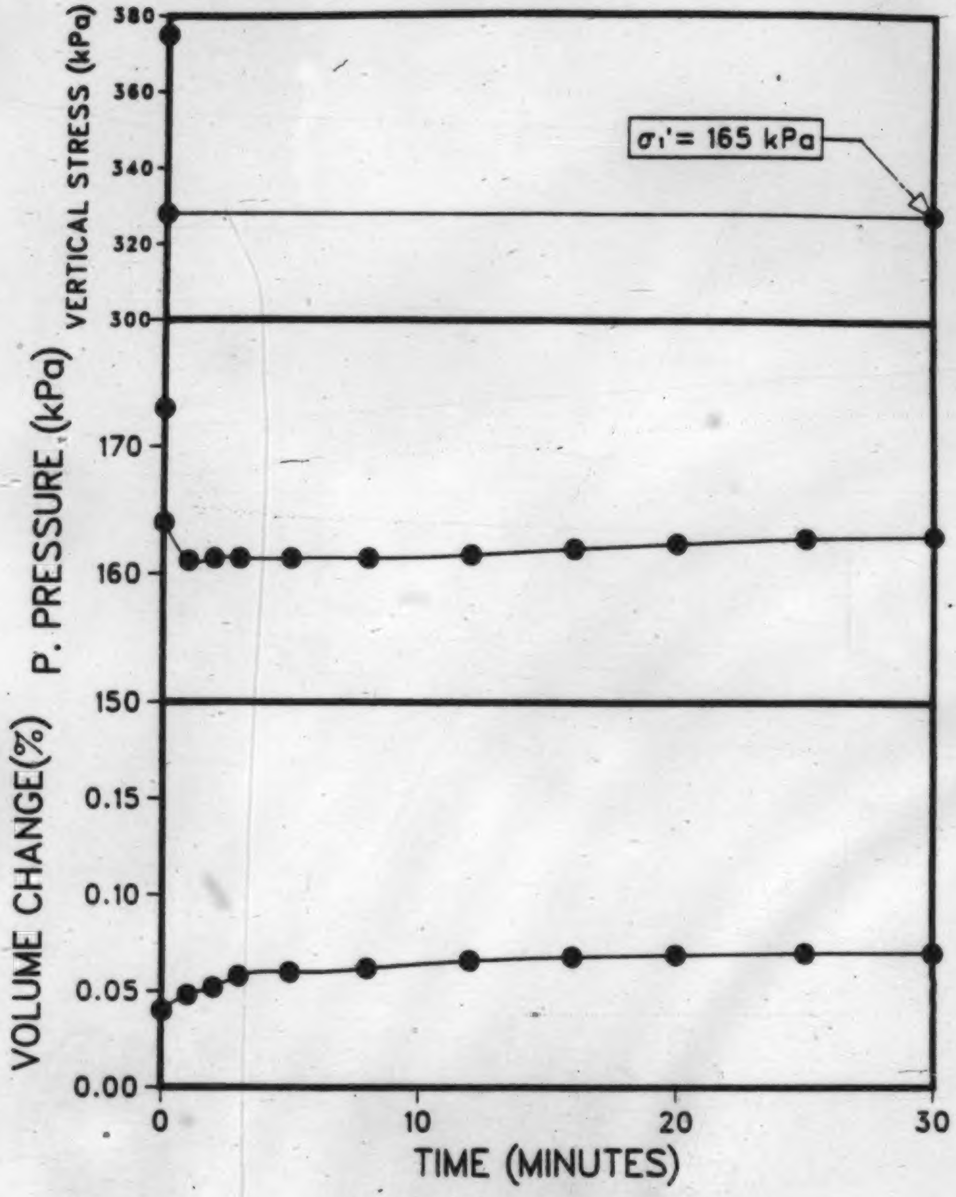

Figure 4.15 Increment F from unloading undrained test on lean oil sand sample B-224 at 24°C

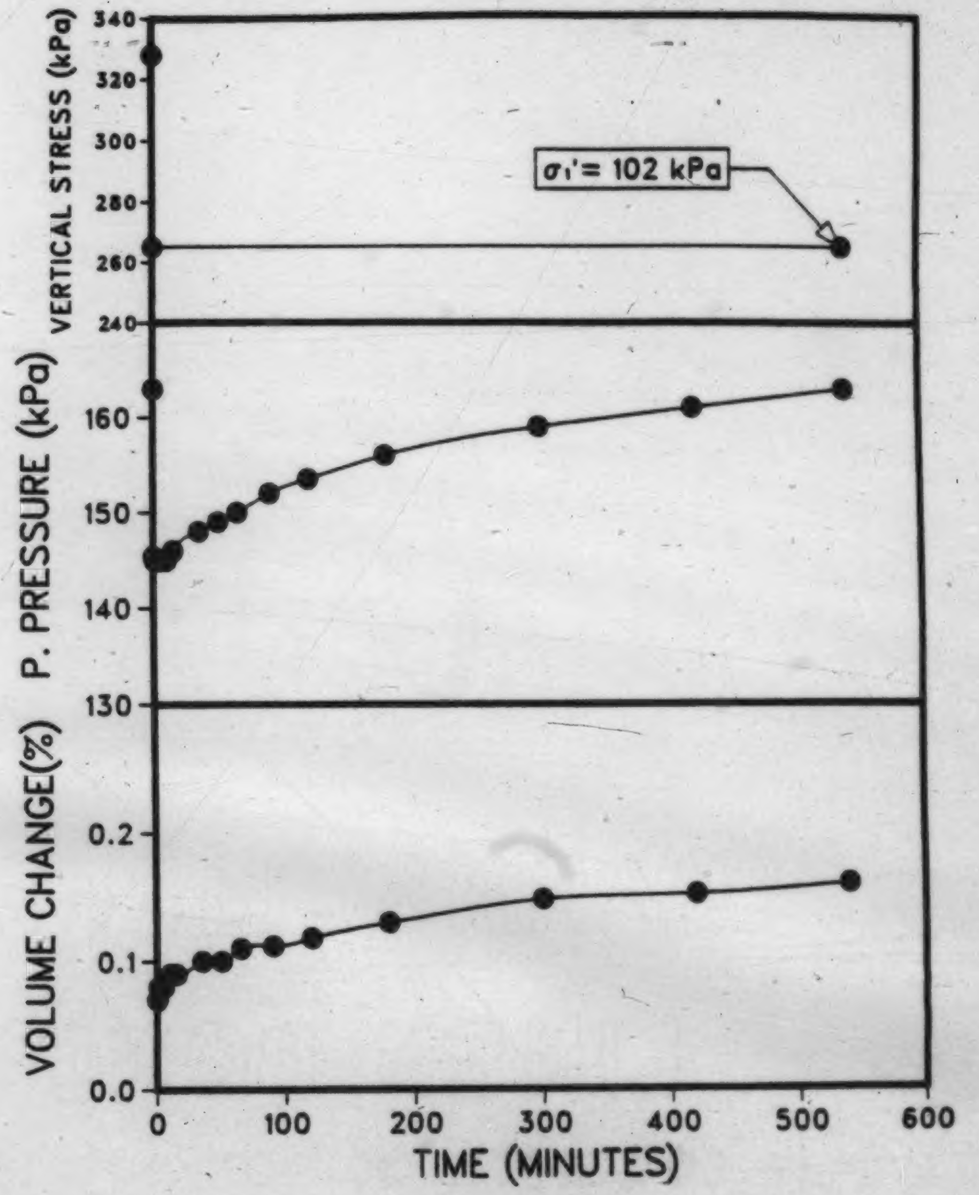

Figure 4.16 Increment G from unloading undrained test on lean oil sand sample B-224 at 24°C

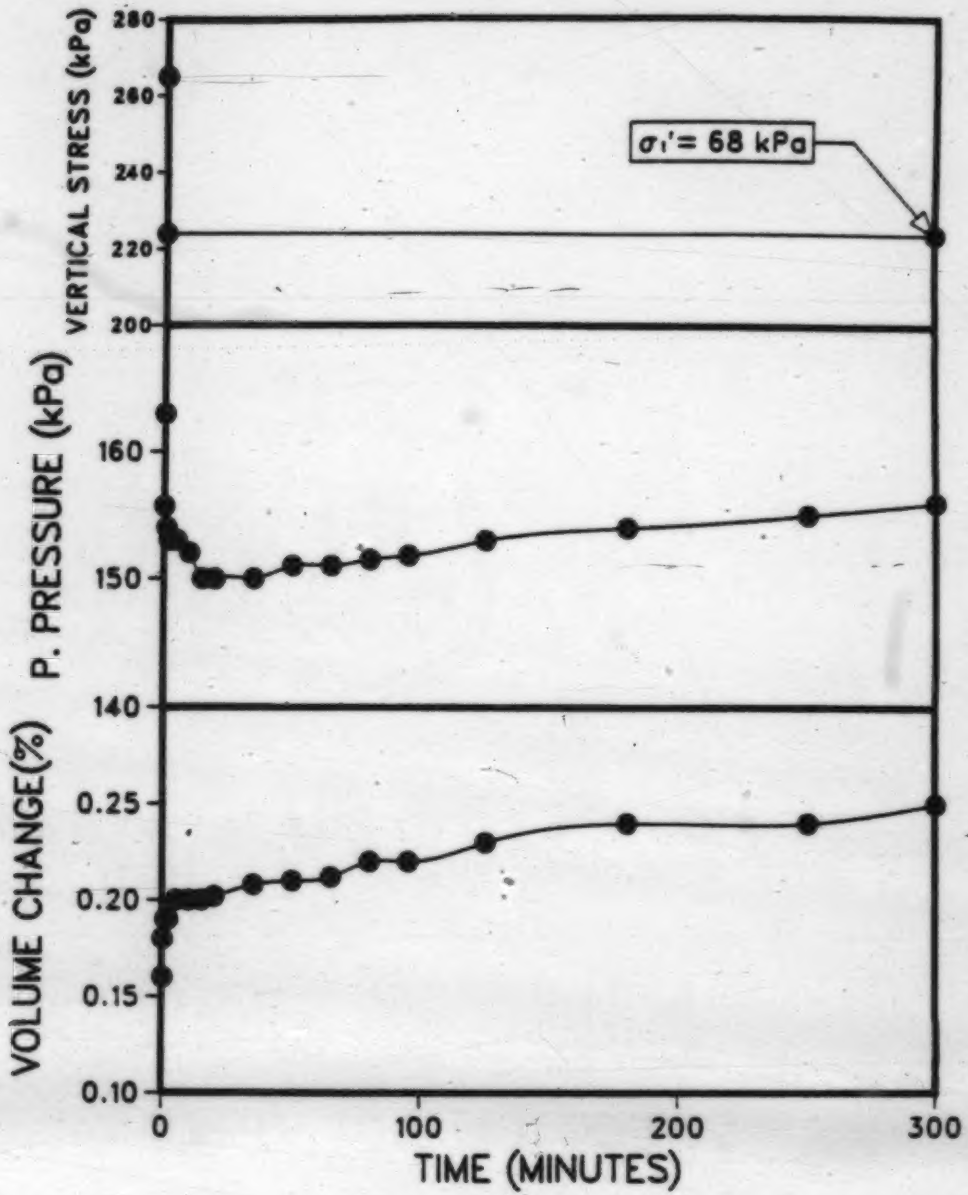

Figure 4.17 Increment H from unloading undrained test on lean oil sand sample B-224 at 24°C

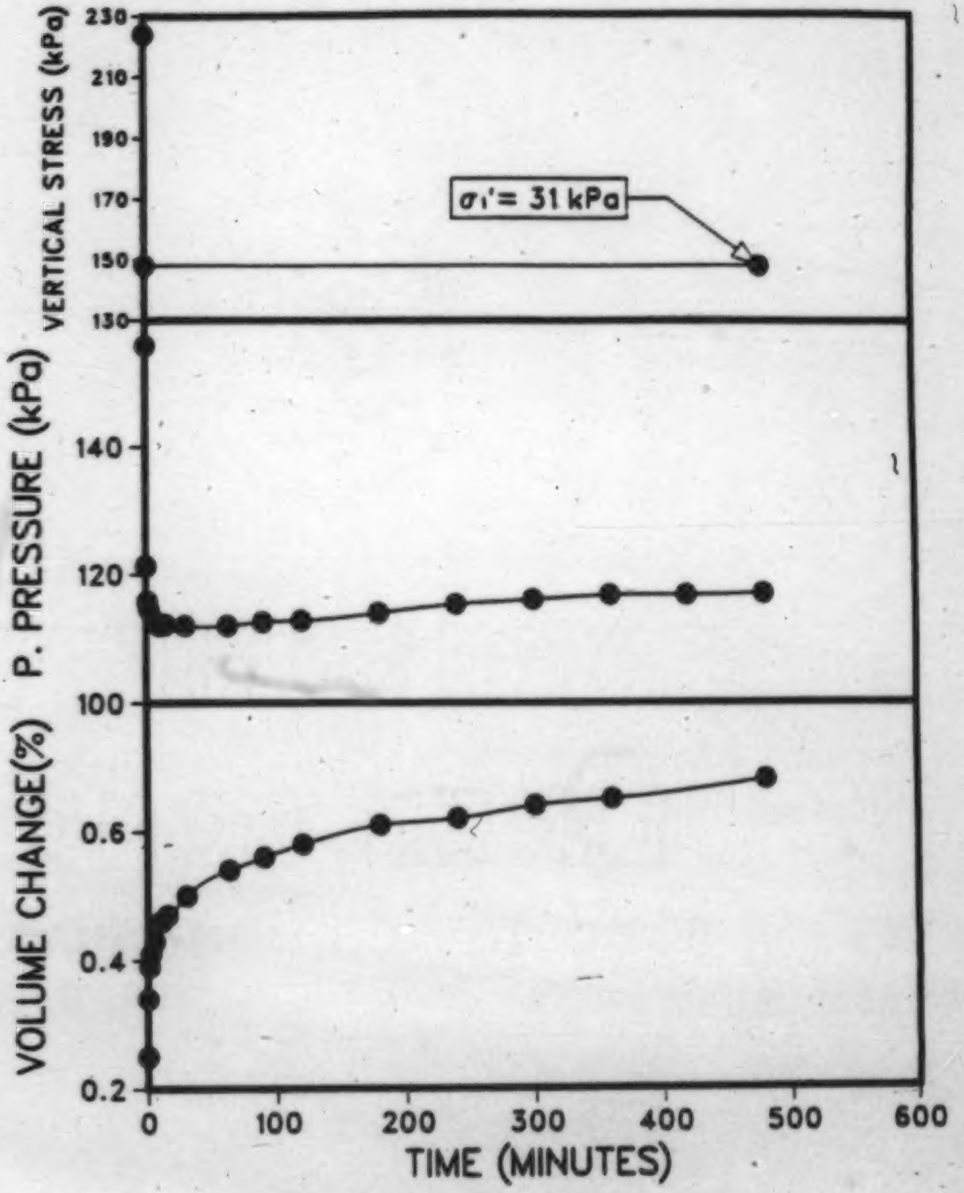

Figure 4.18 Increment I from unloading undrained test on lean oil sand sample B-224 at 24°C

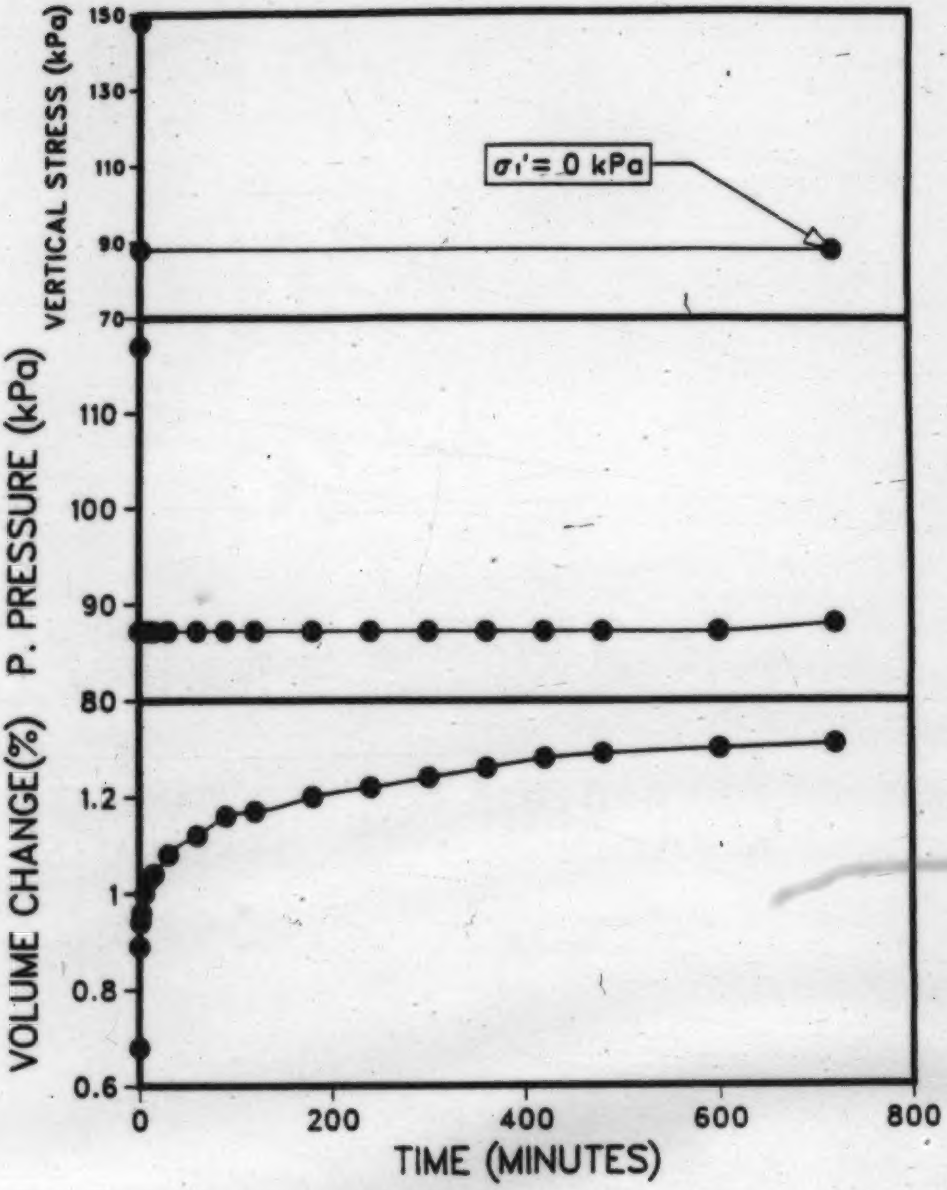

Figure 4.19 Increment J from unloading undrained test on lean oil sand sample B-224 at 24°C

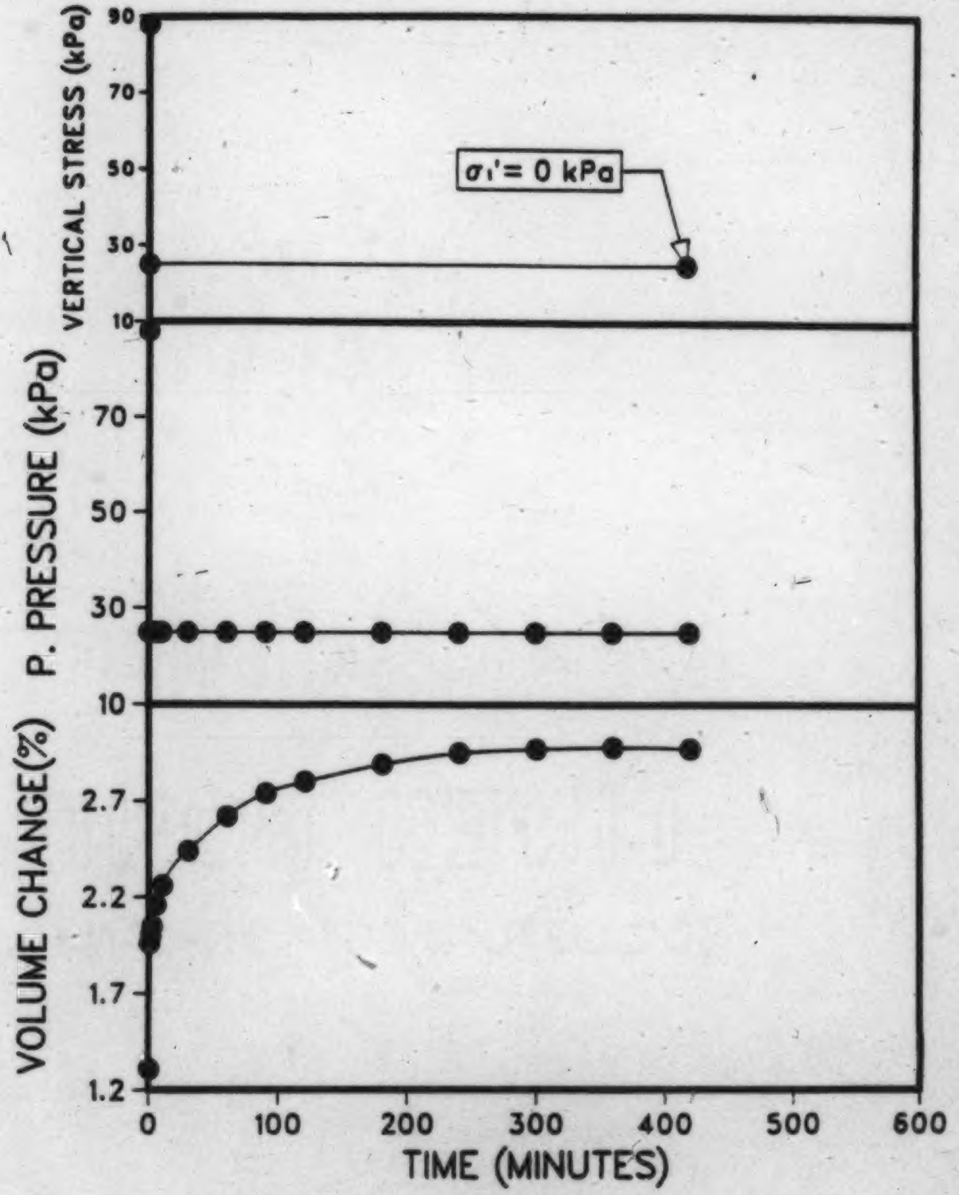

Figure 4.20 Increment K from unloading undrained test on lean oil sand sample B-224 at 24°C

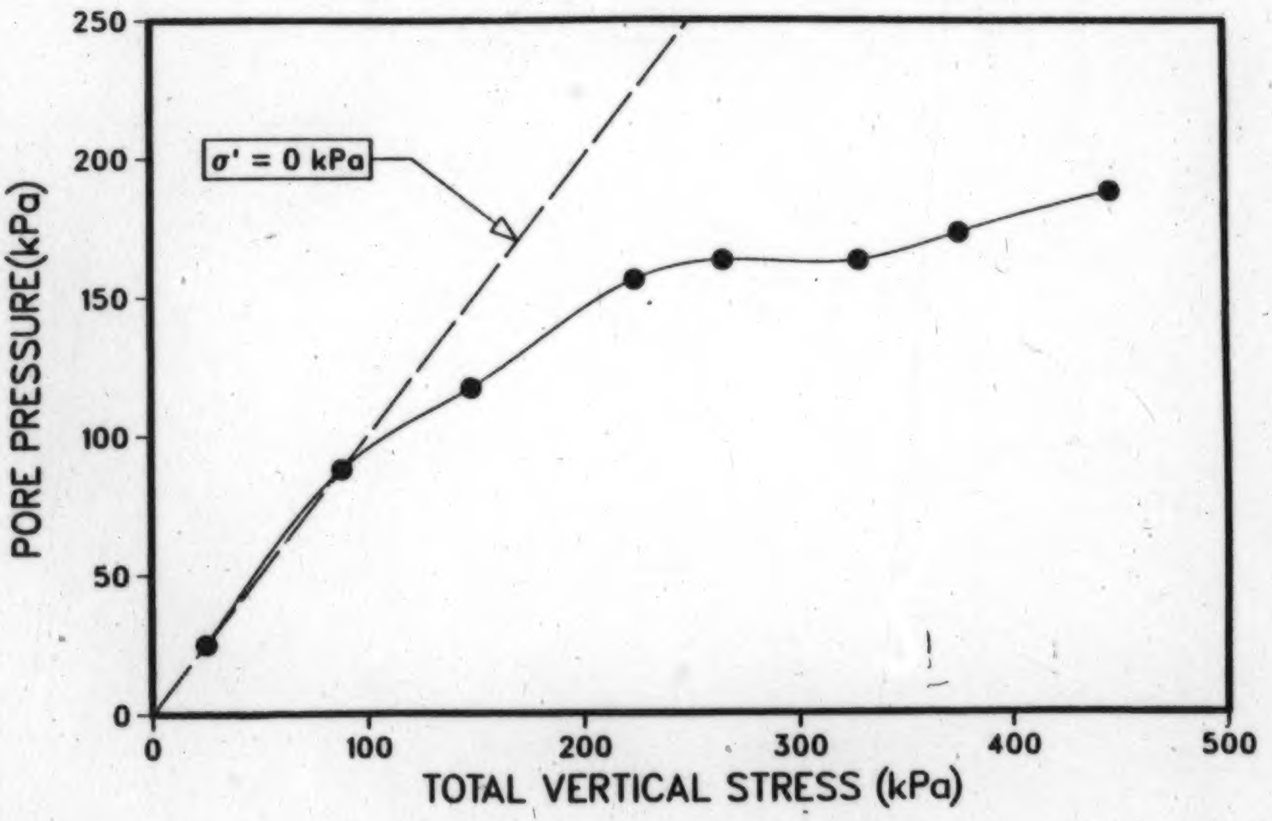

Figure 4.21 Undrained equilibrium curve for lean oil sand sample B-224 at 24°C

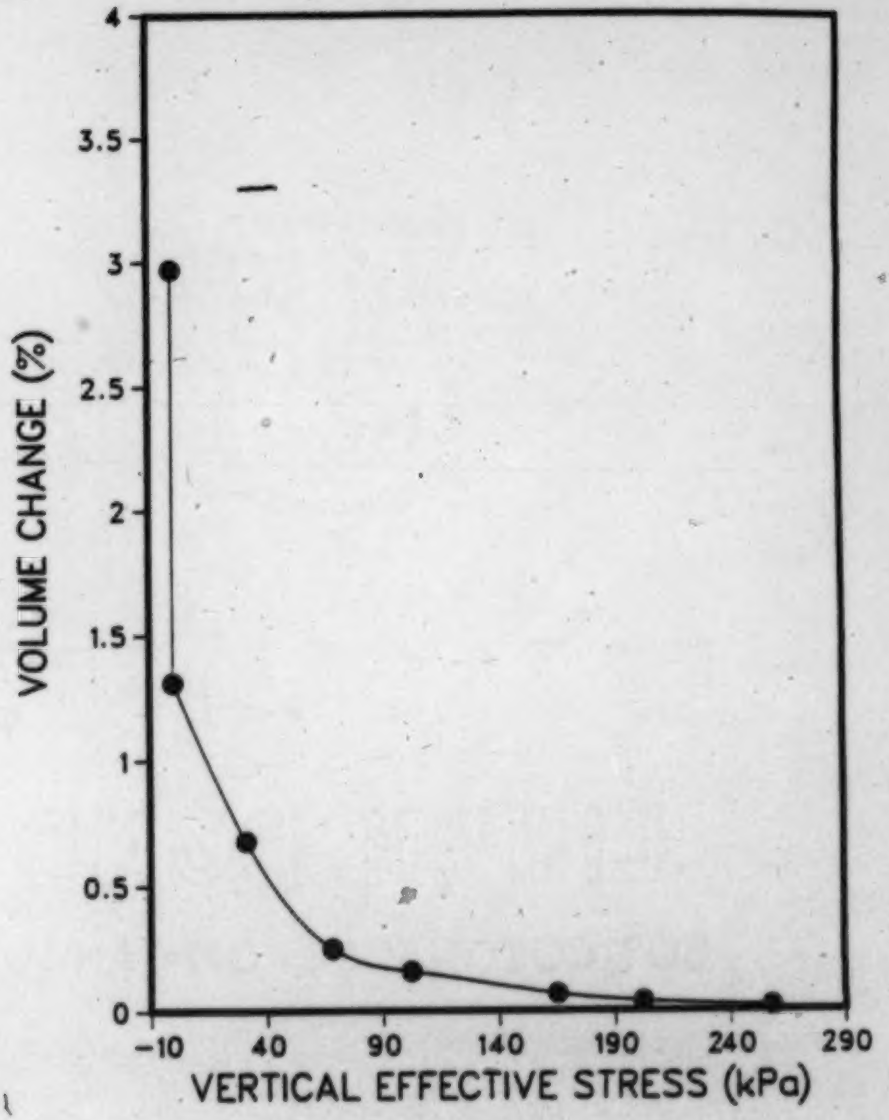

Figure 4.22 Stress vs. strain curve for lean oil sand sample B-224 at 24°C

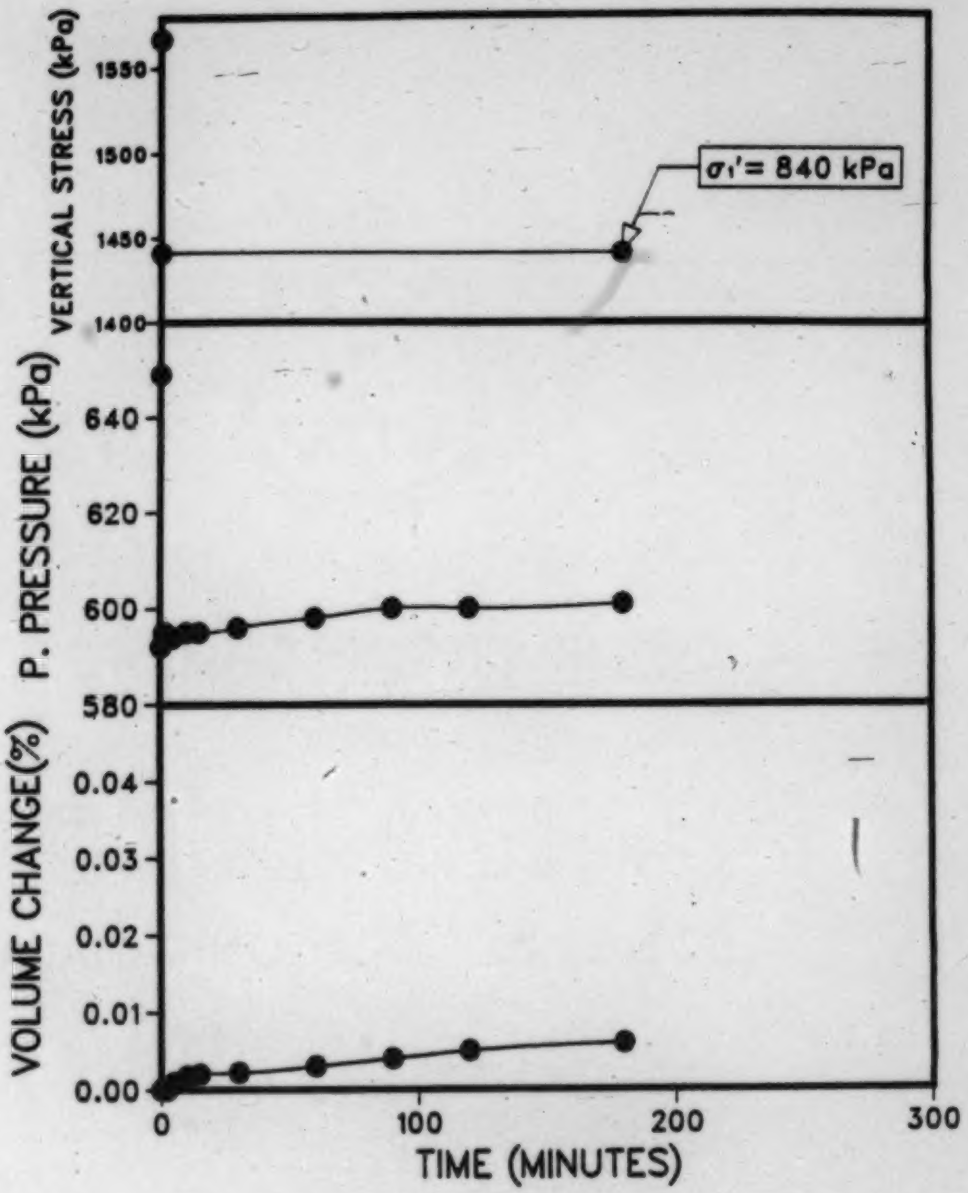

Figure 4.23 Increment A from unloading undrained test on rich oil sand sample RB-5-5 at 24°C

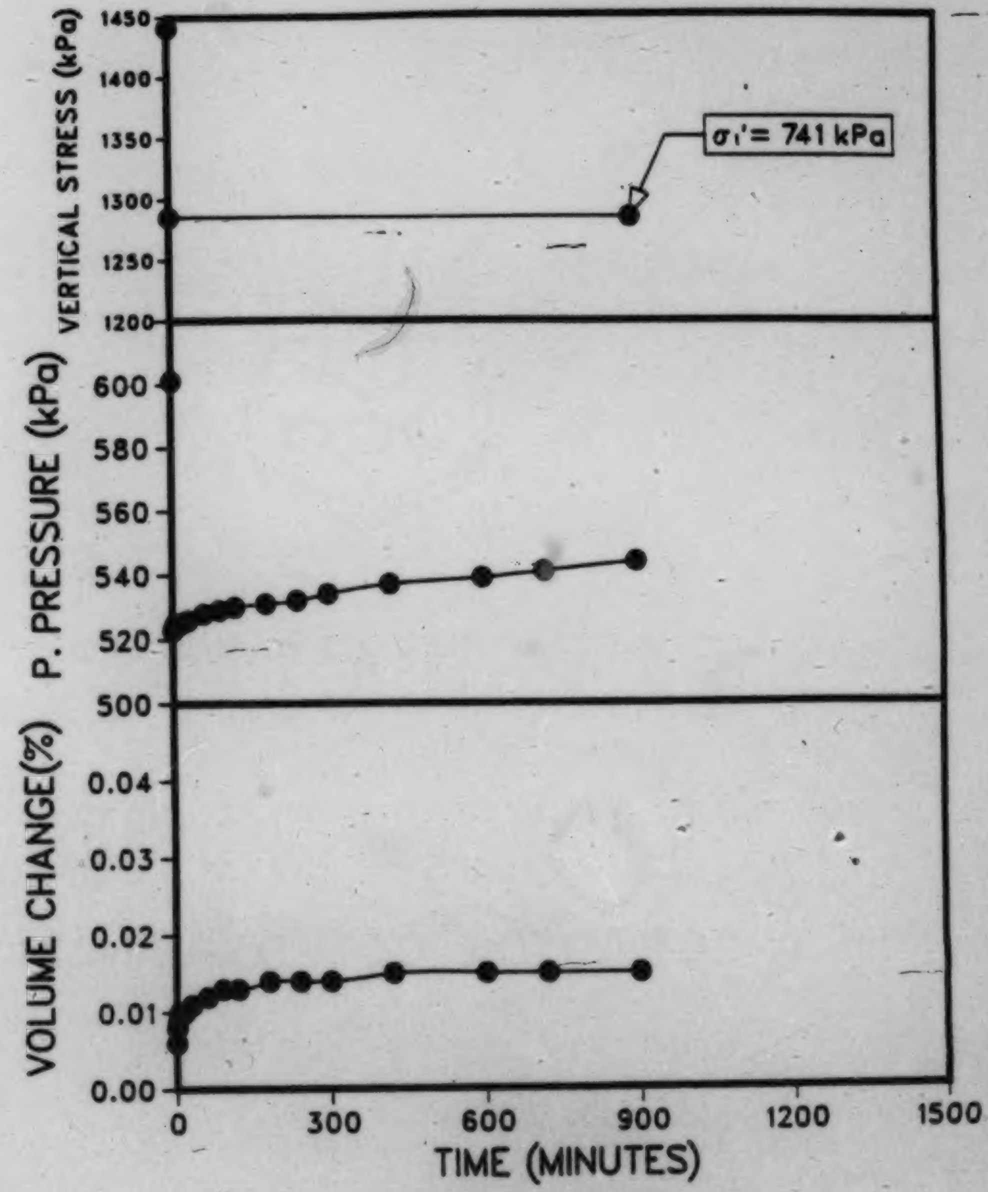

Figure 4.24 Increment B from unloading undrained test on rich oil sand sample RB-5-5 at 24°C

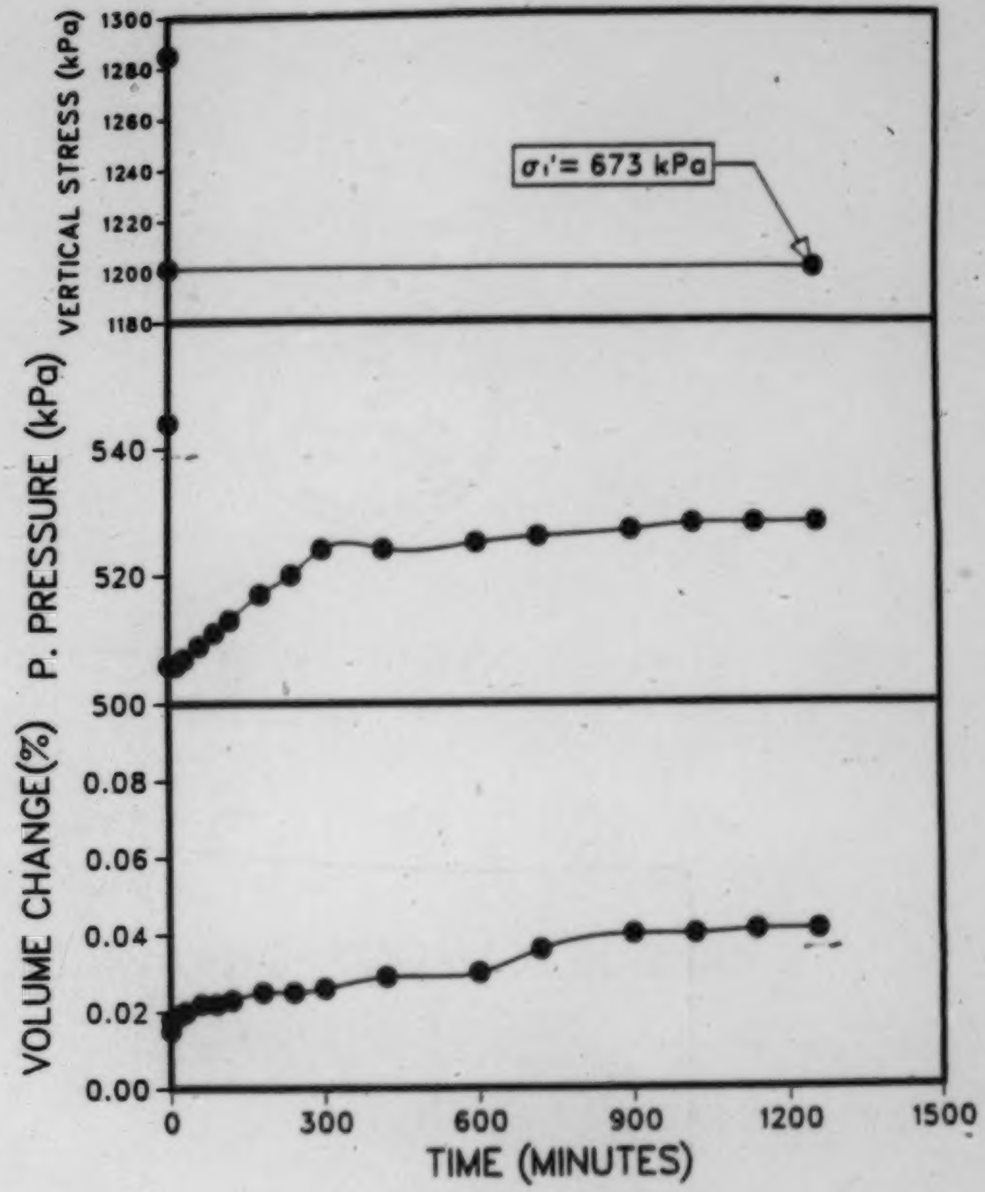

Figure 4.25 Increment C from unloading undrained test on rich oil sand sample RB-5-5 at 24°C

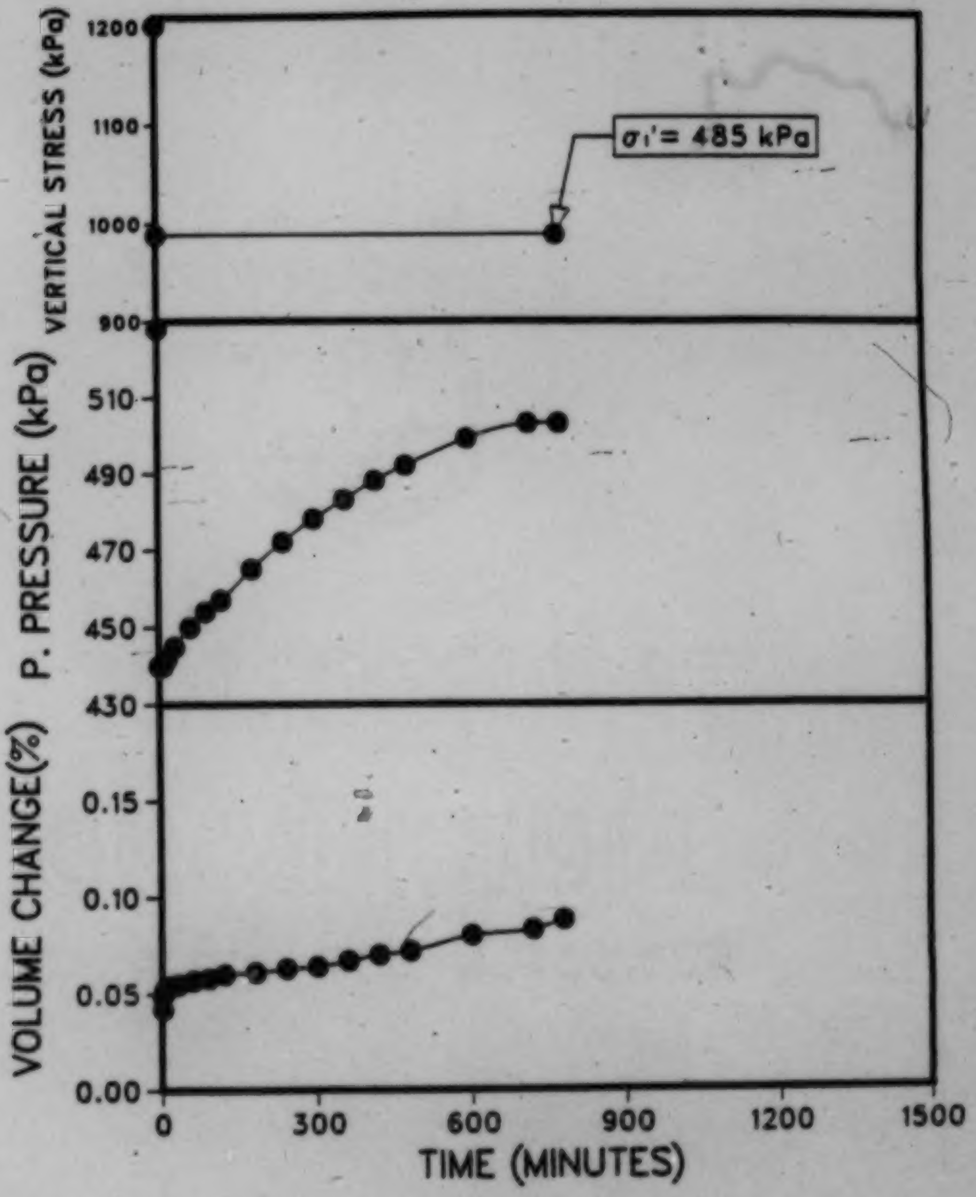

Figure 4.26 Increment D from unloading undrained test on rich oil sand sample RB-5-5 at 24°C

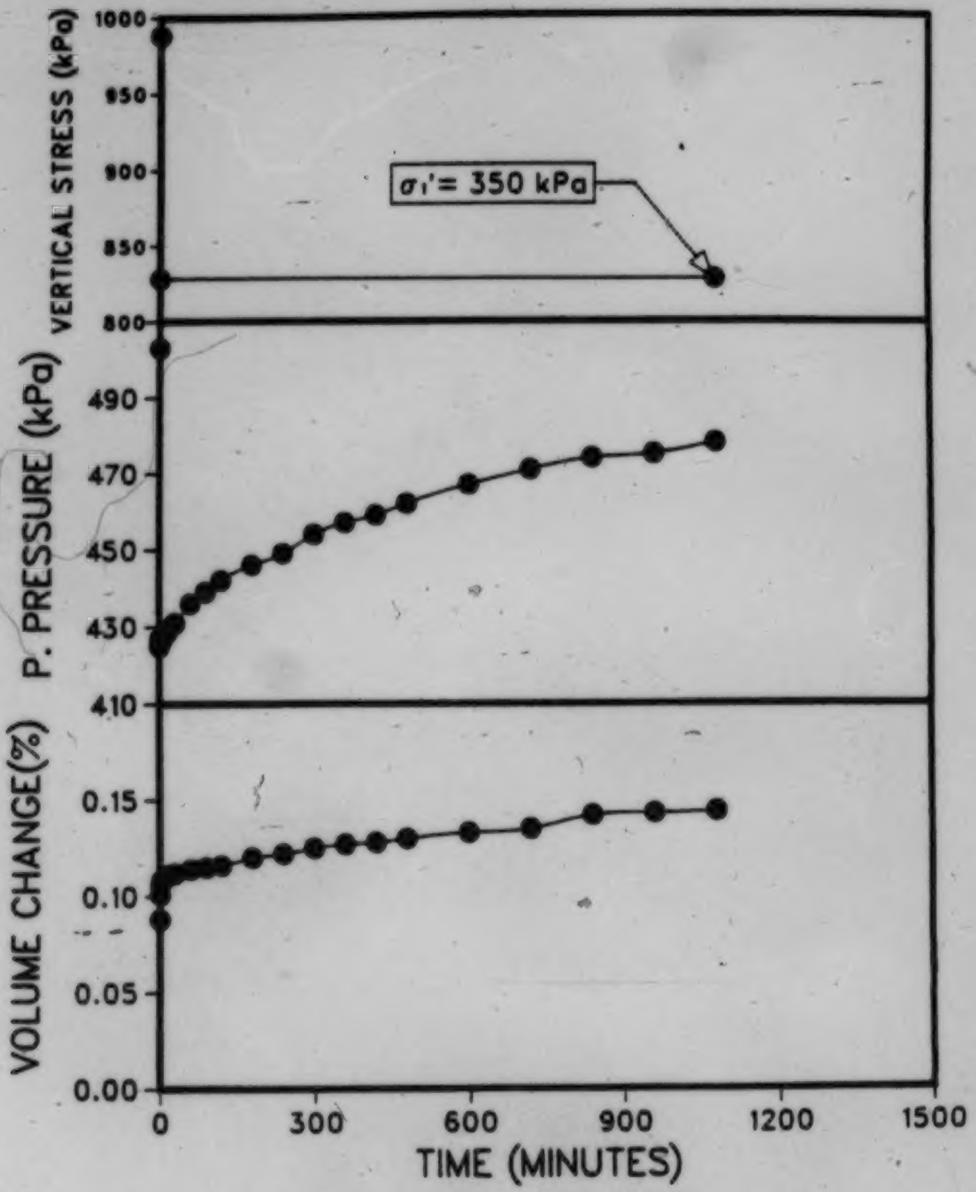

Figure 4.27 Increment E from unloading undrained test on rich oil sand sample RB-5-5 at 24°C

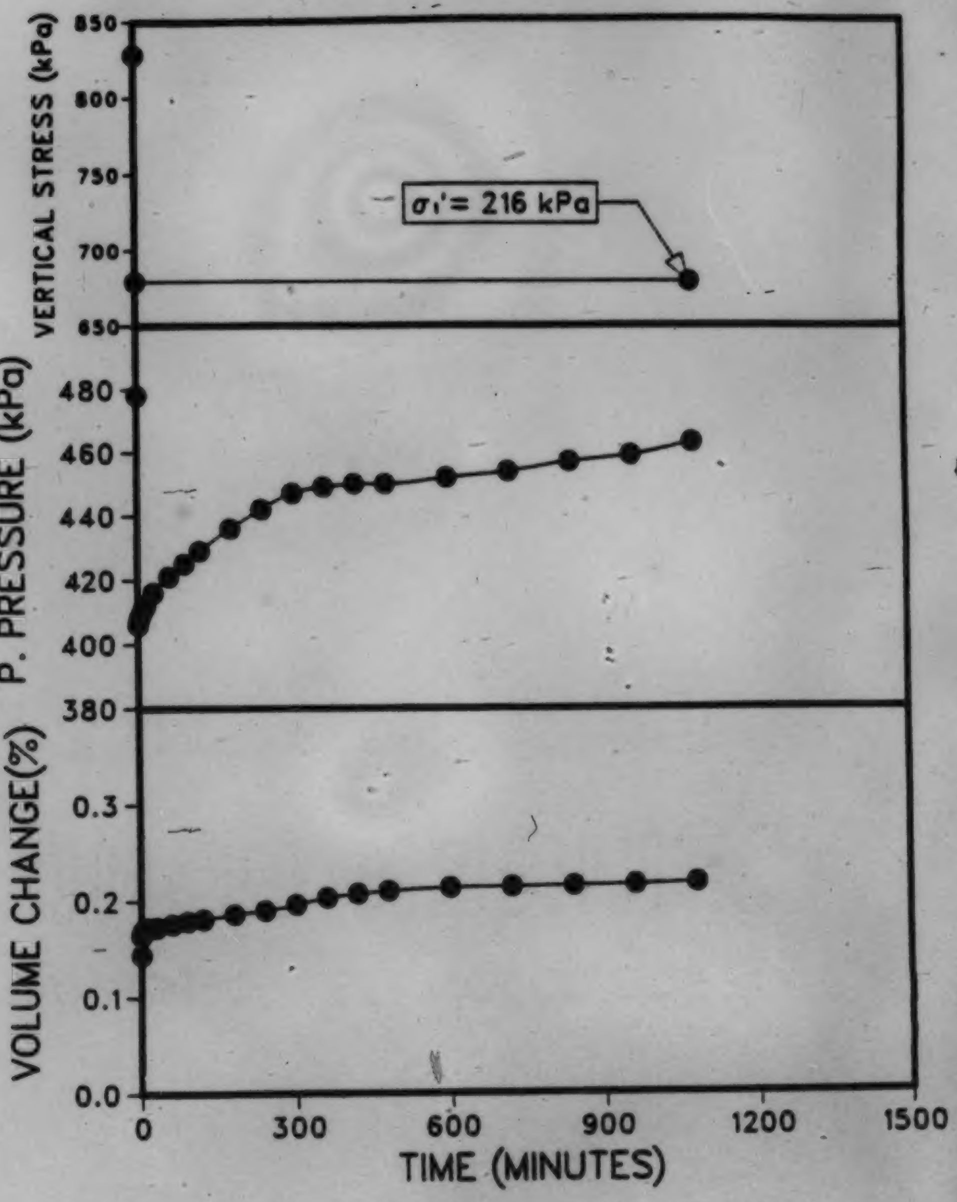

Figure 4.28 Increment F from unloading undrained test on rich oil sand sample RB-5-5 at 24°C

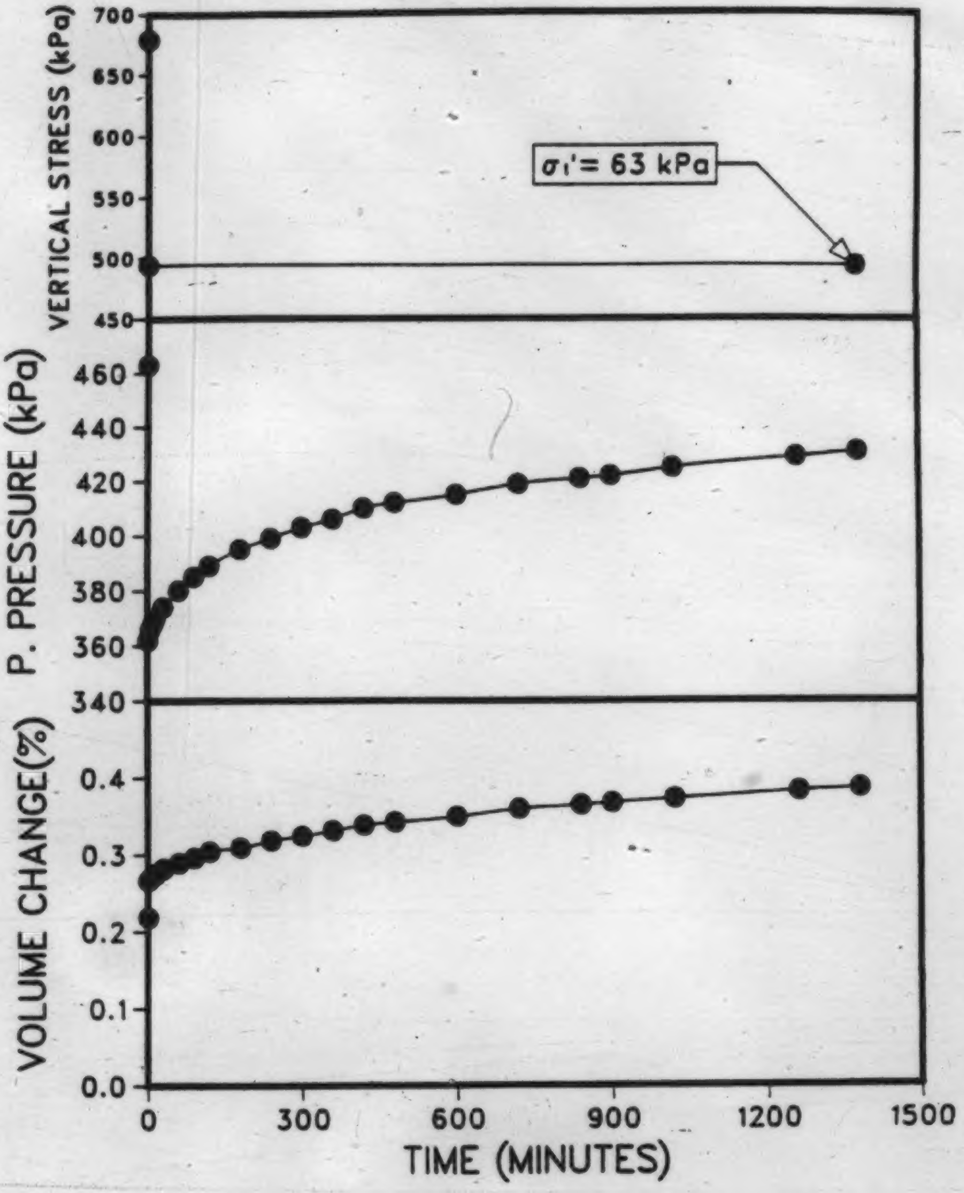

Figure 4.29 Increment G from unloading undrained test on rich oil sand sample RB-5-5 at 24°C

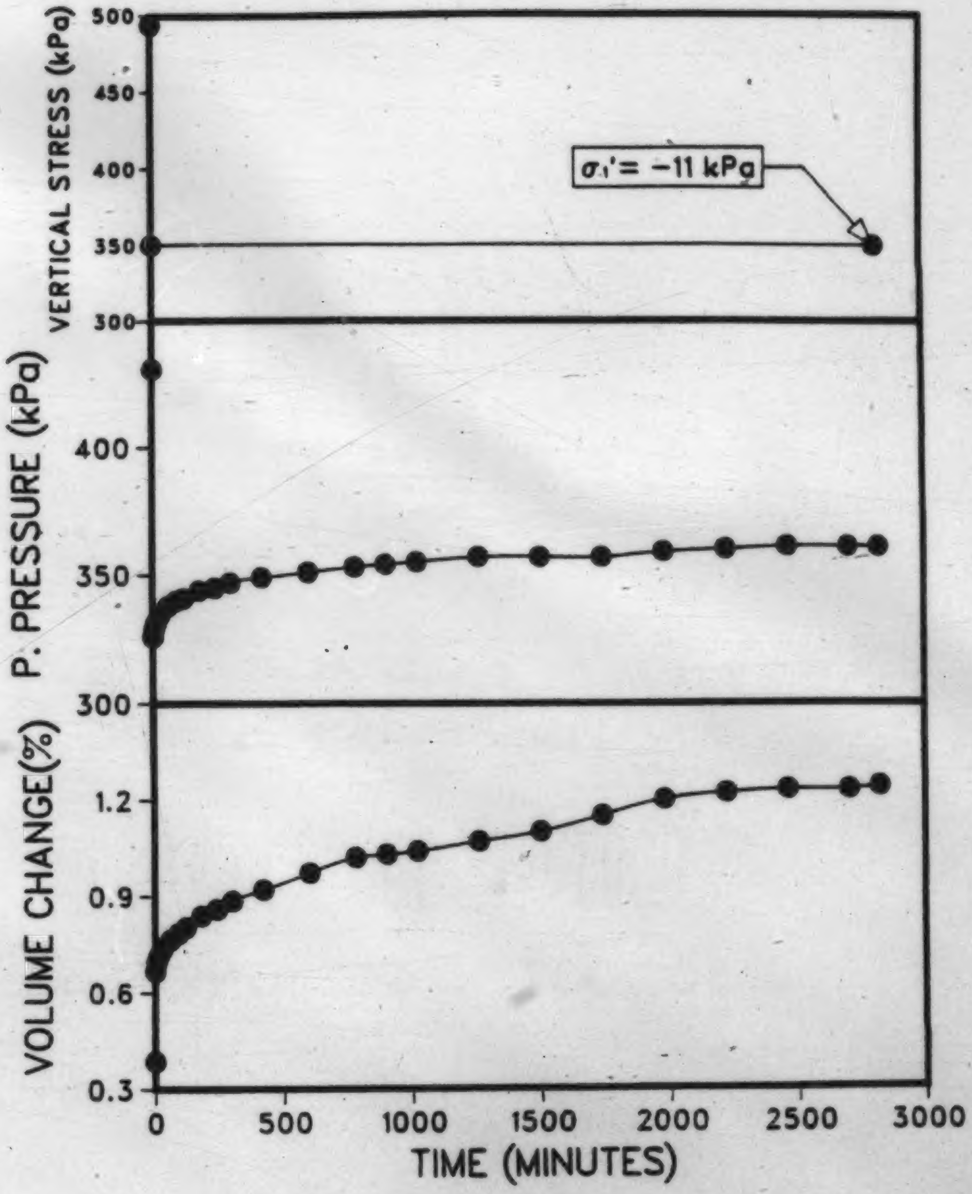

Figure 4.30 Increment H from unloading undrained test on rich oil sand sample RB-5-5 at 24°C

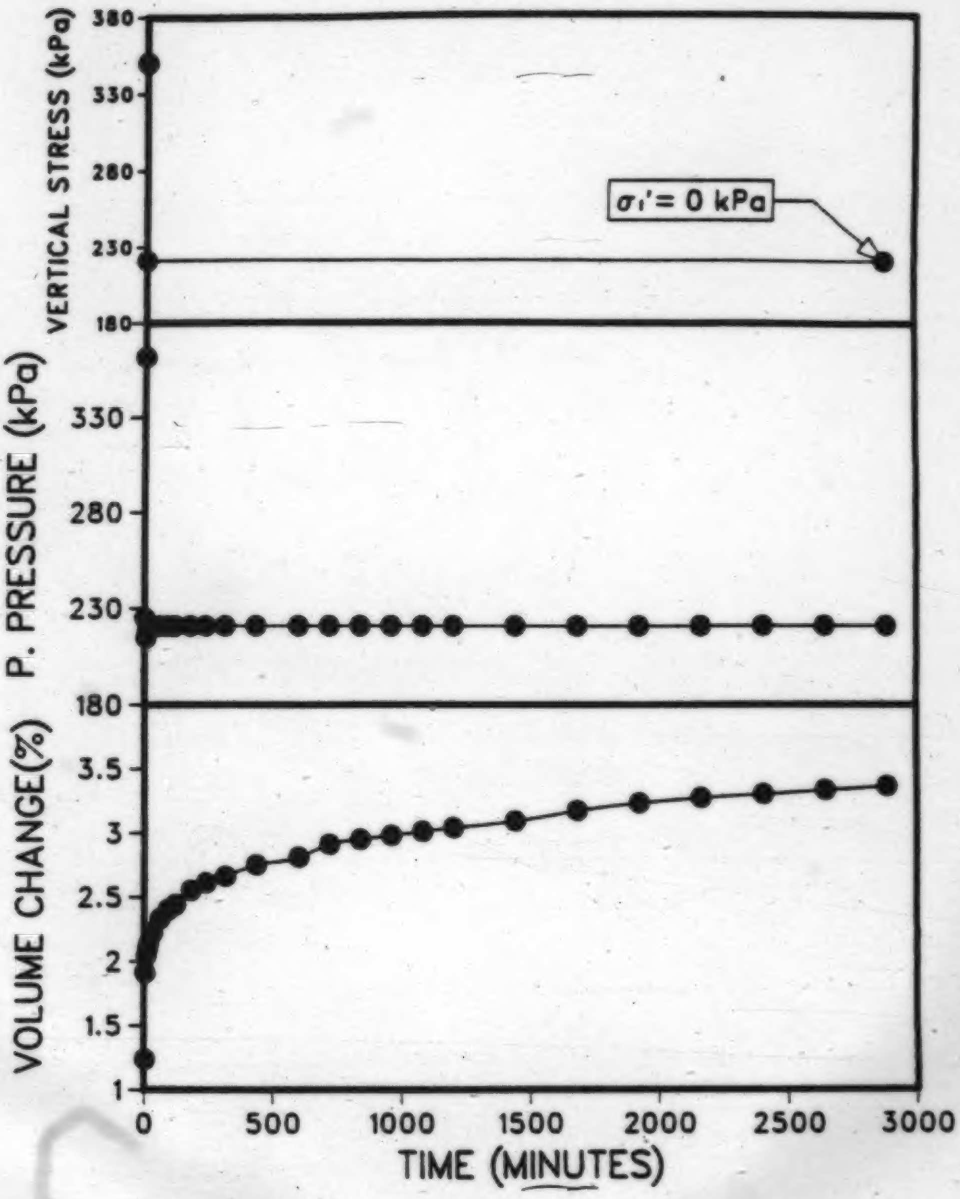

Figure 4.31 Increment I from unloading undrained test on rich oil sand sample RB-5-5 at 24°C

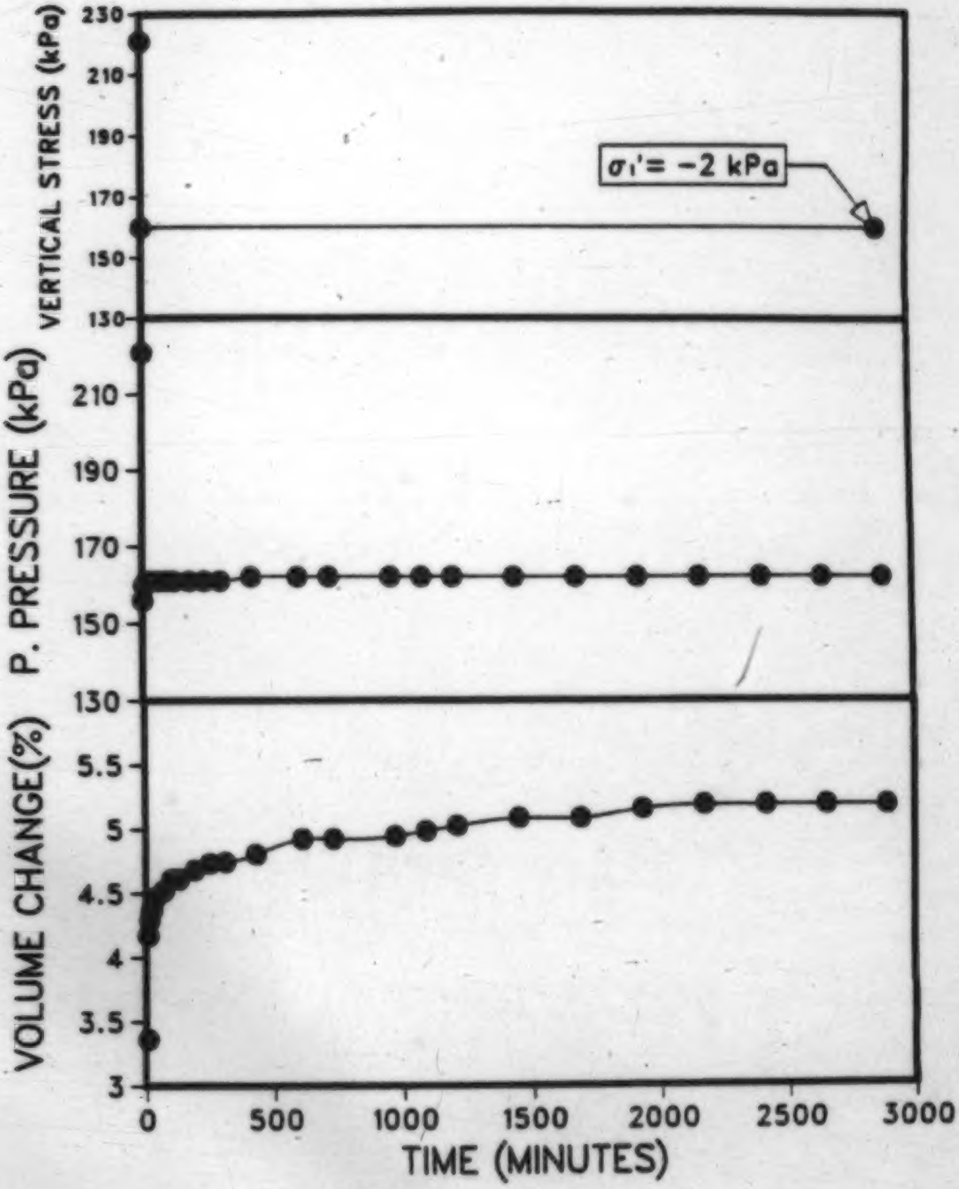

Figure 4.32 Increment J from unloading undrained test on rich oil sand sample RB-5-5 at 24°C

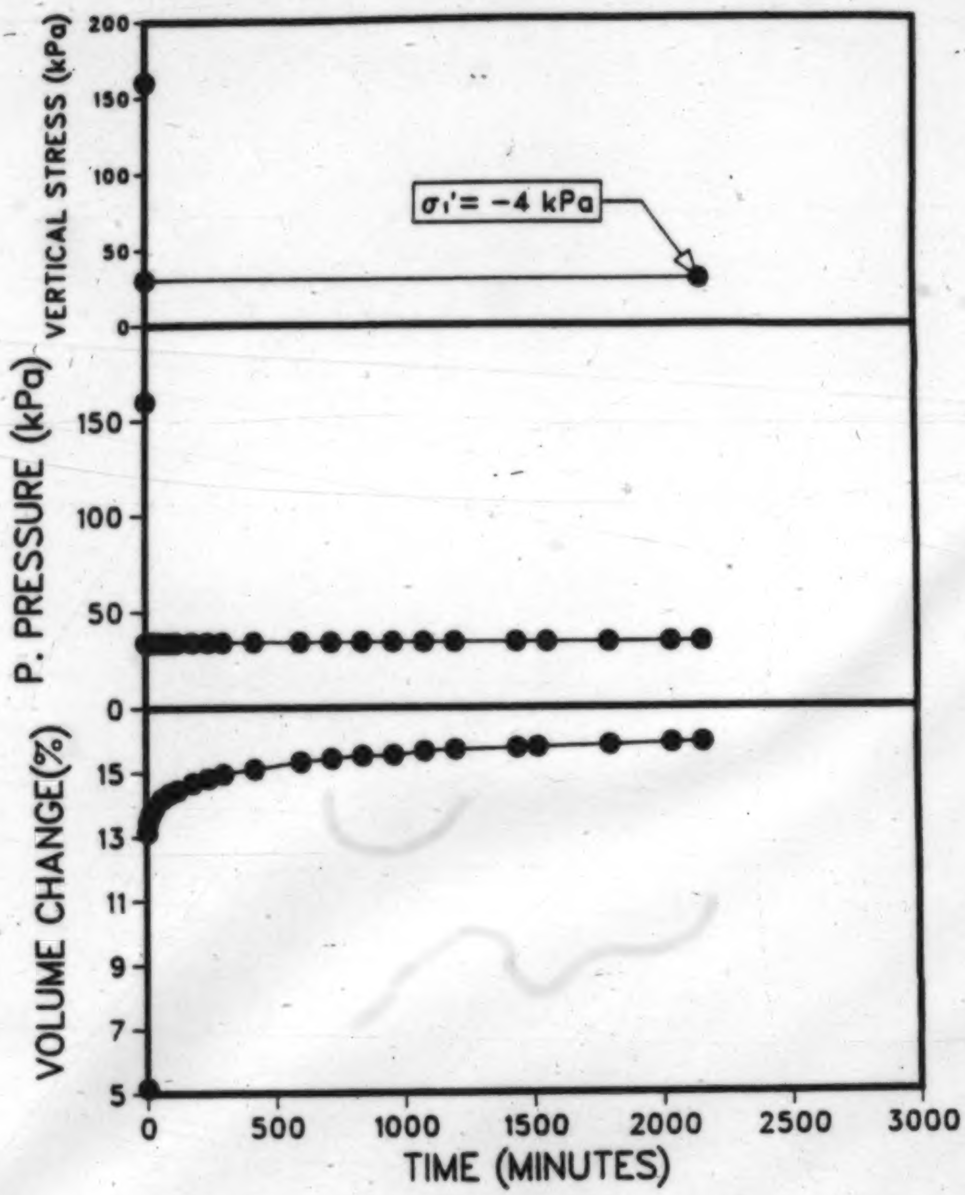

Figure 4.33 Increment K from unloading undrained test on rich oil sand sample RB-5-5 at 24°C

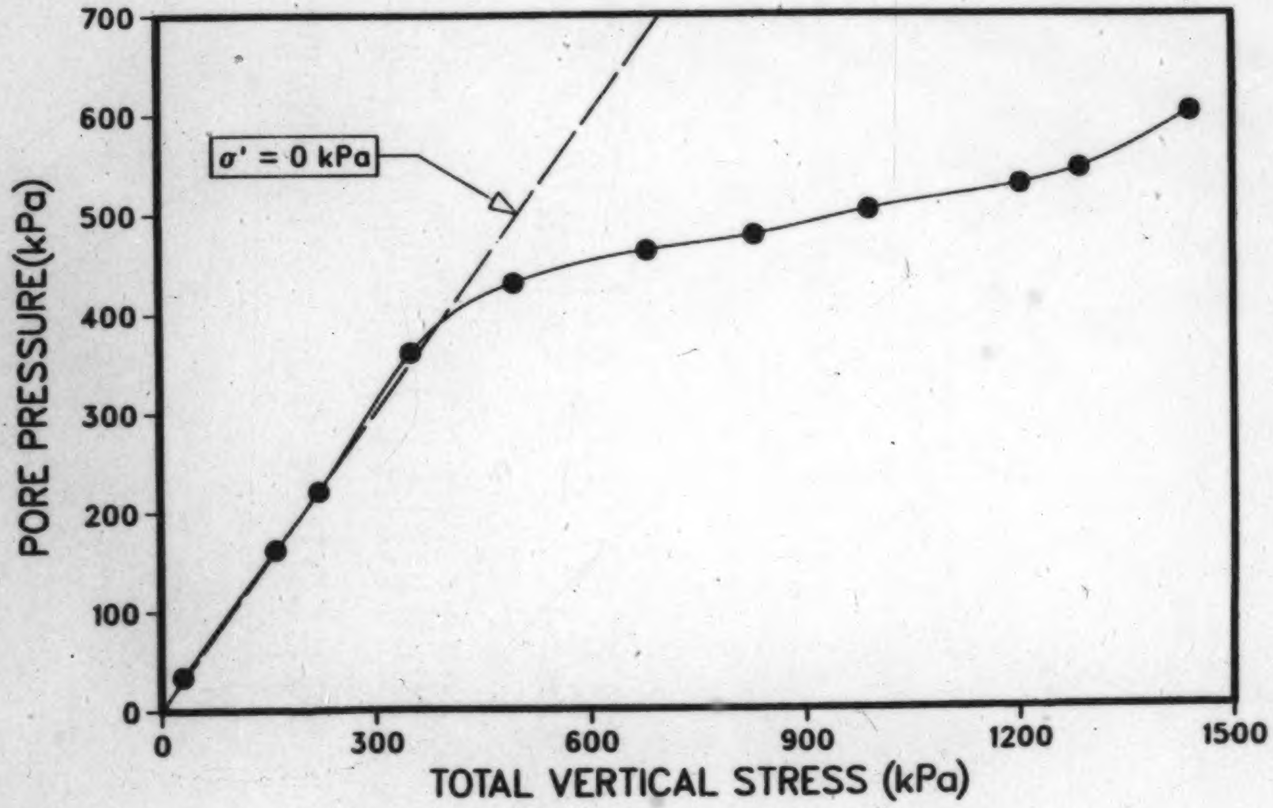

Figure 4.34 Undrained equilibrium curve for rich oil sand sample RB-5-5 at 24°C

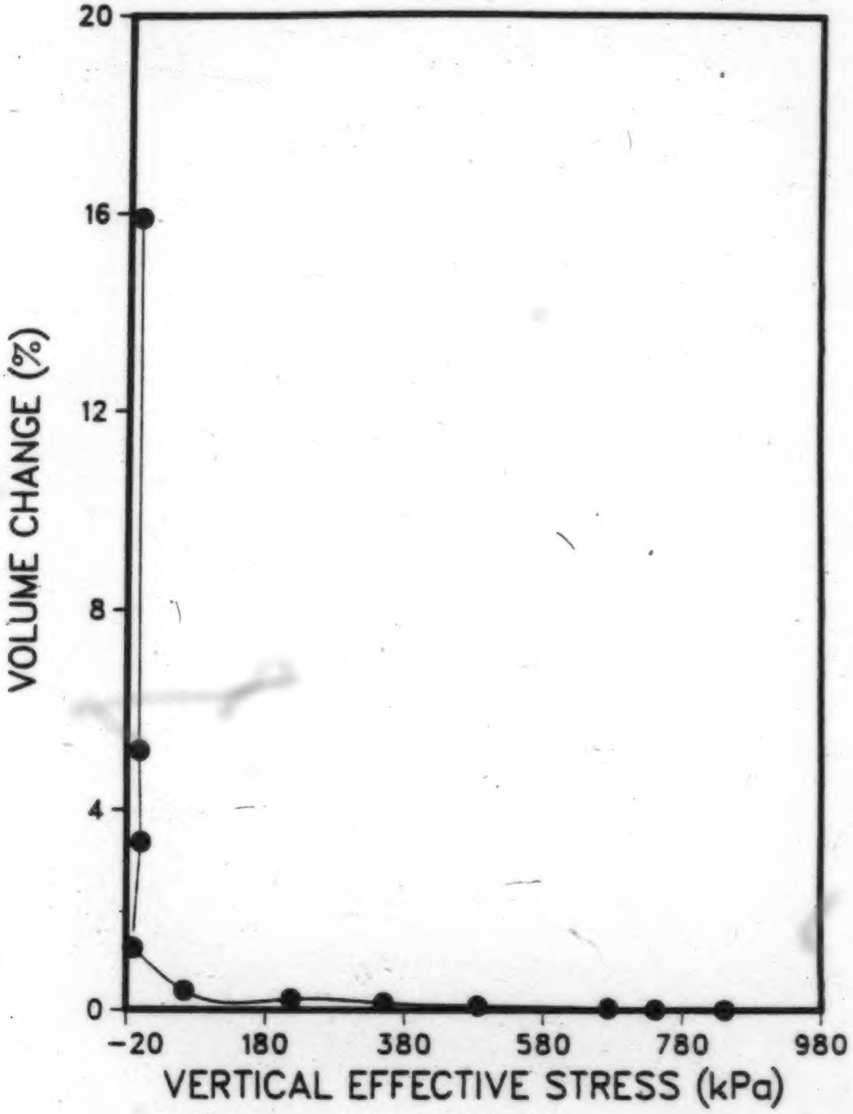

Figure 4.35 Stress vs.strain curve for rich oil sand sample RB-5-5 at 24°C

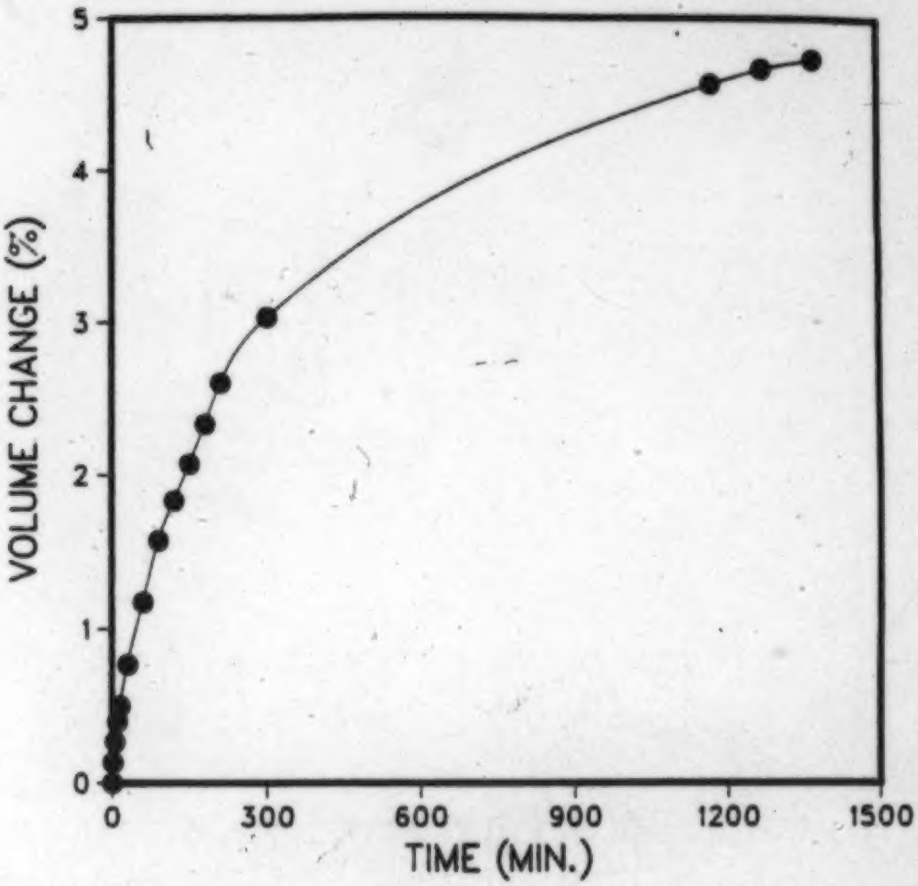

Figure 4.36 Unloading drained test on lean oil sand sample B-222 at 24°C with a vertical load of 8 kPa

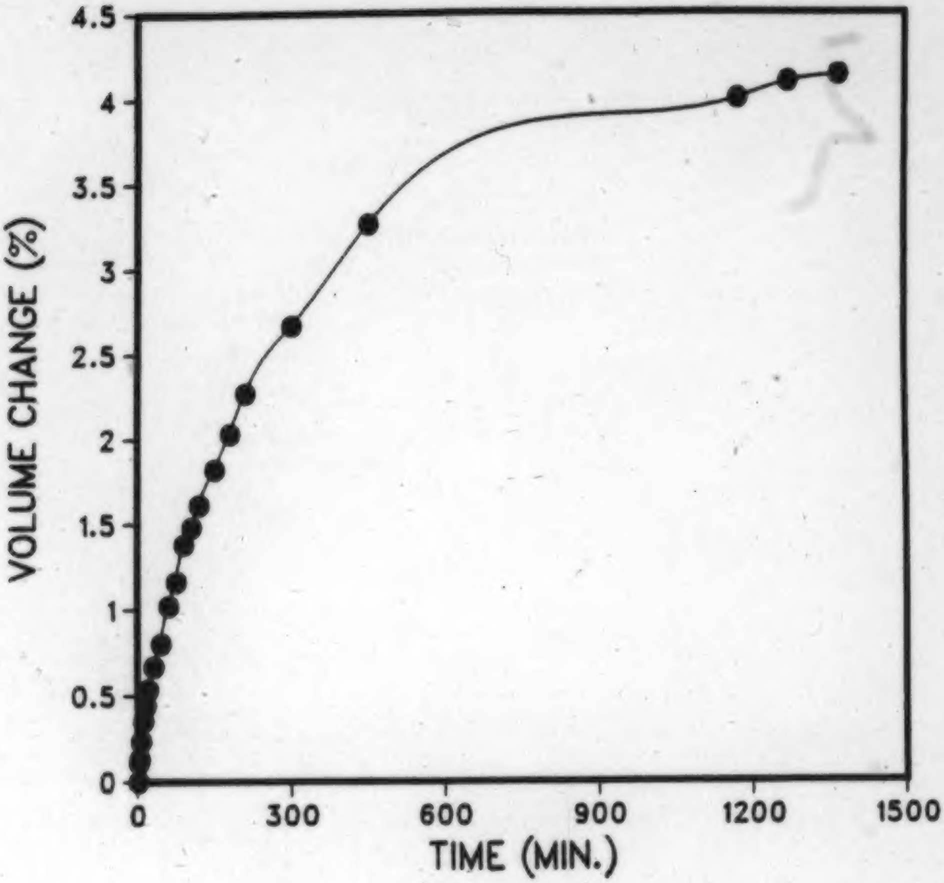

Figure 4.37 Unloading drained test on lean oil sand sample B-223 at 24°C with a vertical load of 300 kPa

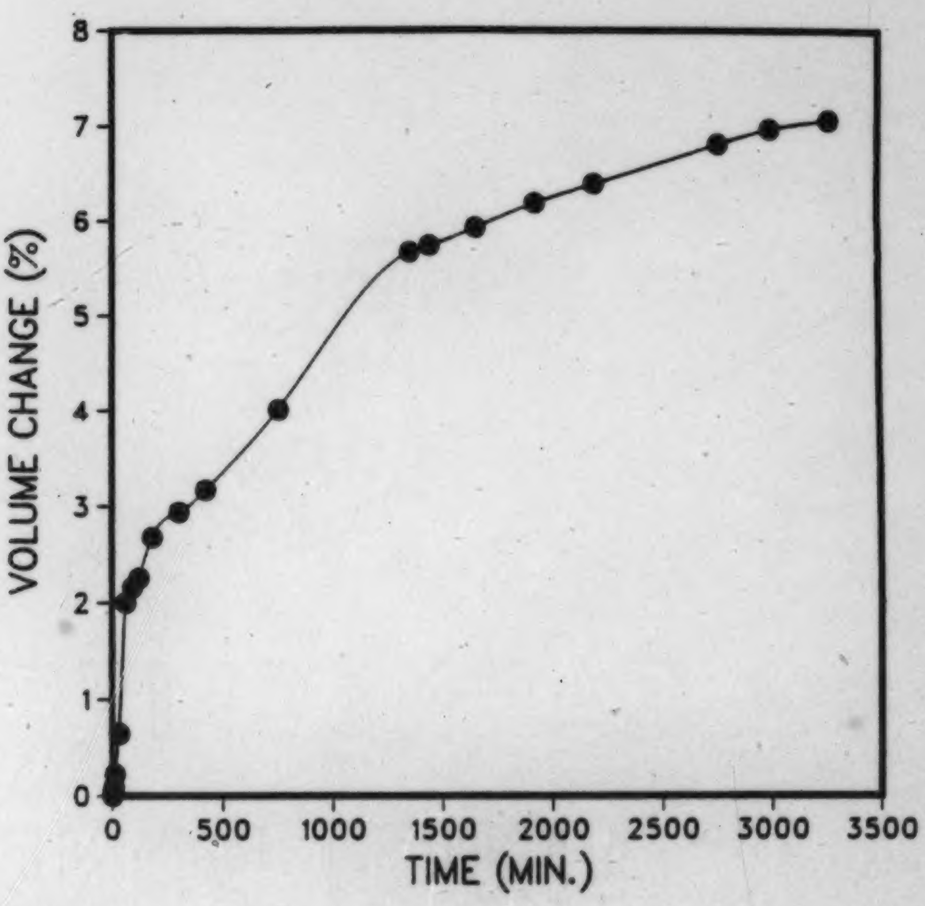

Figure 4.38 Unloading drained test on lean oil sand sample B-225A at 24°C with a vertical load of 120 kPa

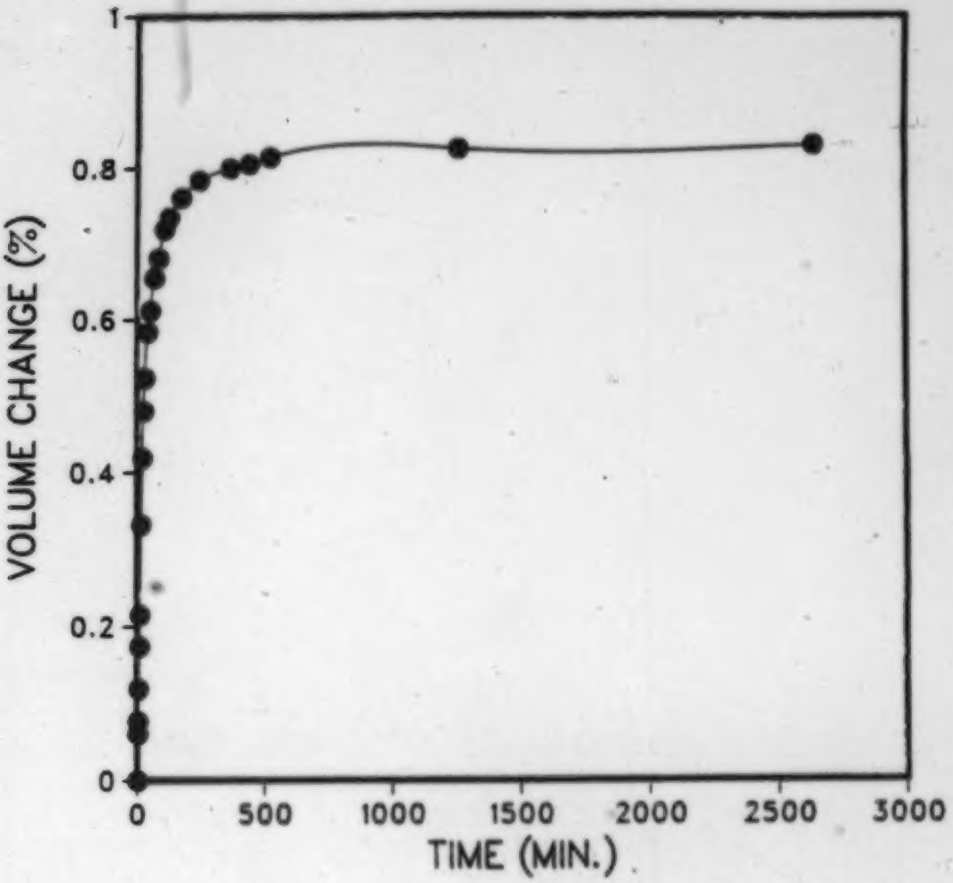

Figure 4.39 Unloading drained test on rich oil sand sample RB-5-1 at 24°C with a vertical load of 8 kPa

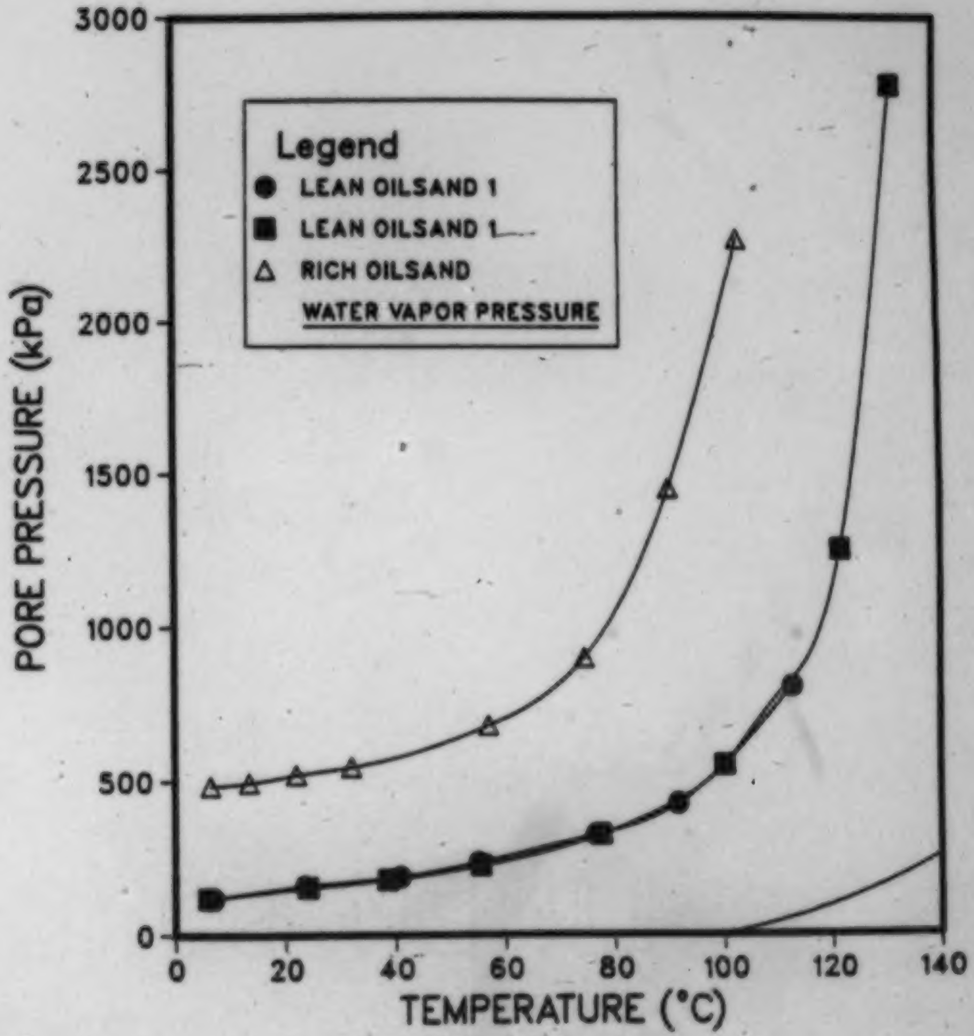

Figure 4.40 Effect of temperature on the gas saturation pressure for lean oil sand samples and a rich oil sand sample

5. EVALUATION OF DATA

5.1 TIME DEPENDENT BEHAVIOUR

5.1.1 Time Dependent Behavior of Tailing Sand Samples

Sobkowicz's curve fitting method and the associated model is, like most geotechnical models, a phenomological model. That is, he based his model on its ability to accurately curve fit the data points rather than determining all the pertinent parameters and modelling the process exactly. One of the weaknesses of a phenomological model is its inability to be extrapolated with confidence. Therefore in order to use Sobkowicz's model or curve fitting equations, any differences in samples or testing equipment must be checked to ensure that the test results are within the model's limitations

In the work done by Sobkowicz (1982) the gas evolution process was observed for carbon dioxide in a water and sand pack mixture. An empirical curve fitting technique was used to model the pore pressure change and the volume change that occurred during his testing. Equations 2.16 and 2.17 were the two methods used to model the volume change occuring during the gas evolution process.

$$\partial V_{fg}/\partial t=(V_2-V_{fg})/(t+A) \quad 2.16$$

$$\partial V_{fg}/\partial t=E*(V_2-V_{fg}) \quad 2.17$$

Equation 2.17 was used in his modeling as it was the easiest curve fitting technique to use, provided a reasonable fit to the data and has a theoretical basis. The E parameter was what determined the time rate of gas evolution and the model of his test results showed that the E values for his carbon dioxide saturated samples ranged from 0.0002 to 0.03. The small E parameters occurred at the beginning of the tests and as the gas evolved from the sample and the gas saturation increased, the E value rose in magnitude.

The volume changes that resulted from the gas evolution in the tailing sand samples in this research program were also modeled using Equation 2.17 (Figures 5.1 and 5.2). These tests were run at 24°C to compare with the results obtained from the Ottawa sand samples tested by Sobkowicz. Figure 5.3 combines the data obtained from Sobkowicz's testing and the results from sample T-525.

The E values for the tailing sand samples and the Ottawa sand samples are remarkably similar considering the differences in equipment and differences in saturation of the sample. The E values shown in Figures 5.1 and 5.2 are approximately 0.018 to 0.043. These are similar to the values that Sobkowicz obtained from curve fitting his data which had higher gas saturations (his larger E values occurred at gas saturations of 1.5-6%).

To determine the effect of the apparatus on the E value, the changing stress paths associated with the triaxial cell and the oedometer must be considered. The amount of gas which will evolve from the fluid is dependent only upon the fluid pressure and not on the effective stress state of the particle media surrounding the fluid (i.e. the solubility of the gas in the fluid is dependent on the fluid pressure). However, under a constant total stress the change in the effective stress state of the particle media directly affects the fluid pressure. The change in the effective stress state for the triaxial cell is much different than for the oedometer as the horizontal movement is zero for the oedometer and the horizontal stress is controlled by the triaxial cell. The triaxial cell can provide a uniform reduction in the overall effective stress resulting in an approximately equal drop in the pore pressure if the sample is saturated. The oedometer is not designed to measure the horizontal effective stress and as a result it cannot verify the triaxial results.

However, the oedometer will provide results similar to the triaxial cell at low effective stresses (approximately zero) because a change in volume associated with gas evolution will cause a minimal effective stress change and thus a minimal pore pressure change. As a result any test data at low effective stresses should be similar for both the oedometer and the triaxial cell and equation 2.17 should curve fit data from experiments from either test apparatus.

A test on tailings sand was also done at 50°C to determine the effect of temperature on the gas evolution process. The E values were plotted for several of the pressure drop increments and these are shown in Figures 5.4 to 5.6. These E values are an order of magnitude higher than the E values obtained from the tests done at room temperature and the gas evolved so quickly that the volume change can be considered to have occurred almost instantaneously.

5.1.2 Time Dependent Behavior of Lean Athabasca Oil Sand

The data from the oil sand samples was not modeled by equation 2.17 as accurately or as effectively as the data from carbon dioxide saturated sand samples. Table 5.1 lists the various samples that were tested, the associated E values (in terms of an upper and lower bound) and whether the resulting curve fit was excellent or poor. The results listed in this table are the bounds for all the increments that were curve fitted for each of the test samples. In some tests there were several increments that were curve fit and in others there was only one. Only the increments which were near an effective stress of zero were modeled as this was the only condition in an oedometer which accurately follows the model proposed by Sobkowicz (1982).

The testing done on the lean oil sand was done in two groups, the testing done at undrained conditions and the testing done under drained conditions. The unloading undrained tests were carried out at 6°C, 24°C and 60°C; six increments from these tests are curve fitted with equation 2.17 in figures 5.7 to 5.11. In these figures the actual data was not modeled well by equation 2.17. The presence of fractures in the samples was noted and it was felt that they provided a shorter path for the diffusing gases than the path length used in the curve fitting equation (The path length assumed for equation 2.17 is discussed in Appendix E). The fractures were small and appeared random in orientation and density. Some samples showed large fractures but the majority of fractures were small. A further discussion of these fractures and their implication will be discussed in the next section.

In order to significantly reduce the time for the gas to evolve the fracture density must be large and they should also be random to access all the bubbles. The unloading drained test provided a means to check the effect of the effective stress on the samples (this in turn controled the amount of fracturing in the sand matrix). Three unloading drained tests were performed under a vertical effective stress of 8 kPa (the weight of the piston), 120 kPa and 300 kPa. The data from the drained test could be modeled by equation 2.17 because the total stress remained constant, the pore pressure was kept constant at atmospheric pressure and the volume change was monitored with time.

The data from the unloading drained test with a vertical effective stress of 8 kPa was compared with the curve calculated by equation 2.17 and is shown in figure 5.12. As anticipated the data was not modeled well by equation 2.17 and it produced results similar in accuracy to the results obtained from the unloading undrained tests. Figures 5.13 and 5.14 give the data from the unloading drained tests under vertical loads of 120 kPa and 300 kPa respectively. The in situ gas saturation pressure is 128 kPa at 6°C and 170 kPa at 24°C and so one of the other drained tests was run with the vertical effective stress just under these pressures and one test was run with a vertical stress over these pressures. This was done to determine if the loading would have any effect upon the rate of gas evolution.

Figure 5.13 shows that the loading of 120 kPa made the data match the curve fitting equation better, but there was still some variation present. Figure 5.14 however, shows almost a perfect fit between equation 2.17 and the test data; up until this set of data this match had only been obtained from the tailing sand samples. This sample was also the only sample tested which had the vertical effective stress higher than the gas saturation pressure at that temperature.

The above data suggest that the presence of fractures in the lean oil sand samples affected the rate at which the gas evolved by changing the length of the drainage path. When the effective stress is kept higher than the gas saturation pressure then the gas evolution process is effectively modeled by equation 2.17. When the effective stress is less than the gas saturation pressure, there is enough pore pressure built up internally by the evolving gas to fracture the sample even though the pore pressure at the edge of the sample is atmospheric. The actual E values did not significantly change for the unloading drained tests under the various loads. The E values for all three unloading drained tests varied from 0.003 to 0.007 despite the changes in the vertical effective stresses (these E values are about 10 times smaller than the values obtained in the unloading undrained tests).

5.1.3 Drainage Mechanism

The problem of determining whether any curve fitting method that will acceptably model gas evolution appears to be influenced by the type of drainage mechanism exhibited by the sample. Sobkowicz (1982) assumed that the mechanism responsible for gas drainage was the combining of the occluded bubbles to form a path for the gas to flow out of the sample (see Appendix E). The inherent assumption with this model is that the majority of the dissolved gas diffuses toward the coalescing gas bubbles as opposed to diffusion toward the edges of the samples.

The transient behaviour as modeled by equation 2.17 accurately fitted the test results obtained by Sobkowicz on tests done on Ottawa sand. Figures 5.1 to 5.2 show the use of equation 2.17 in curve fitting the transient behaviour of the data from the tailing sand samples. The modeling is again very accurate and would indicate that the drainage mechanism in the tailing sand samples is similar to the gas drainage that was exhibited by Sobkowicz's samples.

The oil sand samples tested appeared to show an additional mode of drainage through the presence of fractures within the sample as discussed in the previous section. Figures 5.15 to 5.17 show the fractures that were observed from samples shortly after testing was complete. These fractures appear to be random in orientation and spacing.

When the oil sand sample data was curve fit by equation 2.17 the fit was generally poor (the gas evolved more quickly than predicted by equation 2.17). The presence of fractures and the inability to get a good empirical curve fit of the data indicate that the fractures are affecting the drainage mechanism. It is important to have a better understanding of the fracturing mechanism to determine the extent of fracturing and what is actually occurring to cause this amount of fracturing. Until this is determined, the gas drainage mechanisms can be modeled by equation 2.17 but a good fit should not be expected.

The fracturing will occur because the total stress is approximately equal to the pore pressure, but much lower than the gas saturation pressure. When the gas evolves the pressure acting on the sand structure is equal to the saturation pressure by the presence of the growing and forming bubbles within the pore spaces. The force from the growing bubbles will result in the presence of the fractures.

The presence of the fractures was also noted in the rich oil sand samples. The curve fitting that was done on the data from the rich oil sand samples produced similar results to those obtained from the lean oil sand. Figures 5.18 to 5.23 show the bounding E values for the tests done on the rich oil sand samples. The results again show a variation from the curve fitting model proposed by Sobkowicz (1982) and it is again assumed that the variation is likely due to the presence of fractures in the sample and the resulting difference in the mode of gas drainage.

5.2 EQUILIBRIUM BEHAVIOR

5.2.1 Solubility Coefficients

The combined solubility coefficient as defined in section 2.2 is the most important equilibrium property arising from the experimental work. It defines the amount of gas present in the bitumen at any given pressure under equilibrium conditions. This combined solubility coefficient can be determined directly from the gas volume versus pressure data from the unloading undrained tests or it can be obtained indirectly from equation 2.6 when the gas types and quantities are known.

The data obtained from the unloading undrained tests was the equilibrium volume of gas that evolved at specific pore pressures. By converting the volumes of evolved gas to amounts of gas or converting the gas volumes to equivalent volumes at atmospheric pressure, the data will form a straight line in accordance with the law of ideal solutions. The slope of this line is the combined solubility coefficient for all the gases in the bitumen and/or water.

The gas samples provide a ratio of gases that evolve and from these percentages the combined solubility coefficient can be obtained indirectly from the existing information in the literature on solubility of gases in bitumen and water.

5.2.1.1 Solubility of Carbon Dioxide in Water

One tailings sand sample was tested to determine the solubility coefficient at room temperature for carbon dioxide in water. The solubility coefficient for carbon dioxide in water is well known over a wide range of temperatures. Also all work done with carbon dioxide was in the linear portion of the solubility curve where Henry's Law is valid.

The solubility coefficient for carbon dioxide in water at 24°C should be 0.83 (cm^3/cm^3)/101 kPa and at 27°C it is 0.76 (cm^3/cm^3)/101 kPa. Tailing sand sample T-925 was run with each increment tested to equilibrium as shown in Figure 5.24 (previous tests were used only to obtain the transient properties of the carbon dioxide in the water). The pore pressure of the sample was incrementally reduced and the volume of the evolving gas measured at each increment. This procedure is shown on Figure 5.24 by moving right to left on the figure where the volume increases as the pressure is reduced. The slope of the line through the data points gives a solubility coefficient of 0.76 (cm^3/cm^3)/101 kPa. The experimental solubility coefficient from sample T-925 is only slightly lower than expected and is due to either contamination by air, slightly higher temperature or diffusion of the carbon dioxide into the connate water.

First, the carbon dioxide saturated water was forced into the sample with compressed air. This pressure will tend to drive the air into solution in the water. Because of the solubility of air in water even a small amount of air in the water will decrease the overall solubility.

Second, the water in the sample was flushed out and replaced by carbon dioxide saturated water. This flushing does not remove all of the water in the sample as the connate water next to the particles does not move when the water flows through the sample. As the carbon dioxide saturated water comes in contact with this connate water there is diffusion of carbon dioxide into the connate water. If this connate water does not get any carbon dixide dissolved into it, then the effective volume of water saturated with carbon dioxide is again slightly less than assumed and this will lower the solubility curve.

Third, a higher test temperature will decrease the solubility of carbon dioxide in water and the temperature necessary to get the solubility coefficient down to 0.76 $(cm^3/cm^3)/101$ kPa is only 27°C. The laboratory is not thermally controlled and the water temperature can fluctuate as the temperature of the room varied quite widely and was often higher than 24°C. The temperature of the water was not recorded and although the temperature was assumed to be 24°C the temperature of the pore liquid could be higher. One purpose of the unloading undrained test is to determine if the combined solubility coefficient could be obtained for the oil sand samples from the oedometer. All three of the above problems associated with the tailing sand were avoided in the testing of the oil sand. The oil sand samples did not require the flushing sequence and this eliminated the first two problems associated with the tailings sand samples. Also the temperature of the sample was closely monitored as the sample had to be warmed up to room temperature before the sample could be tested and as a result the exact temperature of the sample was known.

5.2.1.2 Combined Solubility Coefficents of Gases in Oil Sand

The combined solubility coefficients are obtained from unloading undrained tests as described in section 3.2.2. In the lean oil sand the combined solubility coefficients were obtained at three temperatures to determine the effect of temperature. The lean oil sand samples were available from only one depth and so the samples are all saturated with gases at the same pressure. The combined solubility coefficients obtained from the lean oil sand samples are shown in figures 5.25 to 5.27 and from the rich oil sand samples are shown in Figures 5.28 to 5.32.

The combined solubility coefficient for the lean oil sand (at 24°C) is 0.074 $(cm^3/cm^3)/101$ kPa and from 0.19 $(cm^3/cm^3)/101$ kPa to 0.22 $(cm^3/cm^3)/101$ kPa. for the rich oil sand samples. As the testing temperature increases, the solubility of the gases in the pore liquids is lowered. This requires the pressure be increases if the gases are to be maintained in a dissolved state. The total amount of dissolved gas remains constant (and thus the volume of gas expected is constant when measured at NTP), but the slope of the pressure/volume curve will be flatter to reflect the increase in pressure required to keep the gases in solution. Also, a decrease in the test temperature should decrease the gas saturation pressure and increase the slope (and thus the combined solubility coefficient) of the of the pressure/volume curve.

Two tests were run on the lean oil sand to determine the effect of temperature on the combined solubility coefficient. One test (B-223 as shown in Figure 5.27) was run at 60°C and another test (B-225 as shown in Figure 5.25) was run at 6°C. The combined solubility coefficient for these tests were 0.164 (cm^3/cm^3)/101 kPa at 6°C and 0.044 (cm^3/cm^3)/101 kPa at 60°C as shown in Table 5.2.

The presence of premature gas evolution is also shown here in these figures. The reasons for this premature nucleation of the gas is discussed later in section 5.2.2.2. under the topic of the gas saturation pressure.

5.2.1.3 Combined Solubility Coefficients from Gas Samples

The combined solubility coefficient can also be obtained from the solubility data of gases in bitumen and water and a knowledge of the types and ratios of the gases in the pore liquid. The details of obtaining the combined solubility coefficient from the above information is described in section 2.2. The gases obtained from gas tests, the percentage of water and bitumen in the pore liquid and the combined solubility coefficient are shown in Table 5.3.

The gases measured by the chromatograph appear to also contain some contamination from air. Section 5.2.2.3. describes the reasons in eliminating the oxygen (and nitrogen in the proportion equivalent to that of air). The remaining gases are very consistent in composition and the resulting combined solubility coefficients.

The combined solubility coefficients obtained from equation 2.13 are very close to the values obtained from the actual testing (see Table 5.2). They tended to be slightly higher than the actual values but this could be the result of inaccurate testing of the gases, the result that the actual unloading undrained tests may not have been run completely to equilibrium or that the assumptions used in developing equation 2.13 assumed ideal solutions.

The presence (or lack of) nitrogen makes a significant difference in calculating the combined solubility coefficient and the gas sampling and testing methods are not accurate enough to closely determine the amount of nitrogen.

5.2.2 Gas Saturation Pressure

Both the solubility coefficient and the gas saturation pressure must be obtained to determine the amount of gas present in oil sand. The value of the solubility coefficient for oil sand is shown in the previous section and now an indication of the gas saturation pressure will be obtained.

The gas saturation pressure (also called the bubble point pressure) is an equilibrium condition where the liquid is saturated with the dissolved gas at a set pressure and any additional decrease in pressure will produce the presence of free gas in the sample. Because the gas saturation pressure is an equilibrium condition, there is a unique pressure for the evolution of a specified gas concentration in a liquid when tested at a specific temperature.

This specified amount of gas can evolve at other pressures in the liquid if there is insufficient time to allow the nucleation of the bubbles (thus creating a supersaturation conditon within the liquid) or if the gas concentration in the liquid is not uniform. If a supersaturation condition exists in the liquid, then the gas evolution will appear to start at lower pressures than would be anticipated at truly equilibrium conditions. An uneven distribution of the dissolved gas in the liquid will cause the formation of the gas bubbles to initiate at concentration peaks and this pressure will be higher than the equilibrium gas saturation pressure because gas concentration peaks in the liquid will always be higher than the uniform gas concentration. Sample RB-5-5 gives an example of the presence of concentration peaks which result in premature evolution of the gases in the bitumen. In Figure 5.29 the sample's data is shown and the line showing the combined solubility coefficient. The gas saturation pressure obtained in this thesis assumes a uniform concentration throughout the pore liquids.

The gas saturation pressure of the various oil sand samples can be obtained and compared by two different techniques, the measurement of the in situ pore pressure (and assume that the in situ pore pressure is the pressure at which the gases are dissolved in the pore liquids) and from the samples tested in the laboratory. The gas saturation pressure of the gas in the oil sand can (as a first assumption) be assumed to be equal to the in situ pore pressure. Measurements by Jha, Montgomery and Strausz (1979) demonstrates that the bitumen is degenerating with time at a very slow but measureable rate at in situ temperatures. Over a long period of time the pore liquids should be saturated at the in situ pore pressure. Also, if the total stress is reduced (i.e. stripping of the overburden) the pore pressure will remain approximately constant because the evolving gas will tend to maintain the pressure near the saturation pressure (assuming an undrained condition). When these conditions exist the pore pressure, although not an exact indicator of the gas saturation pressure, will give a good approximation of the in situ gas saturation pressure.

The lean oil sand was obtained from a borehole at the Syncrude plant site near Fort McMurray. The sample of lean oil sand tested was from a depth of 12.8 m as shown in Figure 5.33. There were no pore pressure measurement taken in this borehole and only an approximation to the pore pressure can be made, but the water table was measured in the borehole at a depth of 1.0 m below the surface. Before the plant was built the ground was initially covered by muskeg and as a result the maximum pore pressure expected at the depth from which the sample was taken should be 126 kPa (12.8m of water and hydrostatic pressure conditions).

The rich oil sand was taken from a borehole on the Syncrude mine site as shown in Figure 5.34. There were two rich layers of oil sand identified at this location. The first layer started at a depth of 15 m and went to a depth of 29 m below the mine bench. The second layer started at a depth of 34 m and went to 42 m below the mine bench. The two layers were separated by a clayey layer and intermittent siltstone layers. The depths were measured from the surface of the mine bench. The mine bench at this borehole location is approximately 17 m. below the original ground reference.

Two pneumatic piezometeres were placed at depths of 17.2 m and 38.0 m below the bench. The pore pressure measured in the upper zone was measured at 220 kPa and in the lower layer of rich oil sand was measured at 500 kPa. The water table was consistently measured at a depth of 1.8 m below the bench as measured in a series of boreholes in the area.

The pressures obtained from the two piezometers (as shown in Figure 5.34) indicate that the pore pressures are much higher that the water table indicates and even higher than the hydrostatic pressure from the top of the bench. At the time this excess pore pressure was assumed to be the result of the additional weight from the nearby oil sand windrow. However, the excess pore pressure is much greater by a significant amount in the lower oil sand layer than it is in the upper layer. At the site of the sampled boreholes, the premining surface was at an elevation of 308 m and the area was covered by muskeg. If the oil sand was saturated with gas at the premining pore pressure (assuming hydrostatic pressure) the gas saturation pressure would be 550 kPa in the lower layer which is remarkably close to the pressure measured by the piezometer. The upper layer would have a gas saturation pressure under these conditions of 375 kPa; much higher than the 220 kPa that was measured in the field. The piezometers, although giving different readings gave some indication that the gas saturation pressure may not be as straight forward as initially expected.

The unloading undrained tests done on the oil sand samples can also be used to determine the gas saturation pressure. Figures 5.28 to 5.31 shows the volume of gas evolving from rich oil sand samples which were obtained from this upper layer of rich oil sand. In Figure 5.29 the gas saturation pressure is 375 kPa but the pressure at which the gas started to evolve is 520 kPa. The insitu pore pressures obtained by the piezometers were lower than the gas saturation pressure which means that there is probably free gas present in the oil sand in situ. During testing this free gas is driven back into solution and produces gas concentration peaks at the nucleation sites. If sufficient time is not given to allow the concentration peaks to diffuse down, then as the pore pressure is reduced the gas will evolve at these concentration peaks first. The concentration of gas molecules in these peaks is higher than the average concentration and it results in an apparently higher gas saturation pressure than actually exists.

The data from the unloading undrained tests was used to produce the correct gas saturation pressure in another way. When the volume of gas is corrected to a common pressure at each increment, then the data plots along a straight line (the initial evolving gas does not fall on this line and it indicates the presence of gas concentration peaks). The intersection between the straight line through the data points and the pressure axis indicates the true gas saturation pressure. In Figure 5.29 this produces a gas saturation pressure of 375 kPa at room temperature.

The presence of concentration peaks is more pronounced in the rich oil sand as the diffusion rate in the rich oil sand is lower than in the lean oil sand. As a result the time required to have uniform concentration of gas in the pore liquids is also longer in the rich oil sand samples.

The temperature at which the sample is tested has a significant effect on the gas saturation pressure. The amount of gas dissolved in the pore liquid is constant (except at high temperatures where the bitumen breaks down), but the solubility coefficients of the gases in the bitumen vary with temperature. Thus the gas saturation pressure will be lower when the sample is tested at a lower temperature than when the sample is tested at higher temperatures.

The effect of temperature on the lean oil sand was determined by testing samples at three temperatures 60°C, 24°C and 6°C. The gas saturation pressure varied accordingly as shown in figures 5.25 to 5.27 with the gas saturation pressure at 290 kPa at 60°C, 170 kPa at 24°C and 128 kPa at 6°C. To determine the effect of a wider range of temperatures on gas saturation pressures, an undrained test was done as described in section 3.4.5 (Figure 4.40). This figure shows the increase in gas saturation pressure over a range of temperature, but of interest is the dramatic rise in the gas saturation pressure at higher temperatures. This is due either to a dramatic drop in solubility at higher temperatures, a cracking of the bitumen releasing the gas or the vapourization of the natural gas liquids.

The last option is likely the case as the temperature will cause natural gas liquids like propane, butanes and pentanes to reach their bubble point pressure and enter their two phase regions. The interaction of these components will produce a gas saturation curve similar to that obtained in Figure 4.40; an attempt to produce that curve theoretically requires an equation of state program and that is beyond the scope of this thesis.

Figure 4.40 was obtained from testing two samples of lean oil sand and one rich oil sand sample. Each lean oil sand sample was tested at a series of specified temperatures to determine the saturation pressure at each temperature increment. There was some concern that the effect of forming bubbles to determine the gas saturation pressure might cause a concentration peak and produce an inaccurate gas saturation pressure at subsequent temperature increments, but this does not appear to have happened during the testing. The first test was at 24°C and it was retested at 24°C after the sample was tested at high temperatures and cooled and also after the sample was cooled to 6°C and then warmed back up to 24°C. The results from the two samples tested produced a curve which is very consistent both as the temperature was raised and as it was lowered. This supports the theory that the steep rise in saturation pressure is due to the vapourizing of natural gas liquids and not the cracking of the bitumen which would produce additional gases and require a higher gas saturation pressure on the cooling leg of the test. Finally the gas saturation pressure obtained in this manner at 24°C is very similar to the gas saturation pressure obtained from Figure 5.25 to 5.30 which were also tested at 24°C.

The rich oil sand sample was also tested at various temperatures to determine the gas saturation pressure at each temperature increment. The rich oil sand produced a gas saturation versus temperature curve which was similar in shape as that obtained from the lean oil sand sample (Figure 4.41). The testing procedure only determines when the gas is starting to evolve with the assumption that this is also the gas saturation pressure. For the rich oil sand this was a poor assumption as shown by sample RB-5-2 in Figure 5.28 where the gas evolved at pressures higher than the gas saturation pressure. The gas evolved at pressures that were higher than the gas saturation pressures measured in Figures

5.28 to 5.30 at their respective temperature. However, these figures also show a classic example of the presence of premature gas bubble formation resulting from gas concentraion peaks. For example, the gas saturation pressure in Figure 5.29 is 375 kPa but the gas started to evolve at 525 kPa. As a result an indication of the effect of temperature can be obtained, but the actual gas saturation pressure at various temperatures can only be estimated from this figure when used in conjunction with several of the unloading undrained tests.

The test is very good when the gas concentration is uniform throughout the sample. When gas bubbles have to be driven into solution, sufficient time has to be taken to ensure a uniform gas concentration. Once a test procedure is developed which can assure the uniform gas concentration throughout the sample then this test should be redone.

The gas saturation pressure obtained from the samples tested in the laboratory can now be compared to the pore pressures measured in the field where the in situ temperature of the oil sand is 6°C. The gas saturation pressure in the lean oil sand sample tested at 6°C was 128 kPa. This is approximately equal to hydrostatic pressure starting from the ground surface (the initial pore pressure conditions up to 1973 when the site was drained and the muskeg stripped). After 12 years (the cores were obtained in 1985) there has been no loss of gas by drainage or diffusion. This is not surprising as the drop in pore pressure by drainage was only 10 kPa (1 m of water) and numerous horizontal seams of clayshale exist in the Upper McMurray Formation at this site. The test results do suggest that there is now a small amount of free gas present in the lean oil sand matrix.

There are two layers of rich oil sand located in the borehole from which the rich oil sand samples were obtained and piezometers were located in each of the two layers. The first piezometer was located at a depth of 18.6 m in the first layer of rich oil sand. The pressure at this depth was measured at 220 kPa which is equivilent to 22.4 m. of water. This is 1.8 meters higher than the bench level and 3.6 m higher than the measured water table at the time of drilling for that area. The samples from this rich oil sand layer measured a gas saturation pressure of between 335 and 345 kPa (equivilent to approximately 34.7 m of water). To keep this gas in solution the pore pressure would have a head of water 16.1 to 16.3 m higher than the bench level. There was approximately 17 m of overburden removed from this area and this indicates that the samples were likely saturated with gas from the premining pore pressure conditions. Also, the stripping of the overburden, although causing a decrease in pressure, has not allowed any of the gas to escape. As a result the oil sand is still saturated with gas from the premining in situ pore pressure and the removing of the overburden has allowed a small amount of the gas to evolve but it has not caused the gas to dissipate.

The pore pressure in the second layer rich oil sand measured with a second piezometer at a depth of 38.1 m below the bench was 500 kPa (51.0 m of water). The gas saturation pressure obtained from the sample tested in the laboratory was 530 kPa (54.0 m of water)at 24°C. When the original overburden is added to the 38.1 m depth of sampling then the total height from the original ground level is 55.1 m.

The sample from this second layer is saturated with gas at the premining in situ pore pressure just as the samples in the first layer of rich oil sand. Both of the rich oil sand layers tested produced a gas saturation pressure of one meter below the original premining ground level even though they were vertically separated from each other by 16.5 m of oil sand.

The lower pore pressures measured in the field are to be expected as the unloading of 17 m of overburden would cause some elastic rebound especially in the upper layer of rich oil sand. The extra pore volume from rebound would be filled with evolving gas and thus lower the concentration of gas in the bitumen resulting in a lower pressure requirement to keep the remaining gas in solution. The actual pore pressure at any depth would be conditional on the amount of volume change that has occurred in the oil sand.

5.2.3 Gases Present in Oil Sand

In Table 4.5 the gases measured by the gas chromatograph are listed from the lean oil sand and rich oil sand samples tested. The major gases measured are methane, carbon dioxide, nitrogen and oxygen with some samples giving trace amounts of carbon monoxide, ethane and propane.

The process of flushing the air out the cell was not easily done as the cell was not suited to flushing out all the air. The small drainage ports amd the sharp corners of the cell chamber provide dead spaces which are difficult to purge. Also the sample is not smooth but has small irregularities along the side which can trap air.

The oxygen and a proportional amount of nitrogen were removed from the gas sample as a contaiminent. The work by Jha, Montgomery and Strausz (1979) shows that the bitumen will break down in the presence of oxygen even at in situ temperatures. The oxidation rate of the bitumen was quite slow but definitely measureable, and if this exists naturally then there should not be any oxygen present in the bitumen in situ. As a result all of the oxygen and an air equivilent amount of the nitrogen obtained in the samples was considered a contaminent and subtracted from the gases when the combined solubility coefficient was calculated.

There is a small amount of nitrogen remaining in the gas samples even when all the oxygen and enough nitrogen to make the proportions of air is removed from the gas samples. This could be the result of actual nitrogen gas in the bitumen or from air comtamination in the gas sampling procedure where the oxygen has reacted with the bitumen. It is impossible to determine where this extra nitrogen originates from, but it is instructive to look at the Combined Solubility Coefficients that can be obtained by leaving the nitrogen in or omitting it. The Combined Solubility Coefficient for both cases are shown in Figures 5.35 to 5.36. When the nitrogen is left in the gas sample the Combined Solubility Coefficient is close to the values obtained from the volumes measured in the unloading undrained tests. When all the nitrogen is assumed to be a contaminent, then the Combined Solubility Coefficient is about double the value obtained from the tests. As a result the nitrogen is considered to be part of the in situ gases present in the pore liquids.

Table 5.1 E values obtained by curve fitting oil sand samples

Sample No.	Material	Lower Bound E Value	Upper Bound E Value	Remarks
T-525	Tailing Sand	0.018	0.043	Excellent fit
B-222	Lean Oil Sand	0.003	0.0045	Good fit
B-223	Lean Oil Sand	0.003	0.005	Excellent fit
B-224	Lean Oil Sand	0.014	0.028	Fair fit
B-225	Lean Oil Sand	0.0035	0.007	Excellent fit
B-225A	Lean Oil Sand	0.001	0.005	Fair fit
B-226	Lean Oil Sand	0.006	0.017	Poor fit
RB-5-1	Rich Oil Sand	0.013	0.028	Fair fit
RB-5-2	Rich Oil Sand	0.002	0.008	Poor fit
RB-5-5	Rich Oil Sand	0.0008	0.009	Fair fit

Table 5.2 Combined solubility coefficients obtained from unloading undrained tests

Test No.	Combined Solubility Coefficient (cm³/cm³)/101 kPa	Test Temperature (°C)	Sample Type
T-925	0.76	24	Tailing Sand
B-225	0.164	6	Lean oil sand
B-224	0.074	24	Lean oil sand
B-223	0.044	60	Lean oil sand
RB-5-2	0.194	24	Rich oil sand
RB-5-5	0.187	24	Rich oil sand
RB-5-10	0.186	24	Rich oil sand
RB-5-12	0.19	6*	Rich oil sand
RB-15-8	0.221	24	Rich oil sand

*last increment at 24°C

Table 5.3 Combined solubility coefficients calculated from gases obtained from the gas samples

Sample Number	Bitumen Fraction of Liquid	Water Fraction of Liquid	Average Solubility Coefficient at 24°C in Water & Bitumen			Combined Solubility Coefficient	Temp. °C
			CO_2	CH_4	N_2		
	1.00	0	0.80	0.21	0.069		24
	0	1.00	0.83	0.03	0.016		24
B-227	0.33	0.67	0.82	0.09	0.033	0.11	24
B-228	0.33	0.67	0.57	0.08	0.029	0.080	40
RB-5-4	0.867	0.133	0.80	0.19	0.062	0.20	24
RB-5-7	0.913	0.087	0.80	0.19	0.064	0.15	30
RB-5-8	0.913	0.087	0.80	0.19	0.058	0.20	24
RB-15-1	0.942	0.058	0.80	0.20	0.066	0.22	24
RB-15-2	0.942	0.058	0.80	0.20	0.066	0.19	24

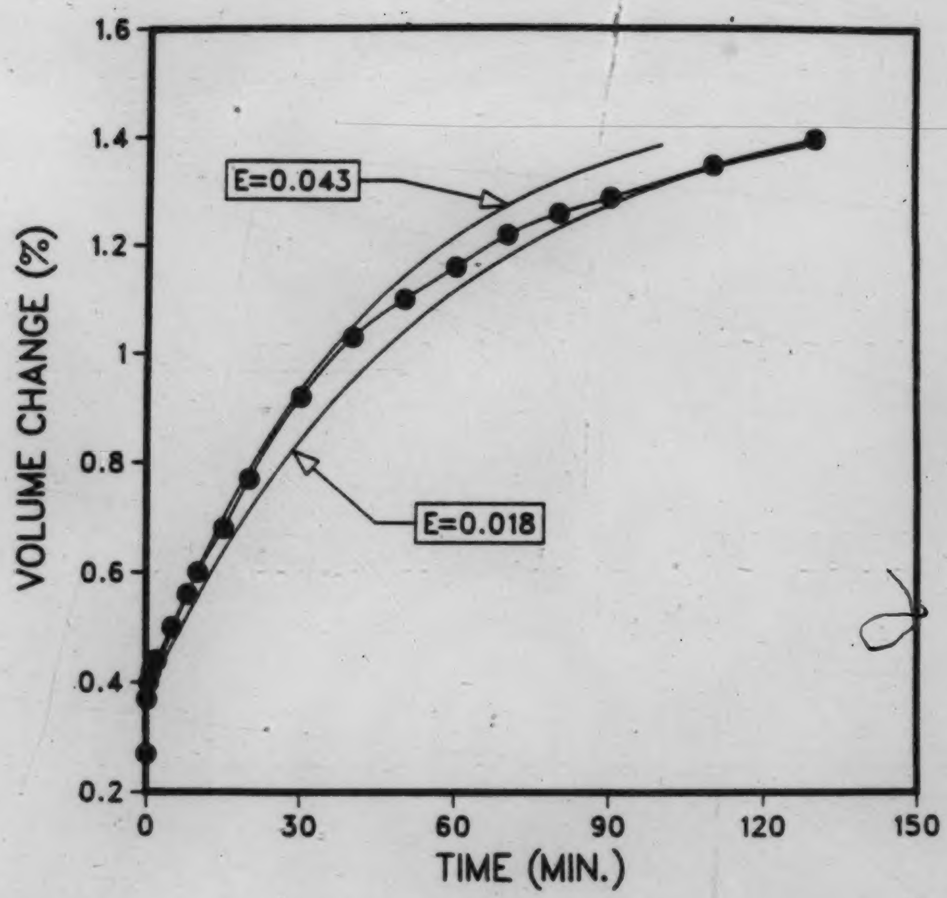

Figure 5.1 E values obtained by curve fitting data from T-525G

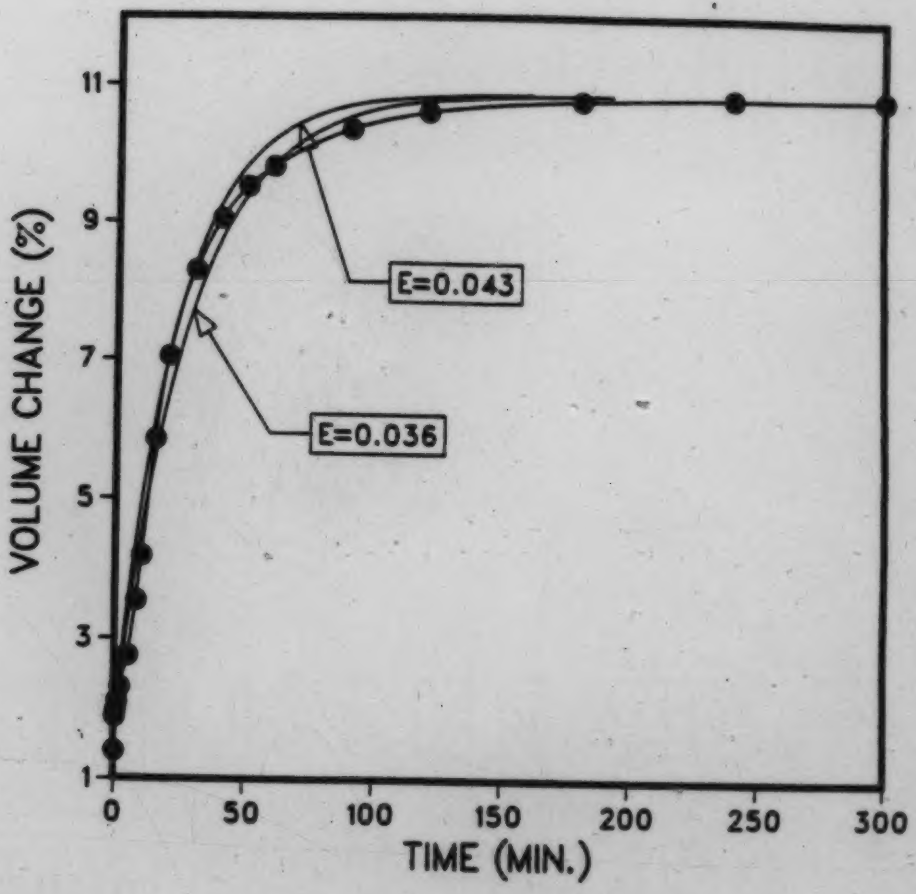

Figure 5.2 E values obtained by curve fitting data from T-525H

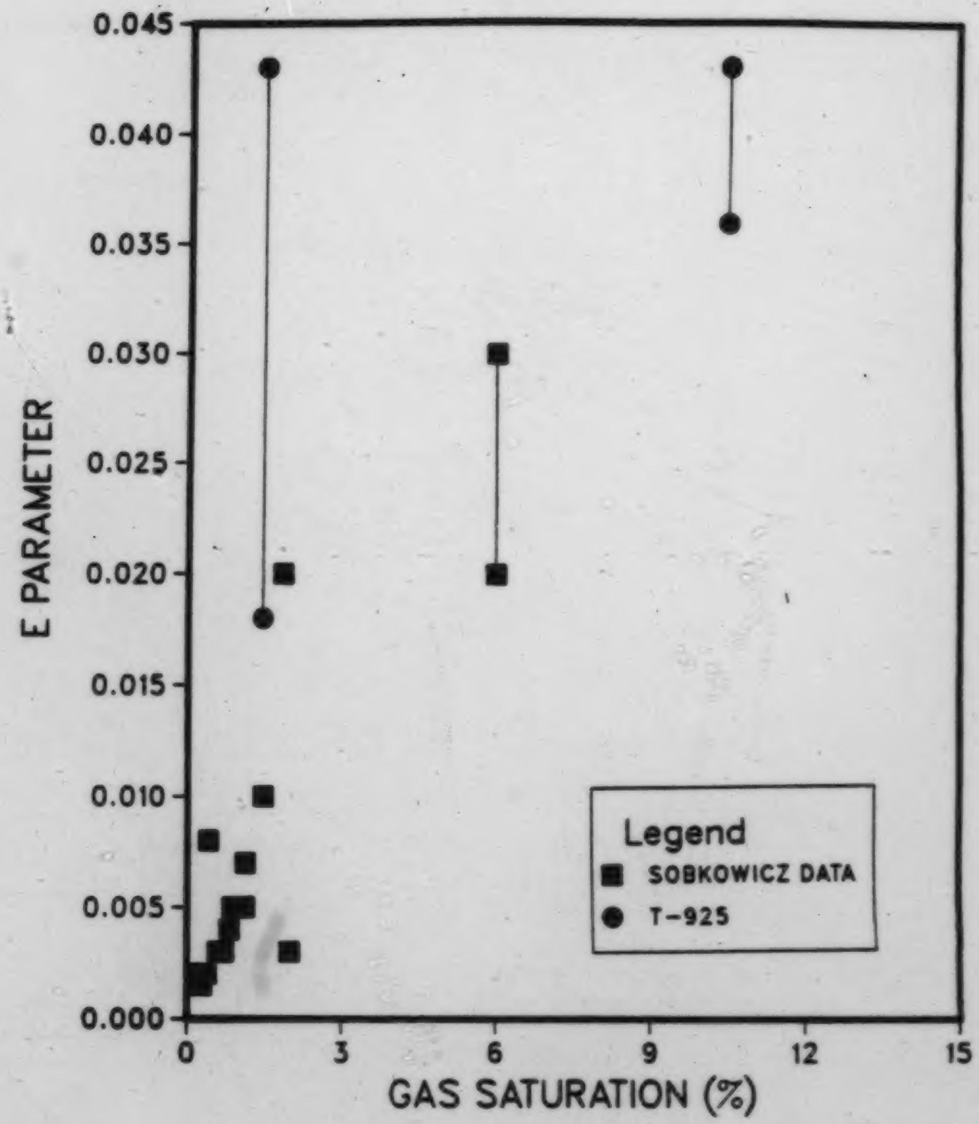

Figure 5.3 Combination of E values from Sobkowicz's data and from sample T-525

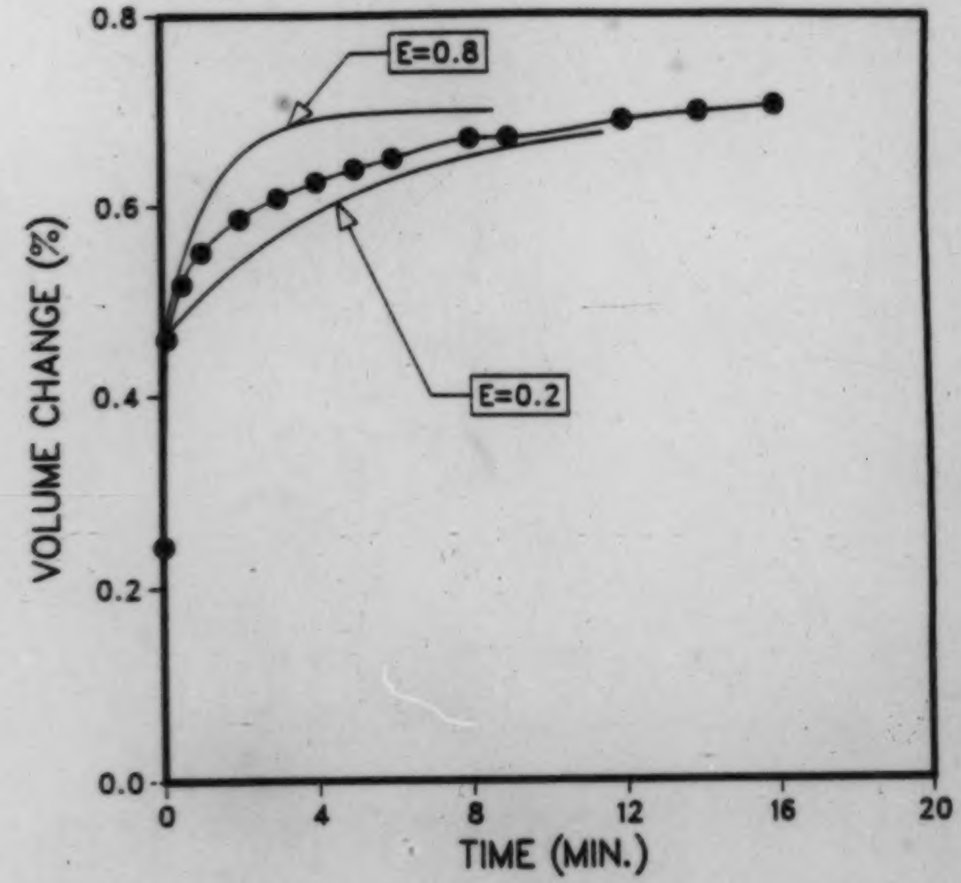

Figure 5.4 E values obtained by curve fitting data from T-350F

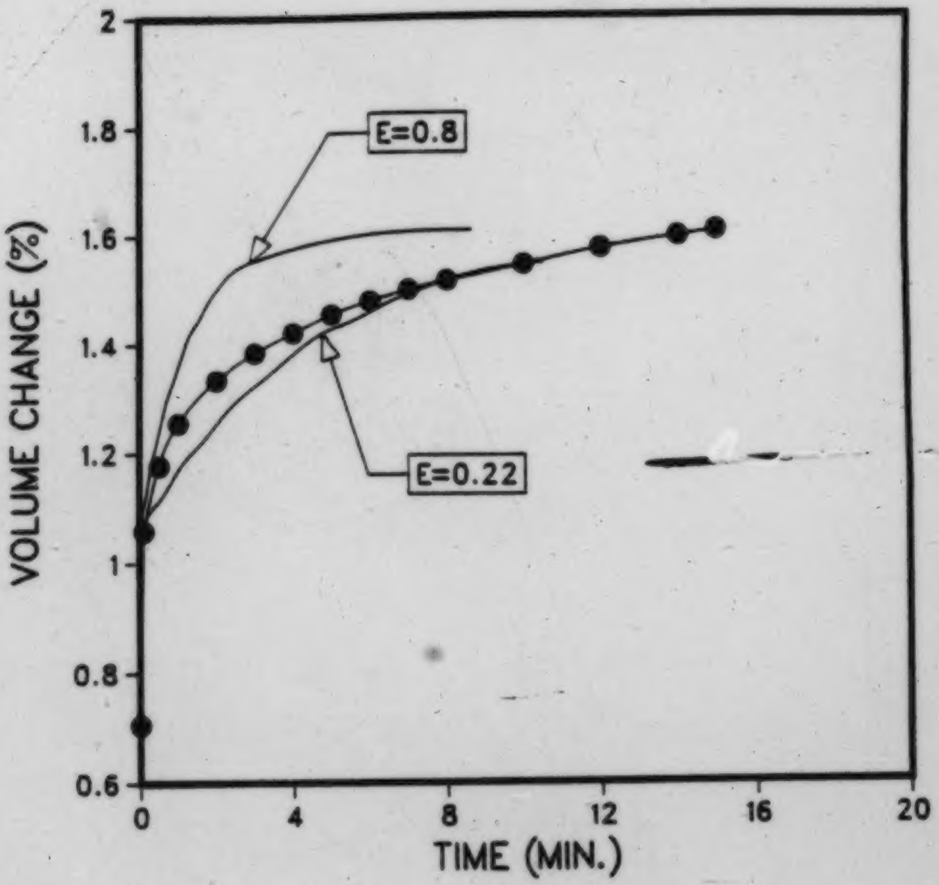

Figure 5.5 E values obtained by curve fitting data from T-350G

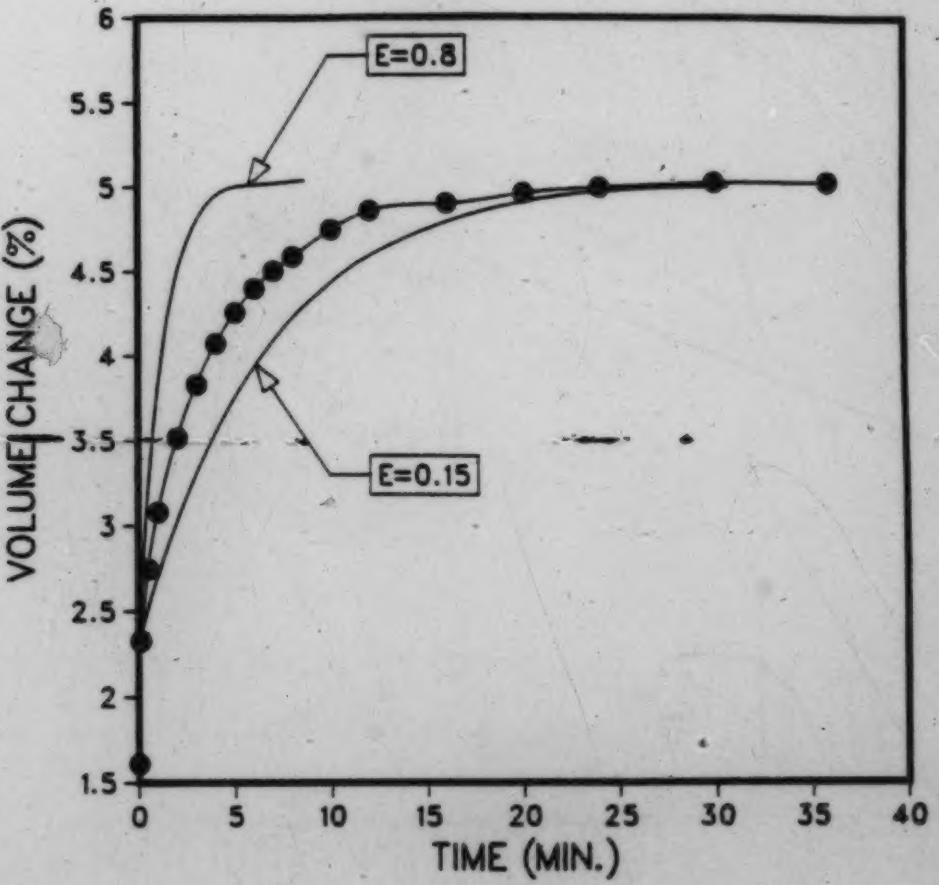

Figure 5.6 E values obtained by curve fitting data from T-350H

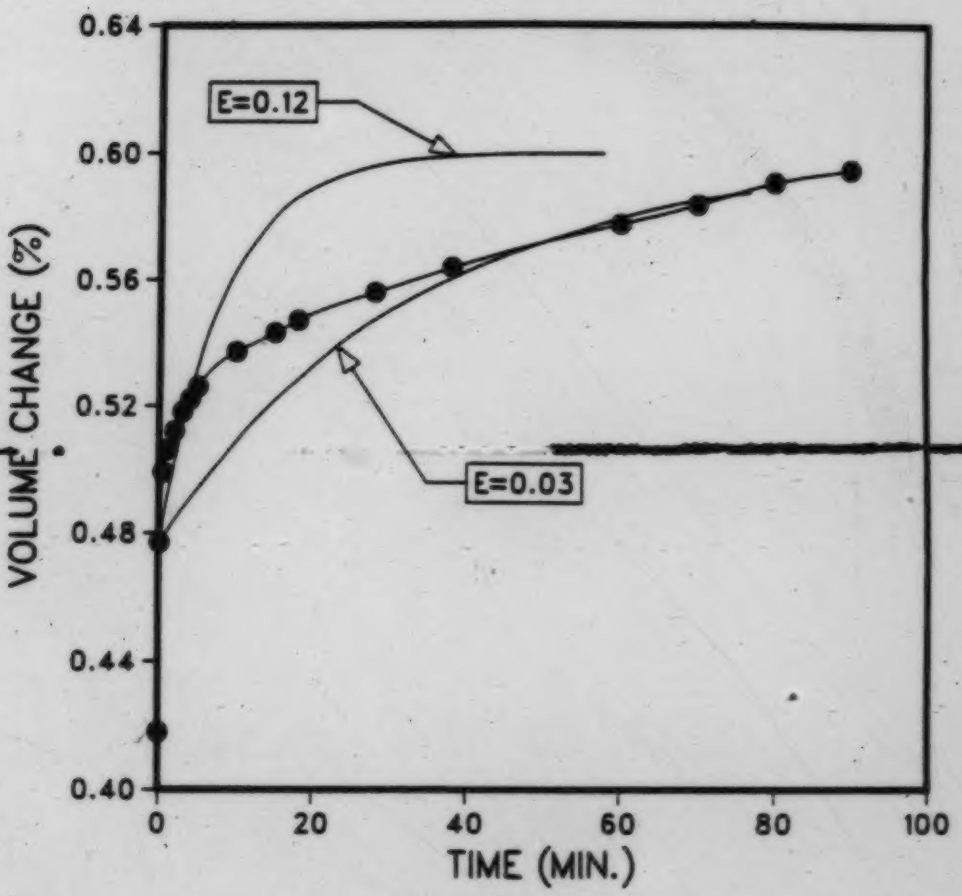

Figure 5.7 E values obtained by curve fitting data from B-223G

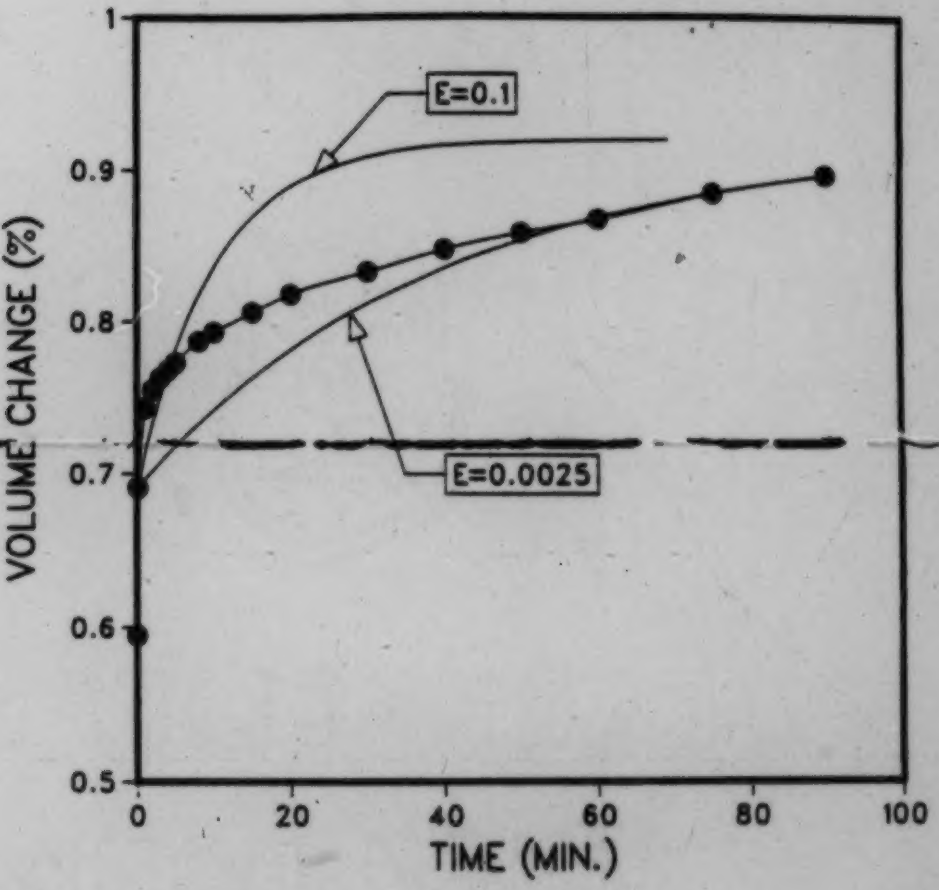

Figure 5.8 E values obtained by curve fitting data from B-223H

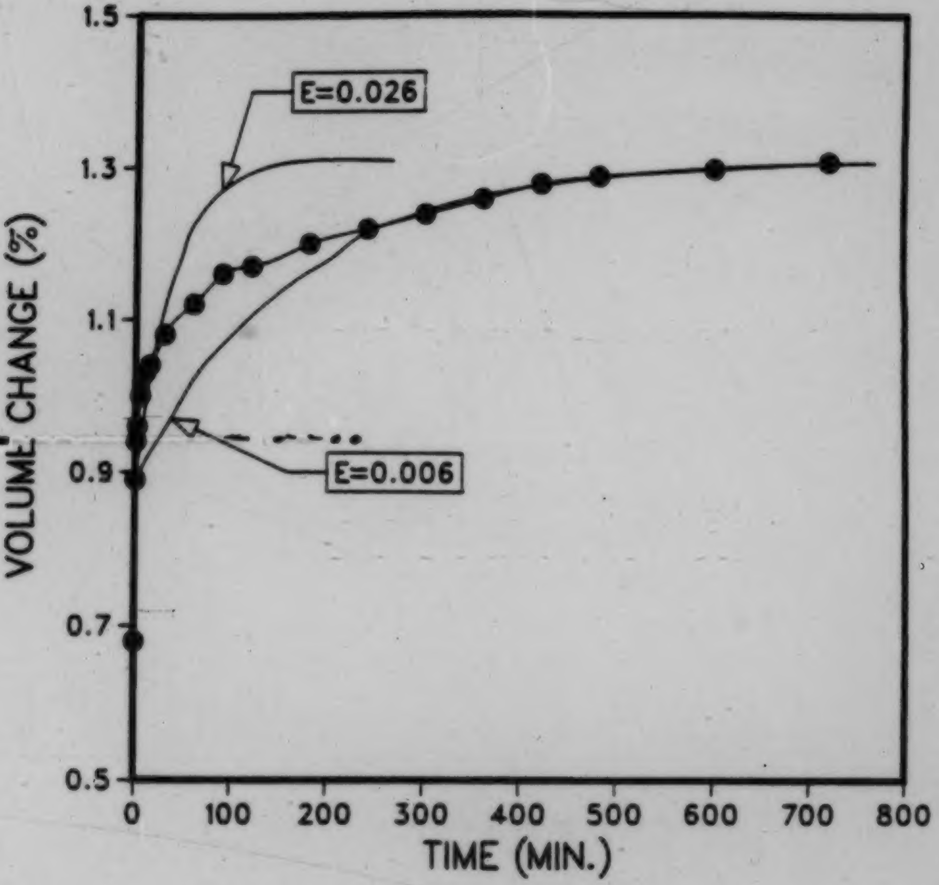

Figure 5.9 E values obtained by curve fitting data from B-224J

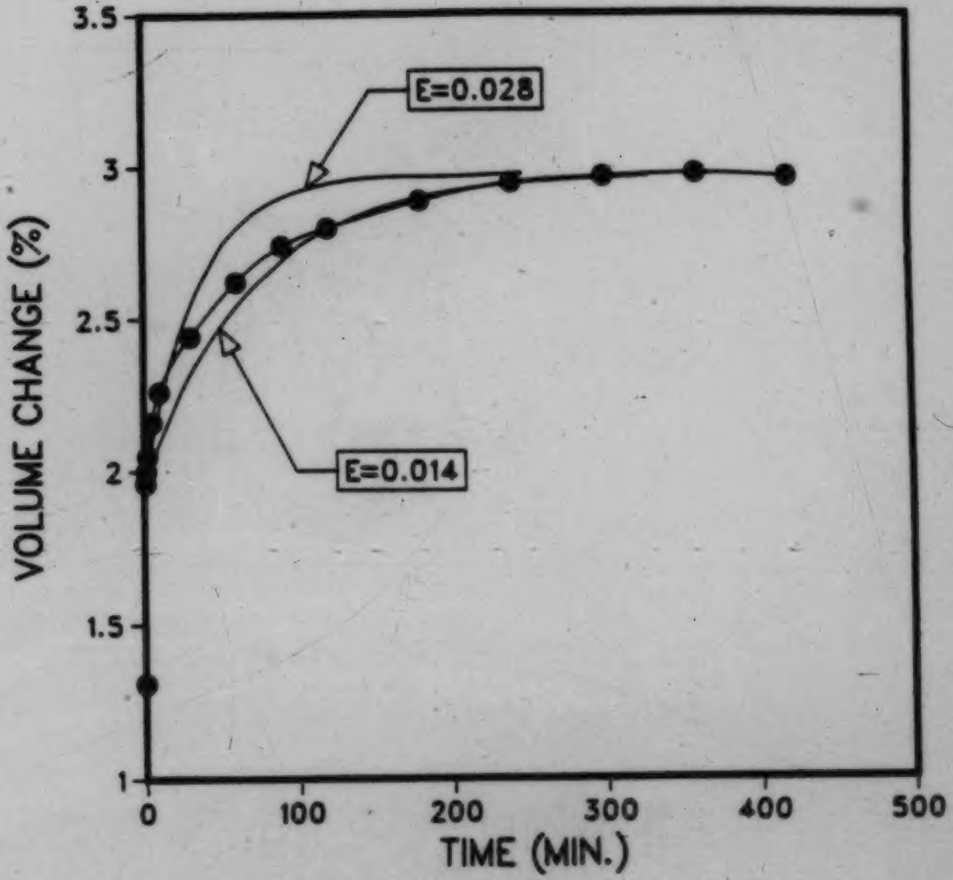

Figure 5.10 E values obtained by curve fitting data from B-224K

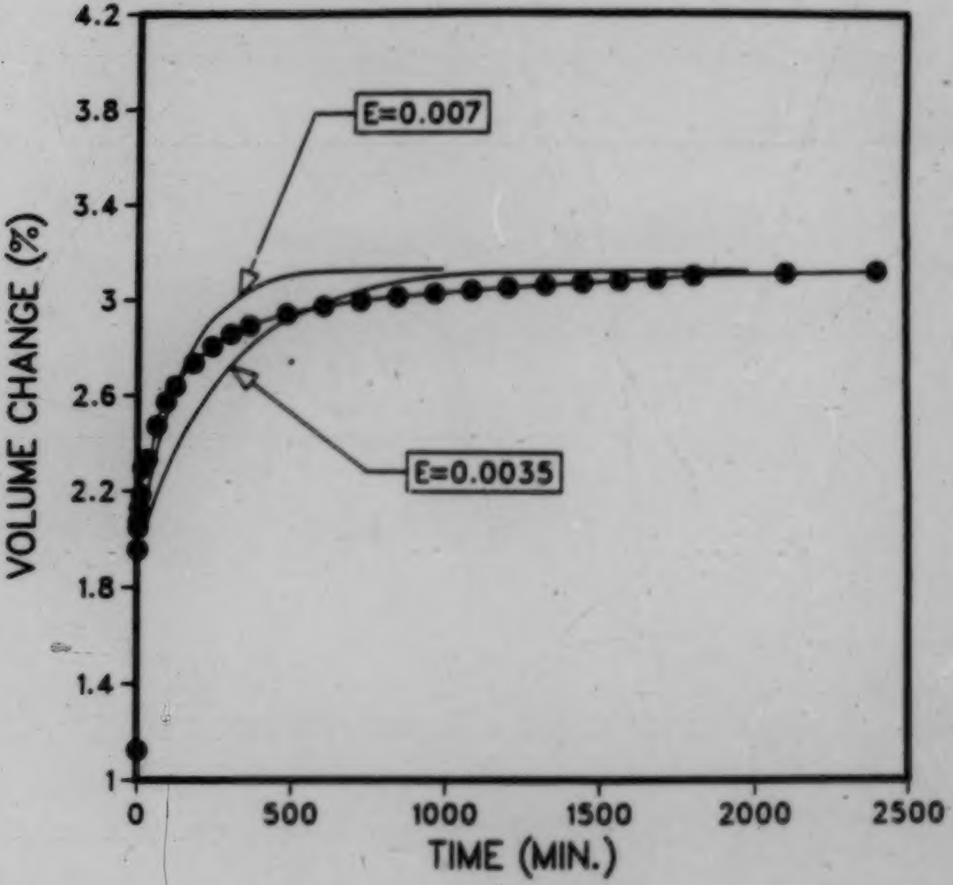

Figure 5.11 E values obtained by curve fitting data from B-225G

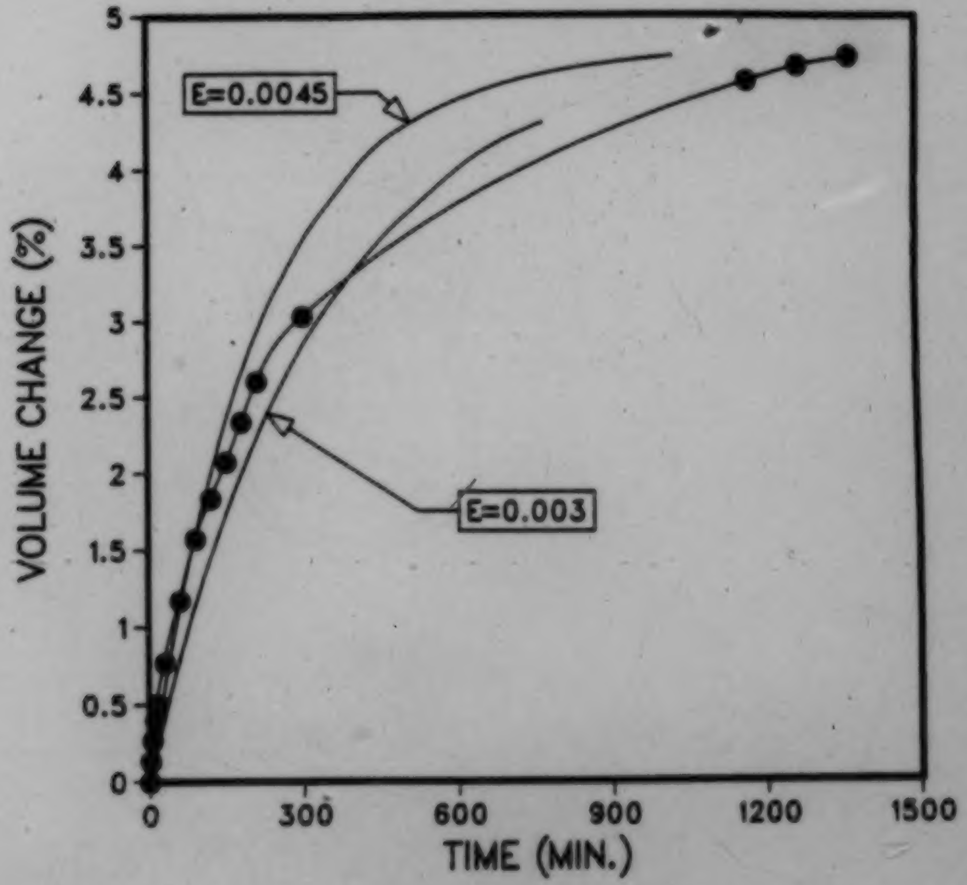

Figure 5.12 E values obtained by curve fitting data from the unloading drained test (B-222)

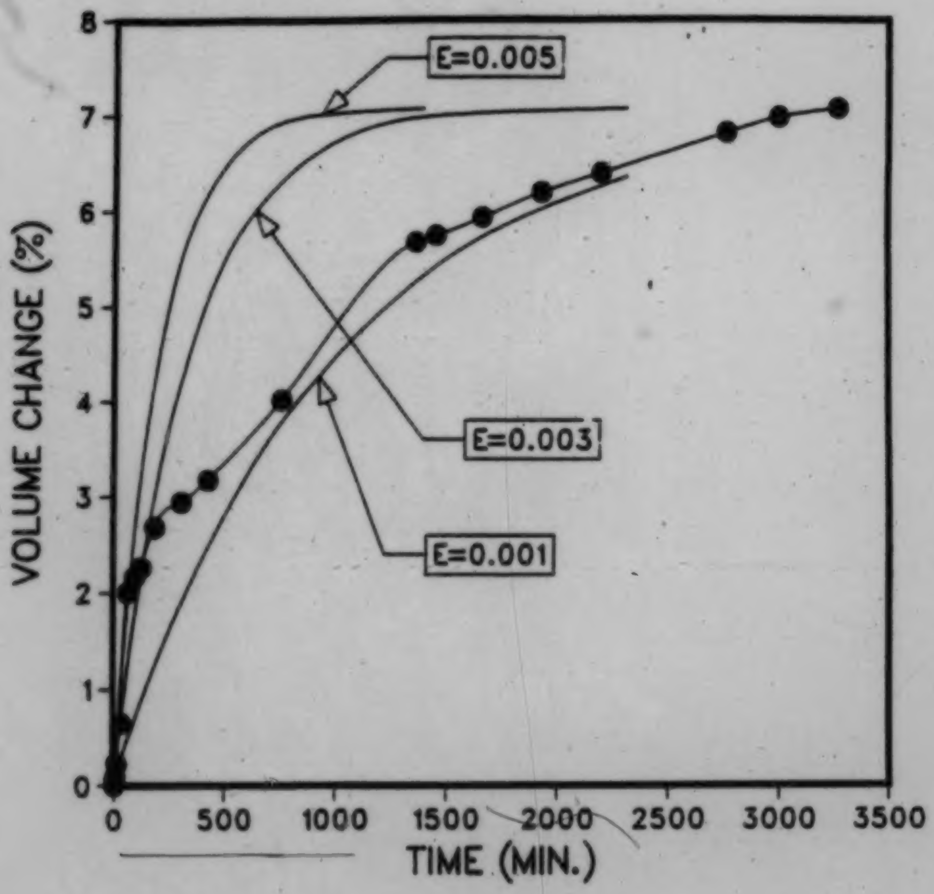

Figure 5.13 E values obtained by curve fitting data from the unloading drained test (B-225A)

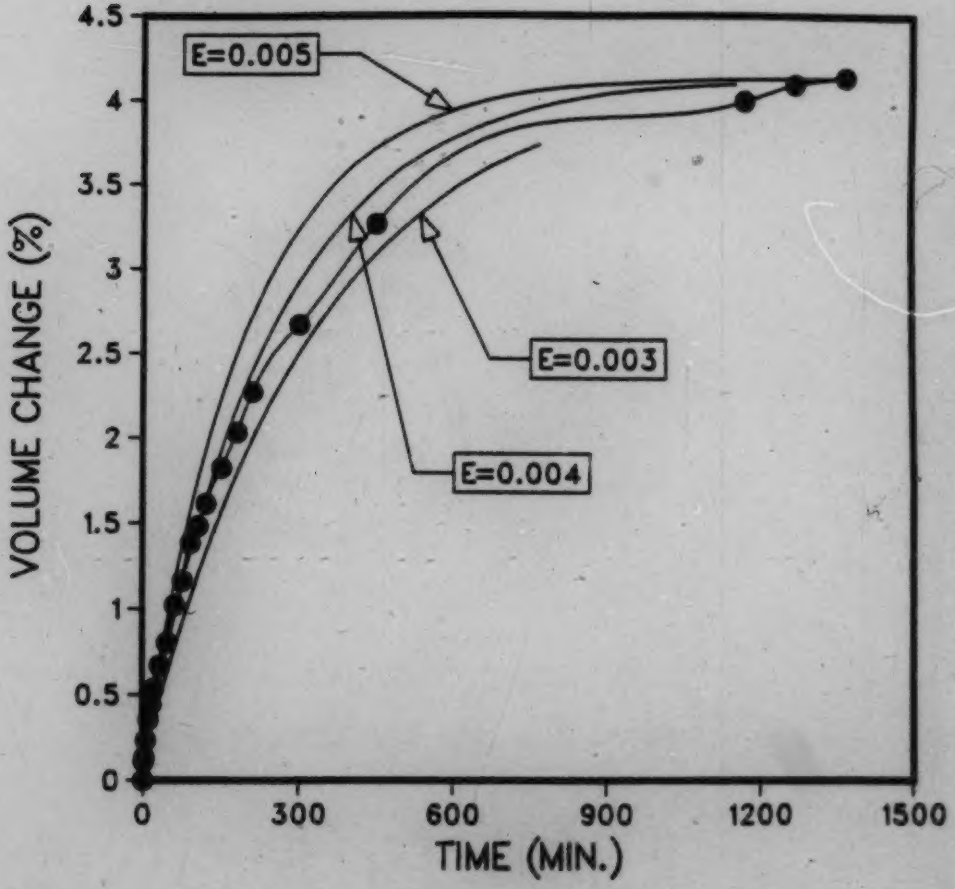

Figure 5.14 E values obtained by curve fitting data from the unloading drained test (B-223)

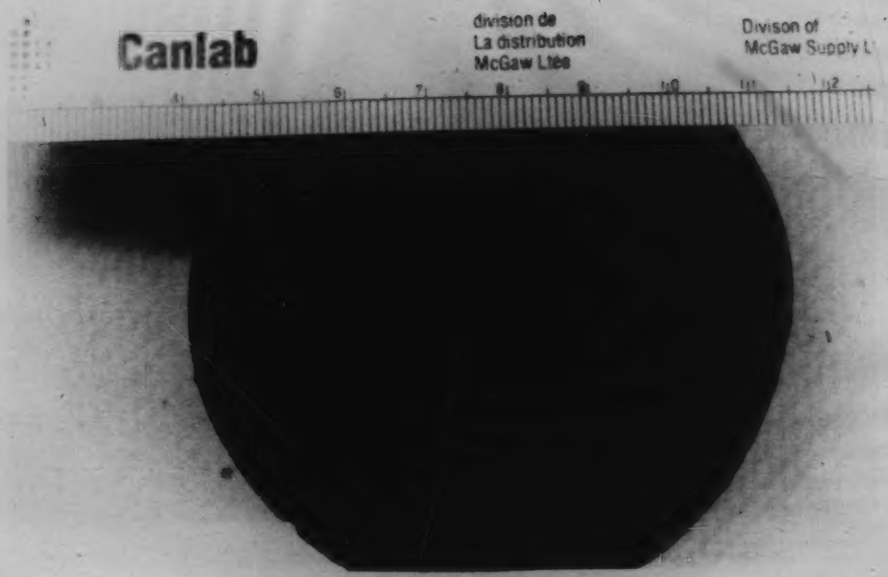
Canlab
division de
La distribution
McGaw Ltée
Divison of
McGaw Supply L

Figure 5.15 Fracturing of lean oil sand sample observed after testing

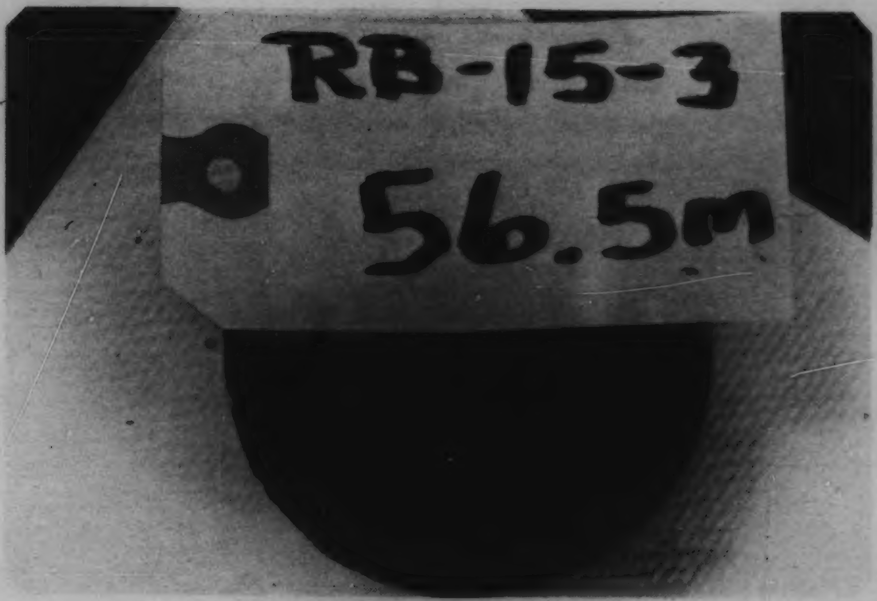

Figure 5.16 Fracturing of rich oil sand sample observed after testing

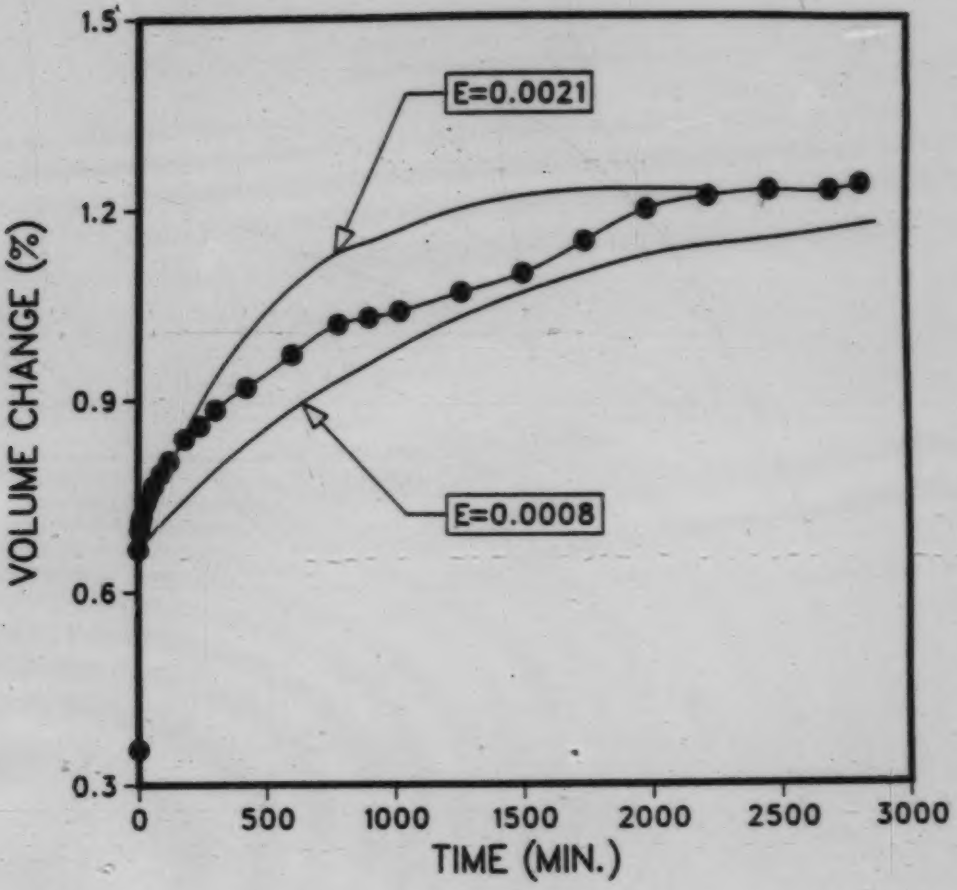

Figure 5.17 E values obtained by curve fitting data from the unloading undrained test (B-5-5H)

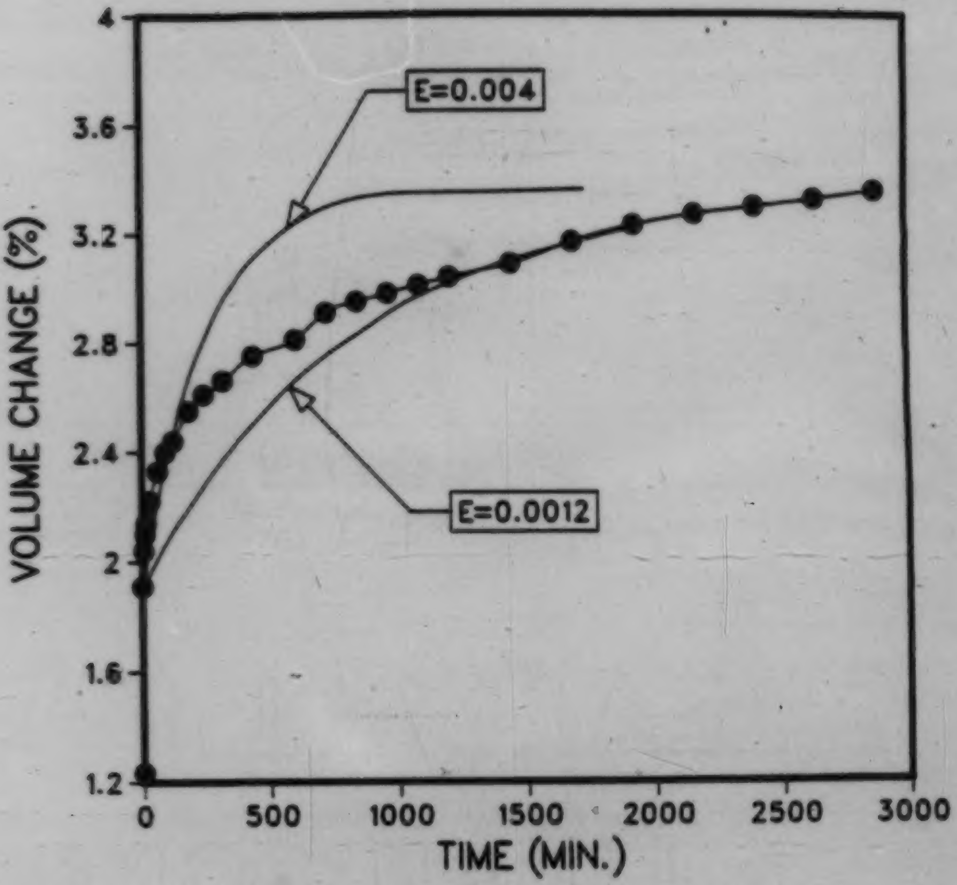

Figure 5.18 E values obtained by curve fitting data from the unloading undrained test (B-5-5I)

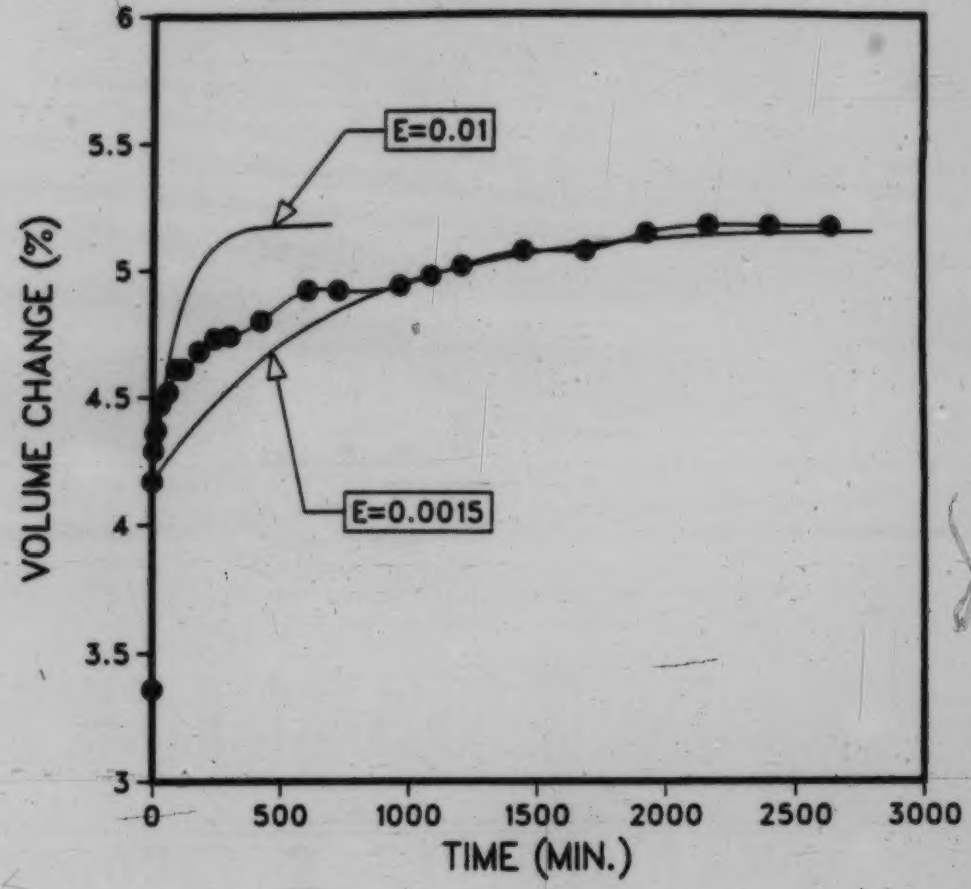

Figure 5.19 E values obtained by curve fitting data from the unloading undrained test (B-5-5J)

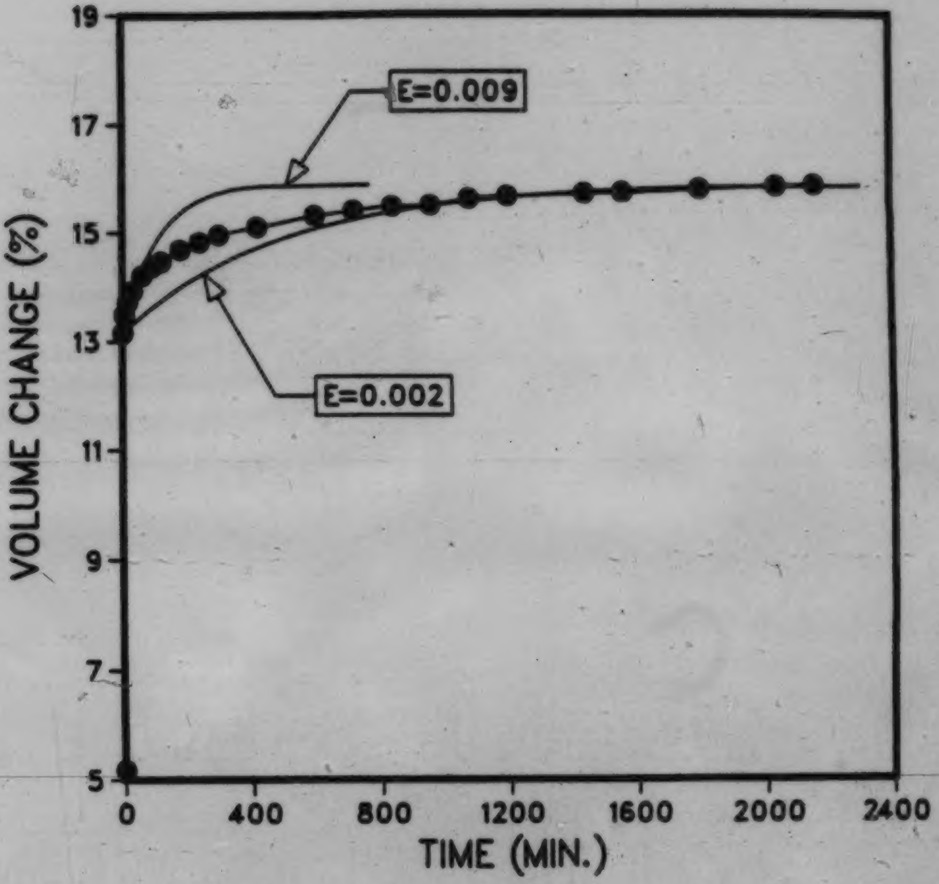

Figure 5.20 E values obtained by curve fitting data from the unloading undrained test (B-5-5K)

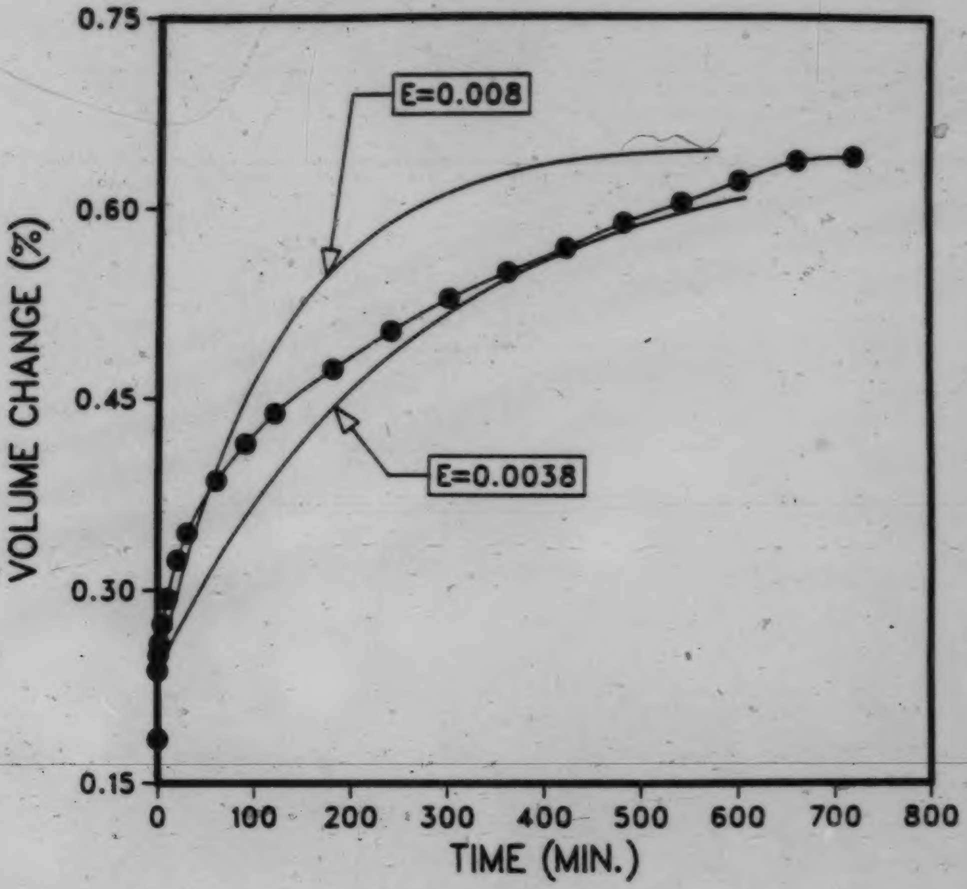

Figure 5.21 E values obtained by curve fitting data from the unloading undrained test (RB-5-2L)

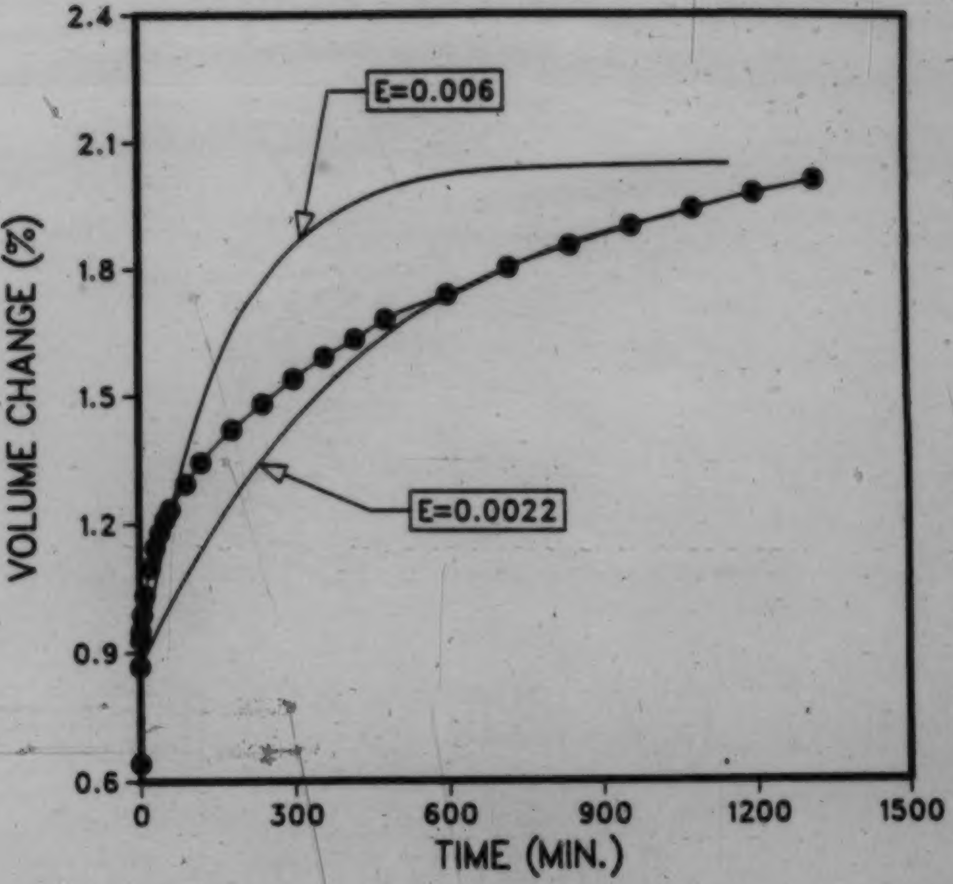

Figure 5.22 E values obtained by curve fitting data from the unloading undrained test (B-5-2M)

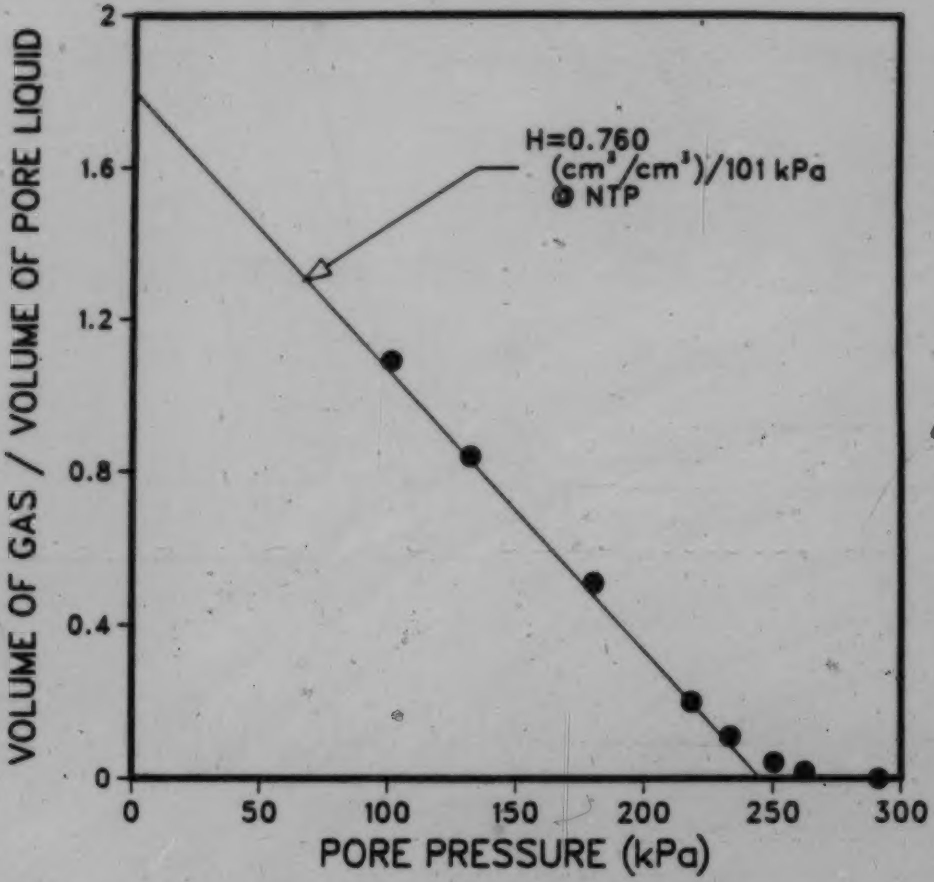

Figure 5.23 Solubility coefficient (H) for carbon dioxide in tailing sand sample at 24°C

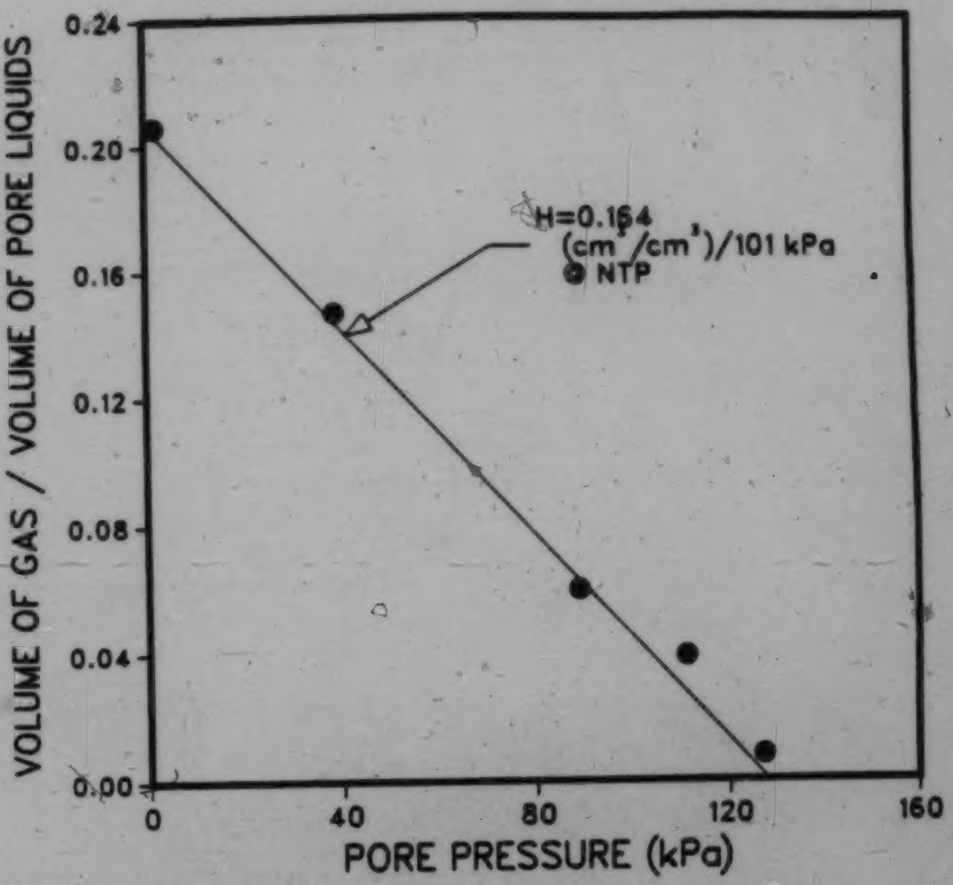

Figure 5.24 Combined solubility coefficient for lean oil sand sample B-225 at 6°C

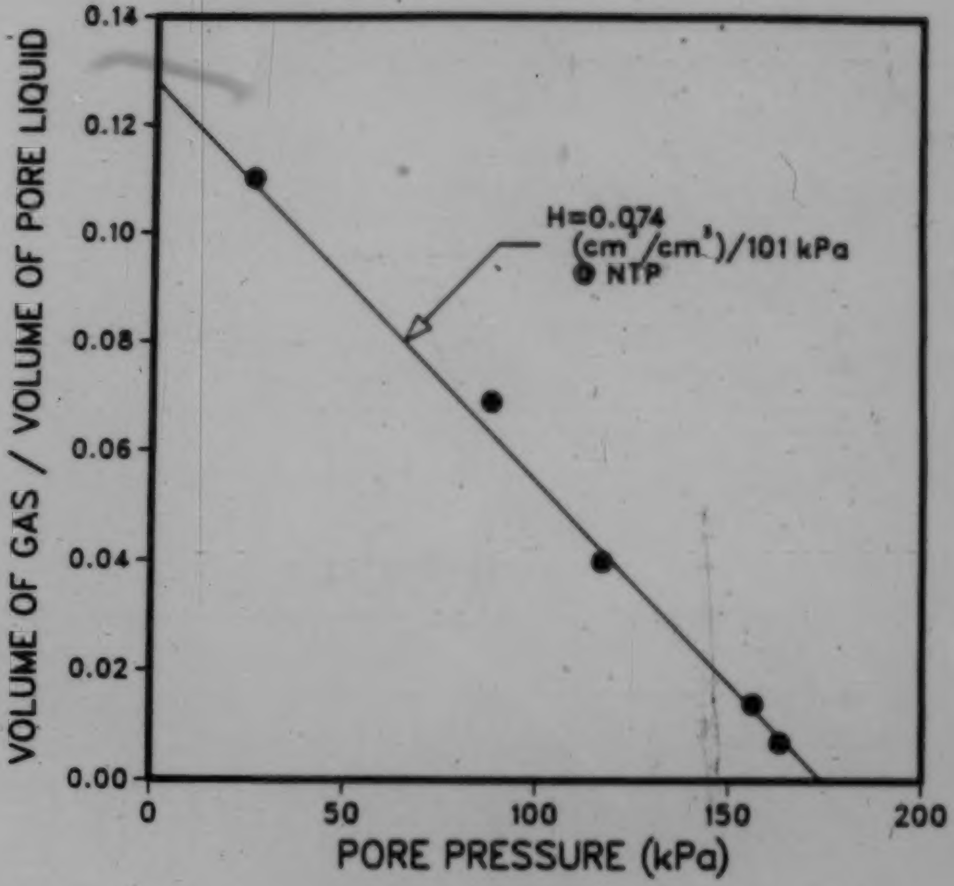

Figure 5.25 Combined solubility coefficient for lean oil sand sample B-224 at 24°C

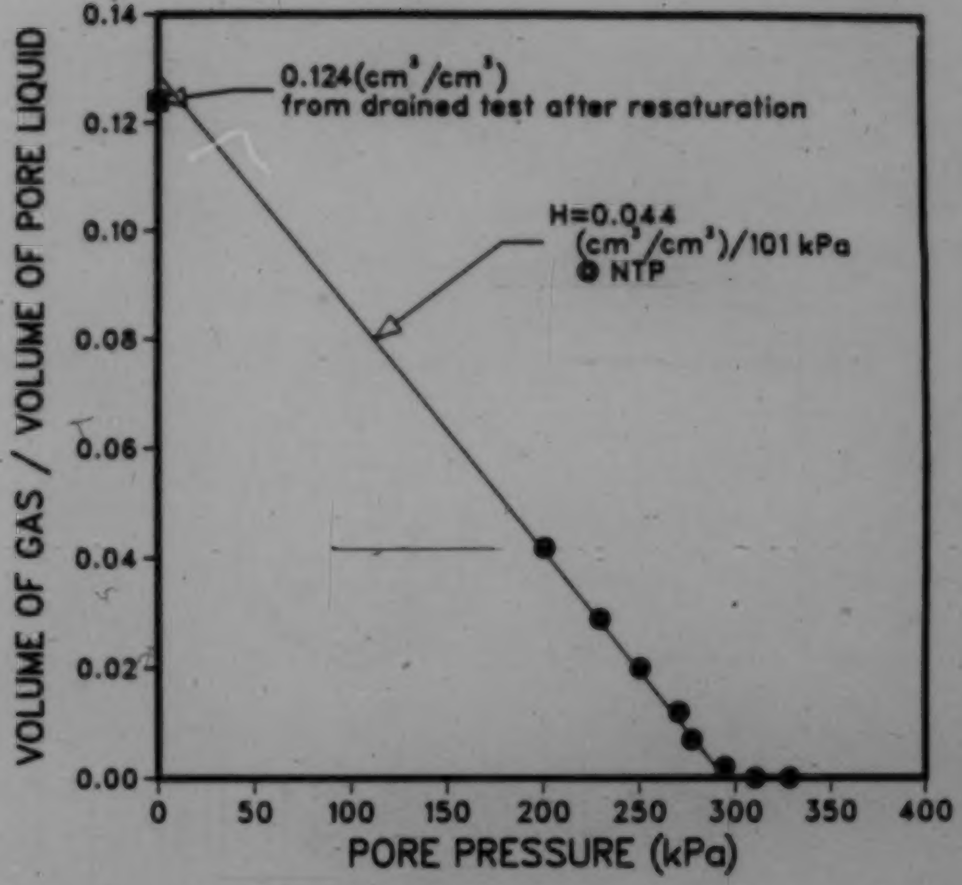

Figure 5.26 Combined solubility coefficient for lean oil sand sample B-223 at 60°C

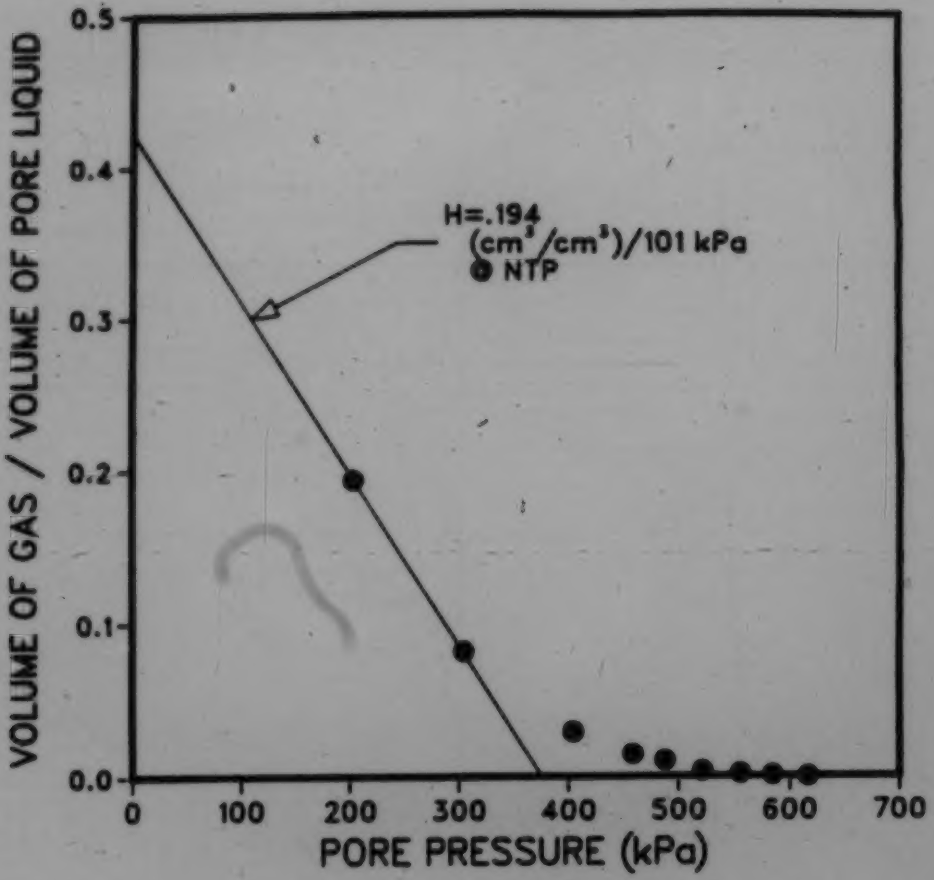

Figure 5.27 Combined solubility coefficient for rich oil sand sample RB-5-2 at 24°C

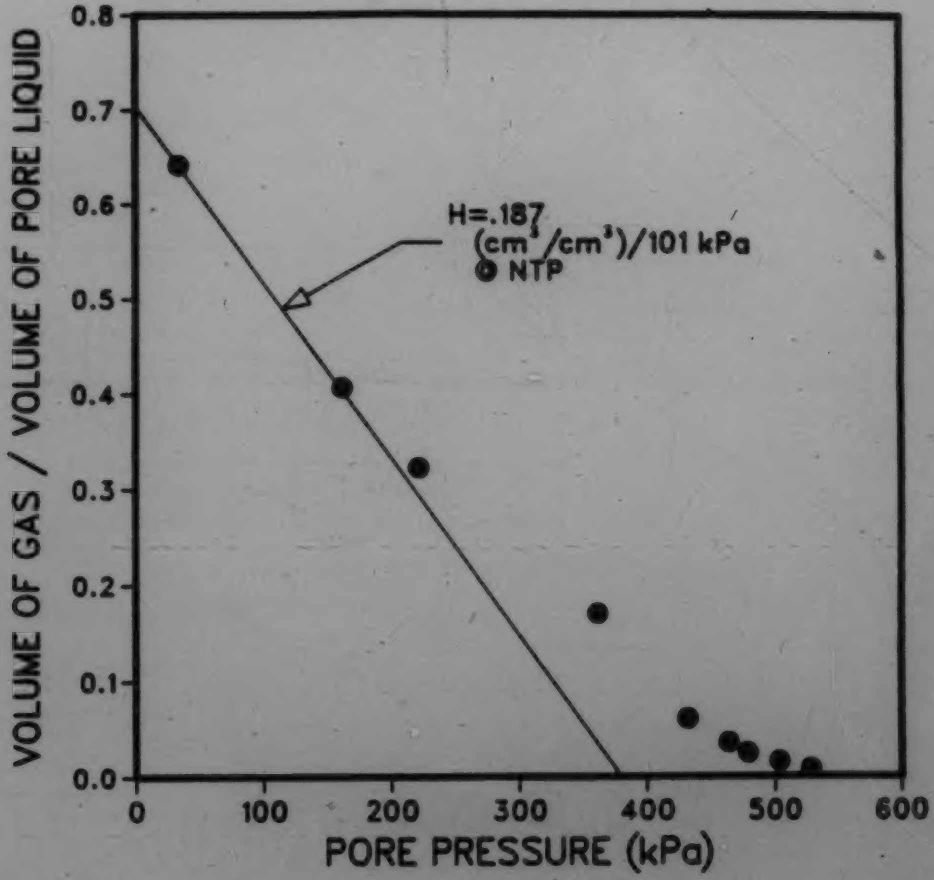

Figure 5.28 Combined solubility coefficient for rich oil sand sample RB-5-5 at 24°C

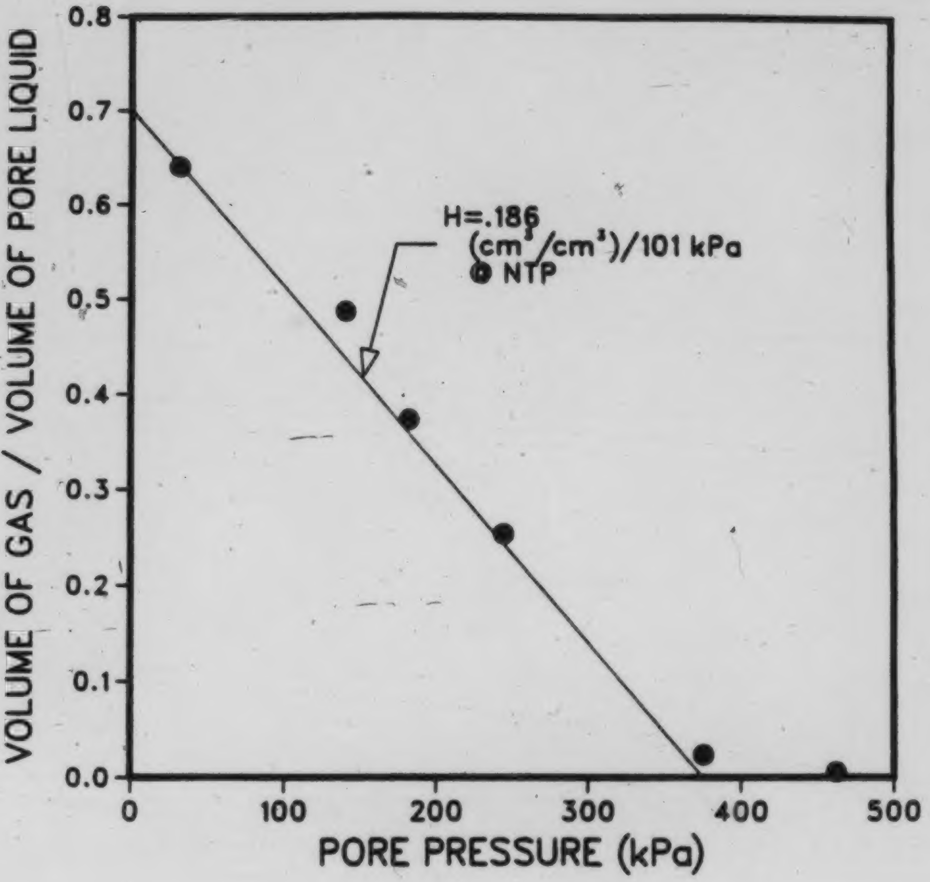

Figure 5.29 Combined solubility coefficient for rich oil sand sample RB-5-10 at 24°C

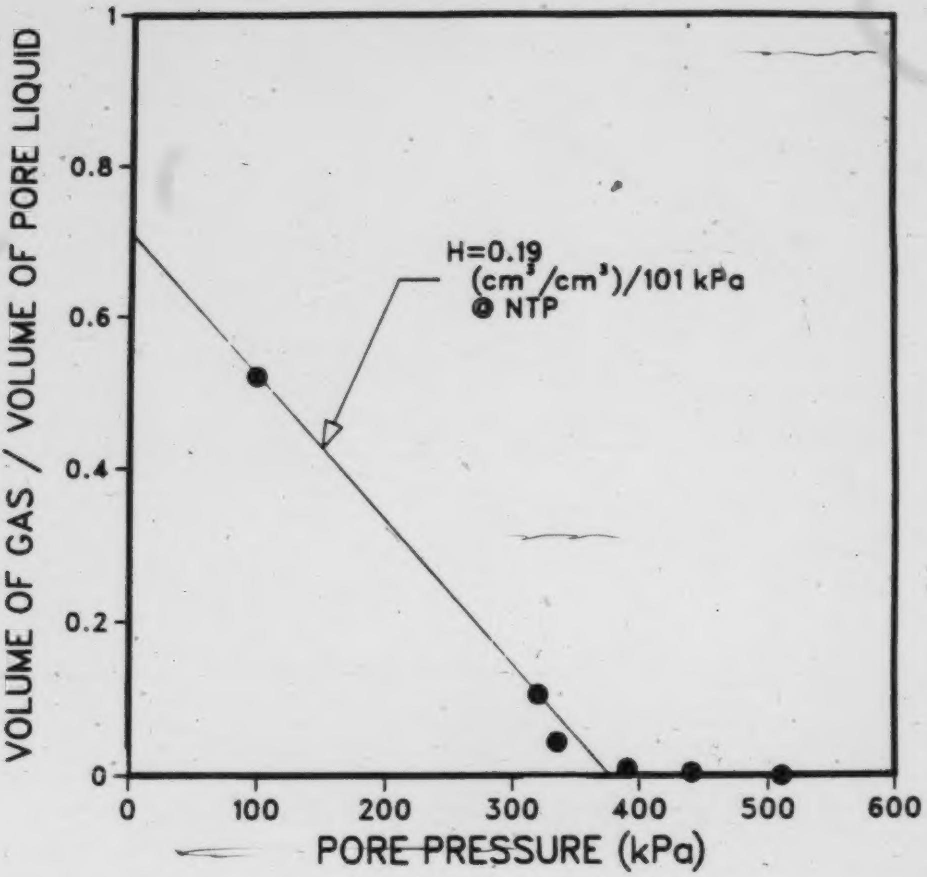

Figure 5.30 Combined solubility coefficient for rich oil sand sample RB-5-12 at 6°C

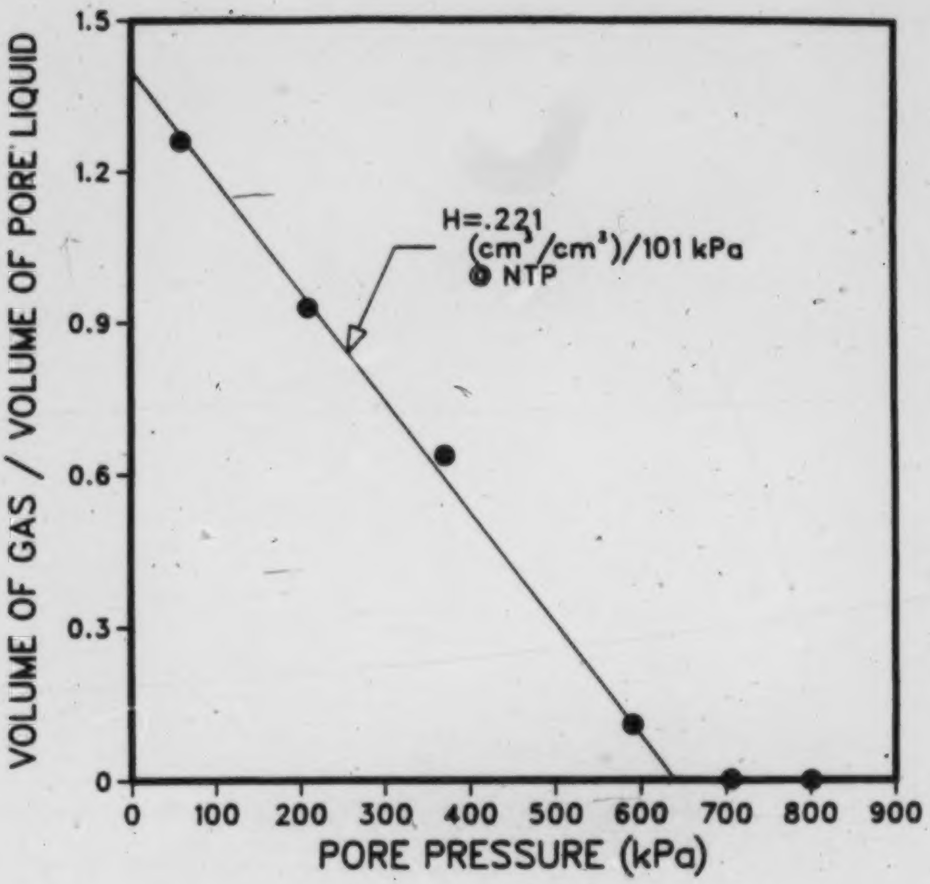

Figure 5.31 Combined solubility coefficient for rich oil sand sample RB-15-8 at 24°C

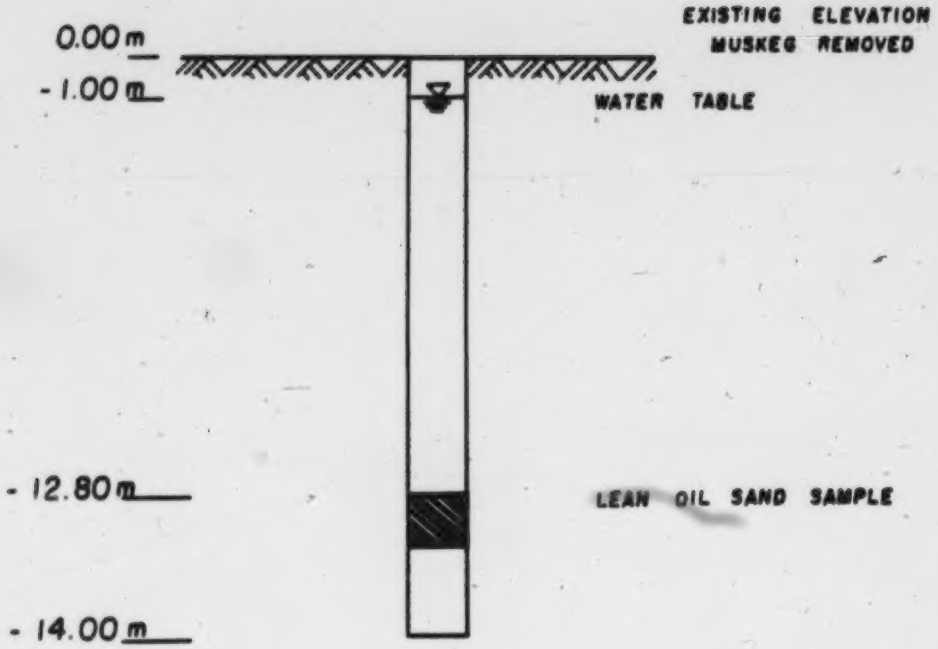
0.00 m
- 1.00 m
- 12.80 m
- 14.00 m
EXISTING ELEVATION
MUSKEG REMOVED
WATER TABLE
LEAN OIL SAND SAMPLE

Figure 5.32 Sketch of the location from which the lean oil sand samples were taken

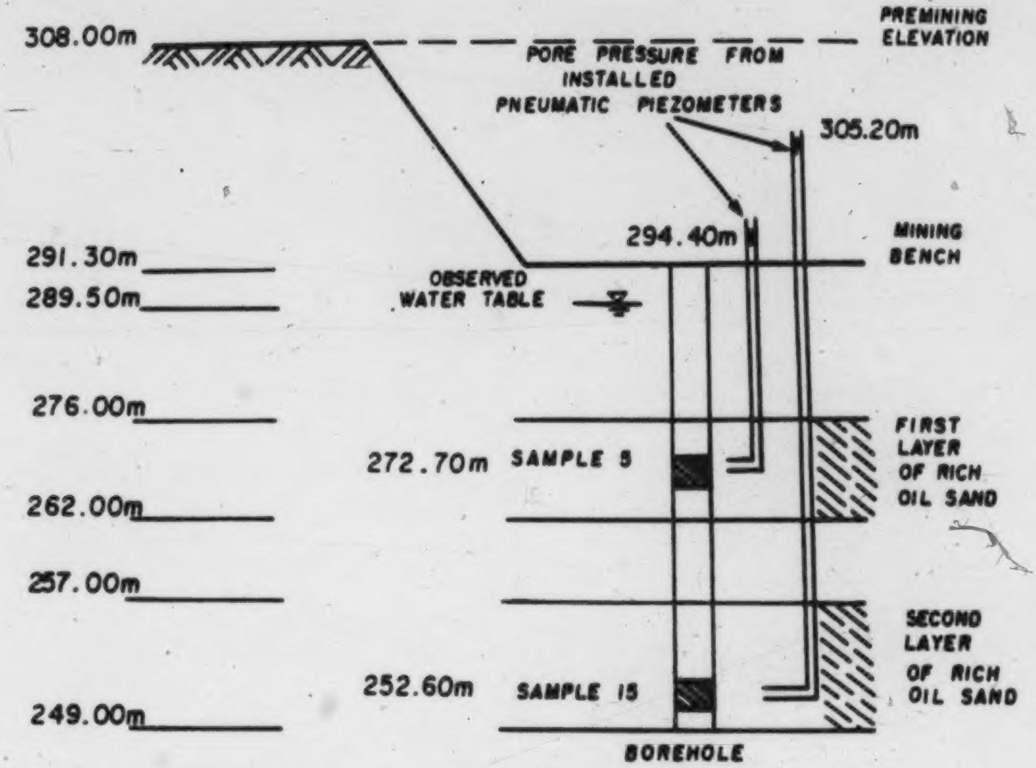
308.00m
PREMINING ELEVATION
PORE PRESSURE FROM INSTALLED PNEUMATIC PIEZOMETERS
305.20m
294.40m
MINING BENCH
291.30m
289.50m
OBSERVED WATER TABLE
276.00m
FIRST LAYER OF RICH OIL SAND
272.70m
SAMPLE 5
262.00m
257.00m
SECOND LAYER OF RICH OIL SAND
252.60m
SAMPLE 15
249.00m
BOREHOLE

Figure 5.33 Sketch of the location from which the rich oil sand samples were taken

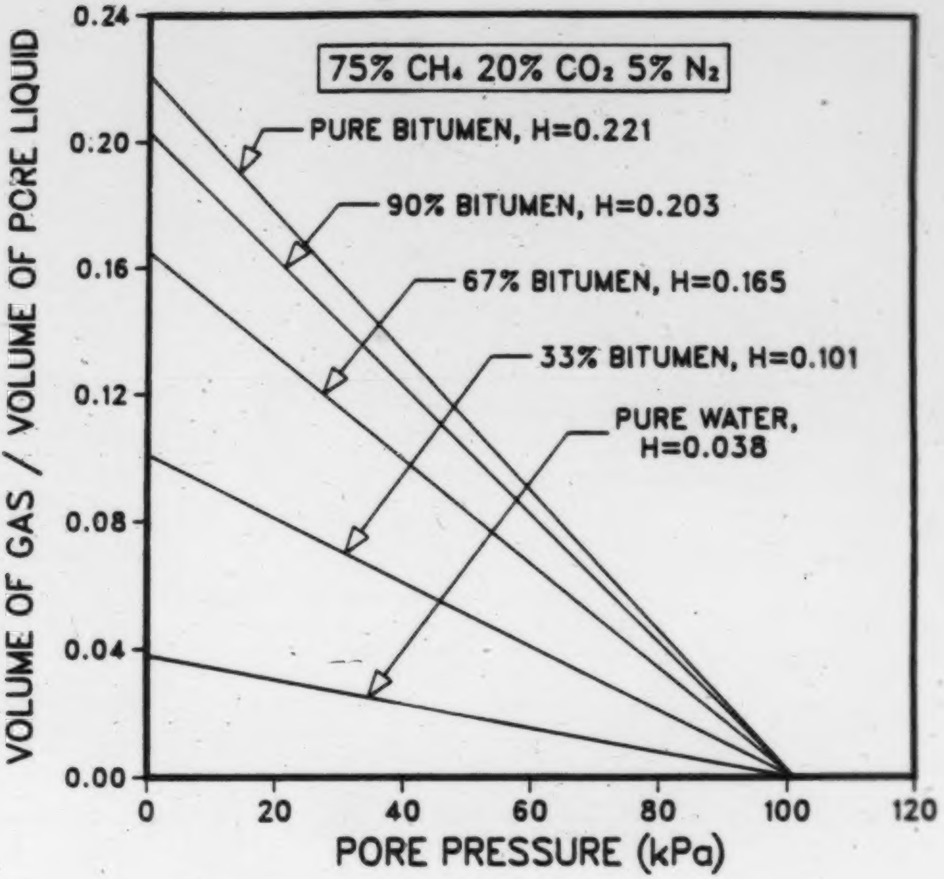

Figure 5.34 Theoretical combined solubility coefficients for oil sand samples at 24°C for a variety of bitumen/water ratios

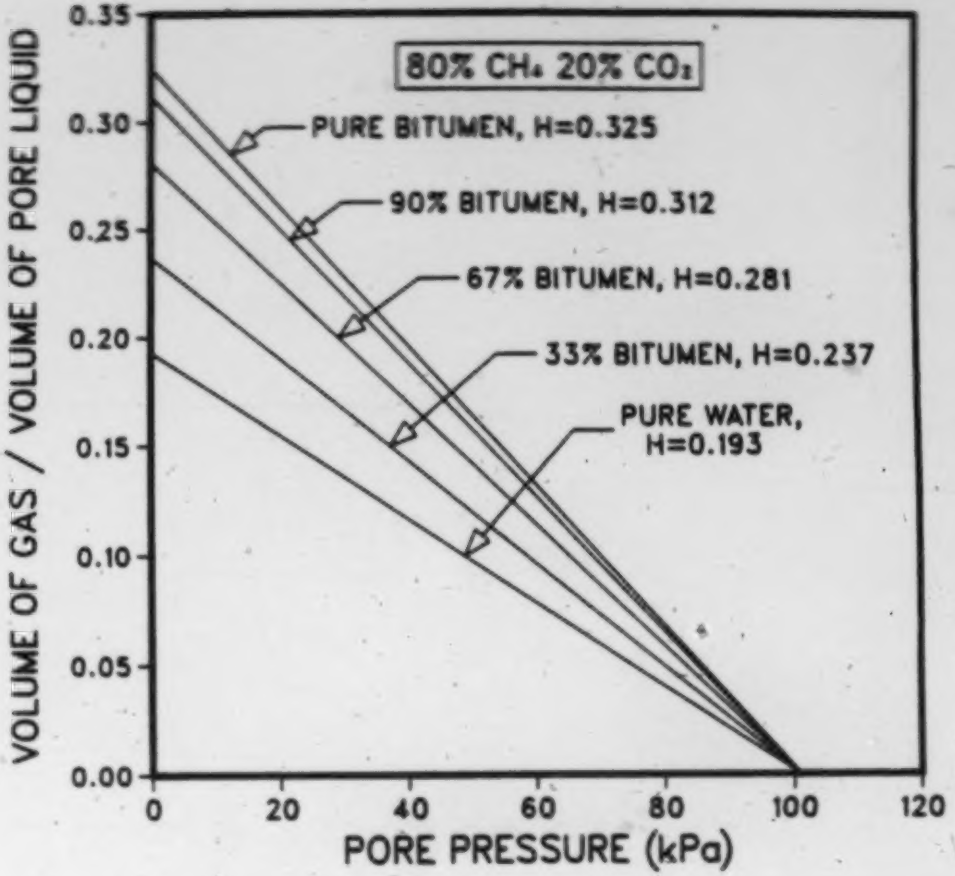

Figure 5.35 Theoretical combined solubility coefficients for oil sand samples at 24°C for a variety of bitumen/water ratios

6. CONCLUSIONS AND RECOMMENDATIONS

6.1 CONCLUSIONS

6.1.1 Sampling

When oil sand samples are being obtained and there is free gas present in the oil sand in situ, care must be taken to restrain the samples during the sampling process until the samples can be frozen. The changing pore pressure is sufficient to cause the free gas to expand and disturb the oil sand matrix. This disturbance can reduce the strength of the sand structure and with larger disturbances it allows the free gas to vent. The Pitcher Tube Samplers was able to restrain the samples sufficiently to prevent the loss of gas from the samples. The samples were not allowed to expand horizontally and these stresses limit vertical expansion. This mechanical restraint was sufficient to prevent the gas from leaving the samples during the sampling and storage process. To our knowledge this is the first time that Athabasca oil sand samples have been obtained where all the in situ gas is still in the samples.

Freezing the oil sand samples keeps this gas in solution. As soon as the samples are at the surface they should be frozen in the shelby tubes and once frozen at -25°C the gas will remain in solution for months. The freezing increases the viscosity of the oil, limits bubble formation and lowers the diffusion rate of the gases in solution.

6.1.2 Testing

The oedometer provided several important advantages over the triaxial cell in determining the gas properties of the oil sand.

1. The oedometer provided a sealed chamber which did not allow any gas to escape. As a result testing could be carried on for many days.
2. It was capable of testing samples over a range of temperatures from 6°C to 130°C. This included tests at the lowered temperature for many days at a time.
3. With the use of an LVDT the volume change measurements could be done with excellent accuracy.

The disadvantages of the oedometer although not serious are still noteworthy.

1. The horizontal stresses are not known and they must be known in order to properly use Sobkowicz's model.
2. The oedometer could not accurately determine the saturation of the sample. Sobkowicz (1982) concluded that the E parameter is dependent upon the liquid saturation of the sample and the oedometer can not give sufficient accuracy of the saturation to use in Sobkowicz's model.
3. The cell is not suitable for accurate gas sampling because of the presence of sharp corners and small ports for flushing.

6.1.3 Equilibrium Properties of Oil Sand

The three major equilibrium properties of oil sands which were analyzedwere the gas saturation pressure, combined solubility coefficient and the types of gases present in the oil sand. The gas saturation pressure of the oil sand is dependent upon the original in situ pore pressures. Also, when the pore pressure is reduced in the oil sand causing some gas to evolve, the gas stays in the pores and is not diffused out of the oil sand.

The Combined Solubility Coefficient

The combined solubility coefficient for oil sand depends on the percentage of water and bitumen that is in pores. A lean oil sand which has 33% of the liquid as bitumen and the rest as water will be able to contain much less gas than a rich oil sand sample (which had as much as 95% of the liquid as bitumen) because the water has a low solubility to methane compared to the bitumen. As a result it is important to determine the percentage of water and bitumen that exists in the oil sand pores.

The types of gas that are present in the oil sand will also affect the combined solubility coefficient especially if there are small quantities of gases which have a very low solubility in the fluid. The presence of 5% of nitrogen makes an enormous difference in the value of the combined solubility coefficient because it adds very little in volume but it requires a large additional pressure to keep it in solution.

The combined solubility coefficients obtained from equation 2.12 for the lean oil sand was 0.074 (cm^3/cm^3)/101 kPa and from 0.19 (cm^3/cm^3)/101 kPa to 0.22 (cm^3/cm^3)/101 kPa for rich oil sand samples at 24°C. The unloading undrained tests were able to give a combined solubility coefficient of approximately the same value that was predicted by the theoretical equation supplemented by data from the literature. For the rich oil sand these varied from 0.18 (cm^3/cm^3)/101 kPa to 0.21 (cm^3/cm^3)/101 kPa at 24°C. The solubility coefficient for the carbon dioxide saturated tailing sand sample was 0.76 (cm^3/cm^3)/101 kPa which was slightly lower than the anticipated value of 0.83 (cm^3/cm^3)/101 kPa. The combined solubility coefficient was obtained over a range of temperatures on some lean oil sand samples. The value at 6°C was 0.164 (cm^3/cm^3)/101kPa, at 24°C was 0.074 (cm^3/cm^3)/101 kPa and at 60°C was 0.044 (cm^3/cm^3)/101 kPa.

Gas Saturation Pressure

The gas saturation pressure for the lean oil sand samples was 170 kPa at 24°C and 128 kPa at 6°C. The gas saturation pressure for samples from the upper layer of rich oil sand was 375 kPa at 24°C (equivalent to 38.2 m of water head) and for the lower layer of rich oil sand was 642 kPa at 24°C (65.4 m of water). The depth of the samples from the original premining elevation was 35 m for the samples from the upper layer of rich oil sand and 55 m for the samples from the lower layer of rich oil sand.

The gas saturation pressure is determined by the in situ pore pressure that was in the ground prior to any mining done above the sample location. For the lean oil sand samples the premining gound conditions had the water table at the surface due to the presence of muskeg and so the saturation pressure will be related to this condition. For the rich oil sand the original water table was near the surface of the overburden and the gas saturation pressure of the sample will be related to the relative distance between the sample and the original pore pressure and not the present pore pressure with the overburden removed.

The gas saturation pressure will vary with temperature because the solubility coefficients of the gas in the pore liquids will vary with temperature; also at higher temperatures the natural gas liquids vapourize and produce additional gases which must also be dissolved. The effect of temperature must not be ignored as the testing done in the laboratory is usually done at a temperature different than the in-situ temperatures of the oil sand samples. The effect at higher temperatures will also seriously affect our ability to keep the samples saturated during testing at elevated temperatures (over 100°C).

Gases Present in Oil Sand

There is some variation in the samples tested but there appears to be approximately 75% methane, 20% carbon dioxide and 5% nitrogen in the oil sand. The amount of nitrogen appears to decrease with depth as the rich oil sand samples which were much deeper than the lean samples have slightly lower amounts of nitrogen than the lean oil sand samples. The oxygen and most of the nitrogen that were obtained in our samples were assumed to be air contamination during testing as the in situ bitumen has been shown to not contain oxygen.

6.1.4 Time Dependent Behaviour

To make use of the model proposed by Sobkowicz (1982) requires an accurate knowledge of the liquid saturation of the sample and the effective stress of the sample. The oedometer was not capable of measuring the liquid saturation to the accuracy required by this model and as a result the model was not used. However, the curve fitting equation used by Sobkowicz (equation 2.17) can be used on data that was obtained from the oedometer at low effective stresses where the volume change due to the evolving gas will not significantly affect the pore pressure. The E values modeling data from the tailing sand samples ranged from 0.018 to 0.043. These values were higher than those obtained by Sobkowicz, but it is within the boundaries he put on his data, especially when the differences in equipment and saturation level are taken into account.

The E values for the lean oil sand varied from 0.12 to 0.001 as the temperature went from 60°C to 24°C. The rich oil sand had E values from 0.008 to 0.0008 at 24°C. The test on the rich oil sand at 6°C was not done at a low enough effective stress to obtain an E value. The E values obtained by curve fitting the data from the unloading drained tests produced resutls which were quite similar to the E values obtained on data from the unloading undrained tests. The change in test procedure did not significantly change the rate at which the gas evolved. Unloading drained tests on a lean oil sand sample subjected to a 300 kPa vertical effective stress produced a transient volume curve which was accurately modelled by equation 2.17 with an E value of 0.004. As the vertical pressure was dropped to 8 kPa (piston load) the data was not modeled well by eqation 2.17 and the bounding E values ranged from 0.003 to 0.0045.

The drainage mechanism for the tailing sand samples was the same as that observed by Sobkowicz with the occluded bubbles joining together to form the drainage paths through the sand pack. The oil sand samples exhibited small fractures which were random in size and orientation. The presence of the fractures changed the drainage mode sufficiently to prevent equation 2.17 from accurately modelling the transient volume data. The only data which was accurately modeled by the E parameter was the tailing sand which was anticipated and the data from the unloading drained tests where the vertical load prevented the fracturing from occurring.

The saturation at which the venting occurred was approximately 82% to 89% for the lean oil sand and varied from 40% to 65% for the rich oil sand. These values were obtained from the final densities of the samples after each experiment.

6.2 RECOMMENDATIONS

The testing of oil sand at in situ temperatures to determine the time dependent behaviour was started but requires much more work to see if this is indeed a matter of concern for shaft and tunnel design. The equipment will require upgrading as well to prevent the variation in volume change due to either minor temperature or pressure variations in testing at in situ temperatures.

The oedometer was capable of testing the equilibrium behaviour quite well but problems existed in determining an accurate gas saturation value at the initial gas evolution stage. The combined solubility coefficient, the gas saturation pressure and the types of gases all require that a significant amount of gas evolve before any accurate results can be obtained. To obtain accurate transient data on gas evolution (especially as bubble formation is initiating) requires the use of a triaxial cell which can accurately map the change in liquid saturation. To obtain this the oil sand samples should be tested in a triaxial cell where a copper membrane is used instead of a rubber membrane. The copper membrane will affect the amount of volumetric change that the sample can be subjected to but the major areas of concern are the initial bubble nucleation and the time required for bubble formation. These should be accurately measured by the copper membranes and the membranes should also prevent the diffusion of the gas out through the membrane.

The saturation level at which venting occurs from the sample is not accurately known and is an important number which must be known before the total volume change of the oil sand can be accurately estimated. The problem of excessive volume change is a major reason for this testing program and the liquid saturation values obtained in this testing of rich oil sand was 40% to 65%. This is a very important number but this kind of variation is not accurate enough.

Closely associated with the venting saturation is the mode of gas drainage. The gas drained from the samples appeared to vary from the drainage along fractures to normal drainage through the joining of occluded bubbles. This variation will affect the venting saturation and the modes of drainage require more research to determine when the various drainage modes occur.

One of the more interesting observations was the production of gases at high temperatures. This production of gas will seriously affect the ability to test oil sand at high temperatures and still keep the samples saturated. The amount of pressure required to keep gas in solution at temperatures over 100°C must be determined to see if it is practical to test saturated samples with significant gas contents at high temperatures.

An oedometer capable of testing at higher temperatures and pressures will determine the gas saturation pressure curve (bubble point curve) for an individual sample. This curve will give an indication of the pressure required to keep the samples saturated at higher pressures and temperatures and enable researchers to obtain accurate geotechnical properties. Also with this curve an indication of the gases present in the sample can be obtained by reproducing the curve with an equation of state.

References

AOSTRA,1984. "The Thermodynamic and Transport Properties of Bitumen and Heavy Oils." Alberta Oil Sands Technology and Research Authority, Technical Report, 471p.

Denoyelle, L. and Bardon, C., 1984. "Diffusivity of Carbon Dioxide into Reservoir Fluids." 86eme Congres Annual Canadian Institute of Mining and Metallurgy, Ottawa, Ontario, April, 29p.

Dusseault, M.B., 1985 Private communications.

Dusseault, M.B. and Morgenstern, N.R., 1977. "Sampling and Testing of Athabasca Oil Sands for Stability Studies." in The Oil Sands of Canada-Venezuela, 1977, CIM Special Volume 17, edited by D. Redford and A. Winestock, pp. 260-269.

Dusseault, M.B. and Scott, J.D., 1984. "Coring and Sampling in Heavy Oil Exploration: Difficulties and Proposed Cures." AAPG Research Conference on Exploration for Heavy Crude Oil and Bitumen, Santa Maria, California, 14p.

Dusseault, M.B. and van Domselaar, H.R., 1982. "Canadian and Venezuelan Oil Sand: Problems and Analysis of Uncemented Gaseous Sand Sampling." in "Updating Subsurface Sampling of Soils and Rocks and Their In-Situ Testing." Engineering Foundations Conferences, Santa Barbara, Calif., Jan., 20p.

Feng, K.K., Cheng, K.C. and Augsten, R., 1984. "Preliminary Evalution of the Methane Production Potential of Coal Seams at Greenhills mine, Elkford, British Columbia." Coal Division Canadian Institute of Mining, vol. 77 No. 871, pp.56-61

Fu, B.C.H. and Phillips, C.R., 1979. "New Technique for Determination of Diffusivities of Volatile Hydrocarbons in Semi-solid Bitumen." Fuel, Vol. 58, Aug., pp.557-560.

Hardy,R.M. and Hemstock, R.M., 1963. "Shear Strength Characteristics of Athabasca Oil Sands." K.A. Clark Volume, Research Council Alberta Information Series No. 45, Edmonton, pp.109-122.

Hepler, L.G. and Smith, W.L., 1975. "Principles of Chemistry." Macmillan Publishing Co. Inc., pp 78-82.

Huculak, M., 1985. "Viscosity of Athabasca Bitumen below

20°C." Unpublished report, University of Alberta, Edmonton, Alberta, 3p.

Jha, K.N., Montgomery, D.S. and Strausz, O.P., 1977. "Chemical Composition of Gases in Alberta Bitumens and in Low Temperature Thermolysis of Oil Sand Asphaltenes and Maltenes." Oil Sand and Oilshales chemical Prcceding Symposium, pp.33-54.

Jha, K.N., Montgomery, D.S. and Strausz, O.P., 1979. "Thermolysis and Oxidation of Alberta Oil Sand Bitumen." American Chemical Society, Division of Fuel Chemistry, 24(3), pp.260-266.

Kissell, F.N., McCulloch, C.M. and Elder, C.H., 1975. "The Direct Method of Determining Methane Content of Coalbeds for Ventilation Design." U.S. Bureau of Mines, Report of Investigation 8043, 17p.

Kosar, K.M., 1983. "The Effect of Heated Foundations on Oil Sands." M.Sc. Thesis, University of Albert, Edmonton, Alberta, 209p.

Lu, B.C.Y. et.al., 1986. "Correlation and Prediction of Solubilities of Gases in Athabasca Bitumen." AOSTRA Journal of Research, Vol. 2, No. 3, pp.139-146.

Martschuk, J., Chan, W.K. and Slawinski, A., 1985. "Basel Aquifer Dewatering at the Suncor Oil Sands Mine." Heavy Oil and Oil Sands Technical Symposium, Calgary, Alberta, Feb., 21p.

McManamey, W.J. and Woollen, J.M., 1973. "The Diffusivity of Carbon Dioxide in some Organic Liquids at 25°C and 50°C." Journal of the American Institute of Chemical Engineering, Vol. 19, No. 3, pp. 667-669.

Mehrotra, A.K. and Svrcek, W.Y., 1982. "Correlations for Properties of Bitumen Saturated with Carbon Dioxide, Methane and Nitrogen, and Experiments with Combustion Gas Mixtures." Journal of Canadian Petroleum Technology, November-December, pp.33-54.

Robinson, D.B. and Associates, 1985. "The Volume and Composition of Gases Dissolved In-Situ in Athabasca Tar Sand." Report written to Syncrude Canada Ltd., 87p.

Robinson,D.B. and Sim, S.K., 1981. "The Behaviour of Bitumen Mixtures during In-Situ Recovery." Progress Report on AOSTRA Agreement 184, 23p.

Schmidt, T., Leshchyshyn, T.H. and Puttagunta, V.R., 1982. "Diffusivity of Carbon Dioxide into Athabasca Bitumen." 33rd Annual Technical meeting of the Petroleum Society of CIM,Calgary, Alberta, Preprint No.82-33-100, 12p.

Sobkowicz, J.C., 1982. "The Mechanics of Gassy Soils." Ph.D. thesis, University of Alberta, Edmonton, Alberta, 531p.

Srajer, V., 1977. "The Saline Creek Diversion Tunnel Fort Mcmurray, Alberta Part 2- Hydrocarbon and Gas Anaylsis." CANMET Mining Research Laboratories Report ERP/MRL 77-119(TR) 39p.

Srajer, V., 1981. "Gas Monitoring Trial at the Gulf-AOSTRA Surmont Lease." CANMET Energy Research Program Mining Research Laboratories Division Report ERP/MRL 81-60(TR), 69p.

Srajer, V. and Barron, K., 1978. "Gas Observations in the Saline Creek Tunnel." CANMET Mining Research Laboratories Report ERP/MRL 78-22(OP), 35p.

Strausz,O.P, Jha, K.N. and Montgomery, D.S., 1977. "Chemical Composition of gases in Athabasca Bitumen in low Temperature Thermolysis of Oil Sand, Asphaltene and Maltene." Fuel, vol. 56, April, pp.114-120.

Svrcek, W.Y. and Mehrotra, A.K., 1982. "Gas Solubility, Viscosity and Density Measurements for Athabasca Bitumen." Journal of Canadian Petroleum Technology, July-August, pp.31-38.

Verma, N.S., 1977. "One Dimensional Compression and Pore Pressure Characteristics of Compacted Soils." Ph.D. Thesis, University of Ottawa, Ottawa, Ontario, Volume 1, 353p.

APPENDIX A - DESCRIPTION OF APPARATUS AND CALIBRATIONS

Measuring Devices

Pressure Transducers

There were three transducers used in the testing apparatus one to measure the pore pressure in the cell, a second to measure the pore pressure at pressures higher than 1725 kPa and a third to measure the pressure acting on the Bellofram Diaphram Air Cylinder. The first transducer (Celesco model PLC S/N 2599) has a operating range of 0 to 1725 kPa. The voltage output versus pressure is shown in figure A.1. The second pore pressure transducer (Viatron model no. 207) has a operating range from 0 to 6900 kPa (see figure A.2 for the calibration curve for this transducer). This transducer was used for pressures above 1500 kPa and also used as a backup measuring system below this value. The first transducer was more sensitive to small pressure changes than the second transducer and was used whenever possible. The third transducer (Celesco model PLC S/N 8414) measured the air pressure acting on the top of the Diaphram Air Cylinder. The actual pressure acting on the top of the sample will be increased in proportion to the cross sectional area of the cylinder to the cross sectional area of the testing chamber. The calibration of the transducer is shown in figure A.3.

Linear Varying Displacement Transducer (LVDT)

The LVDT (Hewlett Packard 24 DCDT 100) was calibrated with the use of a precision micrometer and the results are shown in Figure A.4. Also shown in this figure is the regression analysis of the data points.

Thermal Measurement

There were three Type J (iron-constantan element) thermocouples used in the testing apparatus. These thermocouples were manufactured by Barber-Coleman Company and have a temperature range from 0 to 400°C. The thermocouple in the wall of the cell jacket was used as the temperature input for the Temperature Controller which maintained the temperature at approximately the test temperature. The temperature Controller has a rated accuracy of ±0.5% of the test temperature and has a temperature sampling time of 3 per second. The temperature range of the controler is 0 to 400°C.

During testing the temperature control of the sample was improved with the used of a variable transformer The variable transformer was able to vary the voltage from 0 to 105 volts (95% of the input voltage of 110 volts). The heater used in the test program was a silicon rubber heater fabricated by WATLOW. The heater was a 120 volt AC heater which drew a maximum of 650 watts.

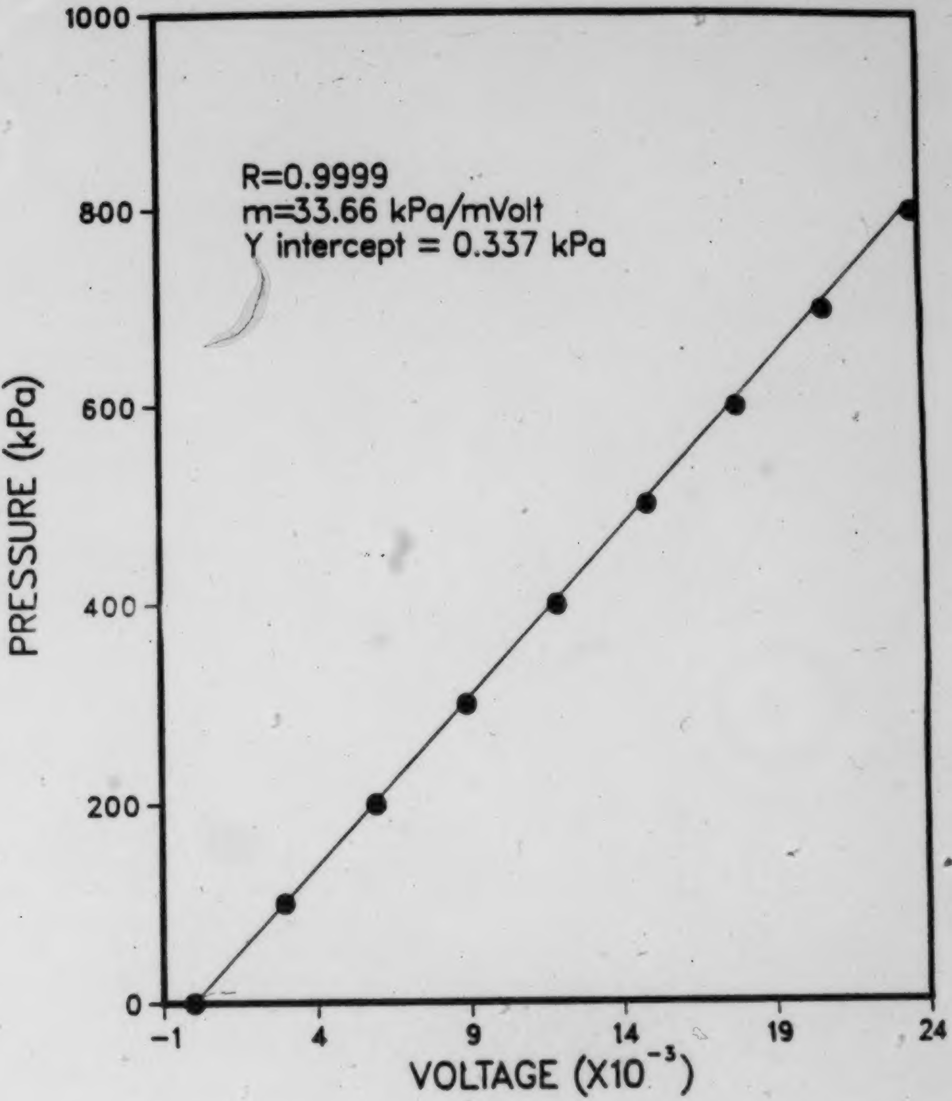

Figure A.1 Calibration curve for the Celesco 2599 pore pressure transducer

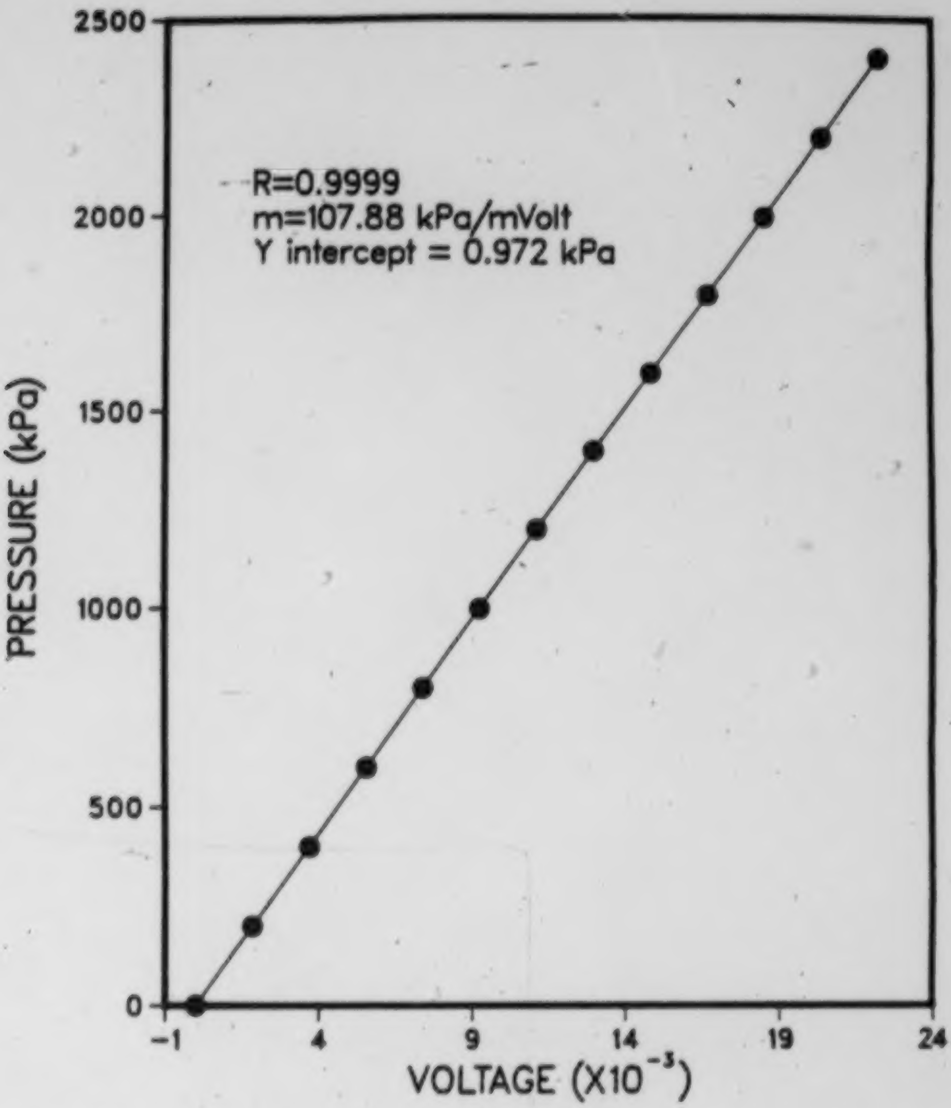

Figure A.2 Calibration curve for the Viatron 207 pore pressure transducer

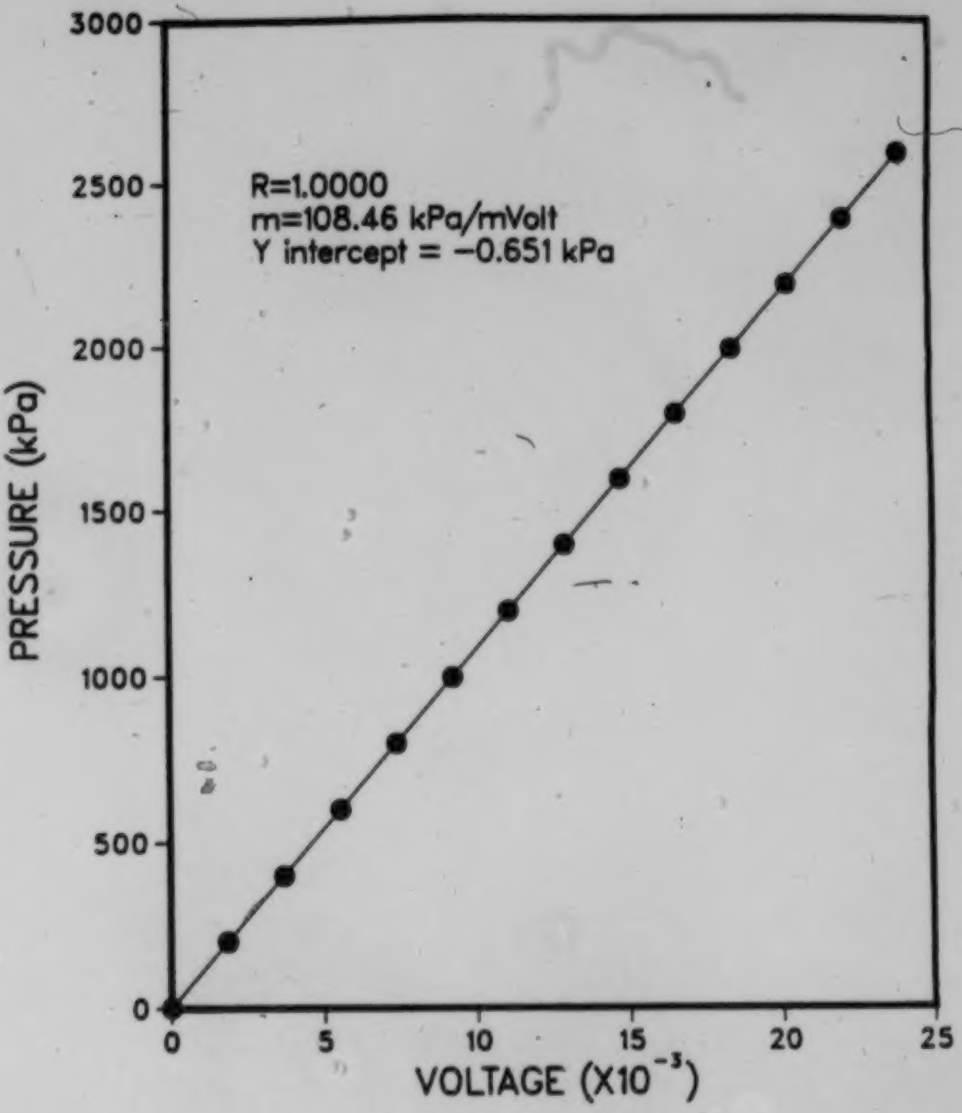

Figure A.3 Calibration curve for the Celesco 8414 pore pressure transducer

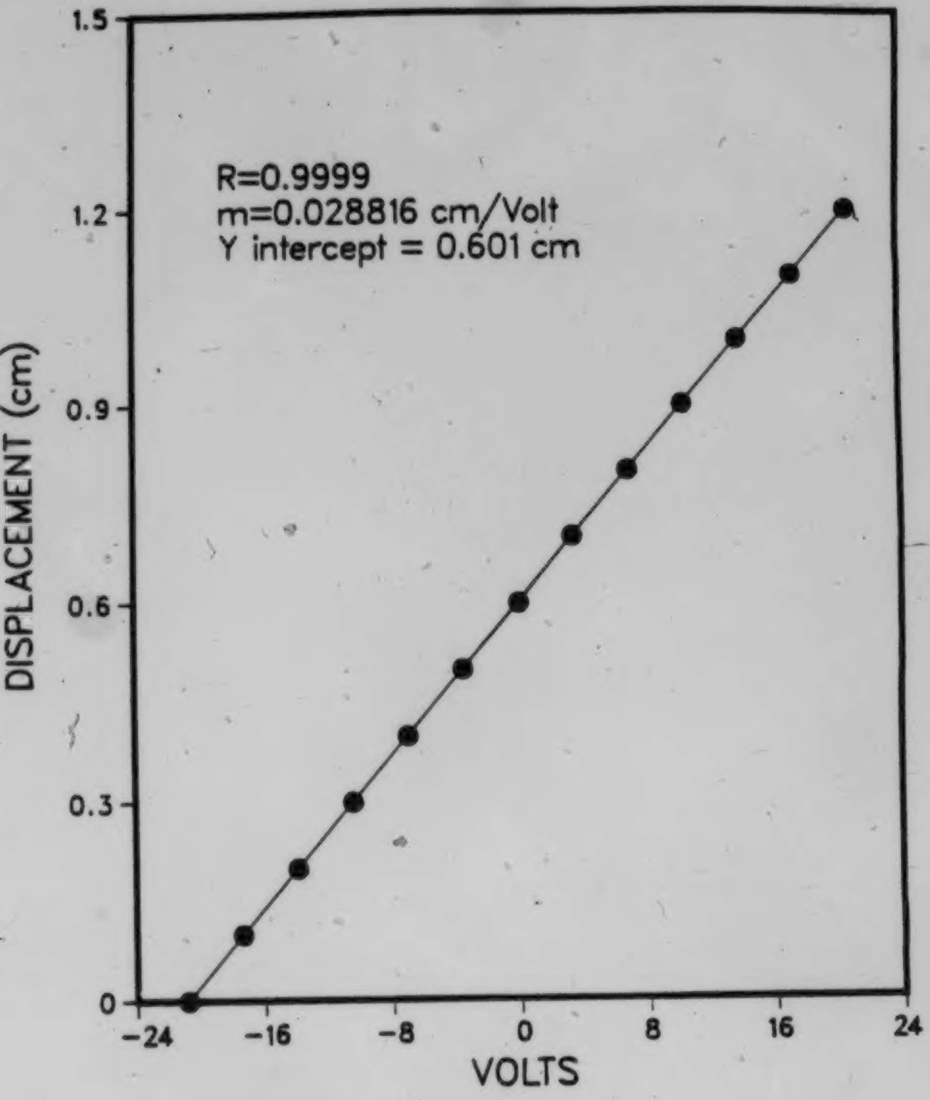

Figure A.4 Calibration curve for the Hewlett Packard DCDT 100 LVDT

APPENDIX B - TESTING ON TAILING SAND SAMPLE AT 50°C

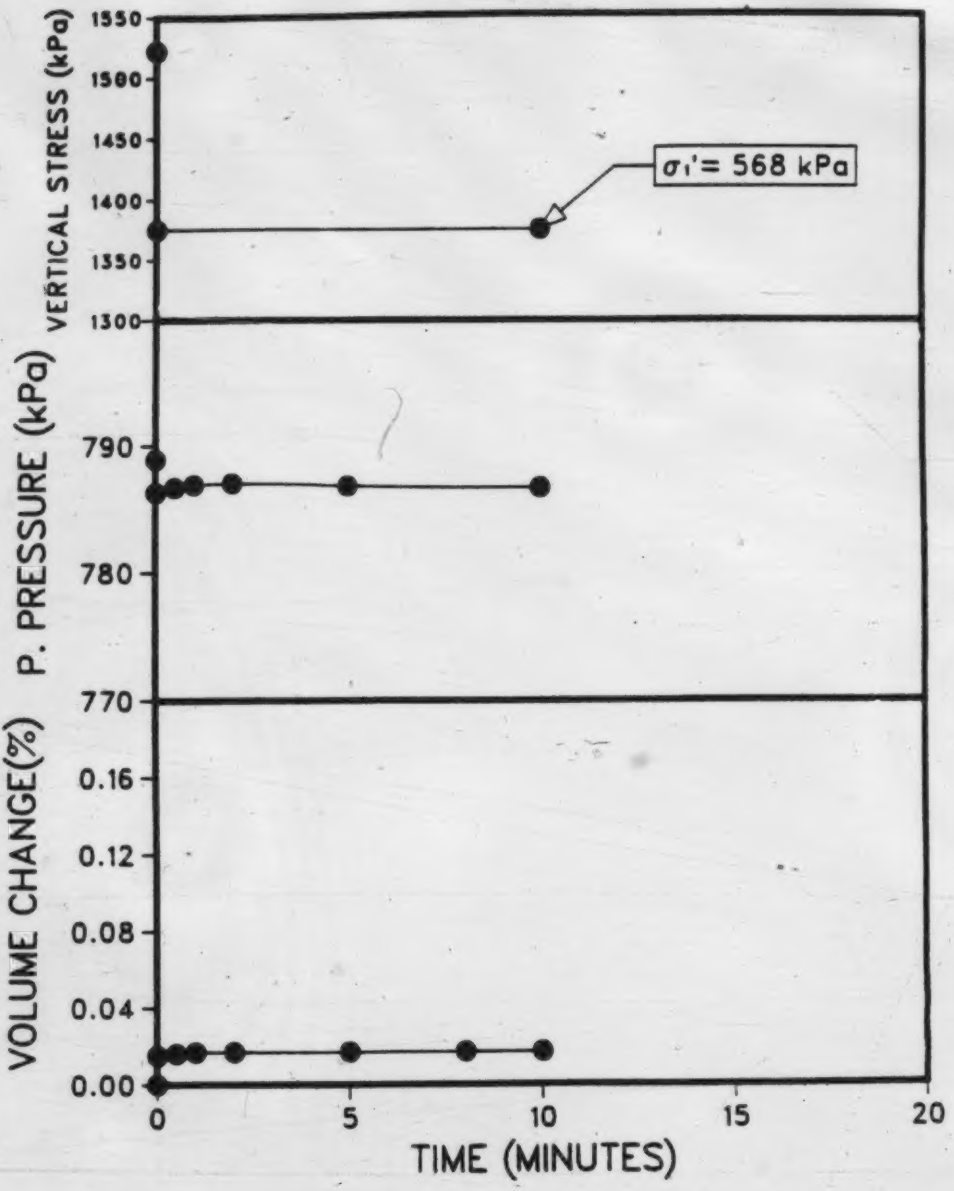

Figure B.1 Increment A from the unloading undrained test at 50°C for T-350

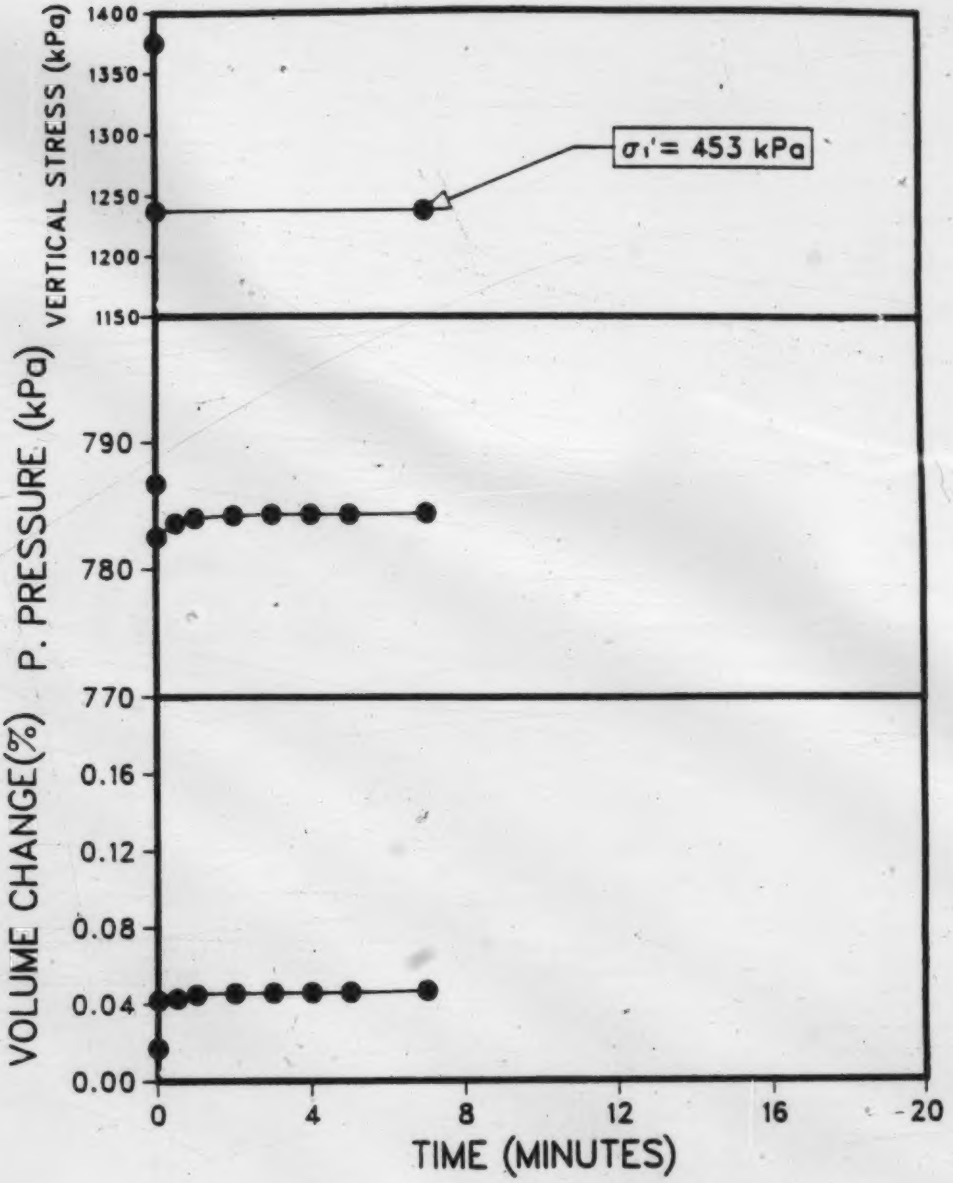

Figure B.2 Increment B from the unloading undrained test at 50°C for T-350

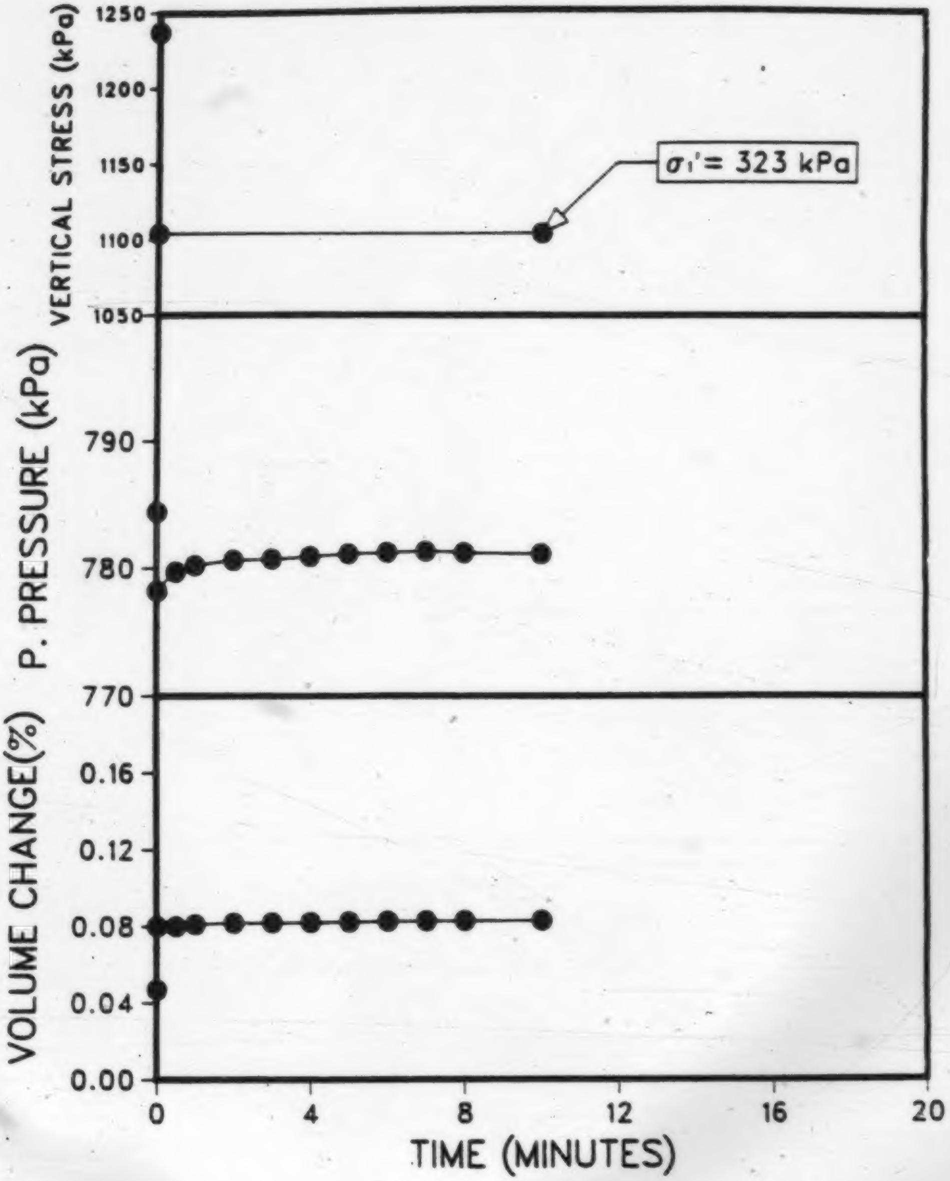

Figure B.3 Increment C from the unloading undrained test at 50°C for T-350

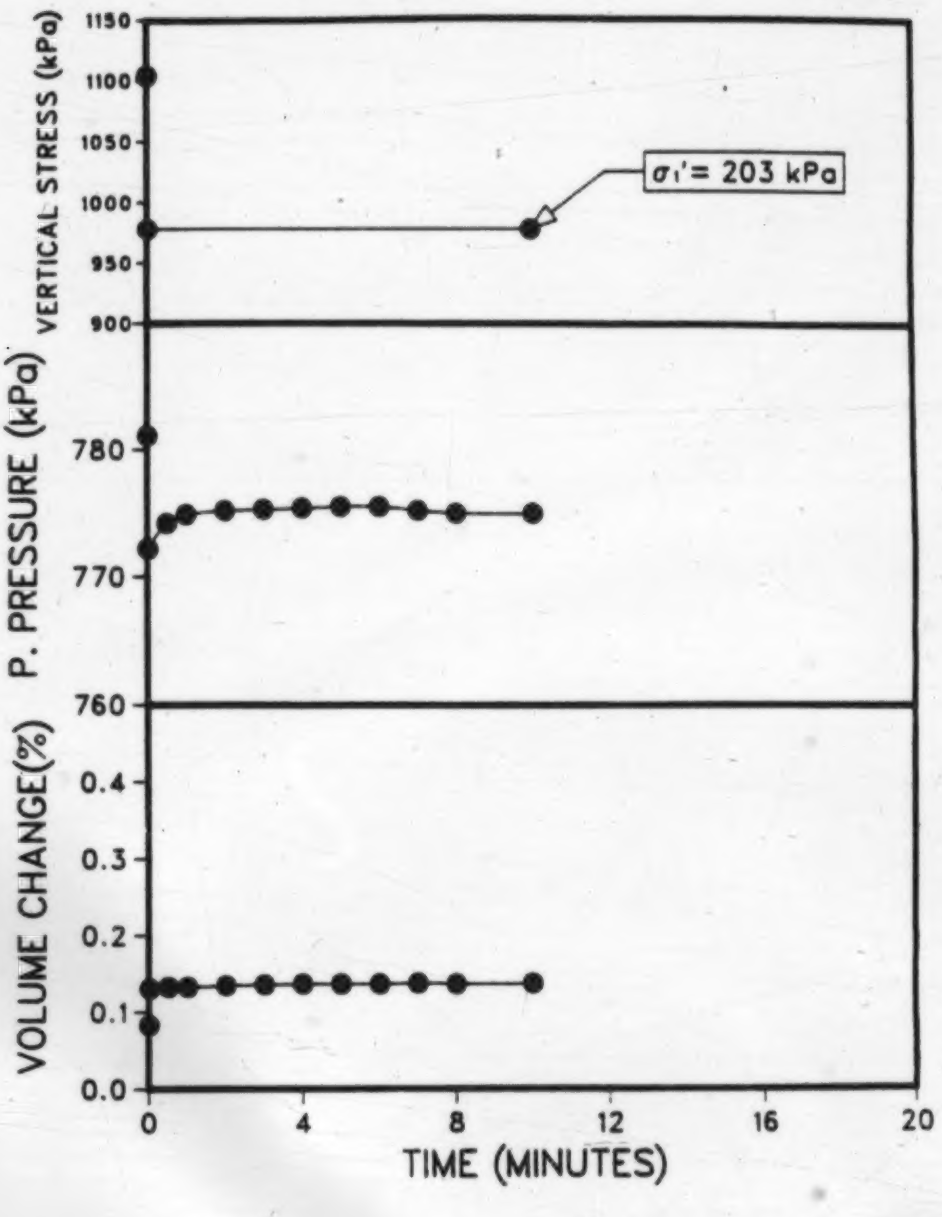

Figure B.4 Increment D from the unloading undrained test at 50°C for T-350

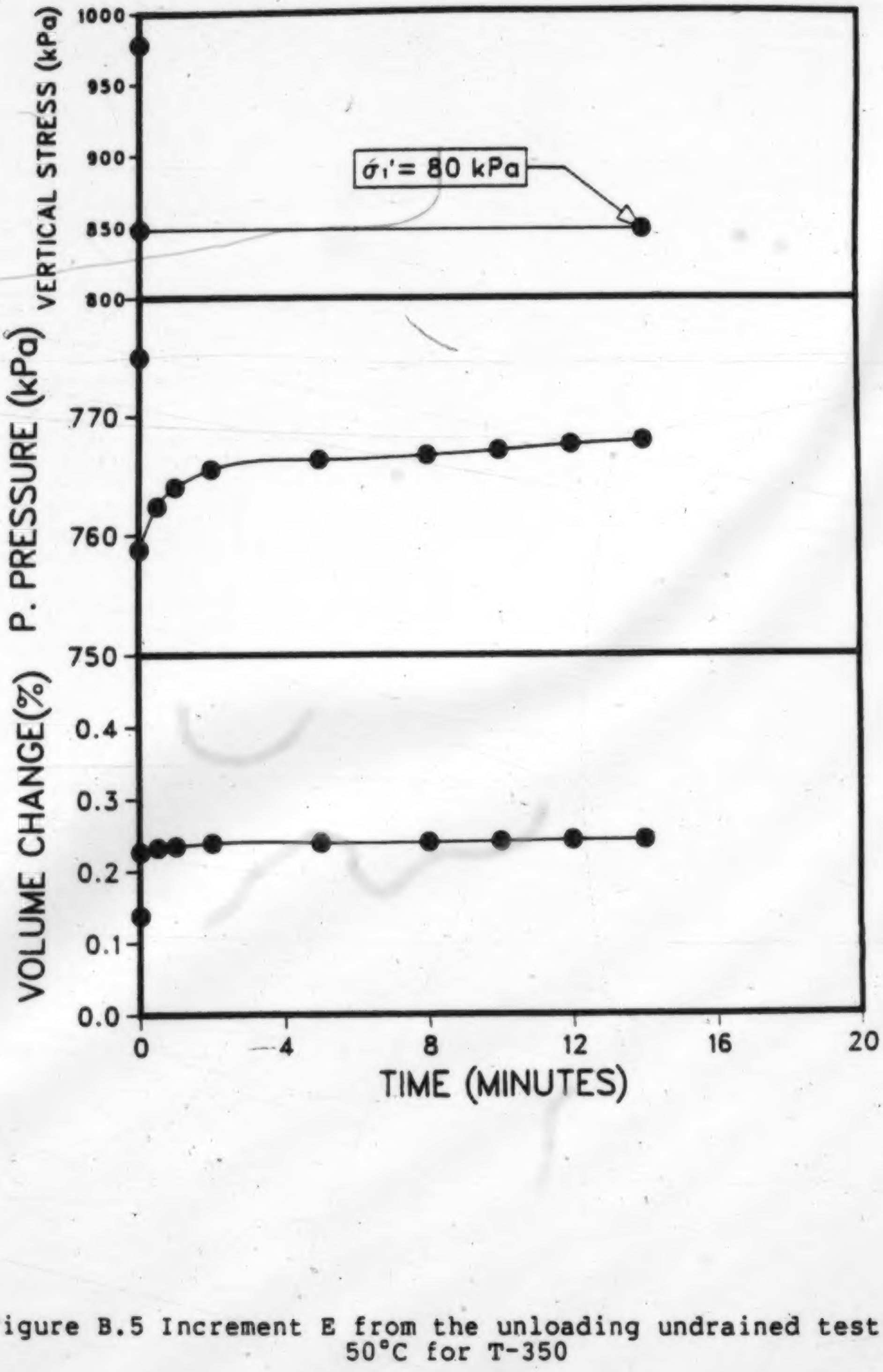

Figure B.5 Increment E from the unloading undrained test at 50°C for T-350

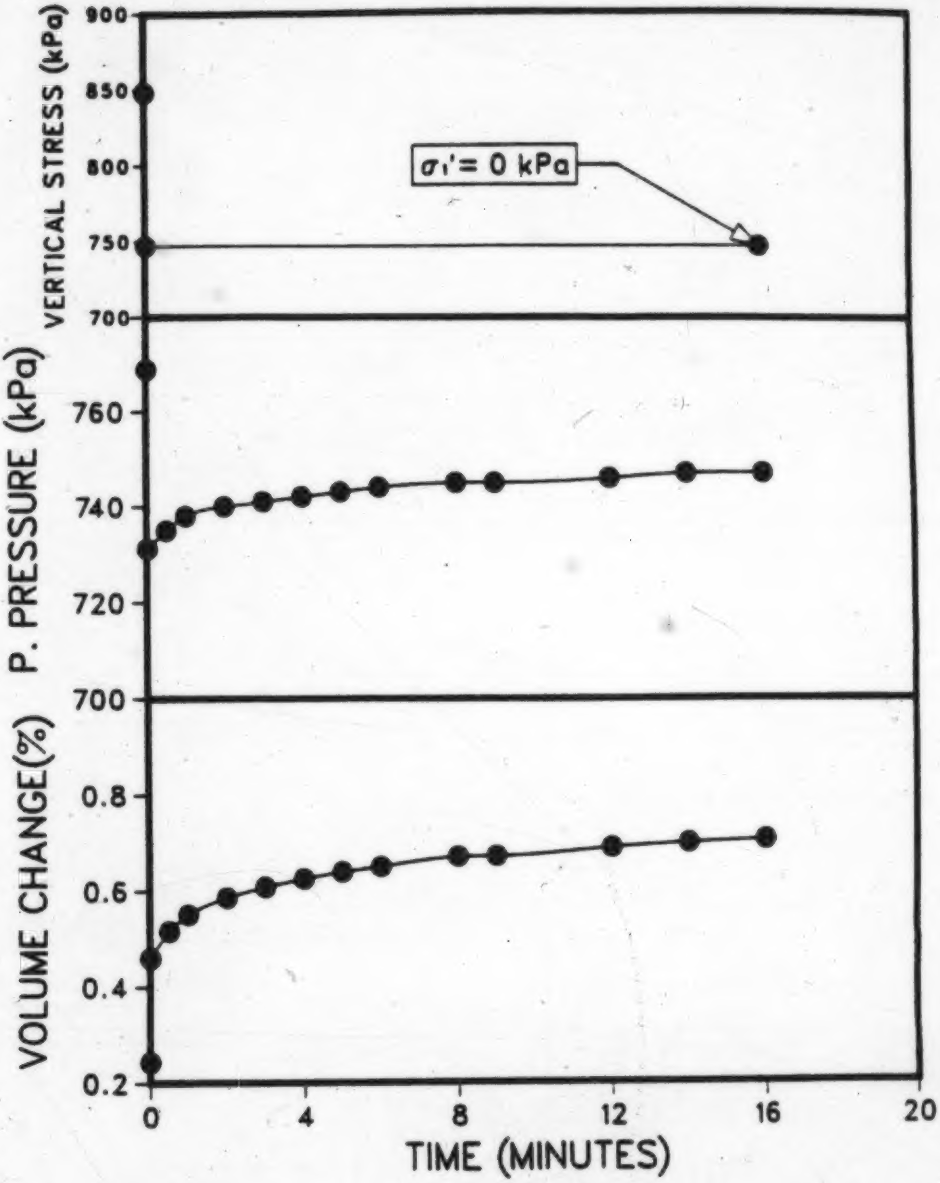

Figure B.6 Increment F from the unloading undrained test at 50°C for T-350

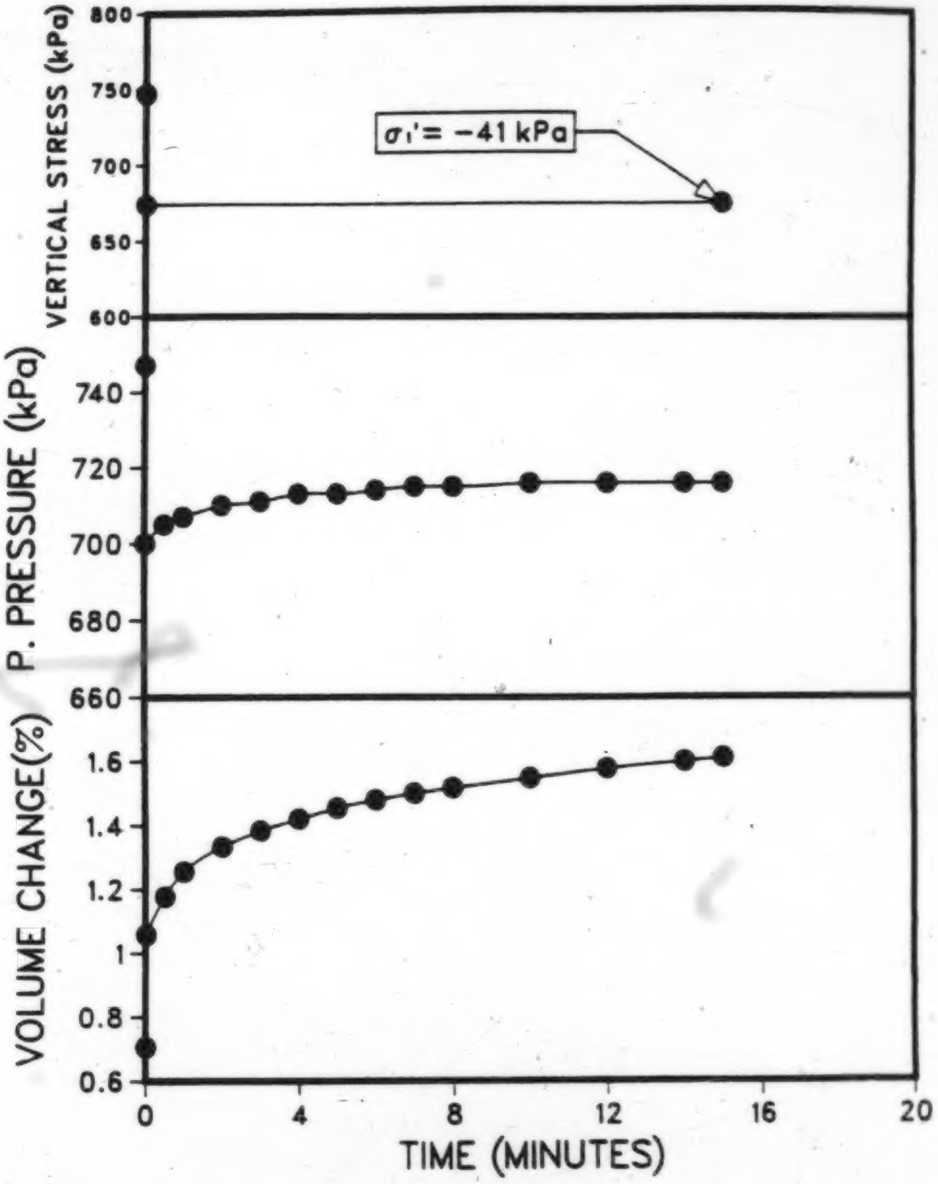

Figure B.7 Increment G from the unloading undrained test at 50°C for T-350

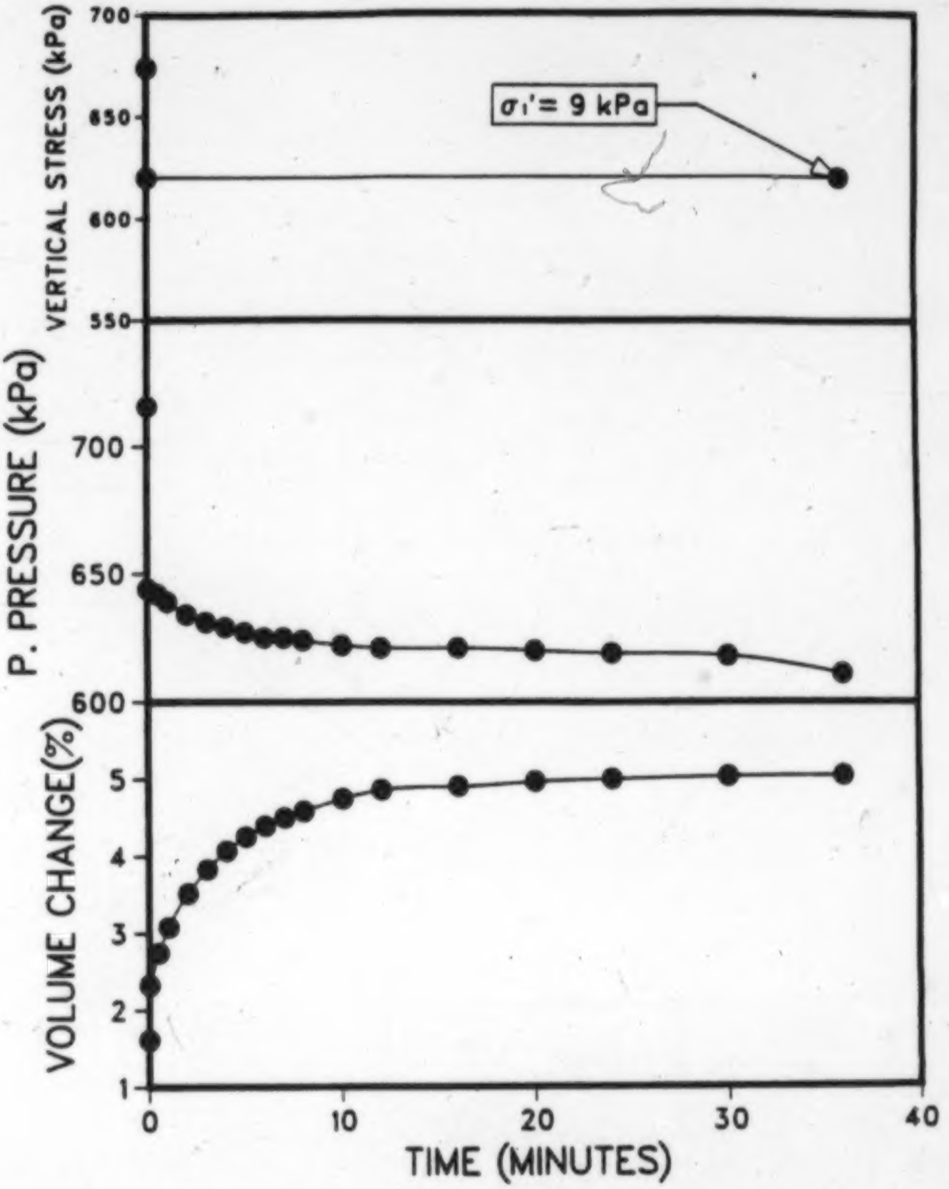

Figure B.8 Increment H from the unloading undrained test at 50°C for T-350

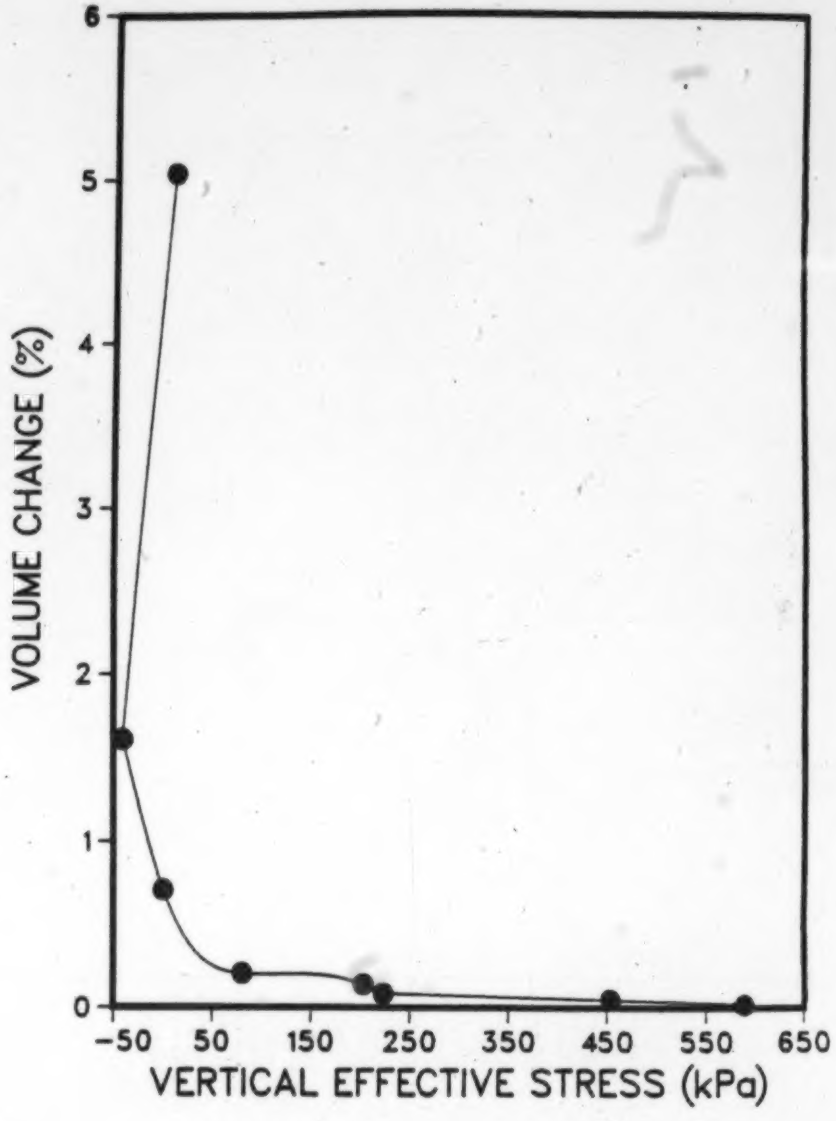

Figure B.9 Stress strain curve for sample T-350

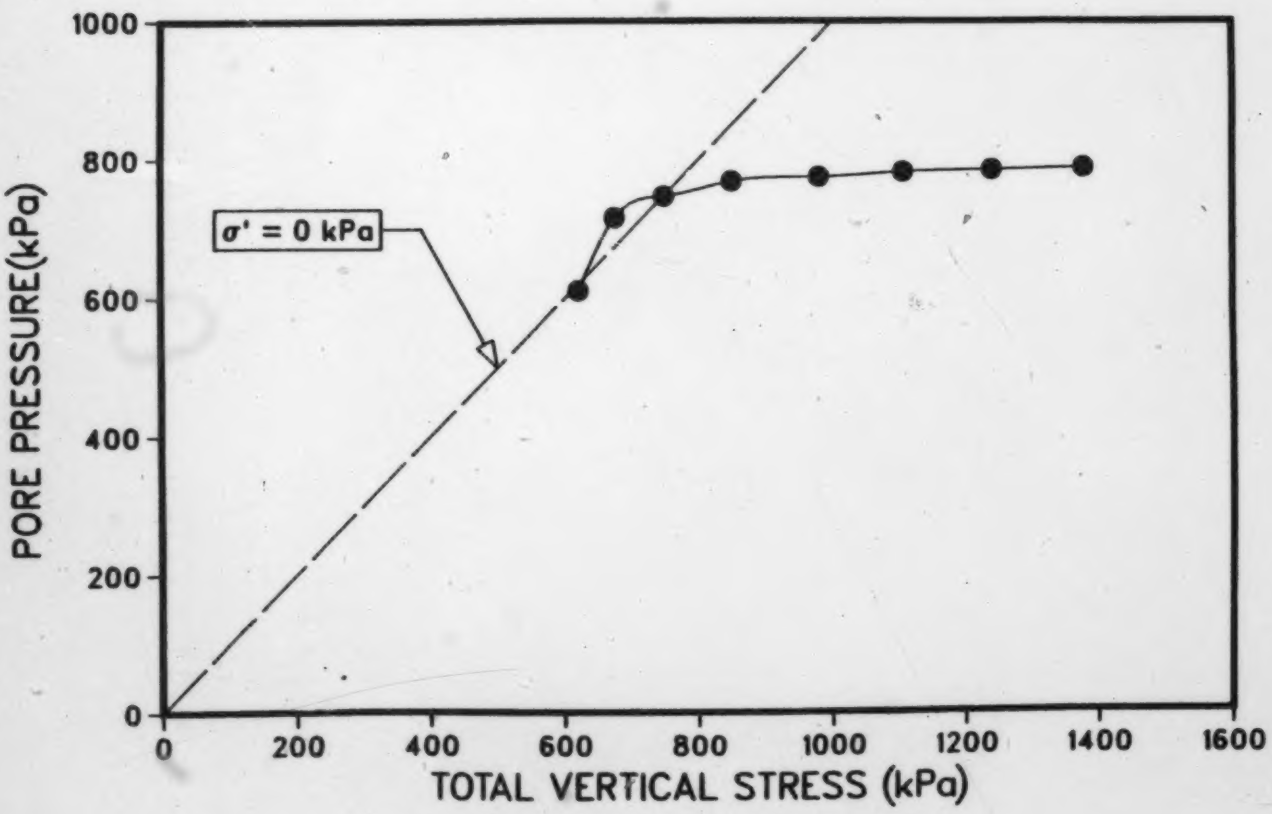

Figure B.10 Unloading Undrained Equilibrium Curve obtained from T-350

APPENDIX C - TESTING ON LEAN OIL SAND AT 6°C AND 60°C

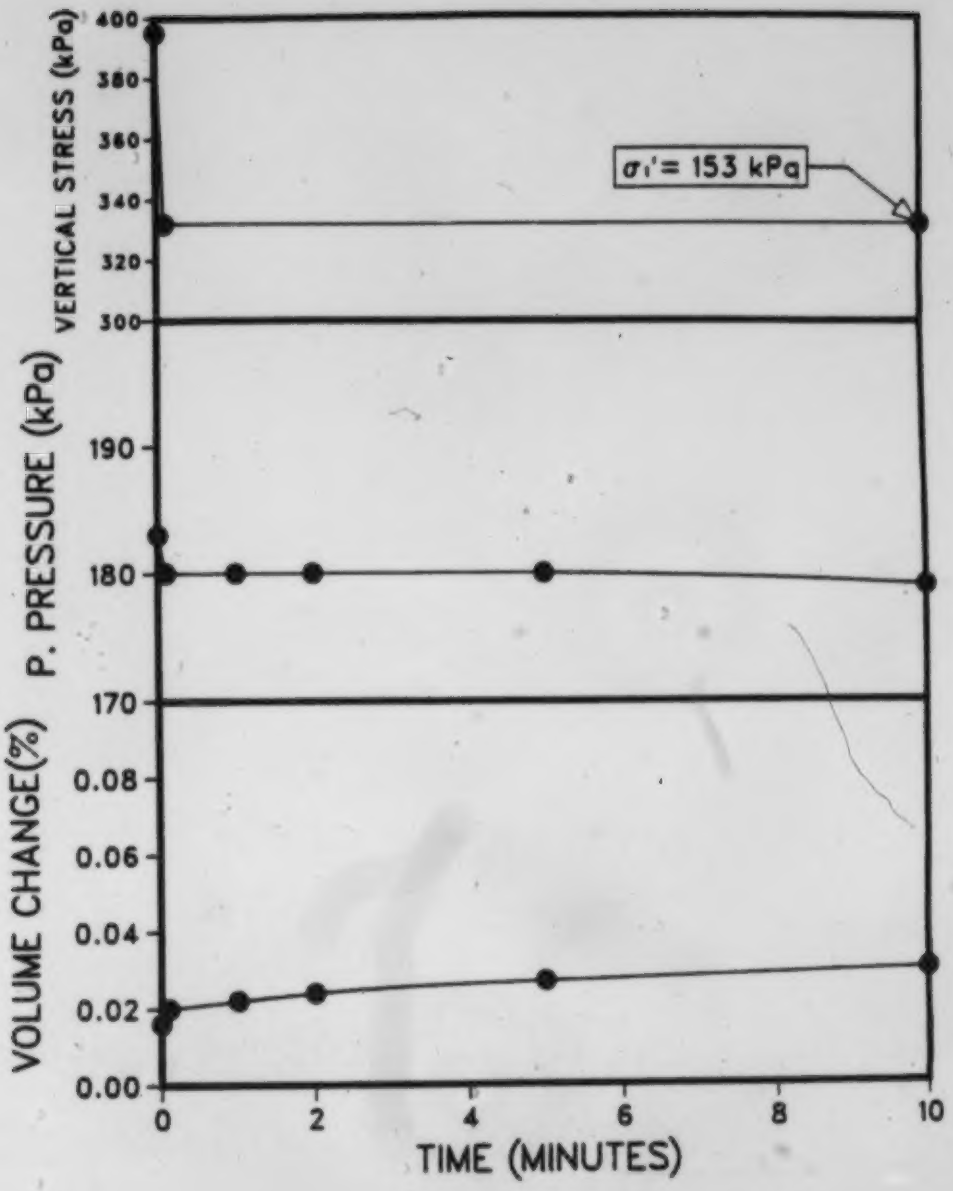

Figure C.1 Increment B from the unloading undrained test at 6°C for B-225

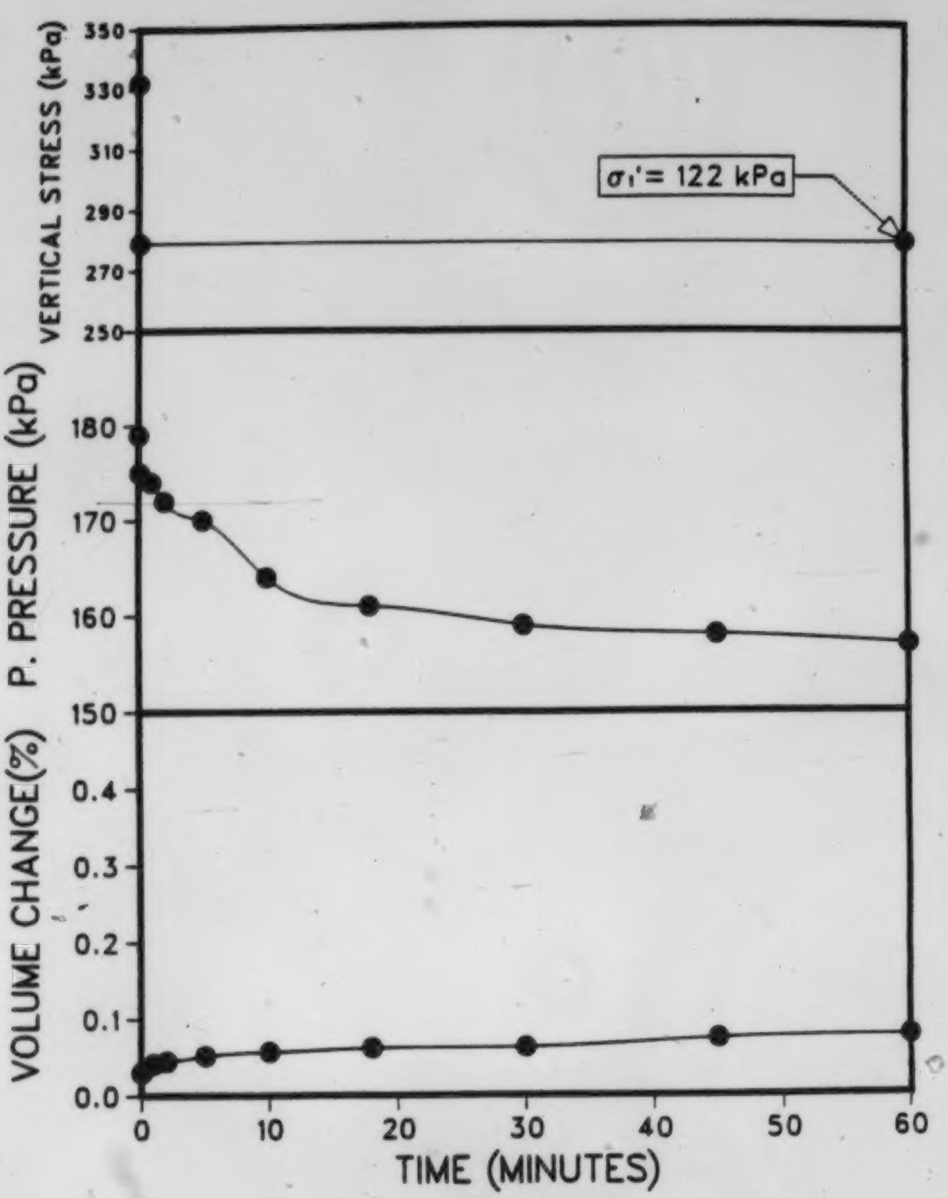

Figure C.2 Increment C from the unloading undrained test at 6°C for B-225

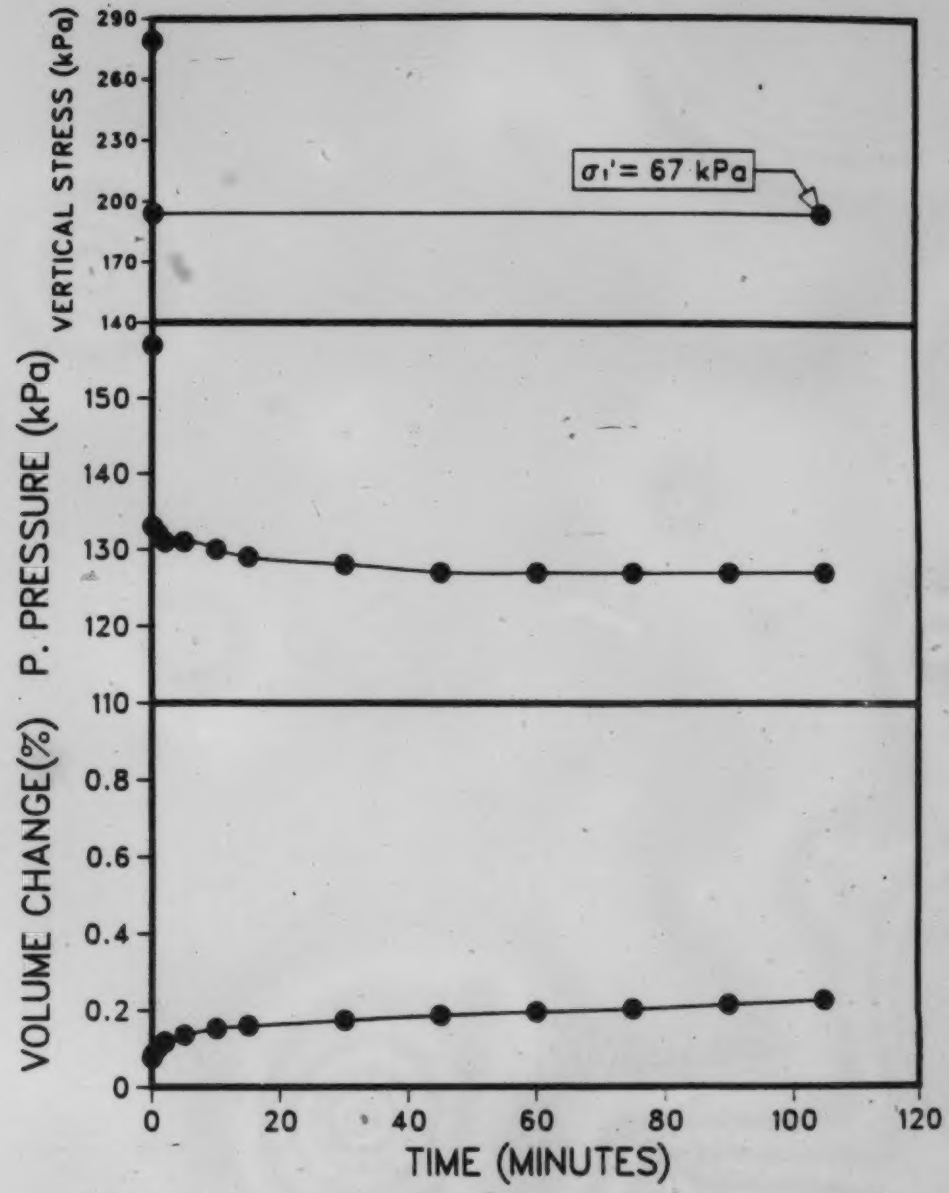

Figure C.3 Increment D from the unloading undrained test at 6°C for B-225

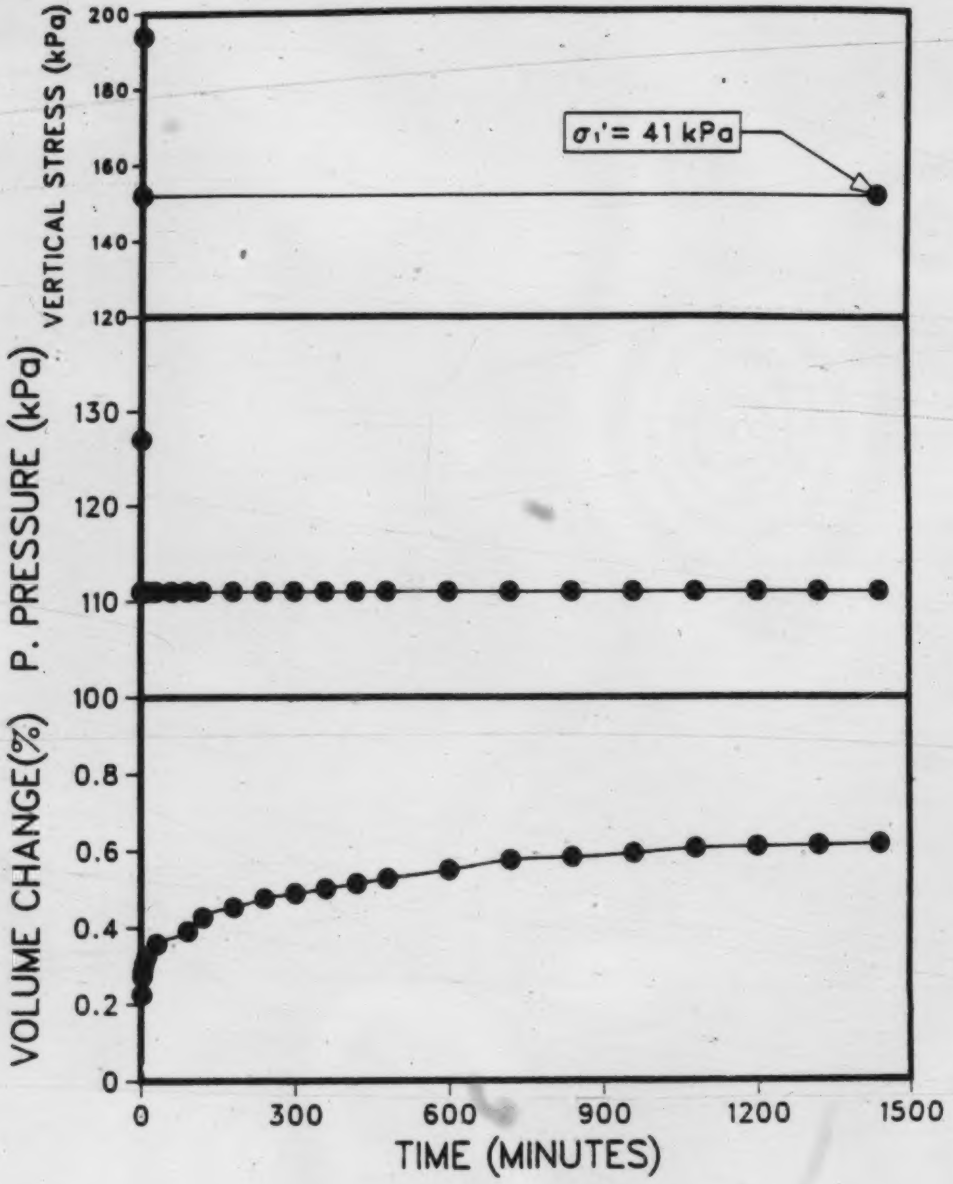

Figure C.4 Increment E from the unloading undrained test at 6°C for B-225

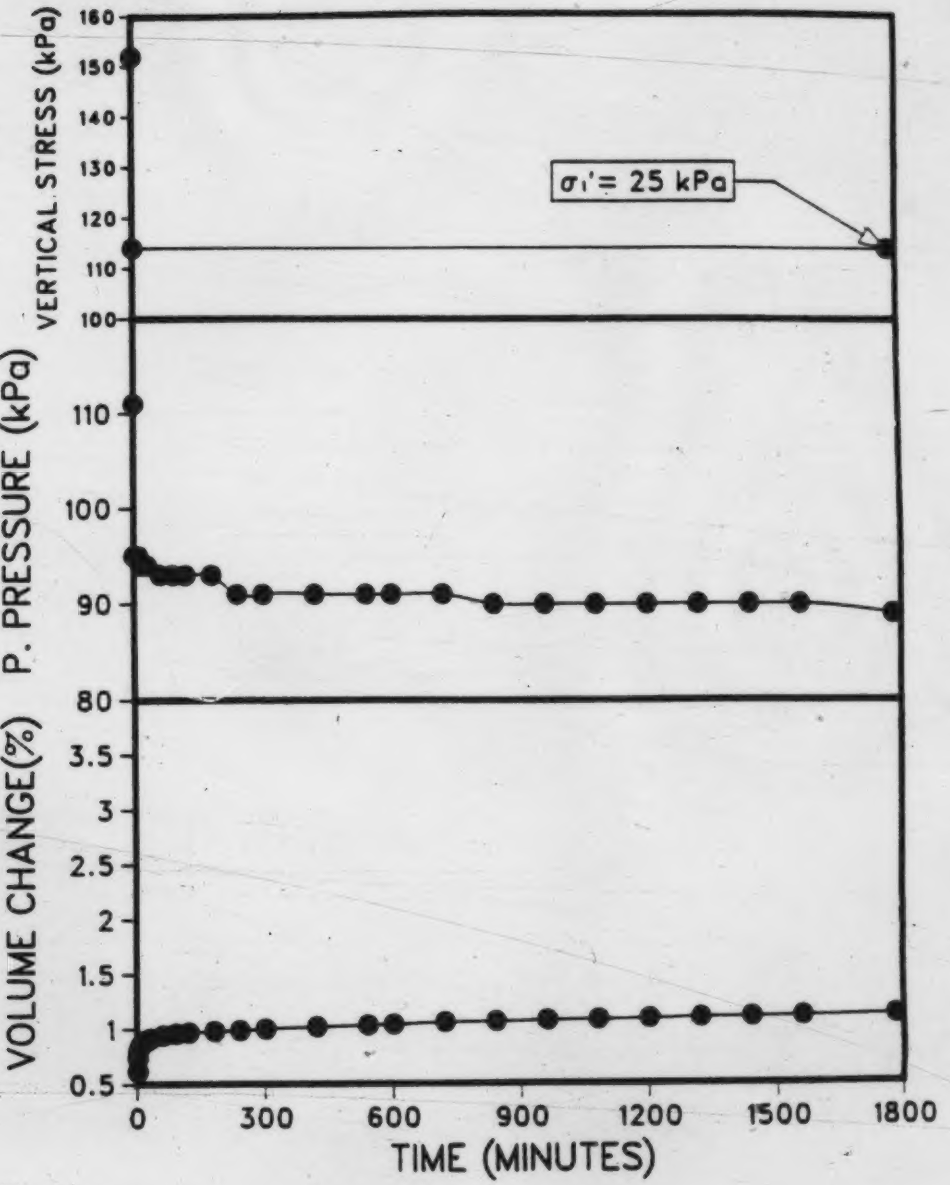

Figure C.5 Increment F from the unloading undrained test at 6°C for B-225

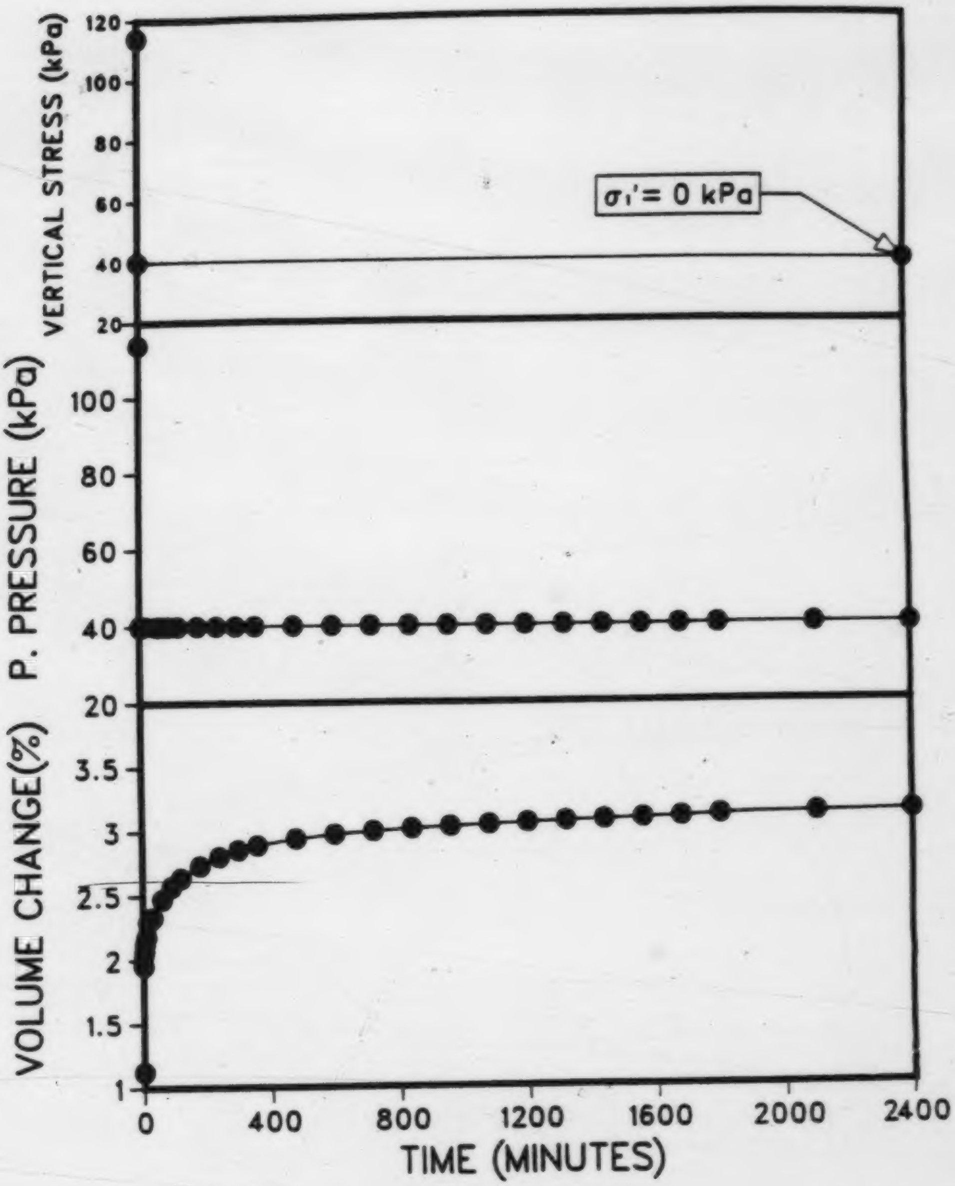

Figure C.6 Increment G from the unloading undrained test at 6°C for B-225

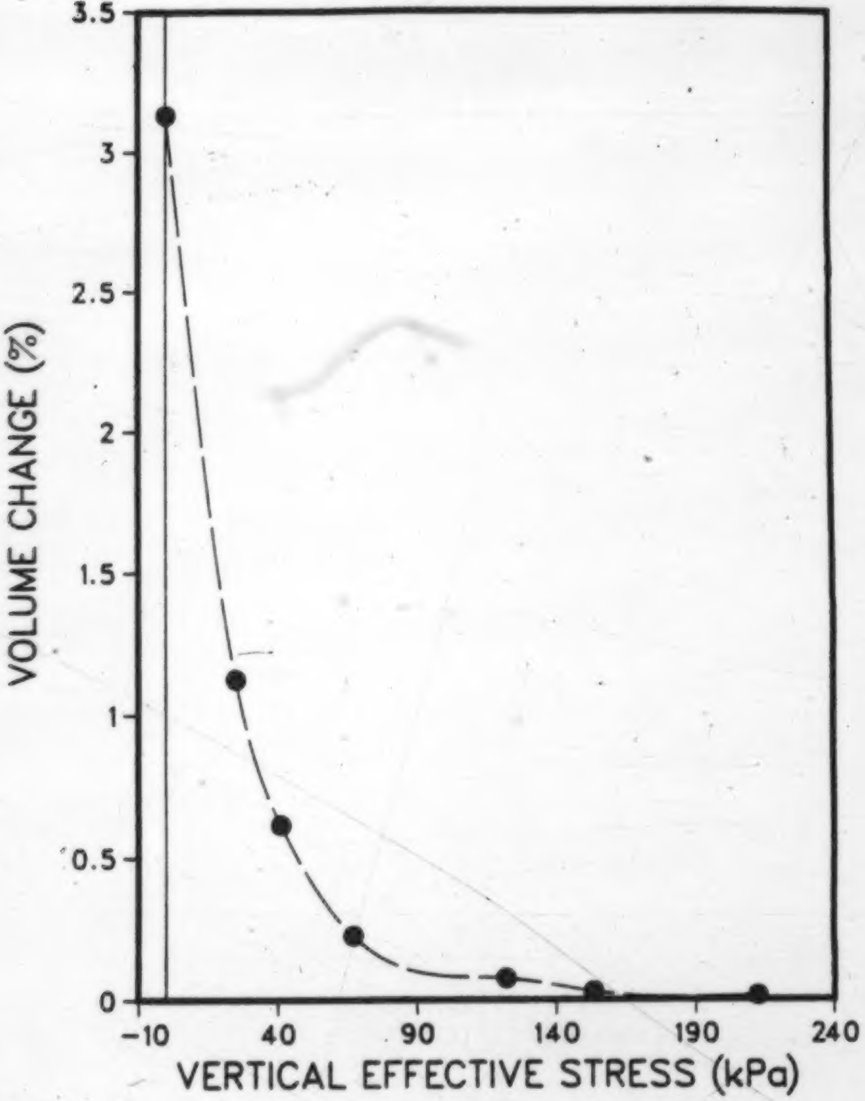

Figure C.7 Stress strain curve for sample B-225

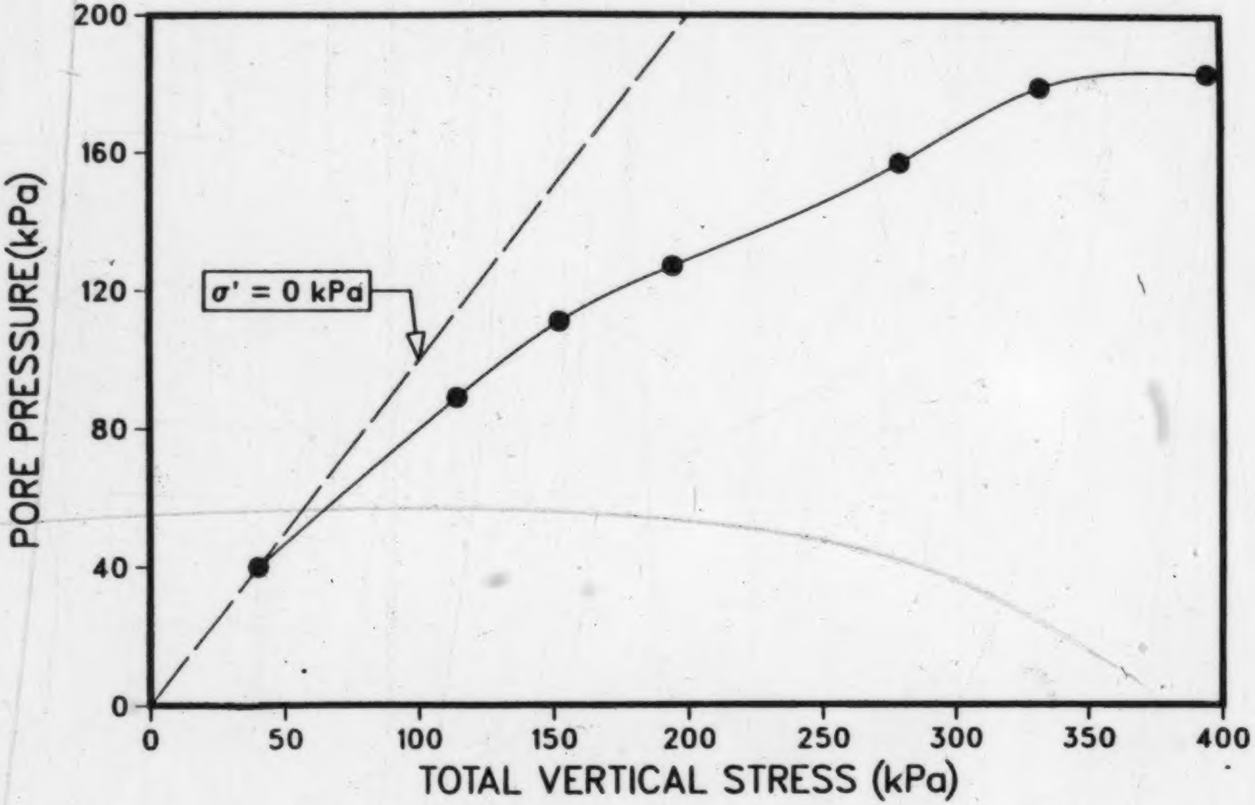

Figure C.8 Unloading Undrained Equilibrium Curve obtained from B-225

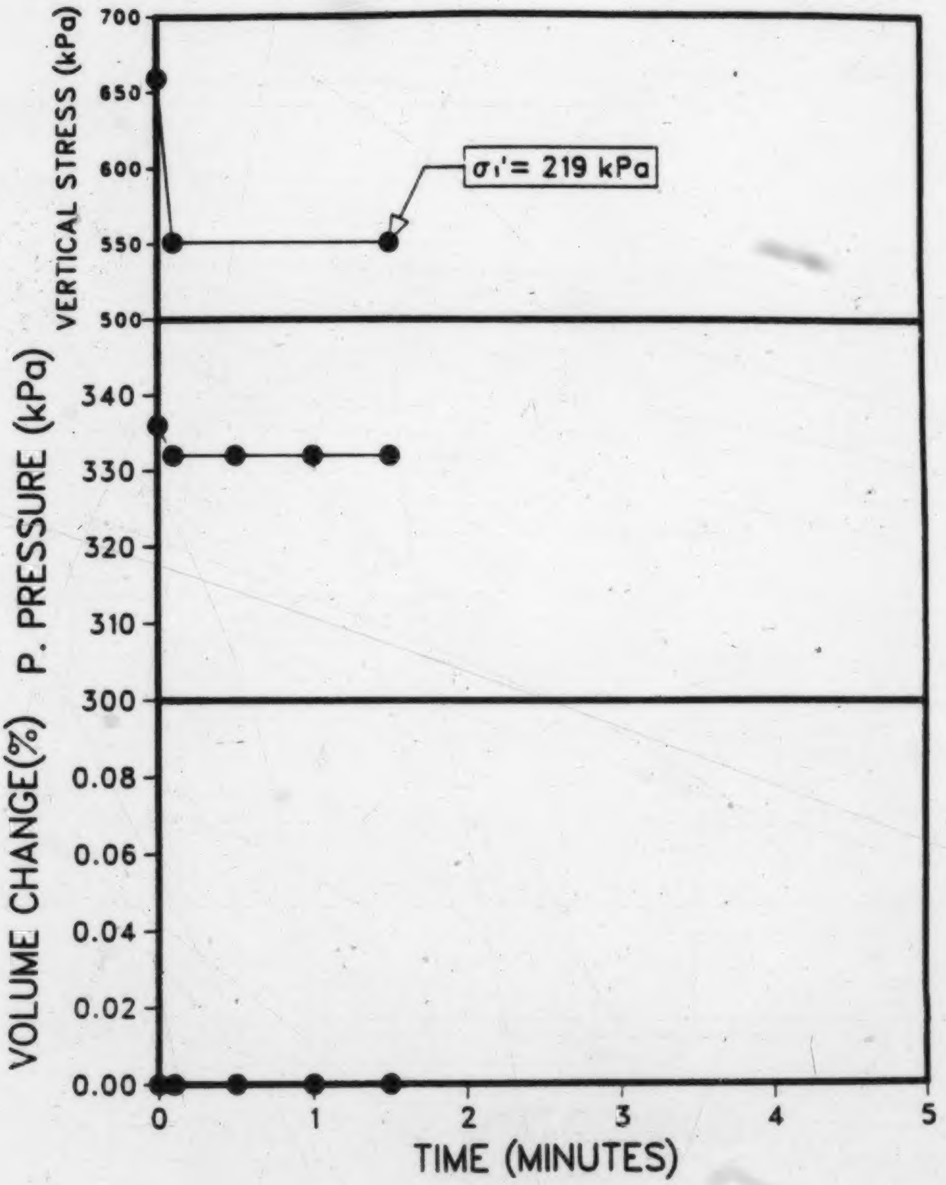

Figure C.9 Increment A from the unloading undrained test at 60°C for B-223

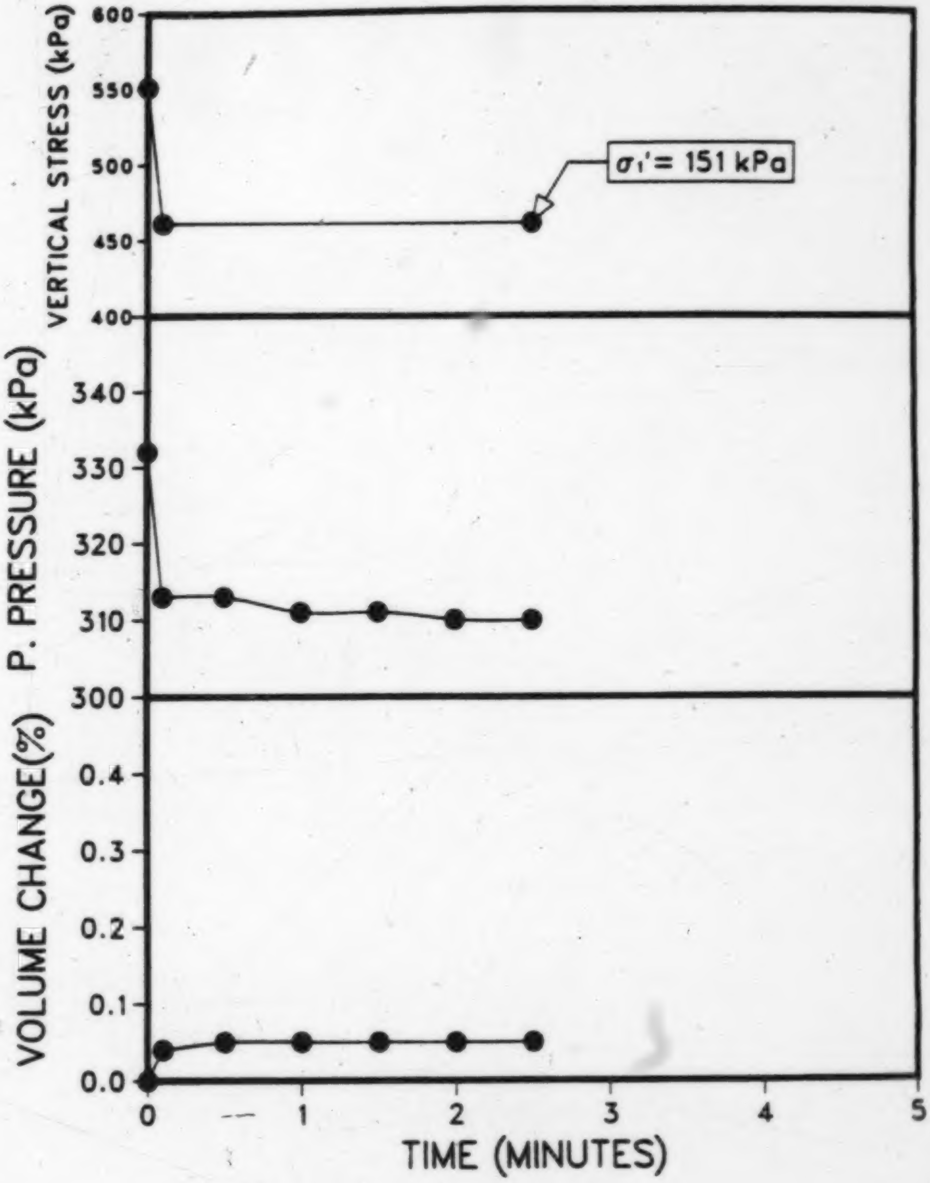

Figure C.10 Increment B from the unloading undrained test at 60°C for B-223

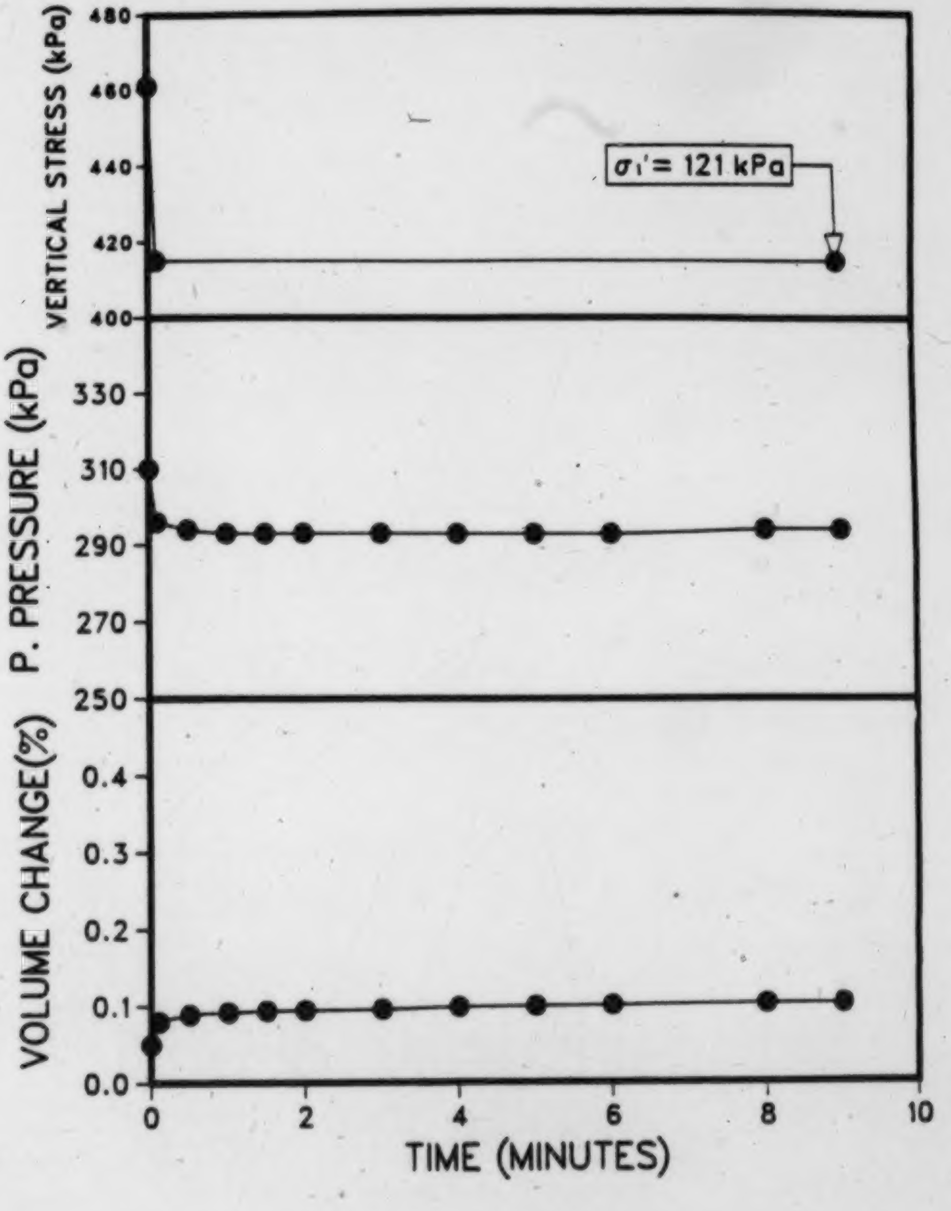

Figure C.11 Increment C from the unloading undrained test at 60°C for B-223

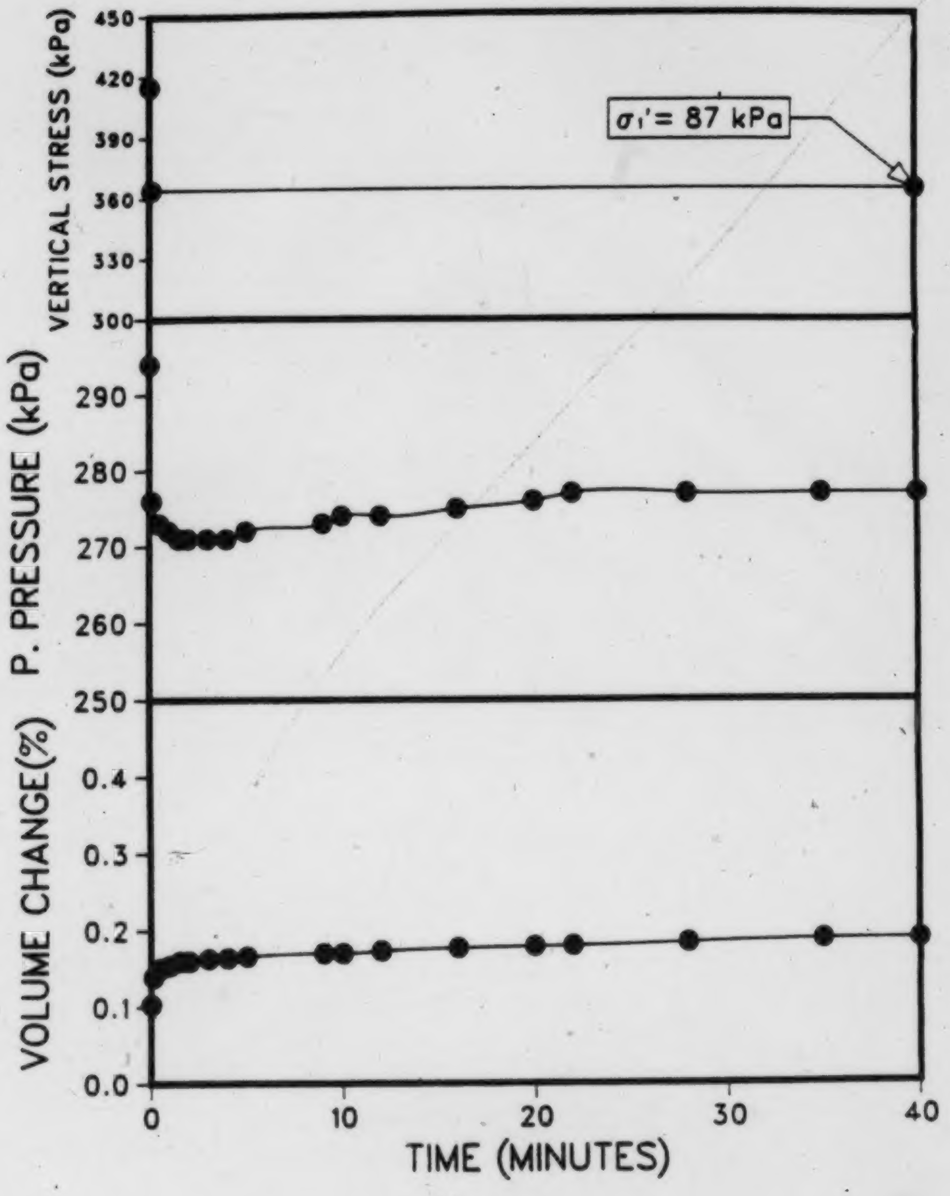

Figure C.12 Increment D from the unloading undrained test at 60°C for B-223

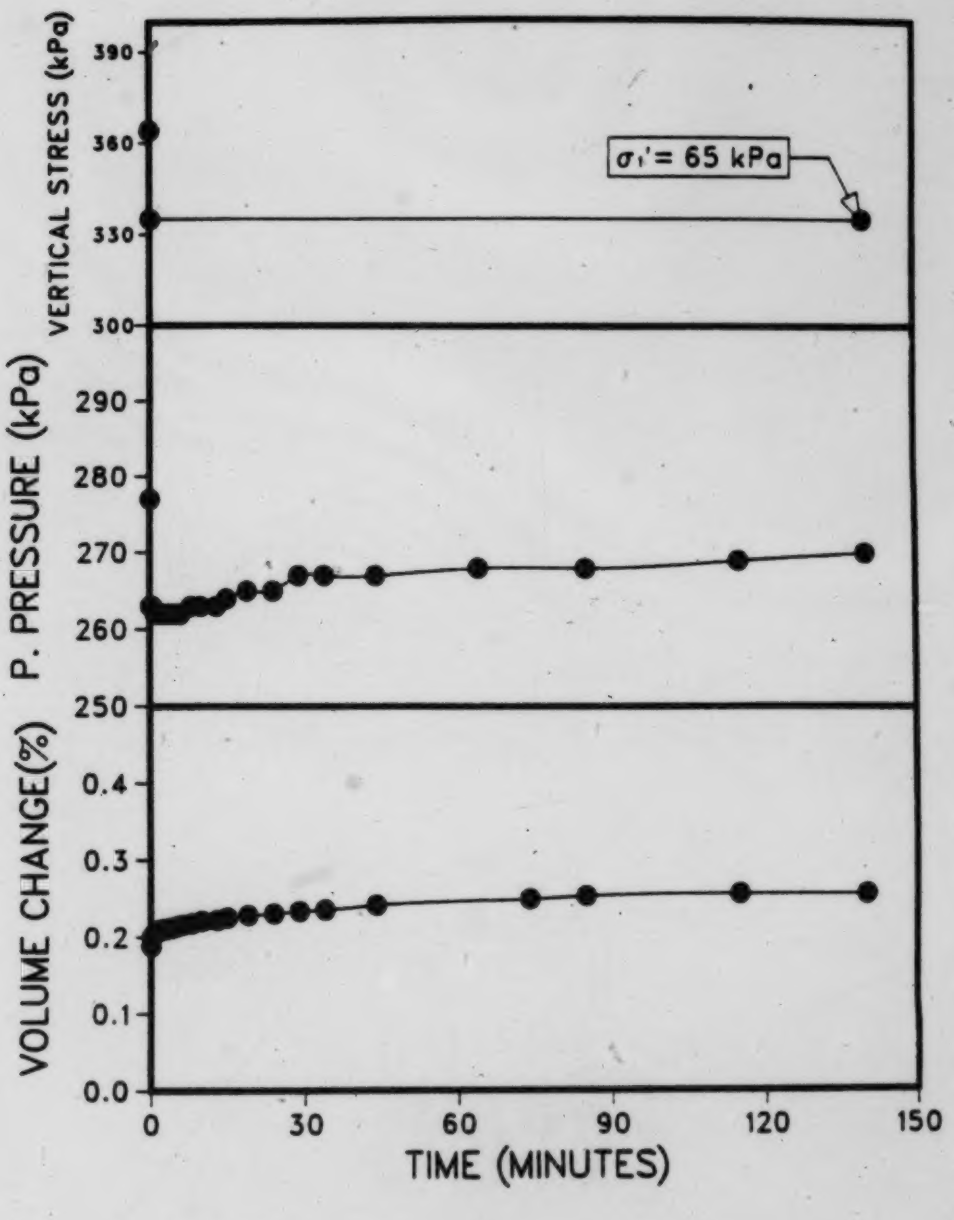

Figure C.13 Increment E from the unloading undrained test at 60°C for B-223

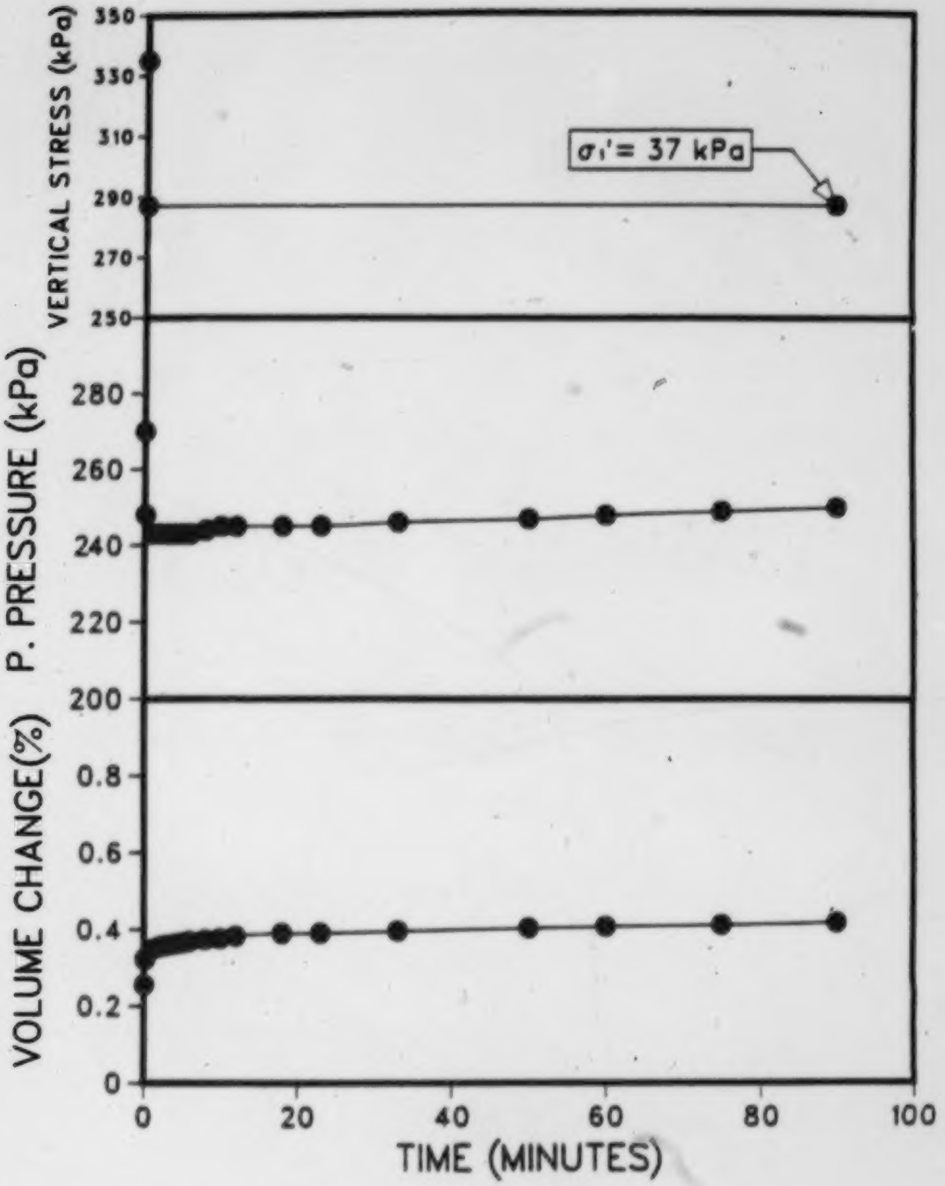

Figure C.14 Increment F from the unloading undrained test at 60°C for B-223

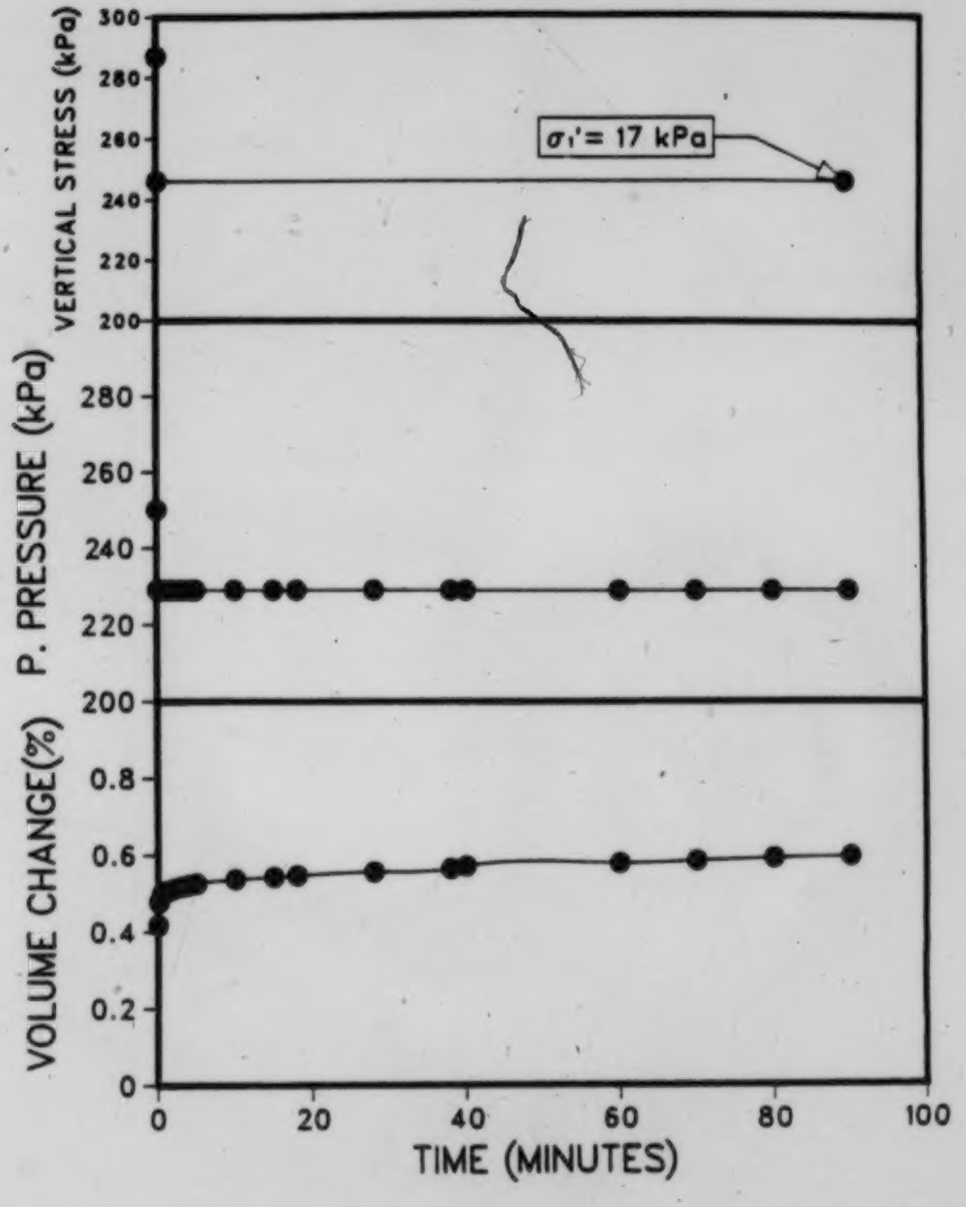

Figure C.15 Increment G from the unloading undrained test at 60°C for B-223

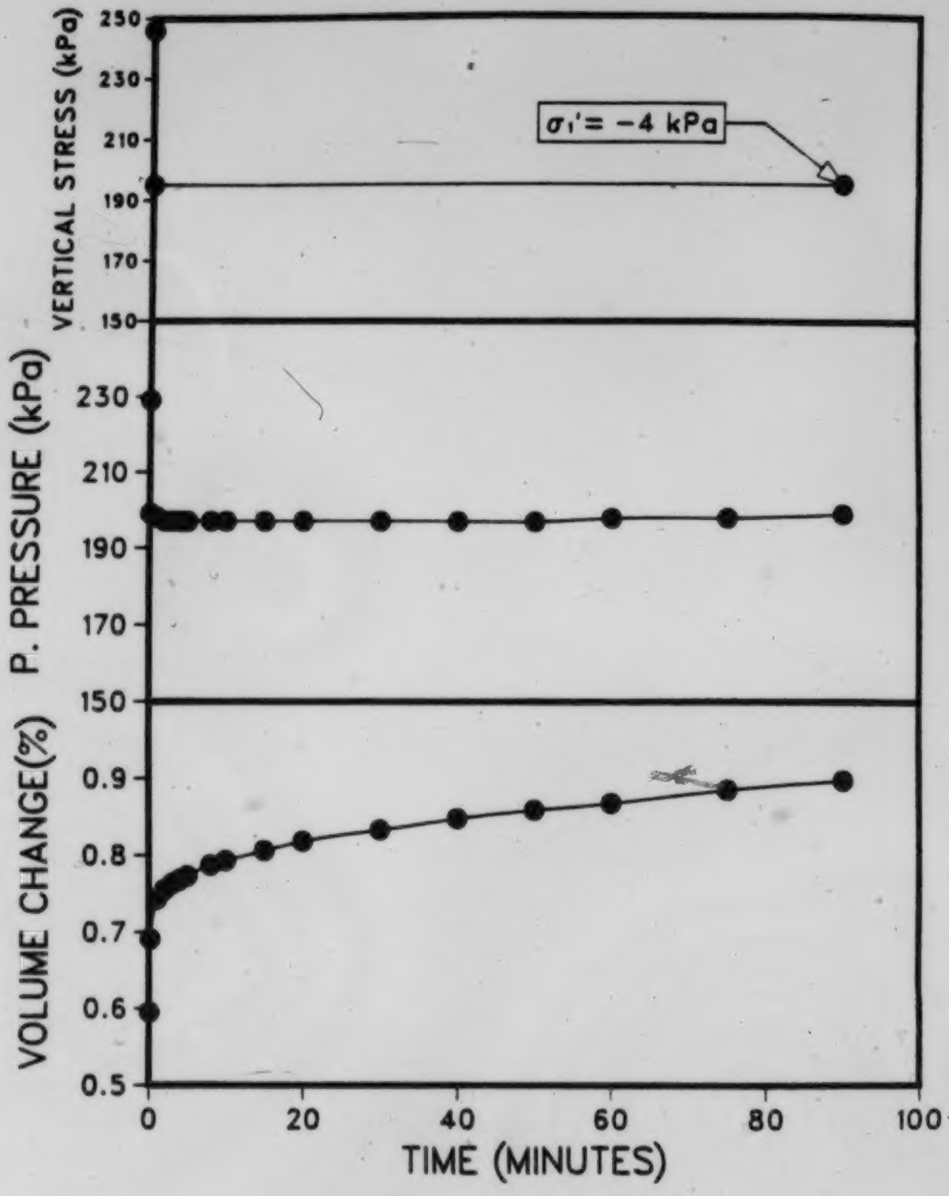

Figure C.16 Increment H from the unloading undrained test at 60°C for B-223

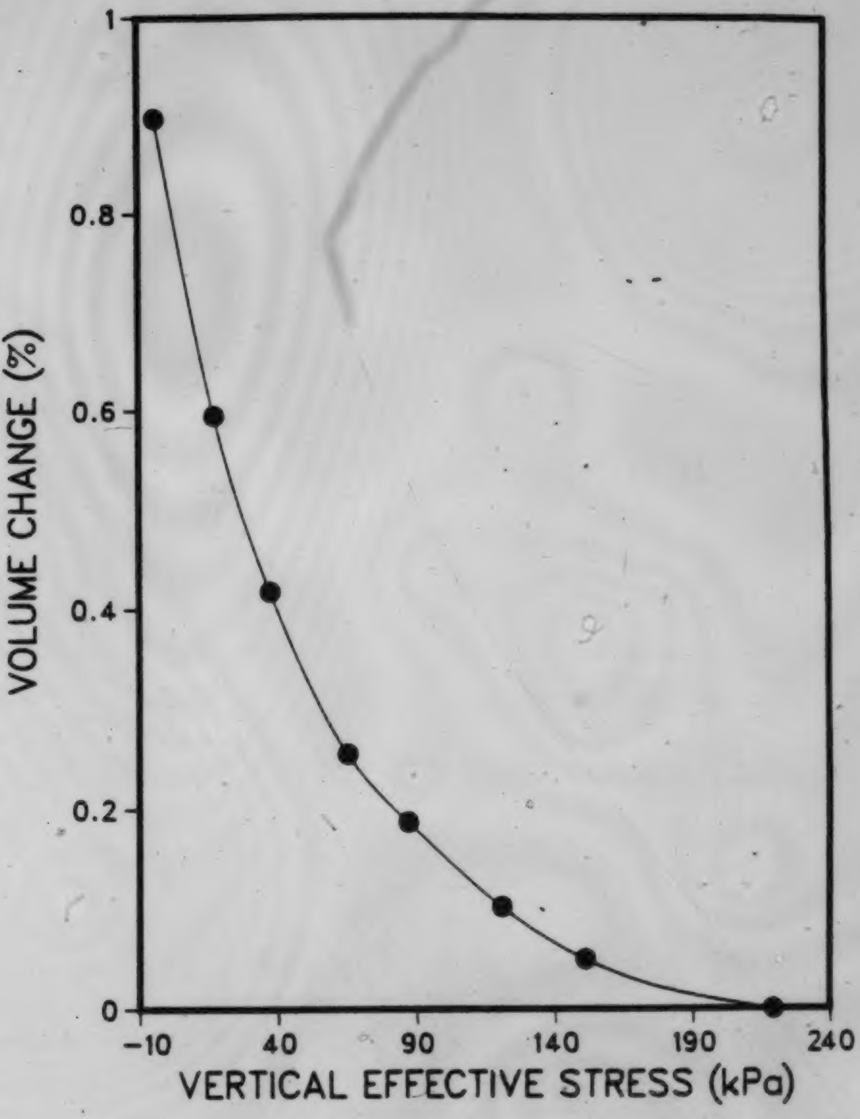

Figure C.17 Stress strain curve for sample B-223

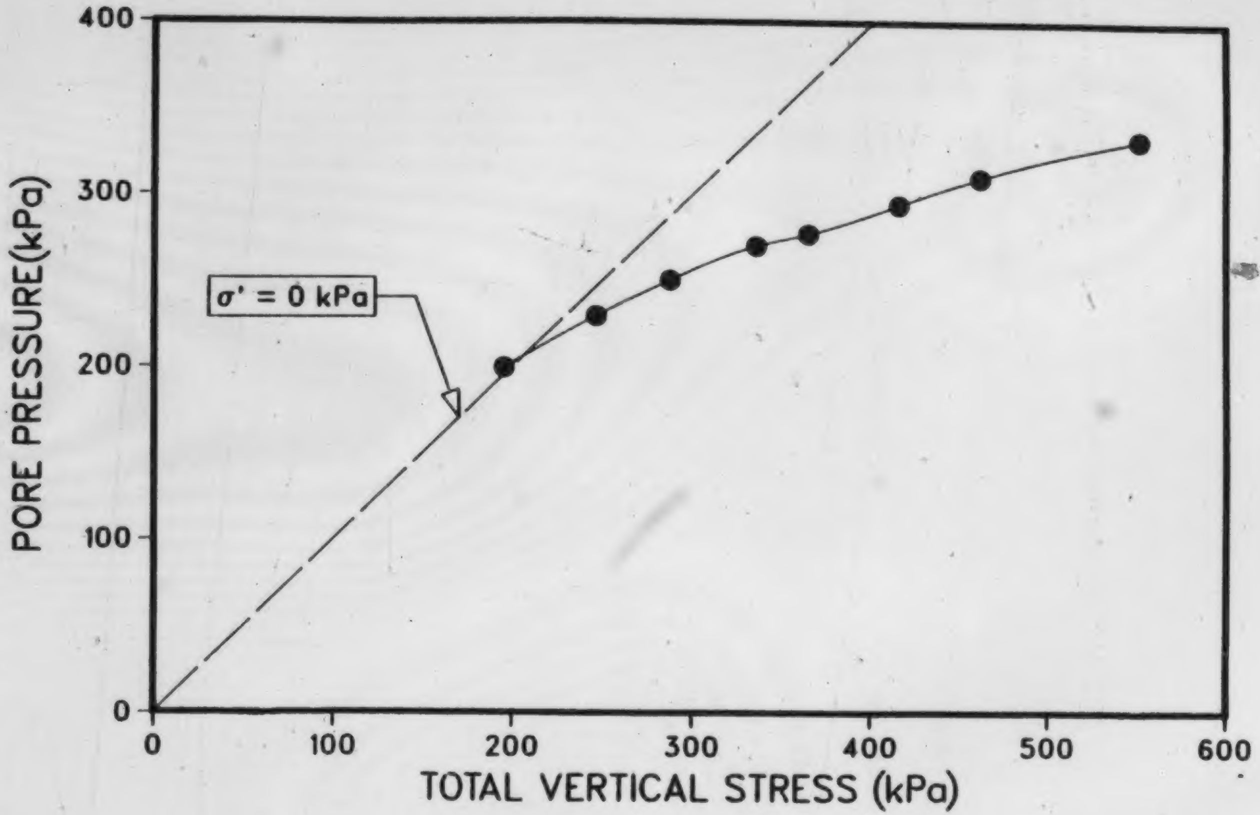

Figure C.18 Unloading undrained Equilibrium Curve obtained from B-223

APPENDIX D - TESTING ON RICH OIL SAND AT 24°C

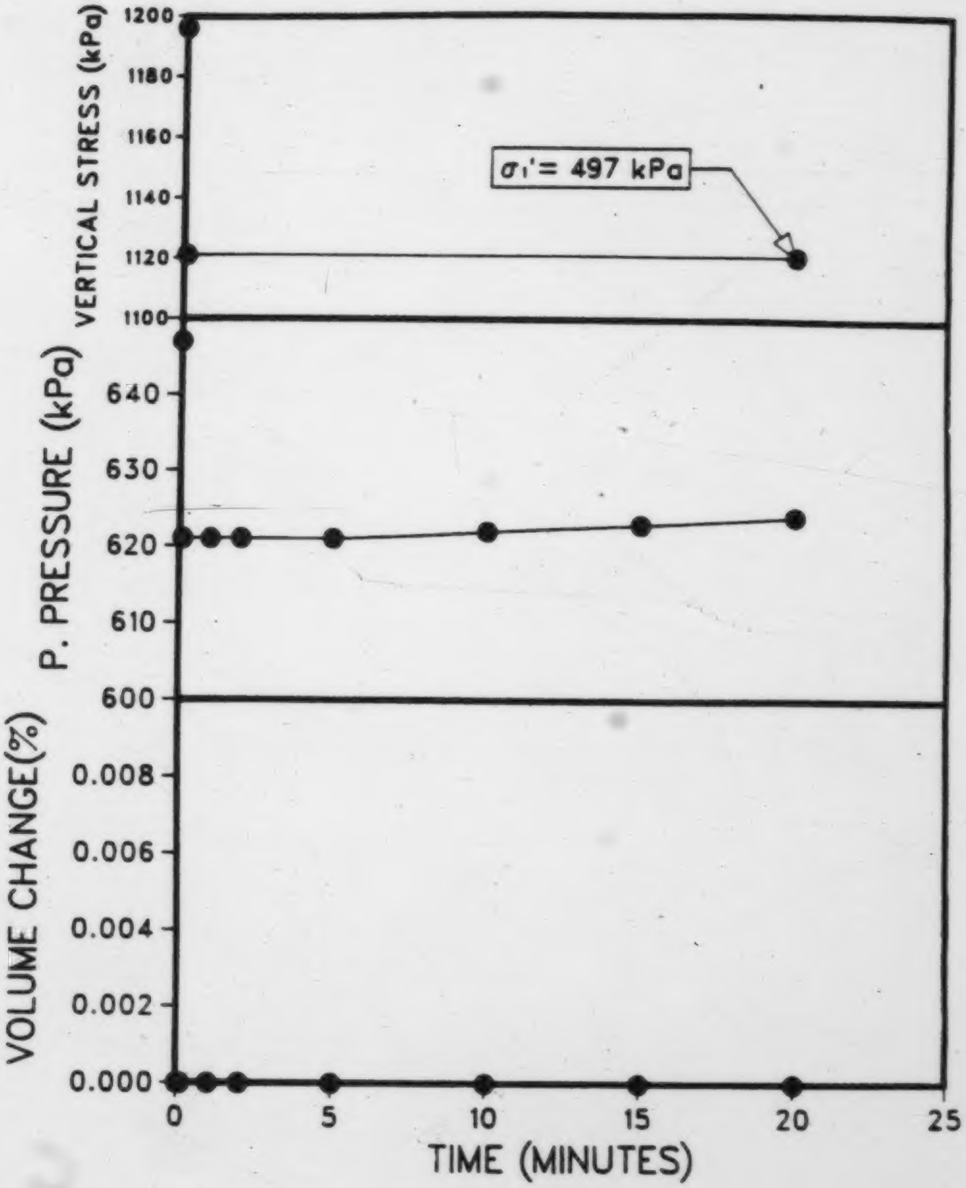

Figure D.1 Increment D from the unloading undrained test at 24°C for RB-5-2

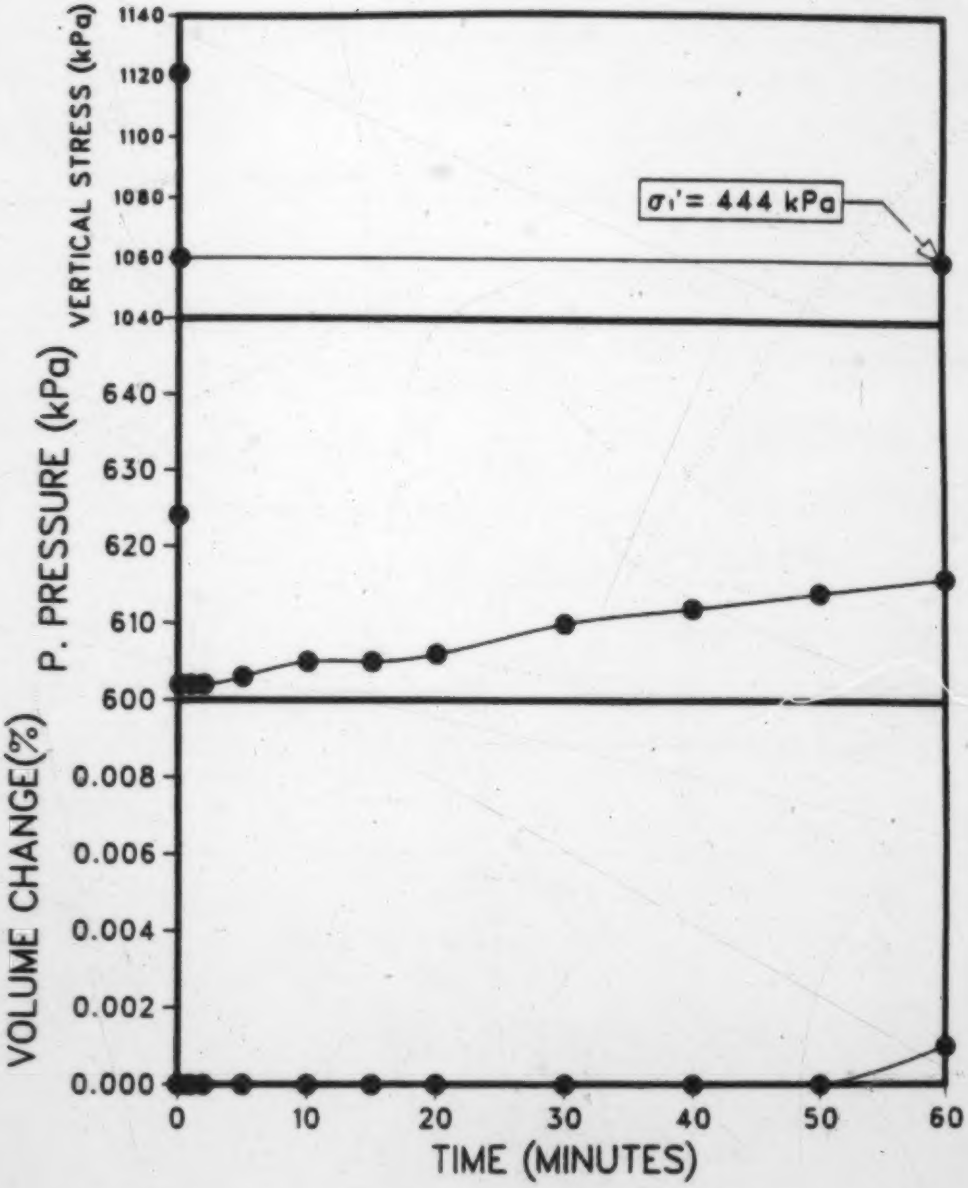

Figure D.2 Increment E from the unloading undrained test at 24°C for RB-5-2

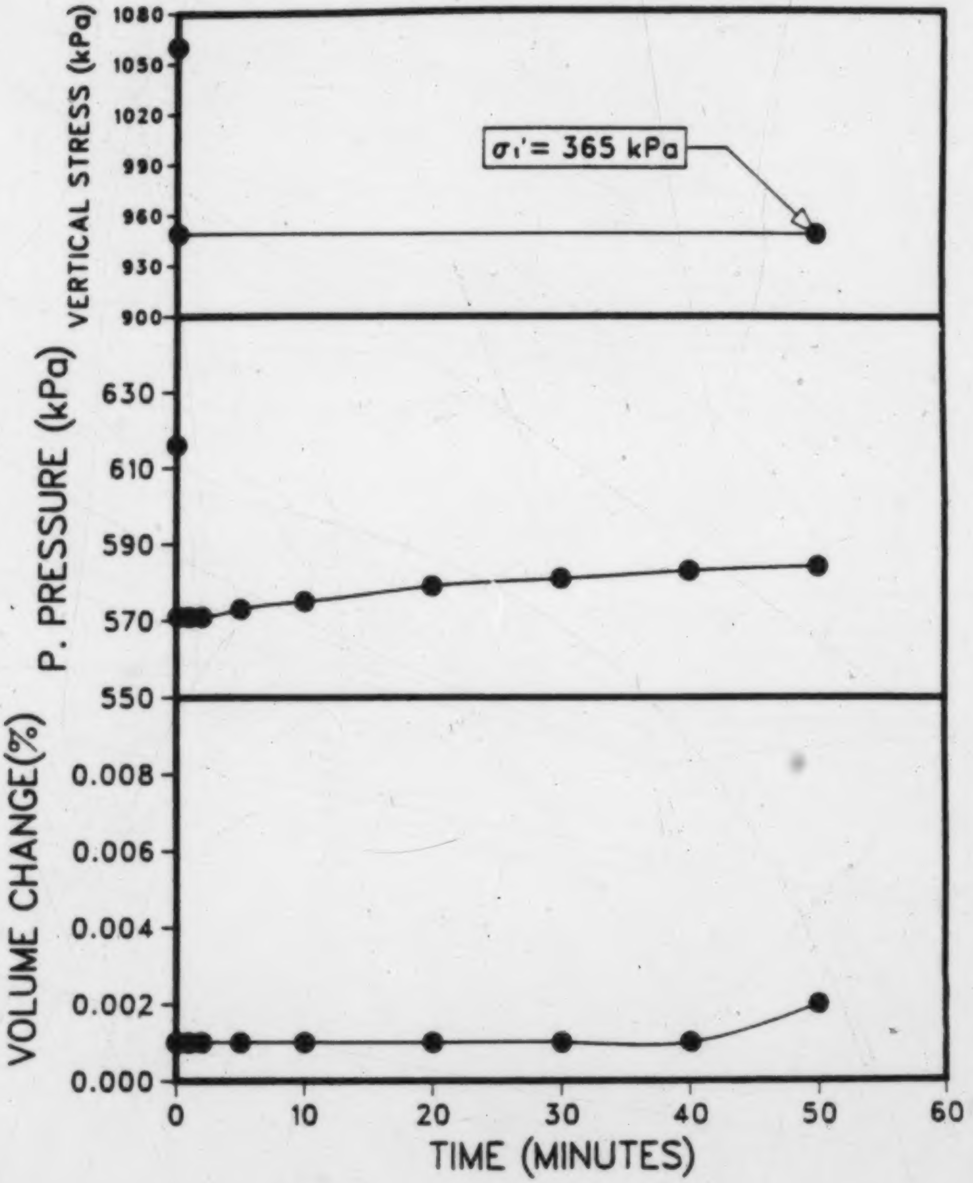

5

Figure D.3 Increment F from the unloading undrained test at 24°C for RB-5-2

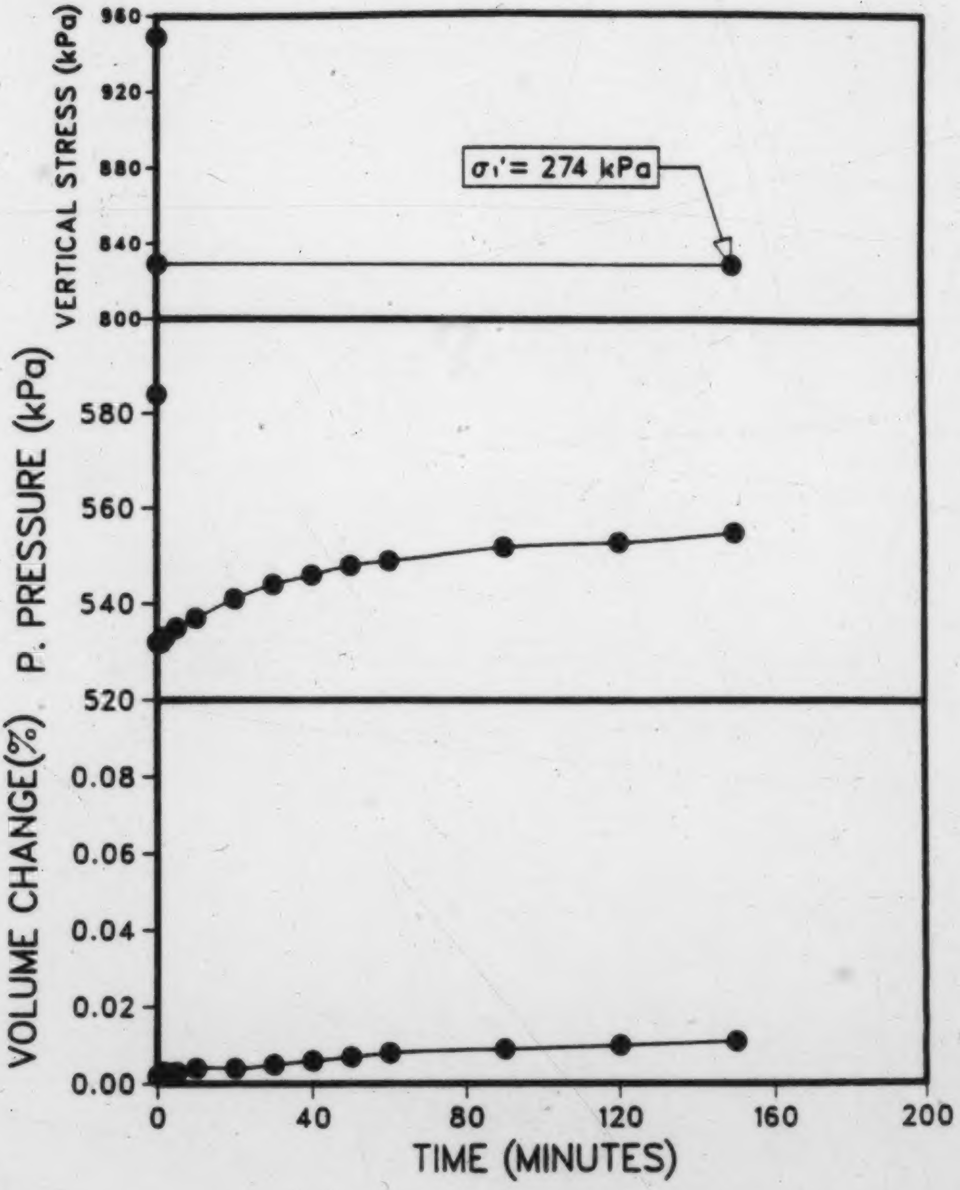

Figure D.4 Increment G from the unloading undrained test at 24°C for RB-5-2

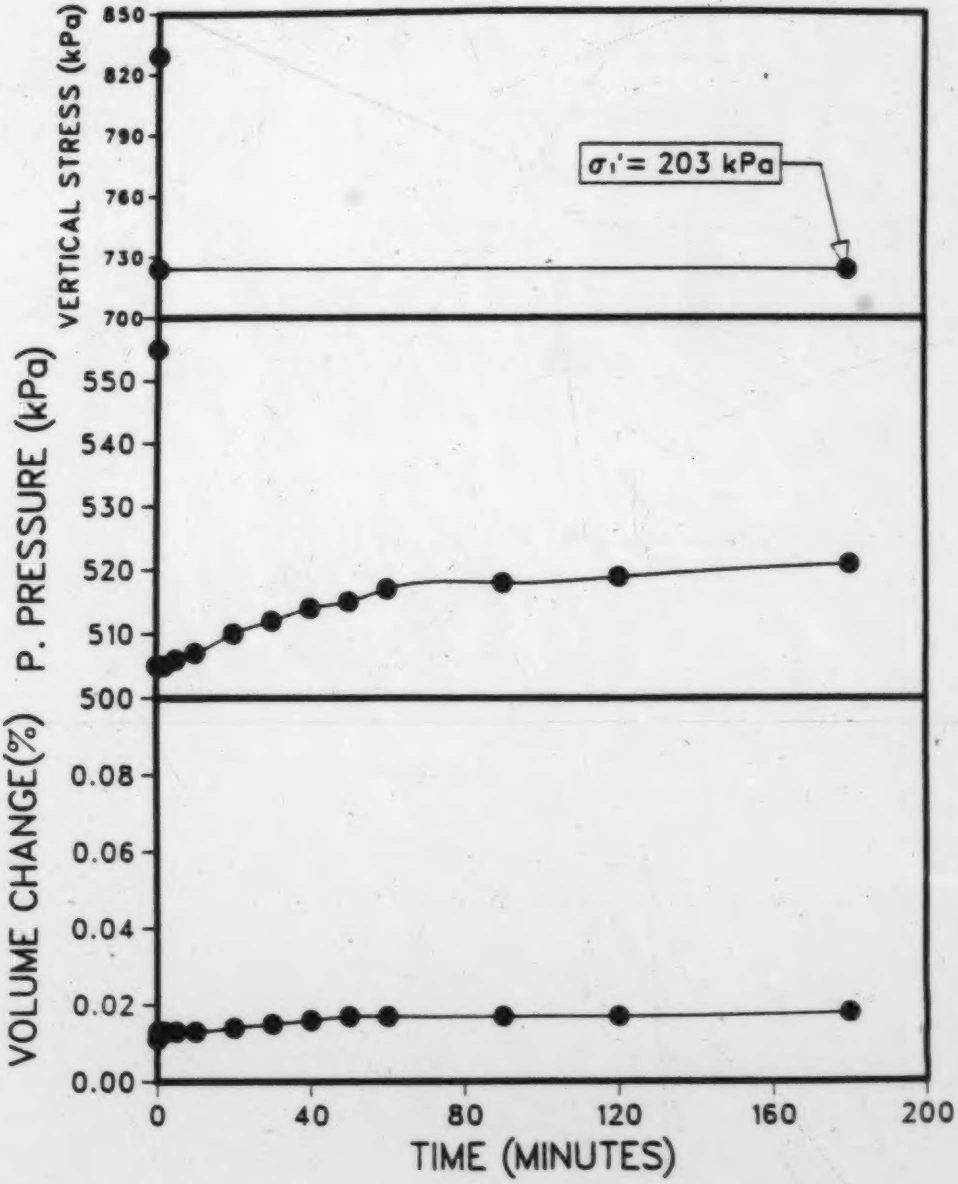

Figure D.5 Increment H from the unloading undrained test at 24°C for RB-5-2

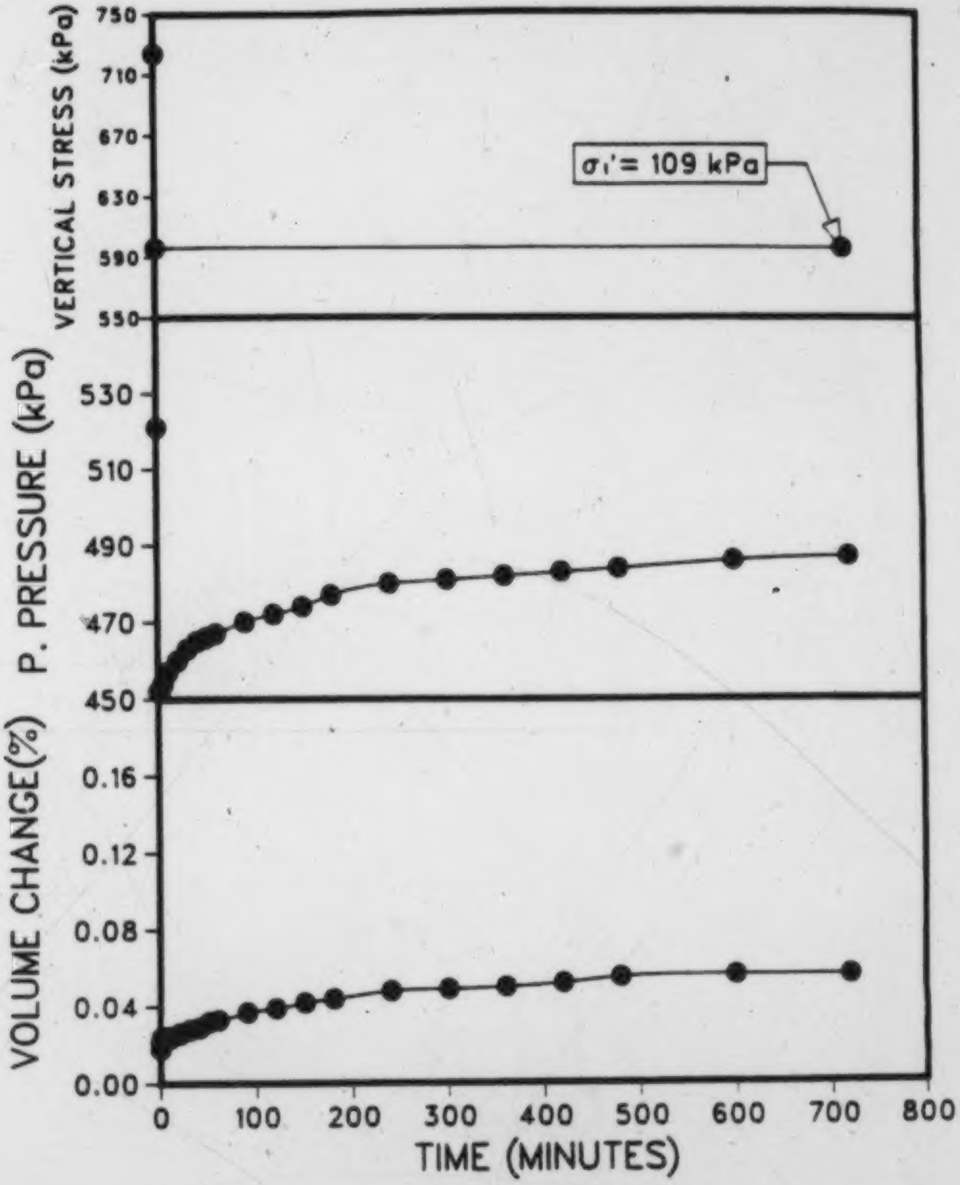

Figure D.6 Increment I from the unloading undrained test at 24°C for RB-5-2

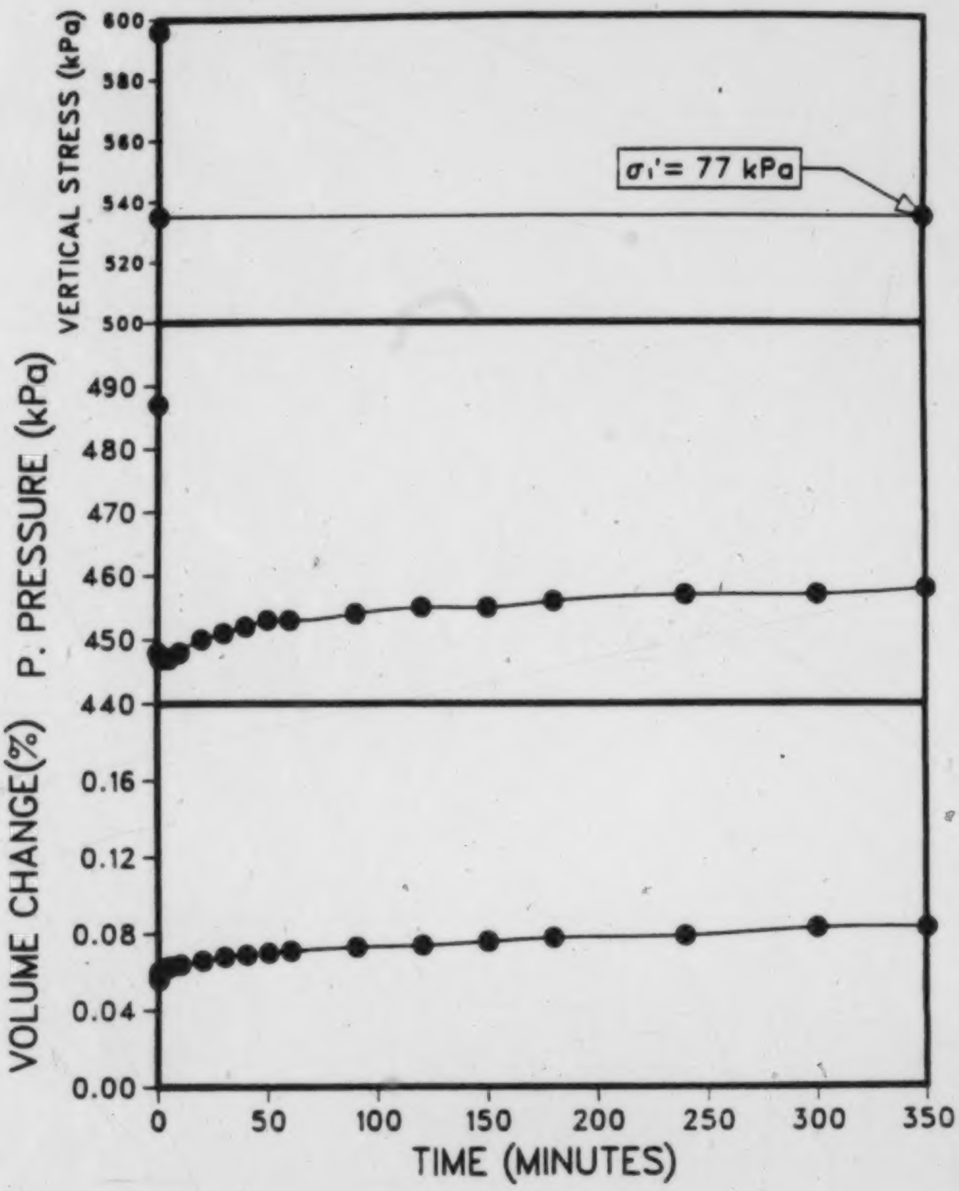

Figure D.7 Increment J from the unloading undrained test at 24°C for RB-5-2

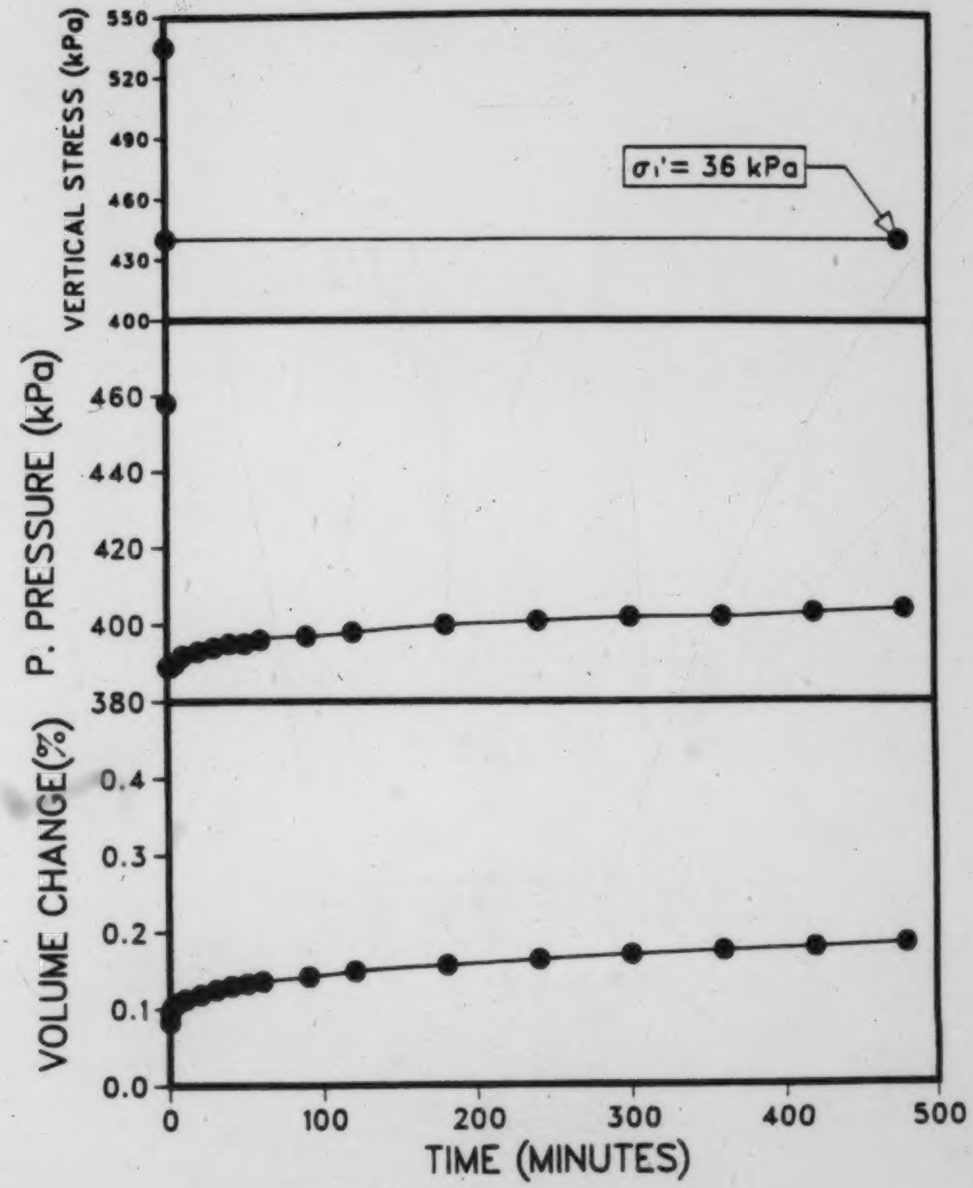

Figure D.8 Increment K from the unloading undrained test at 24°C for RB-5-2

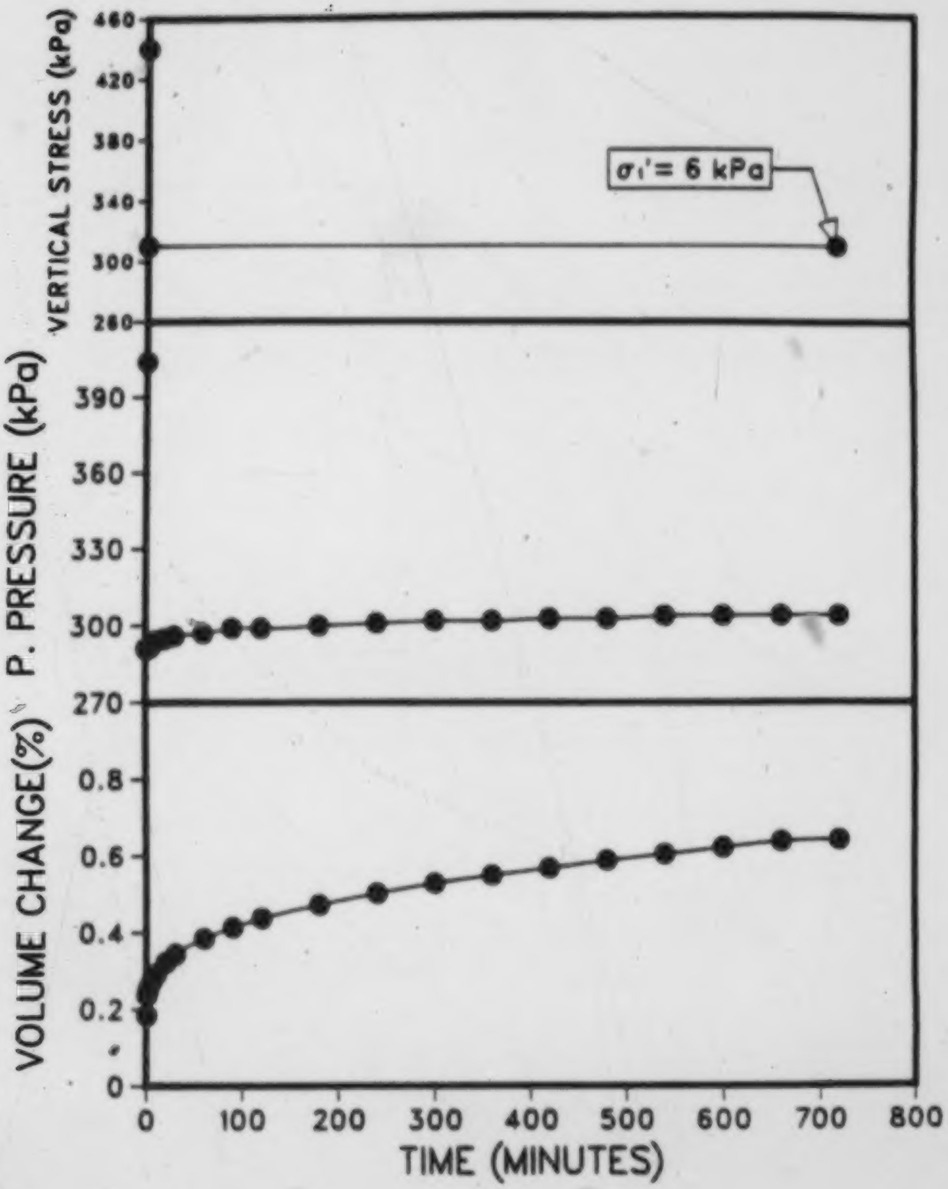

Figure D.9 Increment L from the unloading undrained test at 24°C for RB-5-2

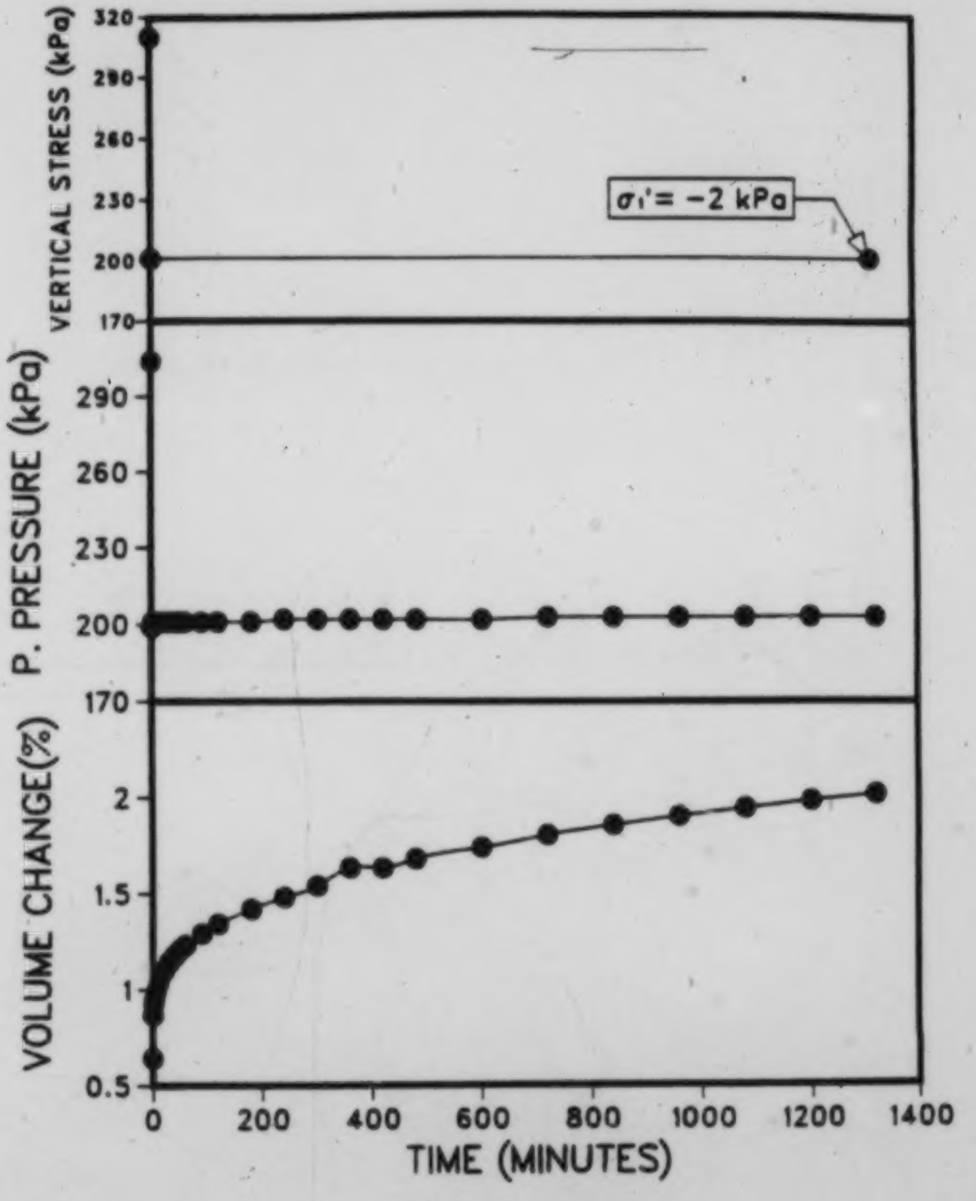

Figure D.10 Increment M from the unloading undrained test at 24°C for RB-5-2

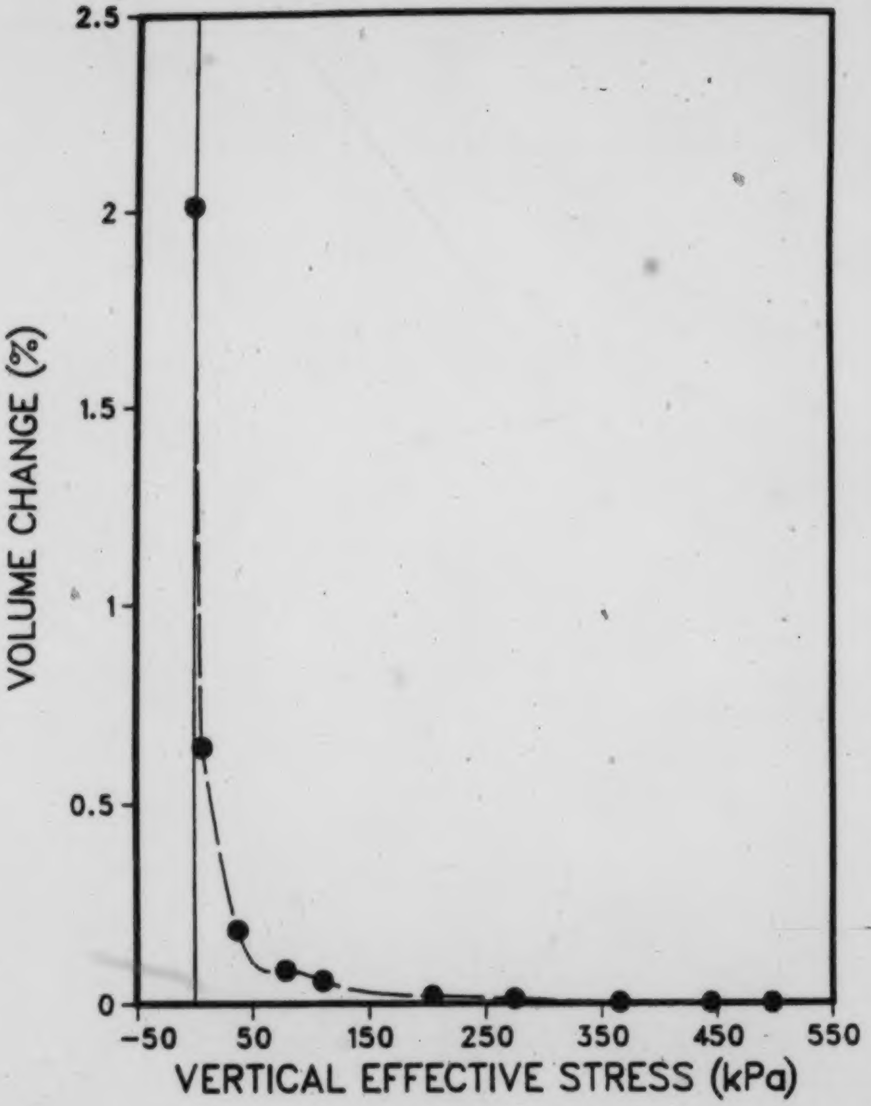

Figure D.11 Stress strain curve for sample RB-5-2

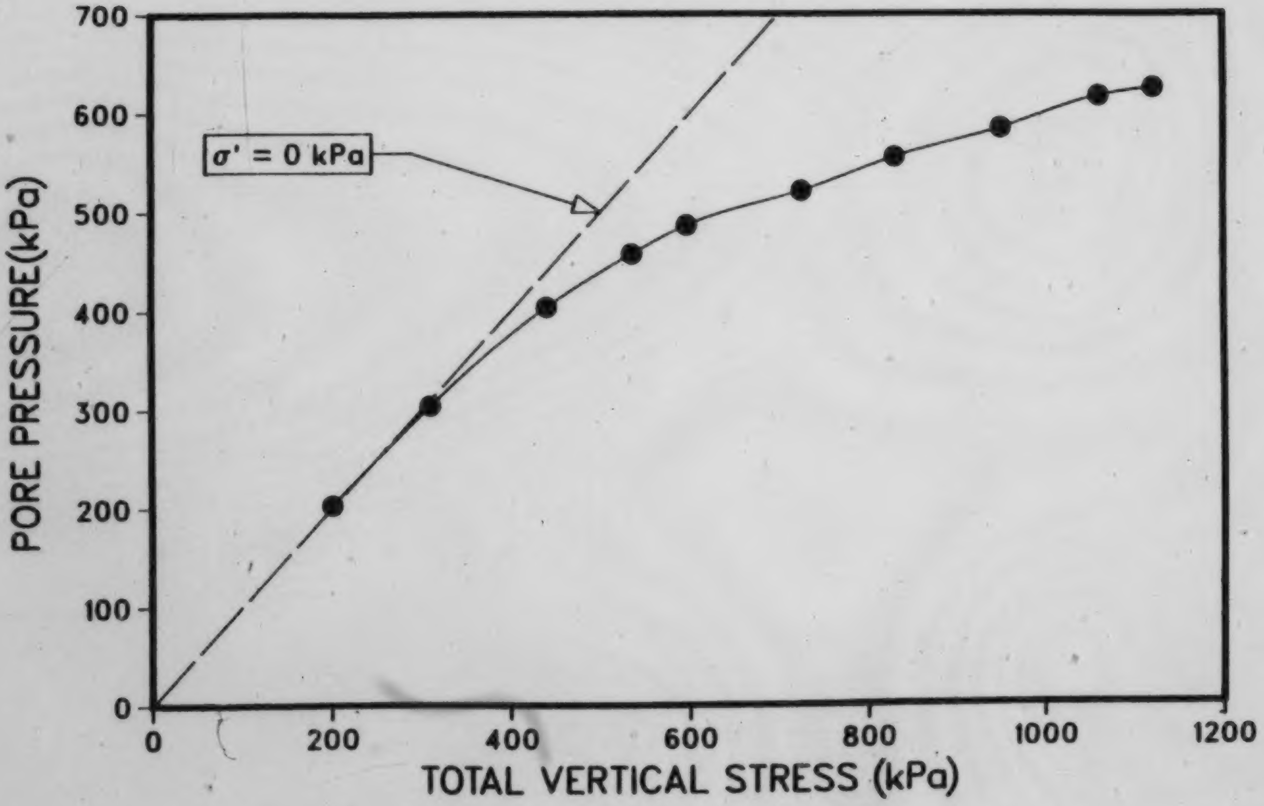

Figure D.12 Unloading Undrained Equilibrium Curve obtained from RB-5-2

APPENDIX E --DIFFUSION EMPIRICAL MODEL

The problem of evolving gas is difficult to analyze because of the presence of complex boundary conditions, the variability of bubble formation, poor understanding of the diffusion coefficient and the lack of understanding of the amount of gas present in the liquid. The boundary conditions are dimensionally complex because of the highly irregular shape of the sand particles and the random orientation of the sand grains in the sand matrix. This random nature of the pore space surrounding the bubble makes an exact solution of the differential equation essentially impossible. The scale effects required to extrapolate the results from the individual bubble to the entire sample would be inaccurate and highly variable. Also the bubbles can move and coelesce and thus change their boundary conditions part way through the diffusion process.

The solubility data of many gases in the bitumen in not known and this is important to determine the actual volume of gases evolving from the pore liquid. Work is progressing in this area but there is still a large void of information.

Finally the diffusion coefficient has only recently been determined for carbon dioxide in bitumen and very little work has been done in determining the diffusion coefficients for other gases in bitumen. Various approximations for determining these diffusion coefficients have been discussed, but they are still only approximations.

As a result of these problems, Sobkowicz (1982) used an empirical relationship to model the actual volume change with time. Equation 2.17 was the empirical curve fitting equation which provided an acceptable fit for his the actual volume change verses time data. This equation has an added advantage because it is similar in form to the theoretical relationships for gas sorption and bubble nucleation.

There are limitations in modeling the transient volume change behavior of a sample with Equation 2.17. Sobkowicz (1982) acknowledged that the E parameter was dependent upon the actual liquid saturation of the sample. In his work on carbon dioxide in water the E parameter varied over an order in magnitude when the liquid saturation of the sample dropped from 100% to 98%. He felt the change in the E parameter was the result of the continual formation and combining of gas bubbles in the pore liquid.

Another limitation of the E parameter is its inability to extapolate the transient nature of any different sample because there is no relationship between this E parameter and the physical properties of the gas in the liquid. To get an E parameter for other liquids requires that the testing procedure be repeated for each different sample. This would be acceptable if the samples could be tested but it is often impossible to collect samples and those which can be obtained are often of unacceptable quality. With this problem the sampling techniques must be greatly improved so that acceptable samples can be obtained, or an effort must be made to correlate the E parameter to the physical properties.

Finally, the E parameter is not able to model behavior which differs significantly from a strictly isolated bubble model. For example the rate of diffusion will occur differently if it is diffusing toward a fracture instead of a bubble and this situation would require a different empirical model. Again this new model will not be related to the actual physical properties, and as a result have the same limitations as equation 2.17. These two empirical models could not be interrelated either because they are empirical.

With the presence of more information in the literature, the diffusion empirical model was developed to take advantage of this data and try to meet some of the shortcomings of the empirical model put forward by Sobkowicz (1982).

DIFFUSION EMPIRICAL MODEL

The diffusion empirical model uses the differential equation for diffusion in spherical coordinates as shown in equation E.1.

$$\partial C/\partial t = K*(\partial^2 C/\partial r^2 + 2/r * \partial C/\partial r) \qquad \text{E.1}$$

This equation forms the basis for the actual diffusion process which actually occurs around bubbles in the sample liquids. The information that is required to solve this equation is the diffusion coefficient and the boundary conditions. The diffusion coefficient can be obtained from Figure 2.2 in section 2.3 when the liquid viscosity and the test pressure are known for the sample.

The boundary conditions comprise two problems, the distance between the bubbles and the volumetric shape of the liquid from which the dissolved gas molecules must evolve. The distance between the bubbles is not known and likely varies considerably. The volumetric shape of the liquid in the sand matrix does change because the shape of the sand pack is highly variable. For simplicity the volumetric shape of the liquid was assumed to be a sphere with the bubble present in the middle. Any shape could be chosen but the spherical one was used because of its simplicity and also because the sphere could be changed to any portion of the sphere and not change the basic nature of the time curve.

The only undetermined quantity left is the distance between the center of the sphere and the outside edge of the sphere (or the distance between bubbles). To empirically curve fit the actual data there must be at least one unknown which can be varied and the radius of the sphere is that unknown for the diffusion empirical model. If the volume change time curve obtained from this model does not give the same curve as the actual data then the volumetric shape of the liquid will have to be changed until we obtain a resulting curve which accurately models the actual data.

When we have a reasonably accurate fit with the actual data then we have obtained an average distance between the bubbles and also an average shape of the liquid containing the gas evolving to the bubble.

In the diffusion empirical model the following assumptions were made:

1. Each gas bubble is at the center of a sphere of liquid.
2. A point sink is present at the center of each sphere. The change in volume of the sphere due to the presence of free gas was not taken into account and the boundaries of the sphere are considered rigid.
3. There was assumed to be no interference between the soil structure and the bubble formation.
4. The diffusion coefficient remained constant throughout the test.

The differential equation was analyzed using a finite difference solution and an explicit formulation stepping forward in time. This procedure was used because of its simplicity and minimal amount of memory required for computation work. Because the concentration of gas in the liquid is uniform as one moves out radially from the center of the sphere, the differential equation is reduced to a one dimensional formulation. The finite difference solution determines the change in concentration that occurs from the outside edge of the sphere to the center using finite difference nodes. To determine the amount of gas that this change in concentration represents, the radial concentration change is integrated over the whole sphere. The volume of gas is obtained by applying the Ideal Gas Law to the amount of evolved gas.

There is an obvious incongruity arising from this model which should be mentioned. In determining the concentration change in the liquid sphere we are assuming that the boundaries are rigid (a point sink). However, we are also calculating a volume of gas as though there is a bubble present in the middle. As a first approximation this is considered acceptable, if the model exhibits merit then this situation should be rectified and the expanding boundary conditions should be inserted into the model.

Equation 2.17 modeled the gas evolution behavior of carbon dioxide in water and so the equation was used as the curve representing the actual behavior of evolving gas. Figures E.1 gives an example of how well the two empirical models correlate. The correlation is almost exact for the full range of the volume change versus time curve but this is not surprising as equation 2.17 is based on the actual diffusion equation. More plots could have been produced but they gave identical results.

If the diffusion empirical model produces the same transient response as equation 2.17 then it should be possible to determine the effect of changing physical parameters on the E parameter of equation 2.17 (i.e. radius and the Diffusion coefficient). Two series of calculations were then done with the diffusion empirical model, the first set of calculations varied the diffusion coefficient and kept the radius of the sphere constant and the second varied the radius of the sphere and kept the diffusion coefficient constant. For each calculation the E parameter was determined which reproduced the curve (as in Figure E.1).

Table E.1 gives the results of the first set of comparative results. The results of the test show that the E parameter is proportional to the diffusion coefficient (equation E.2).

$$E=\underline{k}D \qquad \text{E.2}$$

Table E.2 gives the relationship between the changing radius of the sphere and the E parameter. The diffusion coefficient was kept constant at $2*10^{-6}$ cm^2/sec and by comparing the results it can be shown that the E parameter is inversely proportional to the square of the radius (equation E.3).

$$E=\underline{k}_1 1/r^2 \qquad \text{E.3}$$

With these relationships between the E parameter and the diffusion coefficient and the radius of the liquid sphere, some additional questions can be asked.

1. If we know the diffusion coefficient of a gas in a liquid and have modeled the sample's volume change behavior with time, then the average distance between bubbles can be determined. This can give an indication of the number of bubbles that can be anticipated in the pores between sand particles.
2. The effect of a change in diffusion coefficient on the time taken for the gas to evolve can be determined. This change in coefficient can be due to a temperature change or a liquid change or even a change in the type of gas that is present in the fluid.
3. The presence of a bubble at the center of a sphere will tend to make the distance from the outside of the sphere to the bubble shorter as more gas evolves. This increase in free gas (decrease in saturation) will tend to speed up the gas evolution process and increase the E parameter. In oil sand this can be quite significant as the venting saturation is much lower than it is in water or other liquids with a higher viscosity.

This thesis will not make an attempt to answer these questions as they are beyond the scope of the thesis. The purpose of this appendix is to describe the model and attempt to give some correlations between the empirical model put forward by Sobkowicz and the actual gas evolution properties.

Table E.1 Relationship between E parameter and Diffusion Coefficient

DIFFUSION COEFFICIENT= 2*E-6 cm^2/sec

SPHERE RADIUS cm	E parameter
0.020	.00385
0.024	.00267
0.028	.00196
0.030	.00170
0.038	.00107

Table E.2 Relationship between bubble radius and E parameter

RADIUS OF SPHERE= .02 cm

Diffusion Coefficient (cm^3/sec)	E Parameter
2*E-6	.00385
1*E-5	.0192
8*E-6	.0154
2*E-8	.0000385
2*E-7	.000385

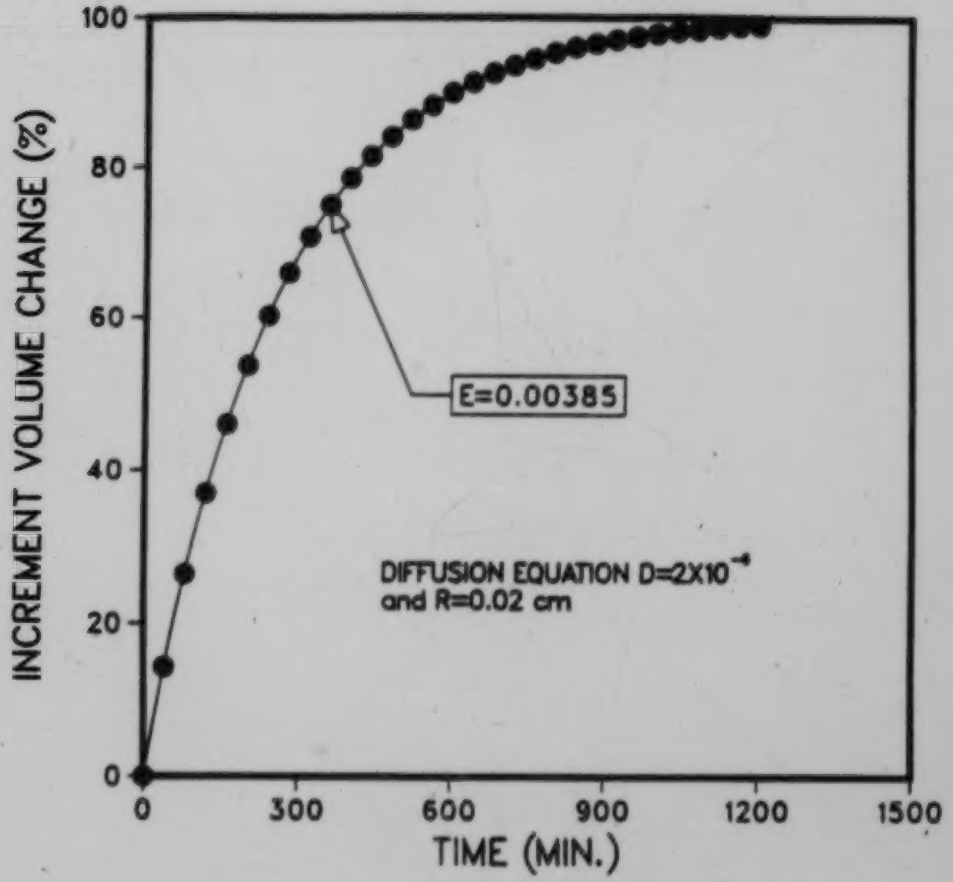

Figure E.1 Correlation between the diffusion empirical model and the E parameter